EMMELIE MARGARETE ECKHARDT

Vaccination and therapeutic strategies against *M. tuberculosis* in the guinea pig model

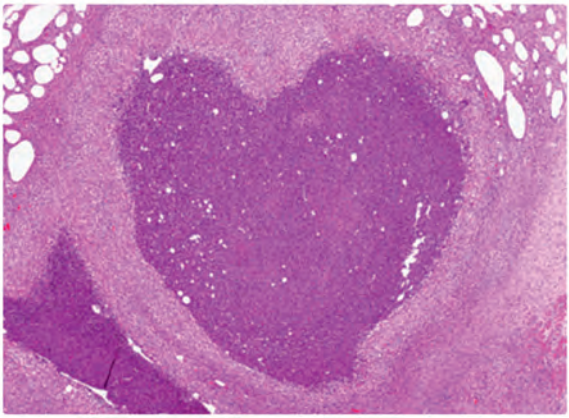

Inaugural-Dissertation zur Erlangung des Grades eines
Dr. med. vet.
beim Fachbereich Veterinärmedizin der Justus-Liebig-Universität Gießen

édition scientifique
VVB LAUFERSWEILER VERLAG

Das Werk ist in allen seinen Teilen urheberrechtlich geschützt.

Die rechtliche Verantwortung für den gesamten Inhalt dieses Buches liegt ausschließlich bei der Autorin dieses Werkes.

Jede Verwertung ist ohne schriftliche Zustimmung der Autorin oder des Verlages unzulässig. Das gilt insbesondere für Vervielfältigungen, Übersetzungen, Mikroverfilmungen und die Einspeicherung in und Verarbeitung durch elektronische Systeme.

1. Auflage 2023

All rights reserved. No part of this publication may be reproduced, stored in a retrieval system, or transmitted, in any form or by any means, electronic, mechanical, photocopying, recording, or otherwise, without the prior written permission of the Authors or the Publisher.

1st Edition 2023

© 2023 by VVB LAUFERSWEILER VERLAG, Giessen
Printed in Germany

édition scientifique
VVB LAUFERSWEILER VERLAG

STAUFENBERGRING 15, 35396 GIESSEN, GERMANY
Tel: 0641-5599888 Fax: 0641-5599890
email: redaktion@doktorverlag.de

www.doktorverlag.de

Aus dem Institut für Veterinär-Pathologie der Justus-Liebig-Universität Gießen
und
dem Friedrich-Loeffler-Institut, Bundesforschungsinstitut für Tiergesundheit,
Greifswald - Insel Riems

Betreuer: Prof. Dr. Jens P. Teifke

Vaccination and therapeutic strategies against *M. tuberculosis* in the guinea pig model

INAUGURAL-DISSERTATION
zur Erlangung des Grades eines
Dr. med. vet.
beim Fachbereich Veterinärmedizin
der Justus-Liebig-Universität Gießen

eingereicht von

Emmelie Margarete Eckhardt

Tierärztin aus Offenbach a.M.

Gießen 2023

Mit Genehmigung des Fachbereichs Veterinärmedizin
der Justus-Liebig-Universität Gießen

Dekan: Prof. Dr. Dr. Stefan Arnhold

1. Gutachter: Prof. Dr. Jens P. Teifke
2. Gutachter: Prof. Dr. Christa Ewers

Tag der Disputation: 16.09.2023

Table of Contents

I. Abbreviations

AG	Arabinogalactan
AM	Alveolar macrophage
APC	Antigen presenting cell
ASC	Antibody-secreting B cell
BCG	Bacillus Calmette-Guérin
CAF	Cationic adjuvant formulation
CAF01	Cationic adjuvant formulation number one
CLR	C-type lectin receptor
DC	Dendritic cells
DC-SIGN	DC-specific intracellular adhesion molecule-3–grabbing nonintegrin
DDA	Dimethyldioctadecylammoniumbromid
DosR	Dormancy survival regulator
DprE1	Decaprenyl-phosphoribose-2'-epimerase
EMB	Ethambutol
GM-CSF	Granulocyte-macrophage colony-stimulating factor
IFN-γ	Interferon gamma
IL	Interleukin
INH	Isoniazid
IV	Intravenously
LAM	Lipoarabinomannan
LM	Lipomannan
M.	*Mycobacterium*
MA	Mycolic Acid
ManLAM	Mannose-capped lipoarabinomannan
mBC	Memory B cell
MDR	Multidrug-resistant
MGC	Multinucleated giant cells
MHC	Major histocompatibility complex

MIC	Minimal inhibitory concentration
Mincle	Macrophage-inducible C-type lectin
MM	Mycomembrane
MR	Mannose receptor
Mtb	*Mycobacterium tuberculosis*
MTC	*Mycobacterium tuberculosis* complex
NHP	Non-human primates
NKT cells	Natural killer T cells
NO	Nitric oxide
NOD	Nucleotide-binding oligomerization domain
PIM	Phosphatidylinositol mannoside
PG	Peptidoglycan
PPD	Purified-protein derivate
PRR	Pattern recognition receptor
PZA	Pyrazinamid
RIF	Rifampicin
ROS	Reactive oxygen species
Rpfs	Resuscitation-promoting factors
RR	Rifampicin-resistant
TCR	T cell receptor
TDB	Trehalose-6,6'-dibehenate
TDM	Trehalose-6,6'-dimycolate
T_H	T helper cell
TLR	Toll-like receptor
TMM	Trehalose monomycolate
TNF-α	Tumor necrosis factor alpha
WHO	World Health Organization
XDR	Extensive drug-resistant

II. Figure Legend

III. Table Legend

1 Initial remarks and objectives

Tuberculosis - mainly caused by *Mycobacterium tuberculosis* (*Mtb*)- is one of the most important infectious diseases worldwide with around one third of the human population being infected. With 1.3 million estimated deaths per year it is the world's leading cause of mortality from a single bacterial pathogen, and 9.9 million new tuberculosis cases developed in 2020 (World Health Organization, 2021).

Currently, the only available tuberculosis vaccine is Bacillus Calmette-Guérin (BCG), a live-attenuated *Mycobacterium bovis* (*M. bovis*) strain, which was developed early in the 20th century and first used in humans in 1921 (Petroff & Branch, 1928). In 120 countries with high tuberculosis rates, over 90 % of infants are vaccinated with BCG and thus protected against severe childhood tuberculosis (Rodrigues et al., 1993; World Health Organization, 2018). A main disadvantage of BCG is that it does not provide protection against pulmonary tuberculosis in adults and therefore is not sufficient to end the global tuberculosis-epidemic.

A further problem is the increase in rifampicin- (most effective first line drug against tuberculosis) and multidrug-resistant tuberculosis (MDR/RR-tuberculosis). Already 3.3 % of new cases and 17.7 % of pre-treated patients were MDR/RR-tuberculosis positive in 2019 (World Health Organization, 2020). This makes a sufficient treatment more difficult or even impossible for extensive resistant tuberculosis (XDR-tuberculosis) cases, in which none of the conventional drugs are effective (World Health Organization, 2018).

The morphologic hallmark of tuberculosis infection and niche of persistence for mycobacteria is the granuloma. Classically, it is composed of a central core of caseous necrosis and mineralization, surrounded by a rim of epithelioid macrophages, multinucleated giant cells (MGC) and a distinct layer of lymphocytes (Ulrichs et al., 2004; Cheville, 2009).

Initially, granulomas were seen only as protective entities of the host against pathogenic mycobacteria, in the meantime it has become clearer that mycobacteria have developed strategies to persist in the hostile environment of a granuloma and that they literally exploit this immunopathologic structure to cause long-term infections (Ehlers & Schaible, 2012).

Mycobacteria have a very particular lipid-rich tripartite cell envelope. On the outer layer a multiplicity of non-covalently bound lipids, glycolipids and lipopeptides can be found (Minnikin et al., 2002). As they have close contact with cellular structures of phagocytes, they can activate innate pattern recognition receptors (PRR) (Sieling et al., 2008; Toyonaga et al., 2014; Yonekawa et al., 2014). These effects of mycobacterial lipids on cells of the innate immune system play an essential role for granuloma formation and maintenance and are often shaped in need of the pathogen (Batt et al., 2020; Dulberger et al., 2020).

Alongside the positive effect of the mycobacterial lipids for the bacteria themselves, they can also be the target for protective immune responses of the host including antibody and T cell activation (Brennan & Nikaido, 1995). There are a number of mycobacterial lipids recognized by CD1 type 1-restricted, adaptive T cells (De Libero & Mori, 2014). Mycolic acids (MAs), a class of long acyl-chained, mycobacterial lipids as well as phosphatidylinositol mannosides (PIM) are essential constituents of the mycobacterial cell wall and induce CD1-restricted T cell responses.

While the existence and the phenotype of CD1-restricted T cells is long known (Porcelli et al., 1992) and their protective role has frequently been postulated (Stenger et al., 1997), it is still poorly understood at what level they contribute to the immune defense against mycobacteria. In this context, it is intriguing that mainly immature dendritic cells (DCs) express CD1, while macrophages, the main host cells for mycobacteria, only express little amounts (Brigl & Brenner, 2004).

In the present thesis the guinea pig model was used to delve in two of the main challenges of tuberculosis research: modern vaccination approaches and anti-tuberculosis treatment. Guinea pigs are well established as an animal model for different aspects of tuberculosis research as vaccine efficacy evaluation (Gong et al., 2020), *Mtb* virulence testing (Palanisamy et al., 2008) or investigation of the immune response to *Mtb* infection (Clark et al., 2014). Coherent with the latter, they are also ideal to elucidate the role of CD1-restricted T cell response in tuberculosis infection, as they expresses functional CD1 type 1 molecules (Dascher et al., 1999) (**publication I**).

The first objective (**publication II)** was to find out whether and how lipid-reactive T cells instruct the formation and maintenance of the granuloma after tuberculosis-infection and to what extent this contributes to immune protection. To this end the presence and reactivity of lipid specific T cells with the morphology and histology of BCG or *Mtb*-induced granulomas was compared. It was demonstrated that PIM_6 is a mycobacterial lipid antigen recognized by T cells. Further, the expression pattern of CD1 in infected tissues and how T cells respond in the presence or absence of vaccine induced memory were shown. Finally, their effect in the immune defense against *Mtb*-infection could be demonstrated. Eventually, this can help to devise new strategies for the development of future vaccines against tuberculosis.

For the second objective (**publication III**), guinea pigs were tested and established as an animal model for testing of the new anti-tuberculosis drug BTZ-043. For this purpose, first pharmacokinetic studies of BTZ-043 in the guinea pig were conducted and finally, the healing potential of BTZ-043 in an *Mtb* challenge trial was tested. Therefore, these studies contribute to an establishment of a new treatment approach against tuberculosis.

2 Introduction

2.1. Tuberculosis

2.1.1 Etiology and epidemiology of tuberculosis

The most important causative agent of tuberculosis is the bacterium *Mycobacterium tuberculosis* (Koch, 1882). *Mtb* is an aerobic, Gram-positive/labile, non-motile rod-shaped bacterium belonging to the family of Mycobacteriaceae. Because of its cell wall composition, it is acid-alcohol-fast and can be stained with Ziehl-Neelsen or Fite-Faraco (Pfyffer, 2015). The generation time of mycobacteria is very slow with 14-20 h and growth in culture therefore needs time.

The origin of mycobacteria is assumed to date back at least 150 million years, accompanying and adapting to humans through history (Barberis et al., 2017). But even in the Middle Triassic period a tuberculosis-like infection in a marine reptile could be detected, suggesting mycobacteria to be actually older than thought (Surmik et al., 2018). Molecular evidence for tuberculosis infection could be already found in mummies from about 1550 BC (Nerlich et al., 1997), but mycobacteria were first isolated by Robert Koch in 1882 (Koch, 1882).

Mtb and seven other mycobacteria (*M. africanum, M. bovis, M. canetti, M. caprae, M. microti, M. mungi, M. orygis, M. pinnipedii*) form the so called "*Mycobacterium tuberculosis* complex" (MTC) (Pfyffer, 2015; Kanabalan et al., 2021). Those bacteria are all able to cause tuberculosis in mammals.

As mentioned above, *Mtb* is the main cause of human tuberculosis, to a lower extent also *M. africanum* causes genuine human-to-human infections (Pai et al., 2016). Their host spectrum is mainly restricted to humans and non-human primates (NHP). By contrast *M. bovis*, another closely related *mycobacterium* of the MTC, efficiently infects several mammalian species among them ruminants causing bovine tuberculosis. *M. bovis* also has extensive zoonotic potential. Before bovine tuberculosis was eradicated in Germany in the late 1960s one third of human tuberculosis-cases were caused by *M. bovis* (Griffith, 1937). Although strict test and slaughtering systems led also in other industrialized Western countries to an eradication of bovine tuberculosis, the past years have witnessed a re-

emergence of the disease in some countries, such as the UK, New Zealand, Spain and also the German-Austrian-Swiss border region, mostly due to uncontrollable wildlife reservoirs and their infections with *M. caprae* (Aranaz et al., 2004; Nugent et al., 2012; Davidson et al., 2017).

Today tuberculosis is still one of the most important infectious diseases worldwide with 1.7 billion people being infected. In 2020 9.9 million new cases developed and tuberculosis caused an estimated 1.3 million deaths, making it the world's leading cause of mortality from a single bacterial pathogen (World Health Organization, 2021).

Only 5-10 % of the population latently infected with tuberculosis will develop an active disease, but especially people with HIV infection (Gupta et al., 2015; Barr et al., 2020), immunosuppression, malnutrition (Cegielski & McMurray, 2004), diabetes (Segura-Cerda et al., 2019; Apt et al., 2020), alcohol abuse and lack of access to public health care are at a much higher risk (Lönnroth et al., 2009; Bloom et al., 2017).

While in most high-income countries there are fewer than 10 new cases per 100,000 inhabitants per year, e.g. only 3 % of worldwide tuberculosis cases are in Europe, in many other countries the tuberculosis incidence is still high. Especially African and Asian countries are highly affected with incidences up to over 500 per 100,000 population per year (World Health Organization, 2020).

As numbers of RR- and MDR-tuberculosis are increasing year by year, treatment success of tuberculosis is getting more and more difficult and currently available drugs and treatment regimens are often not enough to lead to a sustained healing of patients (World Health Organization, 2021) (more on this in 3.5.1).

The World Health Organization (WHO) aims to end tuberculosis until 2030, with 90 % reduction in absolute number of deaths caused by tuberculosis and 80 % reduction in tuberculosis incidence in comparison to 2015 (World Health Organization, 2018). Although current diagnosis, vaccination and treatment averts millions of deaths each year, there is still a large and persistent gap in those areas. With the strategies currently available it is

unlikely that the global goals will be achieved. Therefore, it is inevitable to develop new vaccine, diagnosis and treatment methods.

Furthermore, attention to the tuberculosis-epidemic has declined since the beginning of the COVID-19 pandemic, leading to negative medium- and longer-term consequences for recognising, treating and preventing of tuberculosis (Stop TB Partnership, 2020a, 2020b; World Health Organization, 2020). But not only the biomedical care factors are disrupted because of COVID-19, but now also the poverty-related tuberculosis risk factors are further increasing (Saunders & Evans, 2020).

2.1.2 Clinical signs and pathogenesis of tuberculosis in humans

Unspecific fever, night sweats, weight loss, fatigue and inappetence are some of the initial signs of tuberculosis occurring after 6 to 8 weeks of incubation in humans. In addition, coughing, swollen lymph nodes, haemoptysis and dyspnoea are also common (Suárez et al., 2019). As the disease progresses the symptoms become more specific for the affected organs. A majority of the patients develop pulmonary tuberculosis, and only 15 % extrapulmonary disease (Rodriguez-Takeuchi et al., 2019; Abengozar-Muela et al., 2020). However, clinical disease only occurs in 10 % of the cases. Over 90 % of tuberculosis infected humans develop only a latent form never showing any clinical signs.

Usually tuberculosis is caused by airborne infection: people with active pulmonary disease spread the bacteria trough coughing (Churchyard et al., 2017). Mycobacteria then are inhaled and reach the alveoli of the lungs, the main target location. They then activate various innate immune cells such as macrophages, DCs, neutrophils, and natural killer T cells (NKT) (Sia et al., 2015). A primary focus develops and macrophages phagocyte most of the bacteria. As soon as the regional lymph node is affected, it is called a primary complex (Nieberle, 1929, 1938; Zachary, 2021). It depends on the immune status of the infected person how the disease progresses further: In most cases the bacteria are contained in small granulomas. Bacteria can persist in these lesions over long periods. Eventually the lesions may calcify and become sterile. In cases that are not able to control the bacteria, lesions will grow and will eventually open into the airways. Bacteria may become aerosolised and a dose of fewer than ten bacteria is able to infect new hosts (Pfyffer, 2015).

2.1.3 The formation and role of the granuloma

After infection with *Mtb*, progression of granulomas – hallmarks of tuberculosis-infection - usually begins shortly after with formation of an "innate granuloma", which then can develop to an "immune granuloma" and finally to a "chronic granuloma" (Shaler et al., 2013).

The conformation of granulomatous lesions consists mainly of macrophages (Pagán & Ramakrishnan, 2018), which play an important role in granuloma outcome (Marino et al., 2015) and often develop a "foamy" character during the course of infection (Cáceres et al., 2009; Russell et al., 2009), some neutrophils, DCs and monocytes. In further stages epithelioid macrophages, MGC, plasma cells and an outer layer of B cells, $CD4^+$, $CD8^+$ T cells together with fibroblastic collagen deposition and encapsulation complete the granuloma formation (Ulrichs et al., 2004; Bozzano et al., 2014), while the central core of the granuloma shows caseous necrosis and mineralization. This is also the site where the highest number of mycobacteria are found.

As others have already described the immunopathology of the granuloma at length (Saunders & Britton, 2007; Shaler et al., 2013; Kaufmann, 2016; Pagán & Ramakrishnan, 2018; Woelke, 2020), only a short overview will be given here. After infection, macrophages are binding mycobacteria to their cell surface and internalize them leading to phagocytosis (Schlesinger, 1996). Furthermore, neutrophils (Eruslanov et al., 2005; Eum et al., 2010) and DCs (Wolf et al., 2007) take up the bacteria. Subsequently, different cytokines and chemokines are upregulated and enhance activation of further immune cells (Zuñiga et al., 2012), which consequently leads to a higher number of target cells to infect for bacteria and therefore dissemination of *Mtb*. Attracted trough cytokine signals (e.g. interleukin (IL) 8) T cells are recruited and activated initiating interferon-γ (IFN-γ) production (Birkness et al., 2007). IFN-γ as well as tumor necrosis factor α (TNF-α), which is secreted by infected macrophages, are essential for granuloma formation (Algood et al., 2003; Ly et al., 2007; Bhatt et al., 2015; da Silva et al., 2018). From the innate granuloma mycobacteria or mycobacterial antigens are distributed to the lymph nodes, where antigen-specific T cells are activated by antigen presenting cells (APCs, Guermonprez et al., 2002). Due to chemokine (e.g. CXCL10, CXCL11) attraction, T cells are recruited back to the

primary lesion (Khader et al., 2007), where they surround it and wall it off (Shaler et al., 2013) resulting in a relatively stable state of the granuloma. Further progression with caseous necrosis occurs, when macrophages and other immune cells die in the hypoxic center of the granuloma (Kim et al., 2010), and seldomly caseation occurs due to tuberculous pneumonia with small cavities (Hunter, 2011) .

The ambiguous role of the granuloma in tuberculosis outcome has been topic of many publications (Ulrichs & Kaufmann, 2006; Saunders & Britton, 2007; Rubin, 2009; Ehlers & Schaible, 2012; Reece & Kaufmann, 2012; Guirado & Schlesinger, 2013). For a long time, the granuloma was mainly thought to be a protective entity of the host, where bacteria are walled off inside. This might be true in many cases, as latent tuberculosis-infection is established in over 90 % of infected individuals and will mostly not progress to active tuberculosis. On the outer layer of the granuloma, activated T cells patrol and may keep mycobacteria under control showing an effective immune response (Egen et al., 2008). The inner caseous lesion, however, is devoid of T cells and lined with macrophages in which mycobacteria persist and multiply. As soon as the immunosurveillance wanes, mycobacteria escape the ring of patrolling T cells and reactivate (Ulrichs & Kaufmann, 2006). Therefore, it has become clear that mycobacteria exploit the immune structure of granulomas to cause long term infection as they developed strategies to not only persist, but show enhanced growth in the hostile environment of a granuloma (Davis & Ramakrishnan, 2009; Ehlers & Schaible, 2012). Furthermore, it has been shown that some immunodominant T cell epitopes in mycobacteria (Comas et al., 2010), as well as some mycobacterial lipopeptides (Kaufmann et al., 2016) are highly conserved, leading to the conclusion that mycobacteria provoke the recognition through the immune system and profit from it in some way.

2.2 The mycobacterial cell envelope

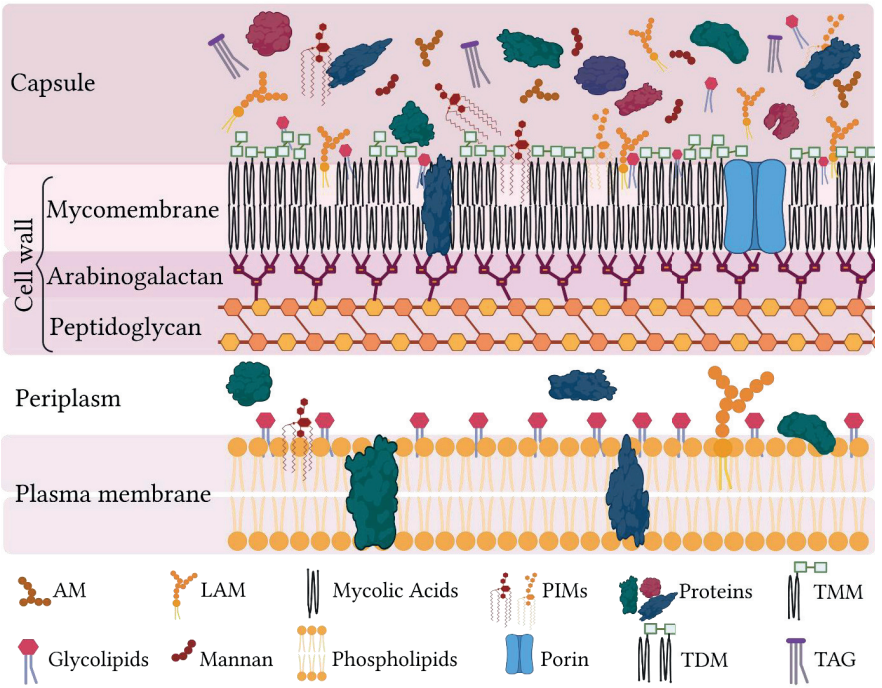

Figure 1: Schematic composition of the mycobacterial cell envelope.

From the outside to the inside the mycobacterial cell envelope consists of a capsule, a cell wall, a periplasm and a plasma membrane. The cell wall itself is composed of a mycomembrane, an arabinogalactan and a peptidoglycan layer. AM: arabinomannan; LAM: lipoarabinomannan; PIMs: phosphatidylinositol mannosides; TDM: trehalose dimycolate; TMM: trehalose monomycolate; TAG: triacylglycerol. Adapted from (Daffé & Marrakchi, 2019) and created with BioRender.com.

Mycobacteria have a very particular multi-layered cell envelope (Figure 1), which differs from those of gram-positive or -negative bacteria. From the outside to the inside this cell envelope is comprised of a 'capsule' outer layer, a complex carbohydrate- and lipid-composed cell wall and a gram-negative bacteria-like (Zuber et al., 2008) plasma membrane composed of phospholipids and proteins (Daffé & Marrakchi, 2019). While the cell-envelope of gram-positive bacteria is made out of less than 10 % and the one from gram-negative out of only around 20 % lipid dry mass (Brennan & Nikaido, 1995), for

mycobacteria it is up to 40 % lipid dry mass (Jackson, 2014; Chiaradia et al., 2017), respectively 60 % in weight (Jarlier & Nikaido, 1994).

The outer capsule of mycobacteria is dominantly composed of polysaccharides and proteins and only small amounts of lipids (2-3 %) (Daffé & Marrakchi, 2019). In detail, the main components are α-glucan, arabinomannan and oligomannosyl-capped glycolipids (Sani et al., 2010), as proteins the 19 and 38 kDa lipoproteins, the 30/31 kDa fibronectin-binding proteins and the 40 kDa L-alanine dehydrogenase and as lipids phosphatidylethanolamine and phosphatidylinositol mannoside in different conformations (Ortalo-Magné et al., 1995).

The mycobacterial cell wall itself is a tripartite structure of the mycomembrane (MM, or outer membrane), arabinogalactan (AG) and peptidoglycan (PG). On one end, AG is covalently attached to PG and on its non-reducing ends to α-alkyl, β-hydroxy long-chain (C_{70}-C_{90}) mycolic acids (Jackson, 2014; Daffé et al., 2017). The MM is composed of the MAs and its derivates as trehalose monomycolate and trehalose dimycolate (TDM, cord factor) together with noncovalently bound, free lipids and lipoglycans: PIMs (more in 3.2.1), phenolic glycolipids, phthiocerol dimycocerosates, mannose-capped lipoarabinomannan (ManLAM), glucose monomycolate, and more (Brennan & Nikaido, 1995; Jackson, 2014; Dulberger et al., 2020). Finally, after a periplasmic space, the plasma membrane forms the innermost layer of the mycobacterial cell envelope being mainly composed of phosphatidylglycerol, diphosphatidylglycerol, PE, phosphatidylinositol and its PIMs (Brennan & Nikaido, 1995). The latter are functioning as an anchor for lipomannan (LM) and lipoarabinomannan (LAM) (Gilleron et al., 2003).

The thick cell wall with its composition of waxes, MAs and lipid compounds is essential for the persistence of mycobacteria and induced immune reaction of the host. The outer layer harbours a unique abundance of non-covalently bound lipids and lipopeptides (Minnikin et al., 2002) that have most intimate contact with cellular and endosomal membranes of phagocytes and are thereby able to activate innate PRR (Sieling et al., 2008; Toyonaga et al., 2014; Yonekawa et al., 2014). The dynamics of the mycobacterial cell envelope, as well as the regulatory pathways and the interactions with the immune system were recently

reviewed in detail (Dulberger et al., 2020) as well as its protective function against antibiotics and the host's immune system (Batt et al., 2020).

2.2.1 Phosphatidylinositol mannosides (PIM)

As described above PIMs are important structures of the mycobacterial cell envelope. They exist in *di-* to *hexa*-mannosylated conformations, with PIM_2 and PIM_6 being the most abundant ones in tested mycobacterial strains (Gilleron et al., 2001). The structure of PIMs has been identified long ago (Ballou et al., 1963; Lee & Ballou, 1965) and their biosynthesis has been described (Guerin et al., 2010; Sancho-Vaello et al., 2017).

PIMs are intermediates in the complex synthesis pathway of mannosylated LAM (Dulberger et al., 2020) and therefore anchor LAM as well as LM in the mycobacterial membrane (Chatterjee et al., 1992; Gilleron et al., 2003).

Structurally, all PIM forms have one mannose residue at position two of the myo-inositol-ring attached, while at position six the number of mannose residues varies from one to five depending on the conformation (Figure 2) (Guerin et al., 2010). In addition, PIM species can also be mono-, di-, tri- and tetraacylated, where fatty acids esterify either at the C_3 from the myo-inositol-ring or the C_2 from the mannose residue (Villeneuve et al., 2005) leading to $AC_{1/2}PIM_{1-6}$ (Driessen et al., 2009). Only diacylated PIM species can be transferred and presented (Cala-De Paepe et al., 2012; Gilleron et al., 2016).

Functionally, PIMs can be recognized by T cells due to presentation by CD1b molecules and CD1e as a cofactor (De Libero et al., 2009; Cala-De Paepe et al., 2012). After presentation by CD1d molecules they can activate NKT cells(Fischer et al., 2004). Further, PIM can induce TNF-α and IL-8 secretion (Briken et al., 2004), but PIM_2 and PIM_6 are described to decrease non-opsonic phagocytic capacity of macrophages (Villeneuve et al., 2005).

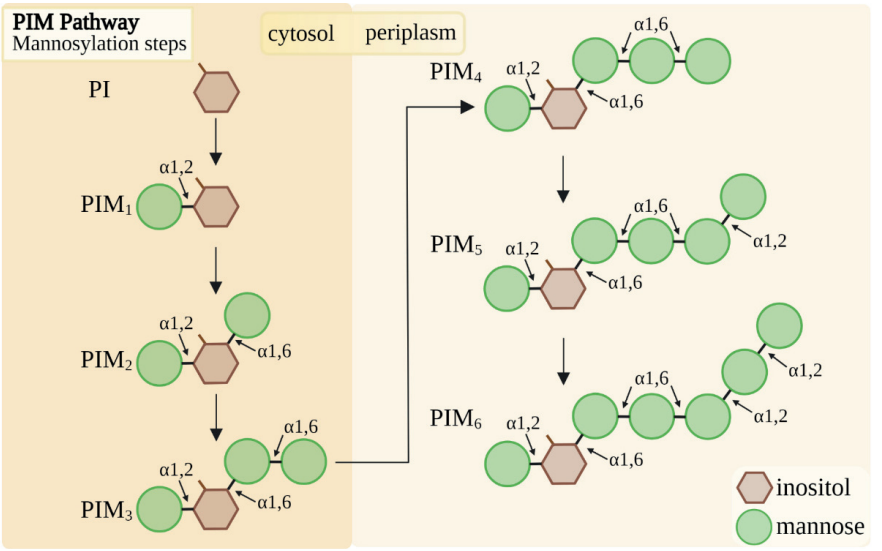

Figure 2: The biosynthetic PIM pathway.

The mannosylation steps from phosphatidylinositol (PI) to phosphatidylinositol mannoside 6 (PIM_6) are shown. Adapted from (Sancho-Vaello et al., 2017) and created with BioRender.com.

2.3 Immune response to *Mycobacterium tuberculosis*

The immune response to *Mtb* infection is a dynamic process between the innate and adaptive immune response, with both the cellular and the humoral compartment (Scriba et al., 2017). Some of the induced responses are leading to reduction or clearance of bacteria while others are more in favor of mycobacteria (Mayer-Barber & Barber, 2015).

2.3.1 Innate immune response to *Mycobacterium tuberculosis*

Alveolar macrophages (AMs) are the first cells to encounter mycobacteria after aerosol-inhalation (Queval et al., 2017; Woo et al., 2018) and are important also in ongoing processes as they are the target cells for *Mtb* (Cambier et al., 2014) and express different cytokines and chemokines (Scriba et al., 2017). Bacteria are recognized via their microbe-associated molecular patterns by PRRs of macrophages. Toll-like receptors (TLRs, especially TLR-2, -4 and -9), nucleotide-binding oligomerization domain (NOD) -like receptors (especially NOD2) and C-type lectin receptors (CLRs, especially Macrophage-inducible C-type lectin (Mincle), Mannose receptor (MR) and DC-SIGN (dendritic cell-specific intracellular

adhesion molecule-3–grabbing nonintegrin)) are just some of the PRRs expressed on AMs and involved in the recognition and binding of *Mtb* having, e.g. ManLAM, PIMs or TDM as their mycobacterial ligands (Berrington & Hawn, 2007; Jo, 2008; Weiss & Schaible, 2015). DC-SIGN, MR, complement receptors and surfactant molecules are important in mediating the phagocytosis of *Mtb* (Schlesinger, 1993; Jo, 2008; Mayer-Barber & Barber, 2015). But as mycobacteria developed ways to reprogram the phagosome-lysosome fusion after infection, this mechanism does not lead to successful elimination of *Mtb*. For example, binding of mycobacterial ManLAM to MR (Kang et al., 2005) resp. PIMs to MR or DC-SIGN (Torrelles et al., 2006) limits phagocytosis. Further, AMs also produce the toxic antimicrobial effector molecules nitric oxide (NO) and reactive oxygen species (ROS) after activation in order to kill *Mtb* (Weiss & Schaible, 2015; Jamaati et al., 2017). Interaction of NO and ROS with the phagosome generates reactive intermediates, which are able to destroy mycobacterial structures, but again *Mtb* evolved mechanisms to counteract (Awuh & Flo, 2017).

The modality of macrophage cell death is influenced by *Mtb* and can vary after *Mtb* infection leading to different outcomes of disease (Mayer-Barber & Barber, 2015). Therefore, mycobacteria induce cytolysis and inhibit apoptosis (Behar et al., 2010), as the latter is associated with containment of bacteria and controlling of disease. Whereas a cytolytic cell death, like necrosis, can occur when the bacterial load of a macrophage reaches a critical number leading to dissemination of *Mtbs* and evasion from the innate immunity (Behar et al., 2010).

Further cells of the innate immune response are also relevantly associated with *Mtb* infection, but will not be further discussed here as they are not of particular interest for this work. Those are DCs (Rodrigues et al., 2020), NKT cells (Brill et al., 2001) and neutrophils (Borkute et al., 2021). The latter are linked to poor outcome in established tuberculosis disease (Lowe et al., 2013).

Recently also another part of the innate immune system has been under focus in tuberculosis research: trained immunity (Netea et al., 2020; Zhou et al., 2021). Reprogramming of the innate immune cells leads to some kind of innate memory response

after *Mtb* infection or vaccination with BCG (Cirovic et al., 2020; Scriba et al., 2020) with non-specific responses to reinfection and resulting in an improvement of disease outcome.

2.3.2 Adaptive immune response to *Mycobacterium tuberculosis*

Infection with *Mtb* does not only induce innate immune responses, but further cellular and humoral adaptive immunity. While T cell-mediated immunity is considered to be crucial for control of *Mtb* infection in humans (Jasenosky et al., 2015), the role of B cells and antibody-immunity has long been neglected (Li & Javid, 2018). Although this is changing recently, the focus of the following paragraphs will be on T cell mediated immunity as this was the focus of my work and only a short overview about B cells and antibodies in tuberculosis immune response will be given.

2.3.3 T cell response to Mycobacterium tuberculosis

Although not leading to sterile immunity, the T cell response is very critical in the control of mycobacterial infection (Winslow et al., 2008; Jasenosky et al., 2015). T cells can be differentiated between CD4 T helper (T_H) and cytotoxic CD8 T cells (Kleinsteuber, 2012). The latter kill infected cells trough production of cytotoxic proteins (Murphy, 2012). CD4 T cells are also able to exert cytotoxicity and kill intracellular bacteria (Mutis et al., 1993; Bastian et al., 2008). However, they are mainly known to express effector molecules (cytokines and chemokines), which activate macrophages and other immune cells and further, they provide help to B cells for expression of pathogen associated antibodies (Kleinsteuber, 2012; Murphy, 2012). Activation of T cells functions via special T cell receptors (TCR) and presentation through major histocompatibility complex (MHC) molecules I or II for peptide or CD1 molecules for lipid antigens (more on CD1 molecules in 2.3.4) (Porcelli et al., 1992; Murphy, 2012).

CD4 T cells can be further divided into T_H1, T_H2 and T_H17 cells being effector T cells producing effector molecules. T_H1 cells mainly target intracellular pathogens such as mycobacteria and activate macrophages via IFN-γ secretion, T_H2 cells mainly target parasites and lead to secretion of immunoglobulin E antibodies and T_H17 cells aim at extracellular pathogens via mucosal immunity using IL-17 as its effector molecule (Kolls & Khader, 2010; Kleinsteuber, 2012; Murphy, 2012).

After infection with *Mtb* T cells are activated in draining lymph nodes of the affected organs resp. regions and migrate back to the infection site, where they take part in granuloma formation (Lin & Flynn, 2015). The importance of CD4 T cell response in tuberculosis becomes especially clear in depletion models of CD4 T cells (Lin et al., 2012) or IFN-γ (Rossouw et al., 2003), as well as natural co-infections of humans with HIV. The infection leads to decreased numbers of CD4 T cells resulting in reactivation and progression of tuberculosis (Selwyn et al., 1989; Geldmacher et al., 2010; Bruchfeld et al., 2015). While CD4 T cells function against mycobacteria mainly depends on secreting of cytokines like IFN-γ, TNF-α or IL-2, CD8 T cells also use their cytolytic function via granule-mediated functions, induction of apoptosis (Lin & Flynn, 2015) or direct killing of *Mtb* via production of granulysin (Stenger et al., 1998).

2.3.4 CD1 molecules

As described in 2.2, mycobacteria have a lipid rich cell envelope. For T cells to recognize those mycobacterial lipid and glycolipid antigens they need to be presented via CD1 molecules (Beckman et al., 1994). After antigen presentation through CD1 molecules, T cells secret IFN-γ, can lyse infected macrophages, or kill bacteria directly (Stenger et al., 1998; Schaible & Kaufmann, 2000).
Information on every aspect of CD1 molecules, like molecular and cellular biology and their function in disease, have been extensively reviewed (Moody, 2007).

There are three groups/types of CD1 molecules in mammals. In humans group 1 includes CD1a, CD1b and CD1c, group 2 includes CD1d and group 3 includes CD1e (Moody, 2007). CD1 molecules are structurally similar to MHC I molecules (Porcelli et al., 1989; Calabi & Milstein, 2000). They are heterodimers consisting of an alpha-chain comprised of three domains noncovalently paired with β2-microglobulin (Figure 3) (De Libero & Mori, 2014). The antigens are bound in a deep hydrophobic antigen binding groove between the α1 and α2 domain (De Libero & Mori, 2014). Detailed conformation and binding grooves diversify between different CD1 subgroups. For example, CD1b has the largest binding groove composed of the A', C' and F' pocket and a T' tunnel (Gadola et al., 2002; Moody et al.,

2005). Therefore, lipid antigens with very long alkyl chains like MAs or PIMs can be bound by CD1b (Gadola et al., 2002; Garcia-Alles et al., 2011).
CD1 type 1 molecules are mainly expressed on APCs like Langerhans cells or granulocyte-macrophage colony-stimulating factor (GM-CSF)/ IL-4-induced monocyte-derived DCs (Schaible & Kaufmann, 2000), but also thymocytes, while CD1d has a broader distribution including further B cells, macrophages or epithelial cells (Moody, 2007).

Functionally, CD1 type 1 molecules have the role to present foreign lipid and glycolipid antigens, e.g. from mycobacteria, to T cells bearing αβ- or γδ-TCRs (Sugita & Brenner, 2000). Therefore, they broaden and elicit the function of the adaptive immune system to recognize and react to different pathogens with (glyco-)lipid antigens (Behar & Cardell, 2000; Sugita & Brenner, 2000).
On the other hand, CD1d molecules restrict either invariant NKT cells bearing a human Vα24Jα18-TCR or other T cells with a diverse non-invariant TCR repertoire (Behar & Cardell, 2000; De Libero & Mori, 2014).
CD1e molecules mainly have the function to process mycobacterial antigens like PIM_6, which then can be presented by other CD1 molecules to T cells (La Salle et al., 2005; Cala-De Paepe et al., 2012).

As CD1 molecules supposedly originated during vertebrate evolution, they are highly conserved between species (Dascher, 2007) and different subsets can be found in mammals, birds and reptiles (Yang et al., 2015). In mammals the number and panel of CD1 isoforms varies between species, so some express one gene for each CD1 subtype, while others might express more or none (Reinink & Van Rhijn, 2016). Mice for example, immunologists most used small animal model, naturally do not express CD1 type 1 molecules and therefore human CD1 transgenic mice have to be used to study the role of CD1 type 1 molecules (Felio et al., 2009). In contrast, guinea pigs naturally express a rich repertoire of CD1 type 1 molecules, including four CD1b and three CD1c molecules (Dascher et al., 1999), making them an ideal small animal model to study the role and importance of those molecules.

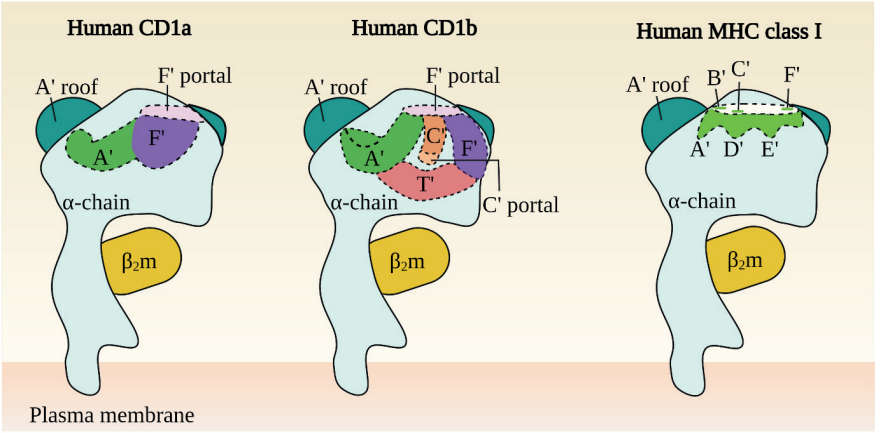

Figure 3: Model of human CD1 and MHC I molecules.

Depicted are two-dimensional structural schemes of human CD1a, CD1b and MHC I molecules with their grooves and pockets. Grooves of CD1 molecules are comprised of up to four pockets (A', C', F' and T'), which are deeper than those of MHC I molecules. Ligands can enter via the C' resp. F' portal. β_2-microglobulin (β_2m) is non-covalently paired to the α-chain. Adapted from (Moody et al., 2005) and created with BioRender.com.

2.3.5 B cell response to Mycobacterium tuberculosis

Although it has long been known that natural infection with *Mtb* induces the onset of B cell response and formation of antibodies, their function has been discussed controversially (Jacobs et al., 2016; Li & Javid, 2018).

When B cells are activated due to recognition of mycobacterial antigens, they clonally expand and differentiate into memory B cells (mBCs) and plasmablasts (Tangye & Tarlinton, 2009). Thus, leading to contemporary secretion of antibodies from plasmablasts and plasma cells. Further, mBCs can differentiate into antibody-secreting B cells (ASCs), when there is a restimulation with known mycobacterial antigens leading to a long-term memory response (Bernasconi et al., 2002). Those ASCs will then secrete antibodies upon stimulation.

Several studies could show that antibodies and memory B cells have a functional effect in *Mtb* infection. Individuals being highly exposed to mycobacteria, but not being infected, had titers of protective antibodies against tuberculosis (Li et al., 2017). Those antibodies

could then provide protection in an *in-vitro*- as well as a mouse model against infection with *Mtb* (Li et al., 2017). Also, the onset of *Mtb*-specific antibodies, IgG-secreting plasmablasts and mBCs could be detected after BCG vaccination (Bitencourt et al., 2021). That there is an important role for the Fc receptor in antibody mediated immunity could be observed (Lu et al., 2016), but further functions of the antibody response against tuberculosis are often speculative (Li & Javid, 2018) and need further research.

2.4 Bacillus Calmette-Guèrin (BCG)

In 2021 the 100th anniversary of the usage of BCG was celebrated. The live-attenuated vaccine strain had been developed during the first world war and was first administered to a human on July 18th 1921 (Singh et al., 2021). Since then, several billion doses have been administered to humans for tuberculosis prevention. BCG is still regularly used in over 120 countries with high tuberculosis incidences, where vaccination programs reach over 90 % of infants (World Health Organization, 2018). Hence they are protected against severe childhood tuberculosis including meningitis and miliary tuberculosis (Rodrigues et al., 1993). Adverse effects like erythema, induration, abscesses, ulceration or local lymphadenitis occur relatively frequent (Dommergues et al., 2009), while severe adverse effects like BCGitis or BCGosis (lymphadenitis and osteitis/osteomyelitis) especially affect immunocompromised, such as HIV-infected children (Yamazaki-Nakashimada et al., 2020). Although, the vaccine reliably protects from severe forms of tuberculosis during early childhood, it does not protect sufficiently against the epidemiologically most relevant lung manifestation, and no other effective vaccine against tuberculosis has been developed so far (Ahmed et al., 2021). Besides usage against mycobacterial infection, BCG is also established as immunotherapy against bladder cancer (Pettenati & Ingersoll, 2018) and discussed in different nontraditional usage approaches (Singh et al., 2021). For its capacity to induce proinflammatory T cell responses as well as trained immunity, its effect against different kinds of non-bladder cancer (Grange & Stanford, 1990; Morra et al., 2017), other respiratory diseases than tuberculosis (Leentjens et al., 2015) including COVID-19 (Berg et al., 2020; Netea et al., 2021) or immunologic diseases like type 1 diabetes or multiple sclerosis is considered (Huppmann et al., 2005; Ristori et al., 2018).

BCG was developed by the physician Albert Calmette and the veterinarian Camille Guèrin at the institute Pasteur in Lille, France (Ahmed et al., 2021). By passaging virulent *M. bovis* 230 times from 1908 to 1921 they succeeded to establish the attenuated vaccine strain BCG (Figure 4). The strain has a very good safety profile (Luca & Mihaescu, 2013) and its' innocuousness was declared by the Health Committee of the League of nations in 1928 (Calmette, 1931). Until 1961, the original BCG Pasteur strain had been *in vitro* passaged 1173 times. A masterseed was established from this material and lyophilized. This resulted in the "BCG Pasteur 1173" strain, which was used in our studies. But also, other laboratories and institutes throughout the world were using and passaging the original BCG strain leading to a total number of 49 BCG substrains today (Behr & Small, 1999; Corbel et al., 2004), of which 14 are currently used as vaccines (Abdallah et al., 2015). Compared to the original strain and each other, they all show genetic differences leading to biochemical, morphological and immunological uniqueness (Abdallah et al., 2015; Kaufmann, 2016). Besides the genetic background and immune status of vaccinated people and the BCG substrain used, also culture conditions can modify the efficacy of BCG vaccination (Abdallah et al., 2015; Guallar-Garrido et al., 2021).

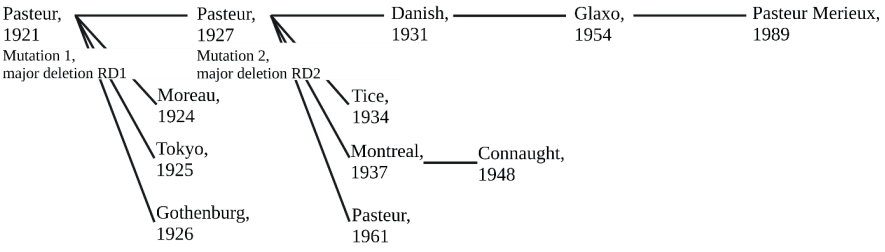

Figure 4: Genealogical tree of BCG vaccine.
All substrains originate from the *M. bovis* BCG Pasteur from 1921. Adapted from (Oettinger et al., 1999) and created with BioRender.com.

2.5 Cationic adjuvant formulation no. 1 (CAF01)

Mycobacteria are intracellular pathogens, which have to be addressed by vaccinations, but are not reachable for antibody approaches. Therefore, it is important that tuberculosis vaccines are able to induce a T cell response. As the role of adjuvants is to enhance the immune response to vaccines, but most common used adjuvants like alum have only major

effects on the humoral immune response (Oleszycka & Lavelle, 2014), they are not suitable for tuberculosis vaccine approaches.

The Statens Serum Institute (Copenhagen, Denmark) was screening for potential adjuvant formulations to find an adjuvant, which could mediate a strong cell-mediated immune response to be used in a tuberculosis vaccine. In this approach they developed the cationic adjuvant formulation no. 1 (CAF01), which is based on cationic liposomes using incorporated mycobacterial pathogen-associated molecular patterns as immunomodulators (Christensen et al., 2009). In CAF01 N',N'-dimethyl-N',N'-dioctadecylammonium bromide (DDA) is used as the antigen delivery system and α,α'-trehalose-6,6'-dibehenate (TDB) as an immunostimulatory (Figure 5). As DDA has a polar head as well as a hydrophobic element it is amphiphilic and dispersible in water. When heated above 47°C it forms lipid bilayers (Christensen et al., 2009) and its features as an immunological adjuvant are well described (Hilgers & Snippe, 1992). TDB is a synthetic, detoxified analogue of TDM (cord factor), making it suitable for vaccine usage because of the decreased size (Christensen, 2017). TDM is, as the cord factor and a MA from the mycobacterial membrane, the key pathogenicity factor and a strong immunomodulator of *Mtb* (Lima et al., 2001). TDM is recognized by and stimulating the CLR Mincle, inducing strong T_H1 and T_H17 immune responses (Huber et al., 2020). Therefore, vaccination with CAF01 induces a strong CD4 T cell response with high levels of TNF-α and IFN-γ (Lindenstrøm et al., 2009), as well as high IL-17 responses (Lindenstrøm et al., 2012), which are all well maintained for over one year.

CAF01 has been tested in different vaccine approaches for some respiratory tract infections such as influenza (Christensen et al., 2017; López-Serrano et al., 2021), tuberculosis (Clemmensen et al., 2021), or COVID-19 (Wørzner et al., 2021) and showed good induction of T cell responses independent of the used animal models. CAF01 in combination with a trivalent influenza split-virion resulted in reduced viral shedding and disease symptoms in ferrets, while local inflammation was not reduced in the nasal cavity (Christensen et al., 2017).

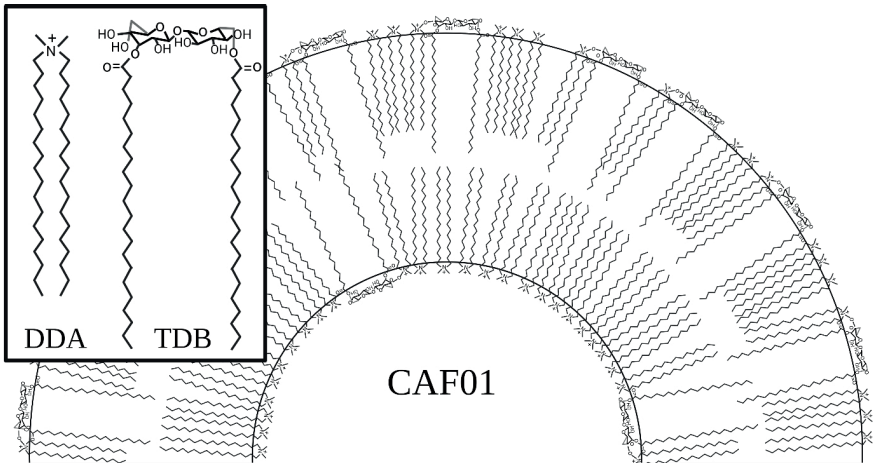

Figure 5: Structural model of a CAF01 liposome.
CAF01 is comprised of N',N'-dimethyl-N',N'-dioctadecylammonium bromide (DDA) and α,α'-trehalose-6,6'-dibehenate (TDB). Adapted from (Christensen, 2017; Pedersen et al., 2018) and created with BioRender.com.

The novel influenza vaccine candidate NG34 HA1 adjuvanted with CAF01 tested in a challenge trial in the pig resulted in reduced pathology and abolished viral load in the lower respiratory tract (López-Serrano et al., 2021). When CAF01 was used to adjuvant the SARS-CoV-2 pre-fusion stabilized spike protein in a mouse model, it induced neutralizing antibodies, but also further elicited CD4 T helper cell response with increased levels of IFN-γ and IL-17 in contrast to other tested adjuvant systems (Wørzner et al., 2021).

Woodworth et al. co-administered BCG with a *Mtb*-specific subunit vaccine (H107), which was composed of antigens not shared with BCG and adjuvanted with CAF01. This resulted in a synergistic vaccine effect with an increased adaptive response (Woodworth et al., 2021). When CAF01 was compared to other adjuvants, its positive effect on eliciting the CD4 T cell response with T_H1/T_H17 character could be demonstrated in different studies, and highlights, how important the right choice of adjuvant depending on the induced immune profile can be (Ciabattini et al., 2016; Knudsen et al., 2016).

Besides CAF01 there are further cationic adjuvant formulations (CAFs) developed, which all use DDA -in two cases combined with squalene- as the delivery system, but combined with different immunostimulators depending on the usage (Pedersen et al., 2018).

2.6 Treatment of tuberculosis

Table 1: First line drugs against tuberculosis.
Adapted from (Vilchèze, 2020) and created with BioRender.com.

Name	Structure	Target
Isoniazid (INH)	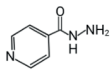	Mycolic Acids
Rifampicin (RIF)	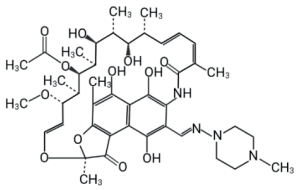	DNA dependent RNA polymerase
Ethambutol (EMB)	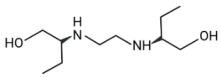	Arabinogalactan, Lipoarabinomannan
Pyrazinamid (PZA)	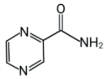	unclear

Since mycobacteria are causing tuberculosis in humans since centuries (Barberis et al., 2017), uncountable numbers of people suffered and died from the so called consumption, lacking sufficient treatment against the fatal disease.

A first approach to cure tuberculosis were treatments at special sanatoria for pulmonary patients in the late 19th and early 20th century first developed in Germany and then spreading to UK, USA and other countries (Daniel, 2006, 2011). The strategy of this regimens included strict rest of mind and body, preferential in open air at any weather conditions and a rich diet (Hurt, 2004), literarily depicted by Thomas Mann in his novel “Der Zauberberg”. The combination of fresh air, increased production of Vitamin D3 through higher UV-irradiation in higher altitudes, modest physical training and healthy diet often induced improvement of patients’ immune system and health (Barberis et al., 2017; Woelke, 2020).

The first real game changer in tuberculosis treatment was the development of antibiotics with antimycobacterial activity. In 1944, streptomycin, isolated from the bacterium *Streptomyces griseus*, was detected to be effective against mycobacteria (Schatz & Waksman, 1944). It was very effective in treatment of tuberculosis, also in advanced forms

of pulmonary tuberculosis, but it didn't take long before streptomycin-resistant strains of *Mtb* evolved (Hinshaw et al., 1947). In combination with para-aminosalicylic acid, another drug with antimycobacterial activity first tested against tuberculosis in 1946 (Lehmann, 1946), the resistance was reduced ("Treatment of Pulmonary Tuberculosis with Streptomycin and Para-Aminosalicylic Acid," 1950), but not overcome. More successful was the introduction of isoniazid (INH) as an anti-tuberculosis drug in 1952 (Vilchèze, 2020). INH targets and blocks the biosynthesis of MAs and therefore the mycobacterial cell wall leading to mycobacterial cell death (Takayama et al., 1972; Vilchèze & Jacobs, 2007). Today, INH is still used as a first line drug against active and latent tuberculosis. The standard treatment regimen against drug-sensitive tuberculosis using the four first line drugs (Table 1) currently consist of a two-month combination of rifampicin (RIF), INH, pyrazinamide (PZA) and ethambutol (EMB) followed by a four-month phase of RIF and INH (Kumar & Kon, 2017). While EMB targets the mycobacterial cell wall synthesis just like INH, RIF targets the RNA polymerase RpoB and the mechanism of PZA is still unknown (Vilchèze, 2020). Although, those drugs with antimycobacterial activity could heal millions of people from tuberculosis in the last 70 years, the increase of resistant mycobacteria are a major threat in the fight against tuberculosis.

2.6.1 Resistant tuberculosis

Since streptomycin has been first used as an antibiotic to treat tuberculosis, mycobacteria resistant to these drugs have been evolving (Hinshaw et al., 1947). Since the 1990s the problem gets more and more relevant (Matteelli et al., 2014) and it can be mainly differentiated between drug-sensitive tuberculosis, RR-tuberculosis, MDR-tuberculosis and XDR-tuberculosis. Also cases of total drug-resistant tuberculosis occur, where none of the used drugs show an effective antimycobacterial activity anymore (Dheda et al., 2014). MDR *Mtb* are resistant to the first-line drugs RIF and INH (Vilchèze, 2020), while XDR-tuberculosis is described as a *Mtb*-strain, which is not only MDR, but shows further resistance to fluoroquinolones and any of the second-line injectable drugs (Table 2) (Matteelli et al., 2014).

Table 2: Grouping of medicines recommended for use in longer MDR-TB regimens. Adapted from (World Health Organization, 2022) and created with BioRender.com.

Group	Steps	Drug
A	Include all three medicines	Levofloxacin / moxifloxacin Bedaquiline Linezolid
B	Add one or both medicines	Clofazimine Cycloserine / terizidone
C	Add to complete the regimen and when medicines from Groups A and B cannot be used	Ethambutol Delamanid Pyrazinamide Imipenem-cilastatin / meropenem Amikacin / (streptomycin) Ethionamide / prothionamide *p*-aminosalicylic acid

In 2019, already 3.3 % of newly treated and 17.7 % of previously treated tuberculosis patients were positive for RR-/MDR-tuberculosis (World Health Organization, 2020). Especially countries of the former Soviet Union are affected (Cox et al., 2004; Merker et al., 2018).

Main reasons for the increasing occurrence of resistances besides poverty, deficient supply of drugs and care of affected populations, are often also lacking compliance of patients (Balabanova et al., 2004; Matteelli et al., 2014; Evangelopoulos & McHugh, 2015). The long and complicated duration of treatment and adverse effects of anti-tuberculosis drugs make incorrect use easy and the strongest risk factor for development of RR-/MDR-tuberculosis (Migliori et al., 2012). The list of possible adverse effects from the first line drugs against tuberculosis is long including hepatitis, gastrointestinal disturbances, peripheral neuropathy, photosensitive dermatitis or optic neuritis (Kumar & Kon, 2017). Therefore, not only effective new drugs or drug regimens are needed for the future, but also shorter treatments and less adverse effects would be major advantages.

In recent years, many new anti-tuberculosis drugs and drug regimens are in the process of development and testing (World Health Organization, 2021). Many of these drugs target the mycobacterial cell envelope with its importance for *Mtb,* and its complexity offers different possibilities to encounter and kill the bacteria (Vilchèze, 2020). But also, the

RNA-, DNA-, ATP- or protein synthesis, as well as further mechanisms of mycobacteria are targeted by emerging drugs (Angula et al., 2021).

Mycobacteria have the capacity to shut down their own metabolism and terminate replication entering the so-called dormancy (Gengenbacher & Kaufmann, 2012; Peddireddy et al., 2017). In this stadium they are extremely resistant to drug treatment. Therefore, resuscitation-promoting factors (Rpfs) or dormancy survival regulator (DosR) genes, which are involved in reactivation of dormant mycobacteria could be used as drug targets to reactivate mycobacteria and make them responsive to classical antimycobacterial drugs (Peddireddy et al., 2017).

Modern approaches to develop new drugs against and tackle resistant tuberculosis give hope to slow down and decrease the emergence of resistant tuberculosis cases.

2.6.2 BTZ-043

Table 3: Structure and target of the anti-tuberculosis drug BTZ-043.
Adapted from (Vilchèze, 2020) and created with BioRender.com.

Name	Structure	Target
BTZ-043	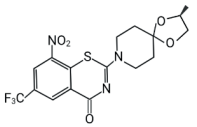	Arabinogalactan, Lipoarabinomannan via DprE1

The benzothiazinone BTZ-043 is one of the new anti-tuberculosis drugs in the global clinical development pipeline currently tested in a Phase I study corresponding to the WHO (World Health Organization, 2021), respectively in a Phase II study corresponding to the German Centre for infection research (DZIF, 2022). It was first suggested as a drug with antimycobacterial activity in 2009 (Makarov et al., 2009).

It is known that BTZ-043 has a very low minimal inhibitory concentration (MIC) and great efficacy *in vitro* against different mycobacteria and *Nocardia brasiliensis* (Makarov et al., 2014; González-Martínez et al., 2015; Gao et al., 2016). Neither in BALB/c mice after acute (5 g/kg) or perpetuated (25 & 250 mg/kg) application (Makarov et al., 2014), nor in genotoxicity and mutagenicity studies with rats BTZ-043 induced any observable negative or adverse effects (Working Group for New tuberculosis Drugs, 2022).

It can also be used in combined drug regimens with other anti-tuberculosis drugs as benzothiazinones induce convincing additive effects with RIF, EMB or INH or synergistic effect with Bedaquillin *in vitro* (Lechartier et al., 2012) and *in vivo* (Makarov et al., 2014).

Like INH and other anti-tuberculosis drugs, BTZ-043 also targets and inhibits the *Mtb* cell wall-synthesis leading to cell lysis and mycobacterial death (Makarov et al., 2009). In detail, BTZ-043 binds covalently to the mycobacterial decaprenyl-phosphoribose-2'-epimerase (DprE1) and blocks it irreversibly (Neres et al., 2012; Trefzer et al., 2012). This results in prevention of formation of mycobacterial cell-wall arabinans, as it is necessary for the composition of arabinofuranose, a constituent of arabinomannan and -galactan (Neres et al., 2012; Trefzer et al., 2012; NCATS Inxight Drugs, 2022). As this mechanism is highly selective for mycobacteria, it does not affect bacteria of the gut microbiota, preventing disturbances of the gastrointestinal tract (NCATS Inxight Drugs, 2022).

Point mutations at the Cys387 position of DprE1 strongly increase the MIC of BTZ-043 and could result in resistance of mycobacteria against BTZ-043 (Makarov et al., 2009; Vilchèze, 2020). So far, however, all 240 clinical isolates of drug-sensitive and MDR-*Mtb* from European hospitals tested for mutations and resistance against BTZ-043 were consistently susceptible (Pasca et al., 2010).

2.7 The guinea pig as a small animal model for tuberculosis

Guinea pigs (*Cavia porcellus*) have been used by Robert Koch in the detection of and research on tuberculosis (Koch, 1882, 1891) and also Calmette and Guérin used these rodents in the development of BCG over hundred years ago (Calmette, 1931; Luca & Mihaescu, 2013). However, even before the discovery of mycobacteria as the causative agent of tuberculosis, guinea pigs were used as an animal model for it (Fox, 1868) and continue to be used today (Bobak et al., 2022).

Guinea pigs are naturally susceptible to *Mtb* (Dharmadhikari et al., 2011) and upon *Mtb* infection develop a similar pathology as seen in humans (Smith et al., 1970; Wiegeshaus et al., 1970; Ho et al., 1978). Granuloma formation, caseation, encapsulation and mineralization as well as forming of primary lesions and dissemination are comparable between human and guinea pig tuberculosis (McMurray, 2014; Orme & Basaraba, 2014).

One big difference is that guinea pigs lack a phase of real latency, an important feature of human tuberculosis (Sakamoto, 2012). A further disadvantage is the limited range of immunological reagents available for guinea pigs (Young, 2009), although in the last years some guinea pig specific antibodies have been developed (Schäfer & Burger, 2012; Banasik et al., 2019) making immunological analyses easier. Nevertheless, guinea pigs are successfully used to investigate the immune response to tuberculosis (Ordway et al., 2007; Clark et al., 2014). Hence, it could be detected, that they express a functional CD1 type 1-system (Dascher et al., 1999; Hiromatsu et al., 2002), which allows for investigation of the T cell response specific for mycobacterial lipid antigens. A detailed summary on the guinea pig as a model for human CD1 type 1 protein function is part of this dissertation (**publication I**).

Guinea pigs have to be used according to the European pharmacopoeia to test tuberculin batches (European Directorate for the Quality of Medicine and Health Care, 2020), because they show a delayed type hypersensitivity reaction after sensitization with tuberculin (Ladefoged et al., 1976). Therefore, a tuberculin skin test is performed to assess the quality of a tuberculin test batch in comparison with a standard tuberculin in a so-called batch potency test.

Guinea pigs are also suitable and frequently used as a small mammalian model for vaccine efficacy evaluation (Gong et al., 2020) and *Mtb* virulence testing (Palanisamy et al., 2008) and there are some standard protocols suggested to obtain consistent data, when using guinea pigs (Creissen et al., 2021). For evaluation, mainly pathological scoring, determination of CFU scores or survival is used. The immunopathogenesis of granulomas in the guinea pig after *Mtb* infection is well described and therefore, staging of granulomas can also be used as a further assessment criterion (Turner et al., 2003).

For the same reasons, guinea pigs are also a good animal model for anti-tuberculosis drug testing (Basaraba, 2008; Yang et al., 2021). Especially, for testing of drugs on persisting mycobacteria in hypoxic areas of the granuloma they are exceptionally suitable (Lenaerts et al., 2007) and exceed mouse models (Yang et al., 2021).

Furthermore, guinea pigs are well-suited to study comorbidity of tuberculosis with other diseases such as diabetes (Podell et al., 2014).

3 Publications

(I) Animal models for human group 1 CD1 protein function

Emmelie Eckhardt, Max Bastian

Molecular Immunology (130), S.159-163

DOI: 10.1016/j.molimm.2020.12.018.

Molecular Immunology 130 (2021) 159–163

Contents lists available at ScienceDirect

Molecular Immunology

journal homepage: www.elsevier.com/locate/molimm

Animal models for human group 1 CD1 protein function

Emmelie Eckhardt, Max Bastian *

Friedrich-Loeffler-Institut, Suedufer 10, 17493 Greifswald – Insel Riems, Germany

ARTICLE INFO

Keywords:
Group 1 CD1
Lipid antigens
T cells
Animal models

ABSTRACT

The CD1 antigen presenting system is evolutionary conserved and found in mammals, birds and reptiles. Humans express five isoforms, of which CD1a, CD1b and CD1c represent the group 1 CD1-molecules. They are recognized by T cells that express diverse αβ-T cell receptors. Investigation of the role of group 1 CD1 function has been hampered by the fact that CD1a, CD1b and CD1c are not expressed by mice. However, other animals, such as guinea pigs or cattle, serve as alternative models and have established basic aspects of CD1-dependent, antimicrobial immune functions. Group 1 CD1 transgenic mouse models became available about ten years ago. In a series of seminal studies these mouse models coined the mechanistical understanding of the role of the corresponding CD1 restricted T cell responses. This review gives a short overview of available animal studies and the lessons that have been and still can be learned.

1. Introduction

In 1979 Andrew Mc Michael and colleagues published a monoclonal antibody that had been raised against human thymocytes (McMichael et al., 1979). Five years later at the "First International Workshop on Human Leukocyte Differentiation Antigens" this antibody ended up first in the list (Bernard and Boumsell, 1984). The surface molecule that the antibody binds to is now known as CD1a. Forty years later we know a lot about the first cluster of differentiation antigens: CD1a belongs to a family of proteins that is comprised of three subgroups. In humans, CD1a, CD1b and CD1c form group 1, CD1d represents the group 2 isoform, and the non-membrane bound CD1e is separated into group 3.

The type 1 group antigens are expressed early during thymocyte development (Blue et al., 1989) and they are functionally expressed on professional antigen presenting cells (Dougan et al., 2007). Group 1 isoforms differ in their intracellular trafficking, with CD1b, CD1c and CD1d recycling to the endosomal network to varying extents (Moody and Porcelli, 2003). We have understood that group 1 CD1 proteins present antigens to CD1-restricted T cells (Porcelli et al., 1989) and we know a large and highly diverse number of lipid antigens. The first CD1-restricted lipid ligands were identified from bacterial pathogens, and many of known antigens are of mycobacterial origin. Mycobacteria express a particularly rich repertoire of glycolipids, lipoglycans, lipopeptides and waxes, all of which represent or harbor potential CD1-ligands (Minnikin et al., 2002). But, in part, this may also be linked to the fact that some of the early work had a professional bias towards acid fast bacteria (Sieling et al., 1995), because also in gram-negative and gram-positive bacteria lipid ligands have been identified (Fairhurst et al., 1998; Visvabharathy et al., 2020).

Beside microbial ligands there have been descriptions of allergic hypersensitivity agents that activate CD1a-restricted T cells in the skin (Agea et al., 2005; Kim et al., 2016; Nicolai et al., 2020) and most importantly it became clear that also endogenous lipid ligands can stimulate CD1-restricted T cells (de Jong et al., 2014d; Kim et al., 2016; Mansour et al., 2016; Roura-Mir and Moody, 2003; Shamshiev et al., 1999; Van Rhijn et al., 2016). The mechanisms how these antigens are loaded into the hydrophobic cavities of the CD1-molecules are understood in some detail, where lipid binding proteins and low pH can promote loading (Cala-De Paepe et al., 2012; de la Salle et al., 2005d; van den Elzen et al., 2005v; Winau et al., 2004). There is a large number of high resolution crystal structures that illuminate our notion of how the lipidic content is accommodated and how the cognate T cell receptor (TCR) interacts with the lipid epitope complexed to the CD1-molecule [reviewed in: (Moody et al., 2005; Shahine, 2018; Zajonc, 2016)], and interesting observations have been made regarding the semi-invariant TCR usage of CD1-restricted T cells (Kasmar et al., 2011; Van Rhijn et al., 2013; van Schaik et al., 2014v).

However, when it comes to understanding the unique functional role

Abbreviations: BCG, Bacille Calmette Guerin; GMM, glucose monomycolate; MA, mycolic acid; ManLAM, mannosylated lipoarabinomannan; PIM, phosphatidylinsositol mannoside; TCR, T cell receptor; TLR, toll-like receptor.

* Corresponding author.
E-mail address: max.bastian@fli.de (M. Bastian).

https://doi.org/10.1016/j.molimm.2020.12.018
Received 11 November 2020; Accepted 9 December 2020
Available online 29 December 2020
0161-5890/© 2020 Elsevier Ltd. All rights reserved.

of CD1a, CD1b and CD1c in antimicrobial defense or immune homeostasis the picture becomes less clear. It has been calculated that up to 10 % of circulating peripheral blood lymphocytes are CD1 type 1 restricted and self-reactive (de Lalla et al., 2011d). Yet, what is their role? CD1a is constitutively expressed on Langerhans cells. In line with that, skin homing T cells recognize endogenous lipids in the context of CD1a under physiological conditions and this may contribute to the orchestration of barrier immunity (de Jong et al., 2010d). But what about the others? What about CD1b-restricted cells that recognize microbial lipids? There were reports that human CD1-restricted T cells have the capacity to identify infected cells and kill intracellular mycobacteria by granule exocytosis of granulysin (Stenger et al., 1998, 1997), but it was later found that this is not an exclusive feature of CD1-restricted cells (Bastian et al., 2008; Dieli et al., 2001; Gansert et al., 2003; Obata-Onai et al., 2002; Sun et al., 2002). Besides, it has never been clearly answered how the cells might encounter their cognate epitope, because macrophages as the main host cell for intracellular mycobacteria do not express CD1b and CD1 expressing cells are sparsely distributed in the tuberculous granuloma, so a mechanism would presumably require antigen shedding or transfer (Randhawa, 1990). So, what are the immunological roles of group 1 CD1 *in vivo*?

2. Animal models for group 1 CD1 function

Answering that question has been hampered by the fact that mice, the immunologists' top animal model, naturally do not express type 1 CD1-molecules. The absence of a functional type 1 CD1 system is a curio of mice and rats, because the CD1 system is phylogenetically very old and all mammals except muroid rodents have large CD1 gene families. CD1 is found in birds, reptiles and mammals, and it has been hypothesized that the genes evolved about 380 million years ago when first tetrapods appeared and are documented in the fossil record (Dascher, 2007). It seems that the early CD1-molecules resembled CD1a, because a homolog of CD1a is the form still found in chickens (Miller et al., 2005) and reptiles (Yang et al., 2015), whereas a rich and diverse panel of several isoforms is found in mammals (S. A. Porcelli and Modlin, 1999). Rabbits for example express two CD1a and one CD1b isoform (Hayes and Knight, 2001), dogs harbor four CD1a, one CD1b and one CD1c molecule, while cattle bear two functional CD1a and three CD1b genes (Nguyen et al., 2015).

3. The guinea pig

Guinea pigs express a rich repertoire of four CD1b and three CD1c isoforms (Dascher et al., 1999), and at least one CD1a-like gene is found in the genome, although it is not entirely clear, whether this one is functionally expressed. Guinea pigs served as the first animal model to investigate the functional role of the CD1 group 1 system. Interestingly, it was described that of the four gpCD1b isoforms, CD1b3 lacks a cytoplasmic targeting signal that is present in human CD1b and CD1c but not CD1a, and which directs the molecules to the endosomal compartment (Dascher et al., 1999). It was later confirmed that CD1b1 colocalizes with MHC-II and a mycobacterial lipoglycan in the late endosomal compartment, while CD1b3 remains at the surface of antigen presenting cells (Dascher et al., 2002). Using specific monoclonal antibodies that distinguish between the isoforms, a particular tissue distribution was observed. For example, while CD1b1 expression is abundant in the thymus, it is relatively scarce in peripheral tissues. By contrast, CD1b3 is widely expressed both on skin resident dendritic-like cells (Dascher et al., 1999) and on circulating but not germinal center B cells (Hiromatsu et al., 2002b).

Guinea pigs have long been used as an animal model in tuberculosis research: Robert Koch and Albert Calmette made use of their high natural susceptibility to mycobacteria (Calmette et al., 1926; Koch, 1882). Hence, direct evidence for a functional role of CD1-molecules came from studies in which guinea pigs were immunized with purified mycobacterial lipids. Liposomes were spiked with a mixture of mycobacterial lipids and used to immunize Dunkin-Hartley guinea pigs. Only when the liposomes were combined with either MPL or QS-21 as adjuvants, mycobacterial lipid specific T cells were induced (Hiromatsu et al., 2002a). Although *ex vivo* guinea pig T cell responses to mycobacterial lipid preparations may in part be directed to MHC-II restricted lipidic peptides (Kaufmann et al., 2016), Hiromatsu confirmed CD1-restriction for a CD8-positive T cell line. In cytotoxicity assays, fibroblasts transfected with individual CD1 isoforms were used as target cells and lysis was observed with CD1b1, CD1b2 and also CD1c3, but not with CD1b3 (Hiromatsu et al., 2002a). When combined with peptides, lipid antigen immunization conferred some protection from mycobacterial challenge and reduction in lung lesion size (Dascher et al., 2003). Again, some protection was observed with guinea pigs that had been immunized with liposomes containing purified diacylated-sulfoglycolipid (Ac2SGL) and phosphatidylinositol-dimannoside (PIM2) (Larrouy-Maumus et al., 2017). In an ongoing study from our group presented at the EMBO CD1-MR1 Conference at Oxford, we provide evidence that the phosphatidylinositol-dimannoside induces immune protection, because after virulent mycobacterial challenge we observed significant T cell responses to a synthetic diacylated-phosphatidylinositol-dimannoside (Ac2PIM2) only in PIM vaccinated but not in mock immunized animals. Vaccinated guinea pigs showed a significant 10-fold reduction in CFU counts and significant reduction in pathology scores.

Group CD1 proteins have low expression in uninflamed tissues, but are inducible *in vitro* (Roura-Mir et al., 2005), and CD1b has been reported in human TB lung granulomas (Chancellor et al., 2017). We are currently investigating the transcription pattern of guinea pig CD1 isoforms in mycobacteria infected tissues, and there is a clear tendency that after virulent challenge, type 1 CD1-expression is elevated in the tuberculous lesion and the corresponding lymph node of protected BCG-vaccinated guinea pigs, compared to mock vaccinated animals. Preliminary *in-situ* hybridization data shows the same tendency (Schinköthe et al., 2019), but it also confirms early reports indicating that CD1-expressing cells are sparsely distributed in human tuberculous granulomas (Chancellor et al., 2017; Randhawa, 1990). Although this may indicate that the timely secretion of macrophage activating cytokines by CD1-restricted T cells contributes to an early control of invading mycobacteria, a comprehensive mechanistical explanation of CD1-restricted immune protection in the guinea pig is still lacking.

4. The bovine model

Another animal that has gained interest in the CD1 field due to its relevance for TB research is the bovine model. Cattle are the natural host for *Mycobacterium bovis*. Although veterinarians have eradicated bovine tuberculosis in many parts of the world through rigorous test-and-cull strategies, the disease has regained attention also in western industrialized countries due to uncontrolled wildlife reservoirs (Domogalla et al., 2013; Drewe et al., 2013; Nugent et al., 2015). Cattle have two functional CD1a and three CD1b isoforms that are differentially expressed on afferent dendritic cells (DCs), lymph node cells or peripheral blood mononuclear cells (Nguyen et al., 2015). As with guinea pigs, vaccination of calves with purified mycobacterial lipids can elicit lipid-specific T cell responses, and mycobacterial glucose monomycolate-specific T cell response could be blocked using a CD1b-blocking antibody (Nguyen et al., 2009). By comparing cattle that were either infected with *M. bovis* (Mbov), a mycobacterium that is closely related to *M. tuberculosis*, or with *M. avium* ssp. paratuberculosis (Map), the causative agent of Johne's disease, it could be demonstrated that both groups readily respond to the corresponding microbial lipid antigens. Interestingly, it was found that Map-infected animals prominently responded to CD1-restricted glucose-monomycolate. Mbov-infected animals were instead stimulated by an unidentified hydrophilic lipid. Although GMM is present in both mycobacteria and shares an identical hydrophilic head group, there was little cross-reactivity between the two groups of animals (Van Rhijn et al., 2009). For veterinarians these findings are interesting, because they open

new avenues for diagnosis and eventually prevention of zoonotic mycobacterial diseases of livestock animals. However, in terms of a mechanistical insight into the function of the CD1-T cell axis, further studies in the cattle model are required.

5. Human CD1 transgenic mice

In 2009 Chyung-Ru Wang's group published a transgenic mouse that carried the entire coding region of human CD1A, CD1B, CD1C and CD1E, including candidate promoters and all open reading frames along with 5′ and 3′ flanking sequences (Felio et al., 2009). The expression pattern of the various CD1-molecules resembled that of human group 1 CD1-molecules. While high expression of CD1a, CD1b and CD1c was observed on thymocytes, in the periphery CD1a was predominantly expressed on skin Langerhans cells, and CD1b was seen to some degree on lymph node dendritic cells. CD1c was abundantly found on B cells and some DC populations, as also seen in humans. As in humans, robust expression of group 1 CD1 was found on *ex vivo* generated DCs. When mice were vaccinated with transgenic DCs pulsed with mycobacterial lipids or were infected either with live-attenuated BCG or virulent *M. tuberculosis*, *ex vivo* CD1-restricted T cell responses to the corresponding mycobacterial lipids could be demonstrated, although the level of reactivity was relatively low. Accordingly, a majority of CD1-restricted T cell lines generated from lipid vaccinated mice were autoreactive. Of 17 T cell lines that are described in this first seminal paper only one was specific for mycobacterial lipids (Felio et al., 2009). Since 2009, Wang and colleagues published a series of papers in which the role of group 1 restricted T cells was further addressed. Using double transgenic mice that carried a CD1b-restricted, mycolic-acid (MA) specific T cell receptor (TCR) in addition to the group 1 CD1-transgene, they could demonstrate that the CD1-restricted T cells are primed in the mediastinal lymph node upon mycobacterial aerosol challenge. Adoptively transferred, MA-specific T cells conferred protection, albeit only a bacterial load reduction of 0.5 $\log_{10}$ was seen (Zhao et al., 2015). The same model was later used to refine the technique of lipid immunization. Using self-assembling PPG-PPS-nanoparticles as carriers for mycobacterial MA, a vaccination vehicle was generated that induced pulmonary, MA-specific T cell responses after intranasal administration (Shang et al., 2018). Using the same transgenic mouse model, very recently a protective effect of CD1-restricted T cells could also be demonstrated against *Staphylococcus aureus*-infections (Visvabharathy et al., 2020).

Conceptionally interesting was also another study, in which the group addressed a phenomenon that was originally observed by Gennaro De Libero. In 2005 he had described that CD1-restricted, autoreactive T cells show elevated reactivity when CD1-expressing APCs are exposed to bacterial danger signals, such as Toll-Receptor-ligands (De Libero et al., 2005). Along that line a double transgenic mouse line was established that expressed an autoreactive, CD1b-restricted TCR along with the human CD1-transgene. A basal T cell mediated autoreactivity was enhanced by TLR-stimulation, and this protected from *Listeria monocytogenes*-infection (Li et al., 2011). So, apart from the direct cognate interaction with specific microbial derived lipids, the modulation of CD1 protein expression could elicit CD1 autoreactive T cells, which could either be protective of pathogenic depending on the disease context.

In considering self-lipid antigen induced autoimmunity, double transgenic mice carrying a CD1b-restricted autoreactive TCR together with the human CD1b-transgene spontaneously developed a severe, psoriasis-like skin inflammation, when lipid metabolism was perturbated by an additional Apoliprotein-E-deficiency that causes phospholipid deposition in skin (Bagchi et al., 2017). This outcome matched certain predictions of human studies published in parallel, where CD1b autoreactive T cells could be identified in the blood, and the molecular basis for autorecognition could be accounted for by direct contact of TCRs of phospholipids presented on CD1b (Shahine et al., 2017). Another transgenic mouse model expressing human CD1a was independently established by the Sugita group (Kobayashi et al., 2012). This model helped to explain poison-ivy dermatitis, which is caused by plant derived lipids, where the presence of human CD1a and CD1a autoreactive T cells strongly promote inflammation (Kim et al., 2016).

Anti-tumor reactivity complements the breadth of immune functions that can be exerted by CD1-restricted T cells. An anti-tumor activity has been described for autoreactive CD1b-restricted T cells (Bagchi et al., 2016). Recently a T cell retargeting approach has been proposed as a therapeutic intervention against CD1c-expressing primary acute myelogenous and B-lymphoblastic leukemia blasts. The transduction of the corresponding CD1c-reactive T cell receptor into mature mouse T cells or iNKT cells lead to the *in vitro* killing of CD1c-expressing malignant cells, and in an ongoing study a CD1c-transgenic mouse model is used to test, whether this approach is functional *in vivo* (Consonni et al., 2019). Although the number of CD1-expressing transgenic mouse models that were investigated during the past ten years is limited, they have clearly contributed to mechanistically explain many observations that have previously been made with human T cells. New and exciting insights can be expected from ongoing and future studies.

6. Non-human primates

Experimental evidence for the role of CD1-restricted T cells is limited for non-human primates. However, it has been shown that rhesus macaques express human group 1 CD1-molecules and that they are so similar to the human orthologues that the corresponding CD1b-expressing DCs are able to stimulate human CD1b-restricted T cell lines (Morita et al., 2008). Despite the fact that rhesus CD1b can present mycobacterial glucose monomycolate, it seems that T cells from BCG immunized rhesus macaques rather respond in a CD1c-restricted manner (Morita et al., 2013a). This contrasts finding in humans where GMM is considered to be exclusively presented by the large cleft in CD1b because its C80 mycolate lipid is presumably larger than the human CD1c cleft (Moody et al., 2000, 1997; Moody et al., 1999). However, this surprising finding might be explained if, when crystalized, primate CD1c proteins are shown to have larger clefts, or if the mycolate lipid protrudes from a small cleft. Similar to humans, GMM-specific rhesus macaque derived T cells displayed a proinflammatory phenotype and extravasated to sites of infection (Morita et al., 2013a), where they secreted macrophage attracting chemokines and expressed perforin and granulysin (Morita et al., 2013b), mediators that are believed to be important for immune defense against virulent mycobacteria (Stenger et al., 1998).

7. Summary

The human transgenic mouse models that became available about ten years ago were indispensable for gaining insight into the life-cycle of CD1-restricted T cells. Mechanisms of thymic selection, sites of first antigen encounter, modes of action, were all elucidated through sophisticated investigations in double or triple transgenic mouse strains on immune-deficient backgrounds, often complemented by adoptive transfer experiments. Many hypotheses regarding the role of CD1-restricted cells that had been formulated from *ex vivo* observations with human cells could be confirmed in the corresponding mouse model: CD1a, CD1b and CD1c proteins are present in different cells and tissues, and human CD1-restricted T cells contribute to immune response in different ways. Autoreactive cells can act as highly sensitive detectors for cellular stress and may form an intermediate between adaptive and innate immunity. Other cells that are specific for microbial lipids fulfil the classical adaptive role of T cells and exert effector functions that are also part of the functional repertoire of classical MHC-restricted T cells. The interest in the group 1 CD1-restricted T cells always had the very practical aim to devise new vaccination strategies or therapeutic interventions, which could be broadly applicable due to the lack of polymorphism in CD1 molecules. The development of new lipid-based

vaccination strategies against pathogens, such as *M. tuberculosis*, is dependent on the availability of naturally susceptible, outbred animal models. As with humans, experiments with cattle, the target species of *M. bovis*, have shown that lipid antigens constitute an important part of the immune targets after natural infection (Pirson et al., 2014). Which of these antigens are protective, how CD1-restricted T cells are best induced, which functional capacities protective T cells need to acquire and how efficient such an immune response really is, has ultimately to be addressed in the target species. There are still many open practical questions that need to be answered.

Authors contribution

E.E. and M.B. have jointly conceptionalized, written and reviewed the manuscript.

Funding

This work was supported by the German Research Foundation (grant number BA 3885/2-1).

Declaration of Competing Interest

The authors declare that they have no conflict of competing interests.

Acknowledgement

We are grateful to Wiebke Lange for excellent support and literature search.

References

Agea, E., Russano, A., Bistoni, O., Mannucci, R., Nicoletti, I., Corazzi, L., Postle, A.D., De Libero, G., Porcelli, S.A., Spinozzi, F., 2005. Human CD1-restricted T cell recognition of lipids from pollens. J. Exp. Med. 202, 295–308.

Bagchi, S., Li, S., Wang, C.R., 2016. CD1b-autoreactive T cells recognize phospholipid antigens and contribute to antitumor immunity against a CD1b(+) T cell lymphoma. Oncoimmunology 5, e1213932.

Bagchi, S., He, Y., Zhang, H., Cao, L., Van Rhijn, I., Moody, D.B., Gudjonsson, J.E., Wang, C.R., 2017. CD1b-autoreactive T cells contribute to hyperlipidemia-induced skin inflammation in mice. J. Clin. Invest. 127, 2339–2352.

Bastian, M., Braun, T., Bruns, H., Rollinghoff, M., Stenger, S., 2008. Mycobacterial lipopeptides elicit CD4+ CTLs in Mycobacterium tuberculosis-infected humans. J. Immunol. 180, 3436–3446.

Bernard, A., Boumsell, L., 1984. The clusters of differentiation (CD) defined by the first international workshop on human leucocyte differentiation antigens. Hum. Immunol. 11, 1–10.

Blue, M.L., Levine, H., Daley, J.F., Branton Jr., K.R., Schlossman, S.F., 1989. Expression of CD1 and class I MHC antigens by human thymocytes. J. Immunol. 142, 2714–2720.

Cala-De Paepe, D., Layre, E., Giacometti, G., Garcia-Alles, L.F., Mori, L., Hanau, D., de Libero, G., de la Salle, H., Puzo, G., Gilleron, M., 2012. Deciphering the role of CD1e protein in mycobacterial phosphatidyl-myo-inositol mannosides (PIM) processing for presentation by CD1b to T lymphocytes. J. Biol. Chem. 287, 31494–31502.

Calmette, A., Guérin, C., Nègre, L., Boquet, A., 1926. Prémunition des nouveaux-nés contre la tuberculose par le vaccin BCG, 1921–1926. Ann. Inst. Pasteur (Paris) 40, 89–133.

Chancellor, A., Tocheva, A.S., Cave-Ayland, C., Tezera, L., White, A., Al-Dulayymi, J.R., Bridgeman, J.S., Tews, I., Wilson, S., Lissin, N.M., Tebruegge, M., Marshall, B., Sharpe, S., Elliott, T., Skylaris, C.K., Essex, J.W., Baird, M.S., Gadola, S., Elkington, P., Mansour, S., 2017. CD1b-restricted GEM T cell responses are modulated by Mycobacterium tuberculosis mycolic acid meromycolate chains. Proc. Natl. Acad. Sci. U. S. A. 114, E10956–E10964.

Consonni, M., Garavaglia, C., Palumbo, A., Astesana, V., de Lalla, C., Mancino, A., Mori, L., De Libero, G., Dellabona, P., Casorati, G., 2019. CD1c Transgenic Mice to Investigate Leukemia Immunotherapy by Retargeted Lipid-Specific T and iNKT Cells. CD1-MR1: Beyond MHC Restricted Lymphocytes. Oxford; 01-05 September 2019.

Dascher, C.C., 2007. Evolutionary biology of CD1. Curr. Top. Microbiol. Immunol. 314, 3–26.

Dascher, C.C., Hiromatsu, K., Naylor, J.W., Brauer, P.P., Brown, K.A., Storey, J.R., Behar, S.M., Kawasaki, E.S., Porcelli, S.A., Brenner, M.B., LeClair, K.P., 1999. Conservation of a CD1 multigene family in the guinea pig. J. Immunol. 163, 5478–5486.

Dascher, C.C., Hiromatsu, K., Xiong, X., Sugita, M., Buhlmann, J.E., Dodge, I.L., Lee, S.Y., Roura-Mir, C., Watts, G.F., Roy, C.J., Behar, S.M., Clemens, D.L., Porcelli, S.A., Brenner, M.B., 2002. Conservation of CD1 intracellular trafficking patterns between mammalian species. J. Immunol. 169, 6951–6958.

Dascher, C.C., Hiromatsu, K., Xiong, X., Morehouse, C., Watts, G., Liu, G., McMurray, D. N., LeClair, K.P., Porcelli, S.A., Brenner, M.B., 2003. Immunization with a mycobacterial lipid vaccine improves pulmonary pathology in the guinea pig model of tuberculosis. Int. Immunol. 15, 915–925.

de Jong, A., Pena-Cruz, V., Cheng, T.Y., Clark, R.A., Van Rhijn, I., Moody, D.B., 2010d. CD1a-autoreactive T cells are a normal component of the human alphabeta T cell repertoire. Nat. Immunol. 11, 1102–1109.

de Jong, A., Cheng, T.Y., Huang, S., Gras, S., Birkinshaw, R.W., Kasmar, A.G., Van Rhijn, I., Pena-Cruz, V., Ruan, D.T., Altman, J.D., Rossjohn, J., Moody, D.B., 2014d. CD1a-autoreactive T cells recognize natural skin oils that function as headless antigens. Nat. Immunol. 15, 177–185.

de la Salle, H., Mariotti, S., Angenieux, C., Gilleron, M., Garcia-Alles, L.F., Malm, D., Berg, T., Paoletti, S., Maitre, B., Mourey, L., Salamero, J., Cazenave, J.P., Hanau, D., Mori, L., Puzo, G., De Libero, G., 2005d. Assistance of microbial glycolipid antigen processing by CD1e. Science 310, 1321–1324.

de Lalla, C., Lepore, M., Piccolo, F.M., Rinaldi, A., Scelfo, A., Garavaglia, C., Mori, L., De Libero, G., Dellabona, P., Casorati, G., 2011d. High-frequency and adaptive-like dynamics of human CD1 self-reactive T cells. Eur. J. Immunol. 41, 602–610.

De Libero, G., Moran, A.P., Gober, H.J., Rossy, E., Shamshiev, A., Chelnokova, O., Mazorra, Z., Vendetti, S., Sacchi, A., Prendergast, M.M., Sansano, S., Torevilsky, A., Landmann, R., Mori, L., 2005. Bacterial infections promote T cell recognition of self-glycolipids. Immunity 22, 763–772.

Dieli, F., Troye-Blomberg, M., Ivanyi, J., Fournie, J.J., Krensky, A.M., Bonneville, M., Peyrat, M.A., Caccamo, N., Sireci, G., Salerno, A., 2001. Granulysin-dependent killing of intracellular and extracellular Mycobacterium tuberculosis by Vgamma9/Vdelta2 T lymphocytes. J. Infect. Dis. 184, 1082–1085.

Domagalla, J., Prodinger, W.M., Blum, H., Krebs, S., Gellert, S., Muller, M., Neuendorf, E., Sedlmaier, F., Buttner, M., 2013. Region of difference 4 in alpine Mycobacterium caprae isolates indicates three variants. J. Clin. Microbiol. 51, 1381–1388.

Dougan, S.K., Kaser, A., Blumberg, R.S., 2007. CD1 expression on antigen-presenting cells. Curr. Top. Microbiol. Immunol. 314, 113–141.

Drewe, J.A., O'Connor, H.M., Weber, N., McDonald, R.A., Delahay, R.J., 2013. Patterns of direct and indirect contact between cattle and badgers naturally infected with tuberculosis. Epidemiol. Infect. 141, 1467–1475.

Fairhurst, R.M., Wang, C.X., Sieling, P.A., Modlin, R.L., Braun, J., 1998. CD1 presents antigens from a gram-negative bacterium, Haemophilus influenzae type B. Infect. Immun. 66, 3523–3526.

Felio, K., Nguyen, H., Dascher, C.C., Choi, H.J., Li, S., Zimmer, M.I., Colmone, A., Moody, D.B., Brenner, M.B., Wang, C.R., 2009. CD1-restricted adaptive immune responses to Mycobacteria in human group 1 CD1 transgenic mice. J. Exp. Med.

Gansert, J.L., Kiessler, V., Engele, M., Wittke, F., Rollinghoff, M., Krensky, A.M., Porcelli, S.A., Modlin, R.L., Stenger, S., 2003. Human NKT cells express granulysin and exhibit antimycobacterial activity. J. Immunol. 170, 3154–3161.

Hayes, S.M., Knight, K.L., 2001. Group 1 CD1 genes in rabbit. J. Immunol. 166, 403–410.

Hiromatsu, K., Dascher, C.C., LeClair, K.P., Sugita, M., Furlong, S.T., Brenner, M.B., Porcelli, S.A., 2002a. Induction of CD1-restricted immune responses in guinea pigs by immunization with mycobacterial lipid antigens. J. Immunol. 169, 330–339.

Hiromatsu, K., Dascher, C.C., Sugita, M., Gingrich-Baker, C., Behar, S.M., LeClair, K.P., Brenner, M.B., Porcelli, S.A., 2002b. Characterization of guinea-pig group 1 CD1 proteins. Immunology 106, 159–172.

Kasmar, A.G., van Rhijn, I., Cheng, T.Y., Turner, M., Seshadri, C., Schiefner, A., Kalathur, R.C., Anand, J.W., de Jong, A., Shires, J., Leon, L., Brenner, M., Wilson, I. A., Altman, J.D., Moody, D.B., 2011. CD1b tetramers bind {alpha}{beta} T cell receptors to identify a mycobacterial glycolipid-reactive T cell repertoire in humans. J. Exp. Med.

Kaufmann, E., Spohr, C., Battenfeld, S., De Paepe, D., Holzhauser, T., Balks, E., Hamelika, S., Reiling, N., Gilleron, M., Bastian, M., 2016. BCG vaccination induces robust CD4+ T cell responses to Mycobacterium tuberculosis complex-specific lipopeptides in Guinea pigs. J. Immunol. 196, 2723–2732.

Kim, J.H., Hu, Y., Yongqing, T., Kim, J., Hughes, V.A., Le Nours, J., Marquez, E.A., Purcell, A.W., Wan, Q., Sugita, M., Rossjohn, J., Winau, F., 2016. CD1a on Langerhans cells controls inflammatory skin disease. Nat. Immunol. 17, 1159–1166.

Kobayashi, C., Shiina, T., Tokioka, A., Hattori, Y., Komori, T., Kobayashi-Miura, M., Takizawa, T., Takahara, K., Inaba, K., Inoko, H., Takeya, M., Dranoff, G., Sugita, M., 2012. GM-CSF-independent CD1a expression in epidermal Langerhans cells: evidence from human CD1A genome-transgenic mice. J. Invest. Dermatol. 132, 241–244.

Koch, R., 1882. Die Aetiologie der Tuberculose. Berliner Klinische Wochenschrift 19, 1–5.

Larrouy-Maumus, G., Layre, E., Clark, S., Prandi, J., Rayner, E., Lepore, M., de Libero, G., Williams, A., Puzo, G., Gilleron, M., 2017. Protective efficacy of a lipid antigen vaccine in a guinea pig model of tuberculosis. Vaccine 35, 1395–1402.

Li, S., Choi, H.J., Felio, K., Wang, C.R., 2011. Autoreactive CD1b-restricted T cells: a new innate-like T-cell population that contributes to immunity against infection. Blood 118, 3870–3878.

Mansour, S., Tocheva, A.S., Cave-Ayland, C., Machelett, M.M., Sander, B., Lissin, N.M., Molloy, P.E., Baird, M.S., Stobs, G., Schroder, N.W., Schumann, R.R., Rademann, J., Postle, A.D., Jakobsen, B.K., Marshall, B.G., Gosain, R., Elkington, P.T., Elliott, T., Skylaris, C.K., Essex, J.W., Tews, I., Gadola, S.D., 2016. Cholesteryl esters stabilize human CD1c conformations for recognition by self-reactive T cells. Proc. Natl. Acad. Sci. U. S. A. 113, E1266–1275.

McMichael, A.J., Pilch, J.R., Galfré, G., Mason, D.Y., Fabre, J.W., Milstein, C., 1979. A human thymocyte antigen defined by a hybrid myeloma monoclonal antibody. Eur. J. Immunol. 9, 205–210.

Miller, M.M., Wang, C., Parisini, E., Coletta, R.D., Goto, R.M., Lee, S.Y., Barral, D.C., Townes, M., Roura-Mir, C., Ford, H.L., Brenner, M.B., Dascher, C.C., 2005. Characterization of two avian MHC-like genes reveals an ancient origin of the CD1 family. Proc. Natl. Acad. Sci. U. S. A. 102, 8674–8679.

Minnikin, D.E., Kremer, L., Dover, L.G., Besra, G.S., 2002. The methyl-branched fortifications of Mycobacterium tuberculosis. Chem. Biol. 9, 545–553.

Moody, D.B., Porcelli, S.A., 2003. Intracellular pathways of CD1 antigen presentation. Nat. Rev. Immunol. 3, 11–22.

Moody, D.B., Reinhold, B.B., Guy, M.R., Beckman, E.M., Frederique, D.E., Furlong, S.T., Ye, S., Reinhold, V.N., Sieling, P.A., Modlin, R.L., Besra, G.S., Porcelli, S.A., 1997. Structural requirements for glycolipid antigen recognition by CD1b-restricted T cells. Science 278, 283–286.

Moody, D.B., Reinhold, B.B., Reinhold, V.N., Besra, G.S., Porcelli, S.A., 1999. Uptake and processing of glycosylated mycolates for presentation to CD1b-restricted T cells. Immunol. Lett. 65, 85–91.

Moody, D.B., Guy, M.R., Grant, E., Cheng, T.Y., Brenner, M.B., Besra, G.S., Porcelli, S.A., 2000. CD1b-mediated T cell recognition of a glycolipid antigen generated from mycobacterial lipid and host carbohydrate during infection. J. Exp. Med. 192, 965–976.

Moody, D.B., Zajonc, D.M., Wilson, I.A., 2005. Anatomy of CD1-lipid antigen complexes. Nat. Rev. Immunol. 5, 387–399.

Morita, D., Katoh, K., Harada, T., Nakagawa, Y., Matsunaga, I., Miura, T., Adachi, A., Igarashi, T., Sugita, M., 2008. Trans-species activation of human T cells by rhesus macaque CD1b molecules. Biochem. Biophys. Res. Commun. 377, 889–893.

Morita, D., Hattori, Y., Nakamura, T., Igarashi, T., Harashima, H., Sugita, M., 2013a. Major T cell response to a mycolyl glycolipid is mediated by CD1c molecules in rhesus macaques. Infect. Immun. 81, 311–316.

Morita, D., Miyamoto, A., Hattori, Y., Komori, T., Nakamura, T., Igarashi, T., Harashima, H., Sugita, M., 2013b. Th1-skewed tissue responses to a mycolyl glycolipid in mycobacteria-infected rhesus macaques. Biochem. Biophys. Res. Commun. 441, 108–113.

Nguyen, T.K., Koets, A.P., Santema, W.J., van Eden, W., Rutten, V.P., Van Rhijn, I., 2009. The mycobacterial glycolipid glucose monomycolate induces a memory T cell response comparable to a model protein antigen and no B cell response upon experimental vaccination of cattle. Vaccine.

Nguyen, T.K., Reinink, P., El Mesilaki, C., Im, J.S., Ercan, A., Porcelli, S.A., Van Rhijn, I., 2015. Expression patterns of bovine CD1 in vivo and assessment of the specificities of the anti-bovine CD1 antibodies. PloS One 10, e0121923.

Nicolai, S., Wegrecki, M., Cheng, T.Y., Bourgeois, E.A., Cotton, R.N., Mayfield, J.A., Monnot, G.C., Le Nours, J., Van Rhijn, I., Rossjohn, J., Moody, D.B., de Jong, A., 2020. Human T cell response to CD1a and contact dermatitis allergens in botanical extracts and commercial skin care products. Sci. Immunol. 5.

Nugent, G., Gortazar, C., Knowles, G., 2015. The epidemiology of Mycobacterium bovis in wild deer and feral pigs and their roles in the establishment and spread of bovine tuberculosis in New Zealand wildlife. N. Z. Vet. J. 63 (Suppl. 1), 54–67.

Obata-Onai, A., Hashimoto, S., Onai, N., Kurachi, M., Nagal, S., Shizuno, K., Nagahata, T., Matsushima, K., 2002. Comprehensive gene expression analysis of human NK cells and CD8(+) T lymphocytes. Int. Immunol. 14, 1085–1098.

Pirson, C., Jones, G.J., Steinbach, S., Besra, G.S., Vordermeier, H.M., 2014. Differential effects of Mycobacterium bovis-derived polar and apolar lipid fractions on bovine innate immune cells. Vet. Res. 43, 54.

Porcelli, S.A., Modlin, R.L., 1999. The CD1 system: antigen-presenting molecules for T cell recognition of lipids and glycolipids. Annu. Rev. Immunol. 17, 297–329.

Porcelli, S., Brenner, M.B., Greenstein, J.L., Balk, S.P., Terhorst, C., Bleicher, P.A., 1989. Recognition of cluster of differentiation 1 antigens by human CD4-CD8-cytolytic T lymphocytes. Nature 341, 447–450.

Randhawa, P.S., 1990. Lymphocyte subsets in granulomas of human tuberculosis: an in situ immunofluorescence study using monoclonal antibodies. Pathology 22, 153–155.

Roura-Mir, C., Moody, D.B., 2003. Sorting out self and microbial lipid antigens for CD1. Microbes Infect. 5, 1137–1148.

Roura-Mir, C., Wang, L., Cheng, T.Y., Matsunaga, I., Dascher, C.C., Peng, S.L., Fenton, M. J., Kirschning, C., Moody, D.B., 2005. Mycobacterium tuberculosis regulates CD1 antigen presentation pathways through TLR-2. J. Immunol. 175, 1758–1766.

Schinkothe, J., Geluk, A., Ottenhoff, T., Christensen, D., Gilleron, M., Bastian, M., 2019. BCG Vaccination Induces Robust PIM-Specific, CD1b Restricted CD4-Positive T Cell Responses in Guinea Pigs, CD1-MR1: Beyond MHC Restricted Lymphocytes. Oxford, 01-05 September 2019.

Shahine, A., 2018. The intricacies of self-lipid antigen presentation by CD1b. Mol. Immunol. 104, 27–36.

Shahine, A., Van Rhijn, I., Cheng, T.Y., Iwany, S., Gras, S., Moody, D.B., Rossjohn, J., 2017. A molecular basis of human T cell receptor autoreactivity toward self-phospholipids. Sci. Immunol. 2.

Shamshiev, A., Donda, A., Carena, I., Mori, L., Kappos, L., De Libero, G., 1999. Self glycolipids as T-cell autoantigens. Eur. J. Immunol. 29, 1667–1675.

Shang, S., Kats, D., Cao, L., Morgun, E., Velluto, D., He, Y., Xu, Q., Wang, C.R., Scott, E. A., 2018. Induction of Mycobacterium tuberculosis lipid-specific T cell responses by pulmonary delivery of mycolic acid-loaded polymeric micellar nanocarriers. Front. Immunol. 9, 2709.

Sieling, P.A., Chatterjee, D., Porcelli, S.A., Prigozy, T.I., Mazzaccaro, R.J., Soriano, T., Bloom, B.R., Brenner, M.B., Kronenberg, M., Brennan, P.J., Modlin, R.L., 1995. CD1-restricted T cell recognition of microbial lipoglycan antigens. Science 269, 227–230.

Stenger, S., Mazzaccaro, R.J., Uyemura, K., Cho, S., Barnes, P.F., Rosat, J.P., Sette, A., Brenner, M.B., Porcelli, S.A., Bloom, B.R., Modlin, R.L., 1997. Differential effects of cytolytic T cell subsets on intracellular infection. Science 276, 1684–1687.

Stenger, S., Hanson, D.A., Teitelbaum, R., Dewan, P., Niazi, K.R., Froelich, C.J., Ganz, T., Thoma-Uszynski, S., Melian, A., Bogdan, C., Porcelli, S.A., Bloom, B.R., Krensky, A. M., Modlin, R.L., 1998. An antimicrobial activity of cytolytic T cells mediated by granulysin. Science 282, 121–125.

Sun, Q., Burton, R.L., Lucas, K.G., 2002. Cytokine production and cytolytic mechanism of CD4(+) cytotoxic T lymphocytes in ex vivo expanded therapeutic Epstein-Barr virus-specific T-cell cultures. Blood 99, 3302–3309.

van den Elzen, P., Garg, S., Leon, L., Brigl, M., Leadbetter, E.A., Gumperz, J.E., Dascher, C.C., Cheng, T.Y., Sacks, F.M., Illarionov, P.A., Besra, G.S., Kent, S.C., Moody, D.B., Brenner, M.B., 2005v. Apolipoprotein-mediated pathways of lipid antigen presentation. Nature 437, 906–910.

Van Rhijn, I., Kim Anh Nguyen, T., Michel, A., Cooper, D., Govaerts, M., Cheng, T.Y., van Eden, W., Branch Moody, D., Coetzer, J.A., Rutten, V., Koets, A.P., 2009. Low cross-reactivity of T cell responses against lipids from Mycobacterium bovis and M. Avium paratuberculosis during natural infection. Eur. J. Immunol.

Van Rhijn, I., Kasmar, A., de Jong, A., Gras, S., Bhati, M., Doorenspleet, M.E., de Vries, N., Godfrey, D.I., Altman, J.D., de Jager, W., Rossjohn, J., Moody, D.B., 2013. A conserved human T cell population targets mycobacterial antigens presented by CD1b. Nat. Immunol. 14, 706–713.

Van Rhijn, I., van Berlo, T., Hilmenyuk, T., Cheng, T.Y., Wolf, B.J., Tatituri, R.V., Uldrich, A.P., Napolitani, G., Cerundolo, V., Altman, J.D., Willemsen, P., Huang, S., Rossjohn, J., Besra, G.S., Brenner, M.B., Godfrey, D.I., Moody, D.B., 2016. Human autoreactive T cells recognize CD1b and phospholipids. Proc. Natl. Acad. Sci. U. S. A. 113, 380–385.

van Schaik, B., Klarenbeek, P., Doorenspleet, M., van Kampen, A., Moody, D.B., de Vries, N., Van Rhijn, I., 2014v. Discovery of invariant T cells by next-generation sequencing of the human TCR alpha-chain repertoire. J. Immunol. 193, 5338–5344.

Visvabharathy, L., Genardi, S., Cao, L., He, Y., Alonzo 3rd, F., Berdyshev, E., Wang, C.R., 2020. Group 1 CD1-restricted T cells contribute to control of systemic Staphylococcus aureus infection. PLoS Pathog. 16, e1008443.

Winau, F., Schwierzeck, V., Hurwitz, R., Remmel, N., Sieling, P.A., Modlin, R.L., Porcelli, S.A., Brinkmann, V., Sugita, M., Sandhoff, K., Kaufmann, S.H., Schaible, U. E., 2004. Saposin C is required for lipid presentation by human CD1b. Nat. Immunol. 5, 169–174.

Yang, Z., Wang, C., Wang, T., Bai, J., Zhao, Y., Liu, X., Ma, Q., Wu, X., Guo, Y., Zhao, Y., Ren, L., 2015. Analysis of the reptile CD1 genes: evolutionary implications. Immunogenetics 67, 337–346.

Zajonc, D.M., 2016. The CD1 family: serving lipid antigens to T cells since the Mesozoic era. Immunogenetics 68, 561–576.

Zhao, J., Siddiqui, S., Shang, S., Bian, Y., Bagchi, S., He, Y., Wang, C.R., 2015. Mycolic acid-specific T cells protect against Mycobacterium tuberculosis infection in a humanized transgenic mouse model. Elife 4.

(II) Donor unrestricted T cells matter: Phosphatidylinositolmannoside vaccination induces lipid-specific Th1-responses and partially protects guinea pigs from *Mycobacterium tuberculosis* challenge

Emmelie Eckhardt, Jan Schinköthe, Marcel Gischke, Julia Sehl-Ewert, Björn Corleis, Anca Dorhoi, Jens Teifke, Dirk Albrecht, Annemieke Geluk, Martine Gilleron, Max Bastian

Submitted to Scientific Reports

(09.01.2023, Manuscript: SREP-23-00073)

Donor unrestricted T-cells matter: Phosphatidylinositolmannoside vaccination induces lipid-specific Th1-responses and partially protects guinea pigs from *Mycobacterium tuberculosis* challenge

Emmelie Eckhardt[1]; Jan Schinköthe[2]; Marcel Gischke[3]; Julia Sehl-Ewert[1]; Björn Corleis[1]; Anca Dorhoi[1]; Jens Teifke[1]; Dirk Albrecht[3]; Annemieke Geluk[4]; Martine Gilleron[5]; Max Bastian[1]*

[1] Friedrich-Loeffler-Institut; Greifswald – Isle of Riems, Germany

[2] Institute of Veterinary Pathology, Faculty of Veterinary Medicine, Leipzig University; Germany

[3] Institute of Microbiology; Greifswald University; Germany

[4] Dept. Infectious Diseases, Leiden, University Medical Center; The Netherlands

[5] CNRS, Institut de Pharmacologie et de Biologie Structurale, Toulouse, France

* Corresponding author – email: **max.bastian@fli.de** phone: +49-38351-71026; Friedrich-Loeffler-Institut; Südufer 10; 17493 Greifswald – Insel Riems, Germany

Keywords

BCG; CD1; DURTs; guinea pig; *Mycobacterium tuberculosis*; Phosphatidylinositolmannoside (PIM); T-cell-immunology; vaccine-development

Abstract

The concept of donor-unrestricted T-cells (DURTs) comprises a heterogeneity of lymphoid cells that respond to an abundance of unconventional epitopes in a non-MHC-restricted manner. Vaccinologists strive to harness this so far underexplored branch of the immune system for new vaccines against tuberculosis. A particular division of DURTs are T-cells that recognize their cognate lipid antigen in the context of CD1-molecules. Mycobacteria are characterized by a particular lipid-rich cell wall. Several of these lipids have been shown to be presented to T-cells via CD1b-molecules. Guinea pigs functionally express CD1b and are hence an appropriate small animal model to study the role of CD1b-restricted, lipid-specific immune responses. In the current study, guinea pigs were vaccinated with BCG or highly-purified, liposome-formulated phosphatidylinositol-hexa-mannoside (PIM_6) to assess the effect of CD1-restricted DURT-cells on the course of infection after virulent *Mycobacterium tuberculosis (Mtb)* challenge. Robust PIM_6-specific T-cell-responses were observed both after BCG- and PIM_6-vaccination. The cellular response was significantly reduced in the presence of CD1b-blocking antibodies, indicating that a predominant part of this reactivity was CD1b-restricted. When animals were challenged with *Mtb,* BCG- and PIM_6-vaccinated animals showed significantly reduced pathology, smaller necrotic granulomas in lymph node and spleen and reduced bacterial loads. Comprehensive histological and transcriptional analyses in the draining lymph node revealed that protected animals showed reduced transcription-levels of inflammatory cyto- and chemokines and higher levels of CD1b-expression compared to controls. Our observations in the guinea pig model suggest that CD1b-restricted, PIM_6-reactive DURT-cells contribute to immune-mediated containment of virulent *Mtb*.

I. Introduction

Bacille Calmette-Guérin (BCG) is still the only licensed vaccine against tuberculosis (TB). It shows limited efficacy against the epidemiologically most relevant lung manifestation of TB, but it protects reliably from severe systemic TB during early childhood [1]. BCG activates different layers of the immune system. This comprises the induction of adaptive memory and an education of the innate immune system, now known as trained immunity [2]. Many prominent protein antigens are targets of protective adaptive immune responses [3]. However, it is likewise clear that mycobacteria display a broad repertoire of complex lipids and lipoglycans that also provoke adaptive immune responses. In a recent publication, we have shown that BCG-vaccinated guinea pigs respond to lipid-extracts with robust T-cell-proliferation [4]. The prominent T-cell-responses are in part due to MHC-II-presented, lipophilic peptides that are present in total lipid extracts of cultured mycobacteria [5]. However, CD1-restricted T-cell-responses have been reported that are directed against structurally well-defined mycobacterial lipid antigens [6-9]. CD1-molecules are antigen-presenting molecules that evolved to present lipid antigens to T-cells. Since CD1-molecules are non-polymorphic, there are no differences in the epitope binding and presentation capacities between different individuals. It is an appealing concept to incorporate such universally binding epitopes as subunit components in future TB-vaccines. For this concept the term donor-unrestricted T-cells (DURTs) has been coined. In addition to CD1-restricted T cells, DURT-cells comprise cells that recognize their antigen in the context of MHC related protein 1 (MR1), butyrophilin 3A1, as well as the nonclassical MHC class Ib family member HLA-E [10]. Among CD1-restricted lipids are phosphatidylinositolmannosides (PIMs), a class of highly glycosylated lipids that form the lipid anchor of lipoarabinomannan in the mycobacterial cell wall [11]. The molecular mechanisms, how lipids are loaded into the hydrophobic binding groove of CD1-molecules are well studied [12, 13]. However, the functional implications of this system are less clear. The development of lipid-loaded CD1b-tetramers was an important milestone for a better understanding of the CD1-T-cell-axis. *Ex vivo* tetramer staining allowed for a phenotypical characterization of CD1a- and CD1b-restricted T-cells and revealed that the majority of these cells was CD4-positive [14, 15]. A deeper understanding on the functional role of CD1-type-1-restricted T-cells in the immune defense against

pathogens has long been hampered by the fact that the most common rodent animal model, the mouse, by nature does not express a functional CD1-type-1-system. A well-established small rodent model that has already been used by the early pioneers of TB-research is the guinea pig [16]. Guinea pigs naturally express a broad panel of CD1-type-1-molecules. Founding studies investigated the repertoire of CD1-isoforms and found four CD1b- and three CD1c-isoforms that are functionally expressed in the guinea pig [17, 18]. Detailed molecular analyses indicated that the CD1b1- and CD1b4-isoform are functionally relevant in their resemblance to human CD1b-molecules [19]. Furthermore, in a series of publications it was demonstrated that lipid-vaccinated guinea pigs are at least partially protected from virulent *Mycobacterium tuberculosis (Mtb)*-challenge [20-23]. So, the protective effect of lipids in general has been shown, but the precise nature of the immune response triggered has yet to be described. It is unclear, which lipids are presented during mycobacterial infection. It has to be further clarified, which cells respond to CD1b-restricted lipids and where they encounter their antigen. Finally, the effect of CD1-restricted T memory cells on the course of a mycobacterial challenge has to be elucidated. To address these questions and investigate the specific role of CD1-restricted DURT-cells, in the current study, we investigated lipid-specific responses in BCG-vaccinated guinea pigs. Based on previous studies [20] and own unpublished experiments we then vaccinated guinea pigs with liposome-formulated PIM_6 and investigated the effect on the course of infection after virulent *Mtb*-challenge.

II. Material and Methods

II.1 Bacteria

BCG, strain Pasteur$_{1173}$, was obtained from Dr. Walter Matheis (Paul-Ehrlich-Institut, Germany). *Mtb*, strain H37Rv, was kindly provided by Prof. Dr. Stefan H.E. Kaufmann (Max Planck Institute for Infection Biology, Germany). Bacteria were grown in Middlebrook 7H9-Medium (Becton-Dickinson, Germany) enriched with OADC (Becton-Dickinson, Germany) and 0.05% Tween80 (Sigma-Aldrich, Germany).

II.2 Liposomes

The composition and preparation of liposomes corresponded to the Cationic Adjuvant Formulation (CAF01), as described [24]. Briefly, 625 µg dimethyldioctadecylammonium-bromide (DDA, Avanti Polar Lipids) and 125 µg trehalose 6,6'-dibehenate (TDB, Avanti Polar Lipids), solubilized either in chloroform or in chloroform:methanol (9:1), were combined per dose. For PIM_6-liposomes, 25 µg of a highly-purified PIM_6-preparation were added. PIM_6 was purified and characterized by MALDI-TOF-analysis, as described (29). By ESI-mass-spectrometry no contaminating peptides were identified in the batch used for liposome formulation (data not shown). The components were mixed and exsiccated. Subsequently, lipid films were rehydrated with 0,5 ml of Tris-buffered, distilled water and resolubilized by mild sonification. Liposomes were then analysed by thin layer chromatography (TLC), transmission-electron- and fluorescence-microscopy (data not shown).

II.3 Animal experiments

Ethic statement: Female Dunkin-Hartley guinea pigs were obtained from Charles River Laboratories, Sulzfeld, Germany. All animal experiments were approved by the competent authority, the State Office of Agriculture, Food Safety and Fishery in Mecklenburg-Western Pomerania (LALLF MV, 7221.3-1-065/15) and conducted in accordance with the ARRIVE guidelines.

114 *Animal husbandry:* Animals were housed in groups of three in plastic-cages on dust-free wooden
115 bedding. They had free access to dry pellets and water. After completion of the study guinea pigs
116 were anesthetized as described below and euthanized by carbon-dioxide inhalation.
117 *Experimental BCG-vaccination:* One group of guinea pigs (n=8) was administered $1x10^6$ CFUs
118 $BCG_{Pasteur}$ resuspended in 0,5 ml saline subcutaneously to the left axillary region. A control group
119 (n=7) received saline control in parallel. Four weeks after immunization blood was obtained by non-
120 terminal cardiocentesis and processed to analyse cellular immune responses.
121 *Experimental PIM_6-vaccination:* Three groups of six guinea pigs were immunized in parallel (n=18):
122 $1x10^6$ CFUs $BCG_{Pasteur}$, PIM_6-, or empty CAF01-liposomes were resuspended in 0,5 ml saline and
123 administered subcutaneously to the left axillary region. Liposomes were administered three times
124 with an interval of two weeks. Non-terminal cardiocentesis was performed on anesthetized animals
125 before and 28 and 80 days after the first vaccination. Blood was processed to analyse cellular
126 immune responses.
127 *Experimental challenge*: The same vaccinated guinea pigs (n=18) were challenged 84 days after
128 the first immunization, by subcutaneous inoculation of $1x10^3$ CFUs of *Mtb* in the right axillary region.
129 An additional group of non-immunized animals (n=6) was likewise infected. Four weeks after
130 challenge the animals were euthanized. Tissue samples were taken from the injection site, the
131 draining right axillary lymph node, the spleen and the lung. They were used for histopathological,
132 cultural and transcriptional analyses. To analyse the transcriptional profile prior to the challenge,
133 an additional vaccination experiment was performed (n=18).
134
135 II.4 Assessment of cellular immune responses

136 *Antigens*: Phytohaemagglutinin (PHA, Oxoid, Germany) was used as positive control. A total
137 sonicate ($Lysate_{BCG}$) and a chloroform-methanol extract (CME_{BCG}) were produced, as described
138 [4]. Protein antigens, Antigen-85-A and ESAT6 were expressed in *E. coli* and purified as described
139 [25]. For lipid-specific stimulation purified mannosylated lipoarabinomannan (LAM, NR-14848);
140 lipomannan (LM, NR-14850); phosphatidylinositol-hexa-mannoside (PIM_6, NR-14847) and
141 phosphatidylinositol-di-mannoside (PIM_2, NR-14846) all purified from Mtb_{H37Rv}, were obtained from

BEI Resources, NIAID, NIH. For a better comparison this set of four related antigens was obtained from one source. Phthiocerol Dimycocerosate (PDIM, NR-20328) was also obtained from BEI Resources. Glucose-monomycolate (GMM) was purified, as described [6].

Lymphocyte preparation: Peripheral blood mononuclear cells (PBMCs) were isolated using Ficoll-Paque-gradient-centrifugation, as described [26]. Plastic adherent monocytes were incubated overnight at 37 °C and 5% CO_2 in Iscove's-modified-Dulbeco's-medium (IMDM, in-house) supplemented with 5% autologous serum and 5% conditioned hybridoma supernatant containing guinea pig IL4 and GM-CSF to induce CD1-expression (data not shown). Non-adherent responder cells were stored overnight.

Proliferation assay: After overnight incubation, non-adherent responder cells were mixed with CD1-expressing, autologous antigen presenting cells (APCs) at a 3:1 ratio and stained with carboxyfluorescein-succimidyl-ester (CFSE, Enzo Life Science, Germany), as described [26]. Subsequently, $1.3x10^5$ cells per well were seeded in 96-well round-bottom-plates (Greiner Bio-One, Germany) in 100 µl IMDM-medium containing 10% autologous serum. Cells were stimulated in duplicates. Non-stimulated cells served as medium control. CFSE dilution was analysed after 5 days of incubation at 37 °C using a MACS Quant Analyzer (Miltenyi Biotec, Germany).

Flow cytometry: CFSE-negative lymphocytes were further characterized by a triple-staining using allophycocyanin-conjugated mouse-anti-guinea-pig-T-cell-antibody (AbD Serotec, Germany); phycoerythrin-conjugated mouse-anti-guinea-pig-CD4 antibody (AbD Serotec) and biotinylated mouse-anti-guinea-pig-CD8 antibody (kindly provided by Dr. Hubert Schäfer, Robert Koch-Institut, Germany). Binding of biotinylated anti-CD8 antibody was visualized using PE-Cy5.5-conjugated streptavidin (Invitrogen, Germany). Flow cytometry was performed using a MACS Quant Analyzer (Miltenyi, Germany). FlowJo-Software (Version 9.9.6) was used to analyse flow-cytometric data.

II.5 Pathology

Four weeks after the challenge with *Mtb*, guinea pigs were humanely euthanized. Necropsies were performed under BSL3-conditions. Blinded, macroscopic scoring of gross lesions was performed for the right axillary subcutis, right axillary lymph node, spleen, and liver by assessing formation of

granulomas, number and size of granulomas and presence of necrosis. The scores were derived from an ordinally scale of 0–4 based on the modified Mitchison scoring system detailed in supplemental table S1 [27, 28].

II.6 Measurement of bacterial growth

Tissue samples of the spleen were homogenized in 1 ml of PBS containing 0.05% Tween80 (Sigma-Aldrich, Germany). The homogenate was 1:10 serially diluted to a dilution of 10^{-7}. 50 µl of each dilution was plated on 7H11-agar plates (Becton-Dickinson, Germany). Agar plates were incubated at 37 °C for 3 weeks before determining number of CFUs.

II.7 Transcription-analysis

Sample preparation: To determine antigen-specific upregulation of cytokine transcripts non-adherent responder cells and autologous APCs were stimulated as described above. For CD1b-blocking experiments cells were stimulated with PIM_6 in the presence or absence of equivalent amounts of anti-guinea-pig-CD1b- or isotype-matched-hybridoma-supernatant (CD1F2 hybridoma, kindly provided by Steven Porcelli, Albert-Einstein-College; or anti rabies-G-Protein antibody E559, kindly provided by Thomas Mueller, FLI). After 24 hours, cells were washed and solubilized in TRIzol Reagent (Fisher Scientific, Germany). Tissue samples from injection-site-granulomas, draining axillary lymph nodes and spleen were collected during necropsy and put into TRIzol. Tissue samples were homogenised using a gentleMACSDissociator (Miltenyi Biotec, Germany).
RNA isolation and real-time PCR: RNA was isolated using TRIzol and RNeasy Mini Kit (Qiagen, Germany). For qRT-PCR, QuantiTect SYBR Green PCR Kit (Qiagen, Germany) was used. Primers were designed using the NCBI Primer-BLAST tool ((32); see supplemental Table S2). Ct-values were determined and relative transcription-levels were calculated in relation to β-Actin according to the following equation: transcription-level = $1000 \times 2^{(Ct\ b\text{-}Act - Ct\ test)}$.

II.8 Histological analysis

197 *Tissue preparation and staining*: Formaldehyde-fixed, paraffin-embedded (FFPE) tissues were cut
198 at 3 µm, and stained with hematoxylin-eosin (HE) for microscopic analysis, according to standard
199 procedures [29]. Injection-site lesions and axillary lymph nodes were available from five CAF01-
200 and PIM_6-vaccinated animals, from BCG-vaccinated animals one injection-site-granuloma and two
201 lymph nodes were available. Spleen sections were available from all six animals per group. Tissue
202 sections were prepared for immunophenotyping and mRNA-detection as follows.
203 *Immunohistochemistry*: Mycobacteria, B-cells, T-cells and macrophages were detected with
204 primary antibodies described in supplemental Table S3. As secondary antibody a biotinylated goat-
205 anti-mouse-IgG (Vector Laboratories, USA) was used. For visualization of B-cells VECTASTAIN
206 ABC Kit (Vector Laboratories) and for mycobacteria, macrophages and T-cells the EnVision$^+$
207 System (Dako, USA) was used.
208 *In situ Hybridisation (ISH)*: ISH was performed using the RNAscope 2.5 HD Reagent Kit-RED (ACD
209 biotechne, Germany) according to the manufacturer's instructions. Specific probes for guinea pig
210 CD1b1, IFNγ and CXCL10 were custom designed and provided by the manufacturer. According to
211 the manufacturer, the CD1b1-probe does not discriminate between CD1b1- and CD1b4-transcripts.
212 Stainings obtained with the CD1b1-probe are therefore considered synonymous for CD1b1 and b4.
213 As controls, DapB- (negative) and Cp-Ppib-probes (positive) were used (see supplemental Figure
214 S5 for control stainings).
215 *Whole Slide Image (WSI) analysis*: Stained sections were scanned using a digital slide scanner
216 (Hamamatsu, Germany). QuPath software [30] was used to analyse all digitalised images. In some
217 BCG-vaccinated animals, granulomas and lymph nodes were too small to perform histopathological
218 and transcriptional analysis in parallel. In those cases, we prioritized the transcriptional analysis of
219 the expression profiles. For each animal the absolute lesion area in each tissue section of the
220 injection site, lymph node and spleen was determined. Within granulomas, macrophage-rich areas
221 were differentiated from necroses, and the ratio was calculated. In the lymph nodes, regions of
222 interest (ROI) were defined as granuloma and unaltered lymphatic tissue, comprising B- and T-cell-
223 areas. In a number of visual fields representative for the size and type of ROI, the number of

224 mycobacteria, macrophages, B-, T-cells and CD1- or cytokine-expressing cells were counted
225 automatically at 400x-magnification.
226
227 II.9 Statistics
228 GraphPad Prism version 8.1.0 was used to analyse and visualize the data. Quantitative data are
229 expressed as group means. Error bars indicate the standard error of the mean. Data were tested
230 for normal distribution using Shapiro-Wilk and Kolmogorov-Smirnov test. Results from proliferation-
231 assays were analysed by nested-t-tests. qRT-PCR results of PIM_6-stimulated cells were analysed
232 with a Wilcoxon matched-pair-signed-rank-test. For the other data shown, the level of significance
233 was calculated by unpaired-t- or Mann-Whitney-U-test. P-values are expressed as follows: *,
234 $p<0.05$; **, $p<0.01$, ***, $p<0.001$ and ****, $p<0.0001$. Low-case letter “a” indicates a non-significant
235 tendency ($p< 0.1$). Data without symbol did not reach significance. To explicitly indicate “non-
236 significance” some data are labelled with “ns”.

III. Results

III.1 BCG-vaccination induces robust PIM_6-specific T-cell-responses

PBMCs from BCG-vaccinated or control-animals were isolated four weeks after vaccination and stimulated with mycobacterial antigens in the presence of CD1-expressing, autologous APCs. By flow cytometry, the number of proliferated, CFSE low cells was measured. Cells derived from controls only reacted to phytohaemagglutinin (PHA). Cells from BCG-vaccinated animals vigorously responded to BCG-lysate or CME_{BCG}. In addition, there was significant proliferation towards PIM_6. No proliferation was found in response to PIM_2, GMM and PDIM (Fig1A). The phenotype of proliferating cells was analysed by flow-cytometry. The majority of PIM_6-specific cells was CD4-positive. A robust percentage of about 20% was CD4-/ CD8- double negative. A minority of proliferating cells was CD8-positive. For comparison, the CD4/ CD8-distribution was assessed in non-stimulated PBMCs from naïve control guinea pigs, shown in red (Fig1B). The pattern of CD8-positive and double-negative T cells among PIM_6-specific, proliferated cells differed significantly from the normal distribution (p= 0,024 and 0,031, resp.). Transcript levels of a selected panel of T-cell-cytokines were determined by qRT-PCR. β-Actin served as housekeeping gene. PIM_6-stimulation induced in almost all cases an upregulation of the Th1-lead cytokine, IFNγ. This was highly significant. Also, the upregulation of GM-CSF and IL17 reached significance. A non-significant increase was found for IL2 transcripts. No upregulation was observed with TNF-α and IL4, while a non-significant reduction was observed with TGF-β. No upregulation of IFNγ and IL17 and only weak and insignificant upregulation of GM-CSF was observed when cells from naïve control animals were stimulated accordingly (Fig1C). To analyse the dependence on CD1b-presentation, IFNγ-upregulation was measured after PIM_6-stimulation in presence of CD1b-blocking antibody. CD1b-blockade significantly reduced upregulation of IFNγ in comparison to the stimulation without antibodies or in the presence of the isotype-control. Two out of eight animals showed a weak reactivity to PIM_6 and for one animal the isotype control is missing. However, with all animals IFNγ–upregulation was reduced in presence of CD1b-blocking antibody (Fig1D).

III.2 CAF01 adjuvanted PIM_6 induces PIM_6-specific memory T-cell-responses

To investigate the functional role of PIM_6-specific T cells a vaccination- and challenge-experiment was performed. The experimental outline is shown in Fig2A. Three groups of guinea pigs were vaccinated with CAF01-formulated PIM_6, with BCG or with CAF01 alone. Four weeks after first vaccination, blood was obtained and cell proliferation was tested as described above. Cells from animals that received CAF01 alone only showed significant proliferation after stimulation with PHA. After PIM_6-vaccination, significant proliferation was observed in response to PIM_6 and CME_{BCG}, which contains high amounts of various PIM-species. BCG-vaccinated animals showed a vigorous response to BCG-lysate and to CME_{BCG}. Lower but significant was the proliferation to Ag85, LM and PIM_6 (Fig2B). There was a striking difference in the cellular responses between PIM_6- and BCG-vaccinated animals. In PIM_6-vaccinated animals there was almost no reactivity to BCG-lysate that induced the strongest response in BCG-vaccinated animals. To illustrate the specificity of the response, the ratio between number of cells that proliferated in response to PIM_6 and those that proliferated in response to BCG-lysate was separately calculated for PIM_6- and BCG-vaccinated animals (Fig2C). Fig2D shows the time course of PIM_6-reactivity for the three vaccination groups. Before vaccination, there was no proliferation to PIM_6. After 28 days there was a significant response to PIM_6 in BCG- and PIM_6-vaccinated animals. After 80 days, four days before *Mtb*-challenge, there was a clear tendency of PIM_6-reactivity in both groups, but for PIM_6-vaccinated this did not reach significance. Animals receiving only empty CAF01-liposomes did not react to PIM_6.

III.3 PIM_6- and BCG-vaccination of guinea pigs is associated with significant reduction in necrosis and bacterial loads

To assess the role of PIM6-specific T-cells, guinea pigs were subcutaneously challenged with virulent *M.tuberculosis.* Although the subcutaneous infection does not recapitulate the natural route of infection, it allowed for a detailed analysis of the interaction between the site of pathogen entry and the draining lymph node. Four weeks after *Mtb*-challenge, granulomas had developed at the site of infection, in dependence on the vaccination group. Granulomas were prominent and widespread in CAF01-controls. Size and distribution of lesions at the site of infection and in the

draining lymph node and other organs (e.g. spleen and liver) was assessed macroscopically using a semiquantitative scoring system. PIM_6- or BCG-vaccinated animals showed a significantly reduced lesion score compared to the CAF01-controls (Fig3A). Systemic mycobacterial dissemination was absent or significantly reduced as indicated by normal spleens in BCG-vaccinated, and fewer and smaller granulomas in PIM_6-vaccinated animals (Fig3B). Similar observations were made, when the injection-sites, the draining lymph nodes and spleens were microscopically investigated. Percentage of necrotizing granulomas was significantly reduced in PIM_6-vaccinated compared to CAF01-controls (Fig3C and D, I and J). Only in the lymph node this did not reach significance (Fig3F and G). Representative histological sections for all three vaccination groups are shown in supplemental FigS1. By immunohistochemistry the number of *Mtb*-specific spots was assessed in injection-site-granulomas and draining lymph nodes. There was a slight reduction in PIM_6-vaccinated compared to CAF01-controls (Fig3E and H). This tendency was confirmed by quantifying the bacterial loads in spleen homogenates: CFUs obtained after challenge in non-immunized, naïve animals were almost identical to CAF01-controls. By contrast, there was a significant one log reduction in the PIM_6-vaccinated group. In spleens from BCG-vaccinated animals no viable mycobacteria were detected (Fig3K).

III.4 After challenge expression levels of proinflammatory cyto- and chemokines and CD1b-isoforms differ between vaccination groups

Transcript levels of several immune genes were determined in the draining lymph node and the injection-site before and four weeks after *Mtb* challenge. Low transcript levels in the draining lymph node were recorded prior to the challenge. Four weeks after challenge, CAF01-controls showed high levels of proinflammatory cyto- and chemokines. By contrast, PIM_6- and BCG-vaccinated animals expressed significantly lower levels of IFNγ, TNF-α and CCL3, CXCL10 and CXCL11, but elevated levels of TGF-β. At the injection-site, PIM_6-vaccinated animals showed higher transcript levels of IFNγ, CXCL10, CXCL11, cathelicidin and granzyme K as CAF01-controls. The difference was close to significance ($p < 0.1$). BCG-vaccinated animals expressed significantly lower levels of IFNγ and TNF-α, but significantly higher levels of TGF-β, IL12 and IL18. After the challenge, there

was a dramatic decrease of CD1b-expression, which affected all CD1b-isoforms. The decrease was less pronounced in PIM_6- and BCG-vaccinated animals, leaving a significant difference to CAF01-controls (Fig4A). The discrepancy between transcript levels of CD1b1 before and after challenge was significant for CAF01- and PIM_6-vaccinated. For CD1b4 the difference was significant in all three groups. No difference before and after challenge was observed for transcript levels of peptide-presenting MHC-I molecules. In contrast to CAF01-vaccinated animals, PIM_6-vaccinated guinea pigs showed a significant higher level of MHC-II-expression (Fig4B).

III.5 CD1b1/b4-expressing cells localize in T-cell-rich subcapsular areas of draining axillary lymph nodes

To understand the spatial distribution of different cell populations in the draining lymph node, classical immunohistochemistry was combined with *in situ* hybridization four weeks after challenge (Fig5). CD1b1/b4-expressing cells were almost exclusively found in T-cell-areas close to the subcapsular sinus. Only few CD1b1/b4-expressing cells were detected in the macrophage-rich areas of the granuloma. In lymphatic areas of lymph nodes significantly higher numbers of CD1b1/b4-expressing cells were found in PIM_6- compared to CAF01-vaccinated animals. Numerous CD1b1/b4-expressing cells were observed in lymph nodes of BCG-vaccinated animals, but as only two BCG-samples were available the difference only showed a non-significant tendency ($p<0,1$) (Fig5B). A representative comparison between CD1b1/b4-expression in the lymph node of a PIM_6-, a BCG- and a CAF01-vaccinated animal is shown in supplemental FigS2. Distribution of IFNγ-expressing cells showed an inverse pattern: The majority of IFNγ-positive cells was found within macrophage-rich areas of granulomas. In lymphatic areas, IFNγ-expression was less abundant. In PIM_6- and in BCG-vaccinated animals there were fewer IFNγ-expressing cells, although the differences did not reach significance (Fig5C). Within lymph node granulomas, activated macrophages represented the predominant cell type, comprising foamy and epitheloid macrophages, followed by CD3-positive T- and some scattered B-cells (Fig5D). In BCG-vaccinated animals T- and B-cells were more abundant than in other groups. As a prominent Th1-related chemokine also CXCL10-expression was assessed: In correspondence to transcriptional data

obtained by qRT-PCR, a reduction of CXCL10-expressing cells in samples obtained from BCG-vaccinated animals was observed. In lymphatic areas, this finding paralleled the reduced numbers of IFNγ-expressing cells (Fig5D).

IV. Discussion

The role of lipid-reactive T-cells in the fine-tuned interplay between pathogens and immune system is still only partially understood. The current study aimed to elucidate whether lipid-reactive T-cells contribute to immune protection against virulent mycobacteria. For this, guinea pigs are the ideal model, because, in contrast to murine rodents, they naturally express a functional CD1-type1-system [17], they are highly susceptible to mycobacterial infections and develop similar pathology as human TB-patients [31]. In the guinea pig model, BCG-vaccination confers relatively robust protection against virulent *Mtb* [32]. In a first step, we therefore tested the initiation of anti-mycobacterial lipid responses by BCG-vaccination. Of a limited set of different lipid antigens only PIM_6 induced a significant response in BCG-vaccinated guinea pigs. As we used outbred guinea pigs and an indirect stimulation assay to measure PIM_6-reactivity, the nature of that T-cell-response has to be interpreted with caution. However, the fact that prior to immunization no reactivity was observed and also that control animals did not respond to the PIM_6-preparation precludes the possibility that the observed *ex vivo* proliferation to PIM_6 in BCG- or PIM_6-vaccinated animals was due to innate immune activation, e.g. by the TLR2-agonistic activity of PIMs [33]. The reaction represents a *bona fide* recall-response of T-cells that were induced in the course of immunization. BCG-vaccination induced a strong response to the entire breadth of mycobacterial antigens. This is clearly reflected by the strong proliferation to BCG-lysate. Native lipid preparations of mycobacteria are at risk to be contaminated with hydrophobic peptides that can be immunogenic by themselves [4]. We cannot formally exclude the possibility that a certain percentage of the BCG-induced, polyclonal T-cell-response to the PIM_6-preparation reacted to such contaminants. However, results shown in Fig1D demonstrate a significant reduction of PIM_6-induced IFNγ-upregulation in the presence of CD1b-blocking antibodies. This suggests that at least a predominant part of the PIM_6-reactivity depends on CD1b-presentation. This observation significantly contributes to the ongoing discussion on the role of DURT-cells as targets for future TB-vaccines [34]. Very recently, two prospective cohort studies came to the conclusion that BCG vaccination had no effect on CD1b-restricted DURT-cells [35]. However, in this study CD1-restricted T-cells were only tested by flowcytometry using GMM-loaded CD1-tetramers. In our study

BCG-vaccinated guinea pigs also did not respond to GMM. This may indicate that BCG is poorly inducing GMM-specific T cells, but does not necessarily preclude a possible role for CD1-restricted DURT-cells.

Despite the limitation of available tools, we tried to characterize PIM_6-reactive T-cells phenotypically. We observed that the majority was CD4-positive, while a substantial minority was CD4-CD8-double-negative. This pattern differed from normal distribution of CD4- and CD8-positive cells. This corresponds to findings in humans, as it has been shown that the majority of lipid-reactive, CD1b-restricted human T-cells are CD4-positive [15]. In addition, *bona fide* CD1b-restricted T-cell-clones have been described that are double-negative, and it was initially believed that a double-negative phenotype was a marker for CD1-restriction [36, 37].

For specific induction of PIM_6-reactive cells, we formulated PIM_6 in CAF01-liposomes. This was a natural choice, because CAFs have been shown to be immunogenic in several animal models and have entered clinical trials [38]. Their efficacy has already been demonstrated in guinea pigs [25]. In a previous study, we formulated PIMs into CAF01, investigated the biophysical properties of resulting liposomes and tested their protective effect against *Mtb* [20]. However, unvaccinated animals served as controls and mechanistical aspects of the immune protection were not addressed. Since the stimulation with empty CAF01-liposomes, containing Mincle-agonist, TDB [39], could itself induce some immune protection, in the current study, we used animals that received empty CAF01-liposomes as controls. In addition, we investigated the antigen-specific immune response and observed that animals vaccinated with PIM_6-liposomes mounted a focussed response to PIM_6. There was no reaction to immunogenic proteins, such as Ag85, and no additional reactivity to the BCG-lysate – beyond the response to PIM_6. These data are consistent with a model wherein the effect of the PIM_6-vaccination on the trajectory of the mycobacterial challenge infection, as compared to CAF01-controls, can be attributed to PIM_6-specific cells. For the current study, we modified a well-established, parenteral challenge protocol [40]. We are aware that this does not recapitulate the natural route of infection, but subcutaneous inoculation induced a very defined primary complex, consisting of the granuloma at the injection site and corresponding lesions in the draining lymph node. This allowed for a detailed analysis of the lymph node response. In

accordance with our previous study [20], we found fewer and smaller necrotizing granulomas in presence of PIM_6-specific T-cells and overall a significantly-reduced bacterial burden. Compared to CAF01-controls, PIM_6-vaccinated animals showed increased levels of proinflammatory cyto- and chemokines at the site of injection, but reduced levels in the draining lymph node. In combination with reduced pathology, this indicates that preformed, PIM_6-specific T-cells contributed to a more efficient control of mycobacteria at the site of infection. BCG-vaccinated animals showed a different cytokine pattern at the site of injection: They expressed significantly lower levels of IFNγ and TNFα but elevated levels of TGFβ and IL12. This is in accordance with previous reports [41] and may be due to the fact that BCG-mediated protection involves additional immune mechanisms related to trained immunity [42]. To investigate immune processes at the cellular level, we conducted comprehensive microscopic analyses. By ISH we confirmed the reduced expression of IFNγ and CXCL10 in the draining lymph nodes of PIM_6- and BCG-vaccinated animals. The majority of positive cells resided in the macrophage-rich areas of granulomas. The most likely source of IFNγ were CD3 positive T-cells, while CXCL10 was predominantly associated with Iba1-positive macrophages. Important in our context was the distribution of CD1b-expression. High numbers of CD1b1/b4-expressing cells were found at early time points during granuloma development (preliminary data not shown). When granulomas had reached a mature stage, the numbers of CD1b1/b4-expressing cells inside granulomas declined (see supplemental FigS2 and S3). CD1-expression was still detectable, but majority of granuloma-resident macrophages was not associated with CD1b1/b4-expression. This is in accordance with a study that investigated the presence of CD1b-expressing cells in human TB-granulomas. In this study, it was found that individual cells stained positive for CD1b, while the majority of granuloma-resident macrophages was CD1b-negative [43]. Intriguingly, in CAF01-controls fewer CD1-expressing cells were observed than in PIM_6- or BCG-vaccinated animals. Maybe, the maintained CD1b-expression in PIM_6- and BCG-vaccinated was due to a feedback mechanism involving interaction of lipid-reactive T-cells with CD1-expressing APCs. A direct back-signaling is unlikely, as neither MHC- nor CD1-molecules bear phosphorylation-motifs at their cytoplasmic tail. However, a cross-talk has been described for CD1d-restricted NKT-cells that regulates dendritic cell function and possibly maintains CD1d-

436 expression via a GM-CSF-mediated pathway [44, 45]. The close correlation between number of
437 proliferated PIM_6-specific T-cells 28 days after the first immunization and CD1b1- and CD1b4-
438 transcript levels four weeks after challenge points in this direction (see supplemental FigS4A).
439 Another observation in this context was the presence of large numbers of CD1b1/b4-expressing
440 cells in subcapsular areas of draining lymph nodes. This localization is important, because this is,
441 where the lymph from the tributary region enters the lymph node parenchyma. It has been
442 described that mycobacteria-infected macrophages release exosomes from their endosomal
443 compartment that carry high amounts of mycobacterial PIMs- and other mycobacterial lipids [46].
444 It may be that the subcapsular CD1b-expressing cells take up lymph-borne, exosome-packaged
445 lipids and present them to CD1b-restricted T-cells. Hence, the CD1-T-cell-axis could represent a
446 vigilance system that responds to lipid antigens in the lymph and recruits additional immune cells
447 to infected tissues. Along this line, we observed a close correlation between number of T-cells
448 infiltrating the injection-site-granuloma and number of CD1b1-expressing cells in the lymph node
449 (see supplemental FigS4B).
450 Altogether, our study reveals the existence of PIM_6-reactive T-cells in guinea pigs after BCG- and
451 liposome-formulated-PIM_6-vaccination. Our data suggest that this reactivity is at least in part CD1b-
452 restricted. PIM_6-reactive cells contribute to reduced pathology and bacterial loads and seem to
453 have a beneficial influence on the course of infection after virulent *Mtb*-challenge. This underscores
454 the relevance of mycobacterial, non-protein antigens. Clearly, BCG induced a more robust
455 protection compared to liposomal PIM_6, but the small population of PIM_6-specific cells responding
456 to one single, mycobacterial lipid made a significant difference both in terms of pathology and
457 bacterial burden. This shows that the lipid-T-cell-axis can provide a complementary layer of immune
458 protection and emphasises that CD1-restricted, DURT-cells should be considered in future
459 approaches to develop a vaccine against tuberculosis.

Acknowledgements

We are grateful for the courteous provision of important hybridoma cell lines by Branch Moody, Steven Porcelli, Hubert Schäfer and Thomas Müller and kind provision of *M. tuberculosis* H37Rv by Stefan H.E. Kaufmann. We are thankful for the generous supply of research reagents by Tom Ottenhoff and Kees Franken and the US-government funded BEI-program. We are particularly grateful to Wiebke Lange, Silvia Schuparis, Gabriele Czerwinski and Ulrike Zedler for their excellent technical support. We pay tribute to Frank Klipp and all the animal care takers, and we sincerely acknowledge the help of Angele Breithaupt and Svenja Mamerow.

Disclosure

The authors declare no competing interests.

Data Availability Statement

All data relevant to this manuscript is shown.

Author Contribution

E.E. – Experimentation, Data Analysis, Writing; J.S. – Experimentation, Data Analysis, Writing; M.G. – Experimentation, Data Analysis; J. S-E. – Experimentation; B.C. – Critical Infrastructure, Writing/ Reviewing; A.D. – Critical Infrastructure, Conceptualization, Writing/ Correction; J.T. – Critical Infrastructure and Reagents, Conceptualization, Supervision, Writing/ Correction; D.A. – Experimentation, Data Analysis; A.G. – Critical Reagents, Conceptualization; M.G. – Critical Reagents, Conceptualization, Writing; M.B. – Experimentation, Data Analysis, Conceptualization, Funding, Writing

484 **References**

485

486 1. Andersen, P. & Doherty, T. M., The success and failure of BCG - implications for a novel
487 tuberculosis vaccine. *Nat Rev Microbiol* **3**: 656-662 (2005).

488 2. van Hooij, A. et al., BCG-induced immunity profiles in household contacts of leprosy
489 patients differentiate between protection and disease. *Vaccine* **39**: 7230-7237 (2021).

490 3. Mattow, J. et al., Comparative proteome analysis of culture supernatant proteins from
491 virulent Mycobacterium tuberculosis H37Rv and attenuated M. bovis BCG Copenhagen.
492 *Electrophoresis* **24**: 3405-3420 (2003).

493 4. Kaufmann, E. et al., BCG Vaccination Induces Robust CD4+ T Cell Responses to
494 Mycobacterium tuberculosis Complex-Specific Lipopeptides in Guinea Pigs. *J Immunol*
495 **196**: 2723-2732 (2016).

496 5. Bastian, M., Braun, T., Bruns, H., Rollinghoff, M. & Stenger, S., Mycobacterial Lipopeptides
497 Elicit CD4+ CTLs in Mycobacterium tuberculosis-Infected Humans. *J Immunol* **180**: 3436-
498 3446 (2008).

499 6. Layre, E. et al., Mycolic acids constitute a scaffold for mycobacterial lipid antigens
500 stimulating CD1-restricted T cells. *Chem Biol* **16**: 82-92 (2009).

501 7. Gilleron, M. et al., Diacylated Sulfoglycolipids Are Novel Mycobacterial Antigens
502 Stimulating CD1-restricted T Cells during Infection with Mycobacterium tuberculosis. *J Exp*
503 *Med* **199**: 649-659 (2004).

504 8. Moody, D. B. et al., T cell activation by lipopeptide antigens. *Science* **303**: 527-531 (2004).

505 9. Sieling, P. A. et al., CD1-restricted T cell recognition of microbial lipoglycan antigens.
506 *Science* **269**: 227-230 (1995).

507 10. Joosten, S. A. et al., Harnessing donor unrestricted T-cells for new vaccines against
508 tuberculosis. *Vaccine* **37**: 3022-3030 (2019).

509 11. Nigou, J. et al., The phosphatidyl-myo-inositol anchor of the lipoarabinomannans from
510 Mycobacterium bovis bacillus Calmette Guerin. Heterogeneity, structure, and role in the
511 regulation of cytokine secretion. *J Biol Chem* **272**: 23094-23103 (1997).

512 12. Moody, D. B., Zajonc, D. M. & Wilson, I. A., Anatomy of CD1-lipid antigen complexes. *Nat*
513 *Rev Immunol* **5**: 387-399 (2005).

514 13. Moody, D. B. & Porcelli, S. A., Intracellular pathways of CD1 antigen presentation. *Nat Rev*
515 *Immunol* **3**: 11-22 (2003).

516 14. Van Rhijn, I. et al., CD1b-mycolic acid tetramers demonstrate T-cell fine specificity for
517 mycobacterial lipid tails. *Eur J Immunol* **47**: 1525-1534 (2017).

518 15. Kasmar, A. G. et al., CD1b tetramers bind alphabeta T cell receptors to identify a
519 mycobacterial glycolipid-reactive T cell repertoire in humans. *J Exp Med* **208**: 1741-1747
520 (2011).

521 16. Koch, R., Die Aetiologie der Tuberculose. *Berliner Klinische Wochenschrift* **19**: 1-5 (1882).

522 17. Hiromatsu, K. et al., Characterization of guinea-pig group 1 CD1 proteins. *Immunology*
523 **106**: 159-172 (2002).

524 18. Dascher, C. C. et al., Conservation of a CD1 multigene family in the guinea pig. *J Immunol*
525 **163**: 5478-5488 (1999).

526 19. Dascher, C. C. et al., Conservation of CD1 intracellular trafficking patterns between
527 mammalian species. *J Immunol* **169**: 6951-6958 (2002).

20. Larrouy-Maumus, G. et al., Protective efficacy of a lipid antigen vaccine in a guinea pig model of tuberculosis. *Vaccine* **35**: 1395-1402 (2017).

21. Watanabe, Y. et al., BCG vaccine elicits both T-cell mediated and humoral immune responses directed against mycobacterial lipid components. *Vaccine* **24**: 5700-5707 (2006).

22. Dascher, C. C. et al., Immunization with a mycobacterial lipid vaccine improves pulmonary pathology in the guinea pig model of tuberculosis. *Int Immunol* **15**: 915-925 (2003).

23. Hiromatsu, K. et al., Induction of CD1-restricted immune responses in guinea pigs by immunization with mycobacterial lipid antigens. *J Immunol* **169**: 330-339 (2002).

24. Agger, E. M. et al., Cationic liposomes formulated with synthetic mycobacterial cordfactor (CAF01): a versatile adjuvant for vaccines with different immunological requirements. *PLoS One* **3**: e3116 (2008).

25. Commandeur, S. et al., The in vivo expressed Mycobacterium tuberculosis (IVE-TB) antigen Rv2034 induces CD4(+) T-cells that protect against pulmonary infection in HLA-DR transgenic mice and guinea pigs. *Vaccine* **32**: 3580-3588 (2014).

26. Spohr, C. et al., A new lymphocyte proliferation assay for potency determination of bovine tuberculin PPDs. *Altex* **32**: 201-210 (2015).

27. Mitchison, D. A. et al., A comparison of the virulence in guinea-pigs of South Indian and British tubercle bacilli. *Tubercle* **41**: 1-22 (1960).

28. Jain, R. et al., Enhanced and enduring protection against tuberculosis by recombinant BCG-Ag85C and its association with modulation of cytokine profile in lung. *PLoS One* **3**: e3869 (2008).

29. Mulisch, M. & Welsch, U., *Romeis - Mikroskopische Technik*, 19. Edn. Springer, Heidelberg - Berlin, (2019).

30. Bankhead, P. et al., QuPath: Open source software for digital pathology image analysis. *Sci Rep* **7**: 16878 (2017).

31. Clark, S., Hall, Y. & Williams, A., Animal models of tuberculosis: Guinea pigs. *Cold Spring Harb Perspect Med* **5**: a018572 (2014).

32. Keyser, A., Troudt, J. M., Taylor, J. L. & Izzo, A. A., BCG sub-strains induce variable protection against virulent pulmonary Mycobacterium tuberculosis infection, with the capacity to drive Th2 immunity. *Vaccine* **29**: 9308-9315 (2011).

33. Gilleron, M., Quesniaux, V. F. & Puzo, G., Acylation state of the phosphatidylinositol hexamannosides from Mycobacterium bovis bacillus Calmette Guerin and mycobacterium tuberculosis H37Rv and its implication in Toll-like receptor response. *J Biol Chem* **278**: 29880-29889 (2003).

34. Soma, S., Lewinsohn, D. A. & Lewinsohn, D. M., Donor Unrestricted T Cells: Linking innate and adaptive immunity. *Vaccine* **39**: 7295-7299 (2021).

35. Gela, A. et al., Effects of BCG vaccination on donor unrestricted T cells in two prospective cohort studies. *EBioMedicine* **76**: 103839 (2022).

36. Gumperz, J. E. & Brenner, M. B., CD1-specific T cells in microbial immunity. *Curr Opin Immunol* **13**: 471-478 (2001).

37. Beckman, E. M. et al., Recognition of a lipid antigen by CD1-restricted alpha beta+ T cells. *Nature* **372**: 691-694 (1994).

38. Christensen, D., Korsholm, K. S., Andersen, P. & Agger, E. M., Cationic liposomes as vaccine adjuvants. *Expert Rev Vaccines* **10**: 513-521 (2011).

573 39. Desel, C. et al., The Mincle-activating adjuvant TDB induces MyD88-dependent Th1 and
574 Th17 responses through IL-1R signaling. *PLoS One* **8**: e53531 (2013).

575 40. Balasubramanian, V., Guo-Zhi, W., Wiegeshaus, E. & Smith, D., Virulence of
576 Mycobacterium tuberculosis for guinea pigs: a quantitative modification of the assay
577 developed by Mitchison. *Tuber Lung Dis* **73**: 268-272 (1992).

578 41. Ly, L. H., Russell, M. I. & McMurray, D. N., Cytokine profiles in primary and secondary
579 pulmonary granulomas of Guinea pigs with tuberculosis. *Am J Respir Cell Mol Biol* **38**:
580 455-462 (2008).

581 42. Kaufmann, E. et al., BCG Educates Hematopoietic Stem Cells to Generate Protective
582 Innate Immunity against Tuberculosis. *Cell* **172**: 176-190 e119 (2018).

583 43. Chancellor, A. et al., CD1b-restricted GEM T cell responses are modulated by
584 Mycobacterium tuberculosis mycolic acid meromycolate chains. *Proc Natl Acad Sci U S A*
585 **114**: E10956-E10964 (2017).

586 44. Racke, F. K., Clare-Salzer, M. & Wilson, S. B., Control of myeloid dendritic cell
587 differentiation and function by CD1d-restricted (NK) T cells. *Front Biosci* **7**: d978-985
588 (2002).

589 45. Gillessen, S. et al., CD1d-restricted T cells regulate dendritic cell function and antitumor
590 immunity in a granulocyte-macrophage colony-stimulating factor-dependent fashion. *Proc*
591 *Natl Acad Sci U S A* **100**: 8874-8879 (2003).

592 46. Beatty, W. L. et al., Trafficking and release of mycobacterial lipids from infected
593 macrophages. *Traffic* **1**: 235-247 (2000).

594

595 **Captions**
596
597 **Figure 1 BCG-vaccination elicits CD1b-restricted, PIM_6-specific T-cell-responses:**

598 Four weeks after BCG-vaccination PBMCs were isolated. Autologous, CD1b-expressing APCs and
599 non-adherent lymphocytes were stained with CFSE and stimulated with mycobacterial antigens.
600 CFSE dilution was analyzed by flow-cytometry after five days. (A) Seven guinea pigs were control-
601 treated. Eight guinea pigs were BCG-vaccinated. After four weeks, T-cell-proliferation in response
602 to the indicated mycobacterial antigen was assessed. Black bars represent the group mean as
603 determined by nested-data-analysis. Error bars represent the standard error of the mean. Asterisks
604 indicate the level of significance as determined by nested-t-test in comparison to the medium
605 control. (B) CFSE-low, PIM_6-reactive lymphocytes were stained for a general T-cell-marker, CD4
606 and CD8. The small panel at the left shows the gating strategy. The larger pseudo-color graph
607 representatively shows the CD4- and CD8-distribution. The dot blot on the right shows the relative
608 distribution for T-cell-markers in PIM_6-reactive cells four weeks after BCG-vaccination. Red
609 symbols represent the normal T-cell- and CD4-CD8-distribution in PBMCs from naïve control
610 guinea pigs. Asterisks indicate the level of significance as determined by unpaired t-test. (C)
611 Lymphocytes were stimulated with PIM_6 as described above. After 24 hours RNA was harvested.
612 Cytokine-transcript levels were determined by qRT-PCR in relation to β-Actin. Open bars represent
613 non-stimulated controls, black bars represent transcript levels after PIM_6-stimulation. The left panel
614 shows the results for BCG-vaccinated animals, the right panel shows the upregulation of IFNγ, GM-
615 CSF and IL17 for naïve, non-immunized animals. Black bars represent the group mean. Error bars
616 indicate the standard error of the mean. Asterisks depict the level of significance as determined by
617 Wilcoxon-matched-pair-signed-ranked-test in comparison to non-stimulated medium controls. (D)
618 IFNγ-transcript levels were assessed in the presence of CD1b-blocking or isotype-matched control
619 antibodies. Individually colored circles represent transcript levels of eight BCG-vaccinated guinea
620 pigs four weeks after vaccination. Asterisks depict the level of significance as determined by
621 Wilcoxon-matched-pair-signed-ranked-test as indicated.

Figure 2 **CAF01-adjuvanted PIM_6 induces PIM_6-reactive T-cell-responses:**

(A) Six guinea pigs per group were vaccinated three times with CAF01-adjuvanted PIM_6 **[PIM]**, empty CAF01-liposomes **[CAF]** or BCG **[BCG]**. After twelve weeks the animals were challenged with *M. tuberculosis* H37Rv. Four weeks later the animals were euthanized and terminally analyzed. Blood was obtained at the indicated time points. (B) 28 days after first vaccination, PBMCs were isolated from vaccinated animals, stimulated and analysed as described for Fig1A. Asterisks indicate the level of significance as calculated by nested-t-test in comparison to the medium control. (C) The specificity index of the T-cell-response 28 days after vaccination was calculated for PIM_6- and BCG-vaccinated animals by dividing the number of cells that proliferated in response to PIM_6 by the number of $Lysat_{BCG}$-reactive cells. Asterisks indicate the level of significance as calculated by Mann-Whitney-test. (D) The number of PIM_6-reactive T-cells is shown for the different time points tested. Black bars represent the group mean after PIM_6-stimulation, white bars the respective medium control. Error bars indicate the standard error of the mean, asterisks the level of significance as calculated by nested-t-test in comparison to PIM_6-stimulated cells from CAF01-vaccinated controls.

637 **Figure 3** **PIM_6- and BCG-vaccination of guinea pigs is associated with significant**
638 **reduction in necrosis and bacterial load:**

639 Four weeks after s.c. challenge with virulent *Mtb*, PIM_6-vaccinated [**PIM**] and control guinea pigs
640 [**CAF**, **BCG**] were euthanized and necropsied. A gross pathology score shows the overall severity
641 of granulomas as individual sum score (A) or focused at the organ level for the spleen (B), (n=6)
642 per group. (C-J) Tissue sections of the injection-site-granuloma, the draining lymph node and the
643 spleen were stained with hematoxylin-eosin or immunophenotyped using an *Mtb*-specific antibody.
644 The relative area of necrosis within granulomas and the amount of *Mtb*-positive spots per mm^2 were
645 determined for the injection-site-granuloma (C-E), the draining right axillary lymph node (F-H) and
646 for the spleen (I, J). Representative sections are shown from CAF01-vaccinated animals. Black
647 bars represent the group mean, error bars represent the standard error of the mean. Spleen
648 homogenates from the three treated groups and from a group of six non-immunized guinea pigs
649 were cultured and the number of colony-forming units are depicted. Circles indicate individual
650 animals, bars represent the group mean. Asterisks indicate the level of significance as calculated
651 by unpaired-t- or Mann-Whitney-test.

652 **Figure 4** **After challenge expression levels of proinflammatory cyto- and chemokines and**
653 **CD1b-isoforms differ between vaccination groups:**

654 Draining lymph nodes of the site of vaccination or inoculation and injection-site-granulomas from
655 *Mtb*-challenged animals were harvested and homogenized to isolate bulk RNA. Transcript-levels
656 of the indicated immune genes were quantified by qRT-PCR in relation to β-Actin. (A) The left
657 heatmap shows the expression level in the draining lymph node 80 days after vaccination. In the
658 middle the expression level in the draining lymph node, and on the right the injection-site-granuloma
659 four weeks later after virulent *Mtb*-challenge is shown. Columns correspond to respective
660 vaccination groups, rows to the corresponding gene. Expression values are shown as group mean
661 calculated in relation to β-Actin. Asterisks indicate the level of significance, as calculated by Mann-
662 Whitney-test in comparison to CAF01-controls. (B) Bar graphs show selected transcript-levels of
663 antigen presenting molecules in the draining axillary lymph node before and four weeks after
664 challenge. Black bars represent the group mean and error bars the standard error of the mean.
665 Asterisks indicate the level of significance as calculated by unpaired-T-test.

Figure 5 Four weeks after *Mtb*-challenge CD1b1/b4-expressing cells localize in the T-cell-rich subcapsular areas of draining lymph nodes:

Sections of draining lymph nodes were investigated by ISH and IHC. (A) An HE-stained section of the right axillary lymph node from a PIM_6-vaccinated animal is shown in low magnification. The rectangle is shown in higher magnification for consecutive sections stained by IHC for Iba-1 positive macrophages or CD3-expressing T-cells and by ISH for the expression of CD1b1/b4 and IFNγ. Black arrows indicate single positive cells. The number of CD1b1/b4- (B) or IFNγ-expressing (C) cells per mm^2 within lymph node granulomas or the surrounding lymphatic area was quantified. Black bars represent the group mean, error bars the standard error of the mean. (D) Consecutive sections of the same samples were additionally stained for macrophage marker Iba-1, B-cell-marker CD79 or were subjected to ISH using a CXCL10-specific probe. The heatmap shows a comprehensive overview of the numbers of positive cells per mm^2 within the granulomatous or the surrounding lymphatic areas. Rows correspond to the three vaccination groups, columns to the tested surface marker or transcript. Numbers represent group means for five CAF01- or PIM_6-vaccinated and two BCG-vaccinated animals. Asterisks indicate the level of significance as calculated by Mann-Whitney-test in comparison to the CAF01-vaccinated group.

Fig 1

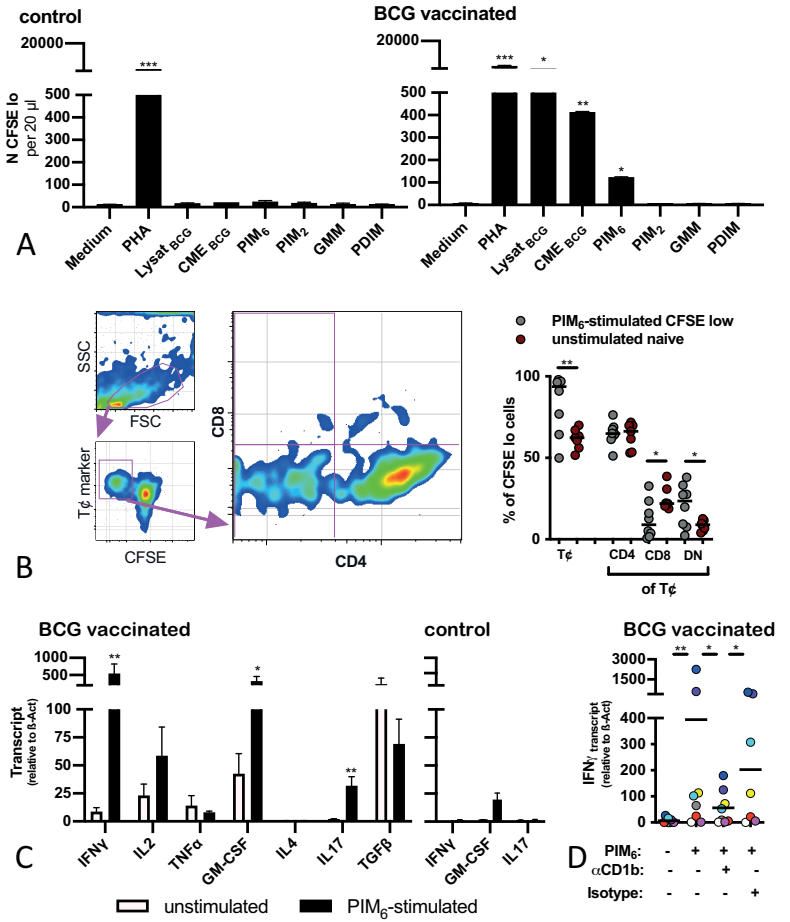
control
BCG vaccinated
N CFSE lo per 20 µl
Medium
PHA
Lysat BCG
CME BCG
PIM6
PIM2
GMM
PDIM
A
SSC
FSC
Tɸ marker
CFSE
CD8
CD4
B
PIM6-stimulated CFSE low
unstimulated naive
% of CFSE lo cells
Tɸ
CD4
CD8
DN
of Tɸ
BCG vaccinated
control
Transcript (relative to ß-Act)
IFNγ
IL2
TNFα
GM-CSF
IL4
IL17
TGFβ
C
unstimulated
PIM6-stimulated
BCG vaccinated
IFNγ transcript (relative to ß-Act)
D
PIM6:
αCD1b:
Isotype:

Fig 2

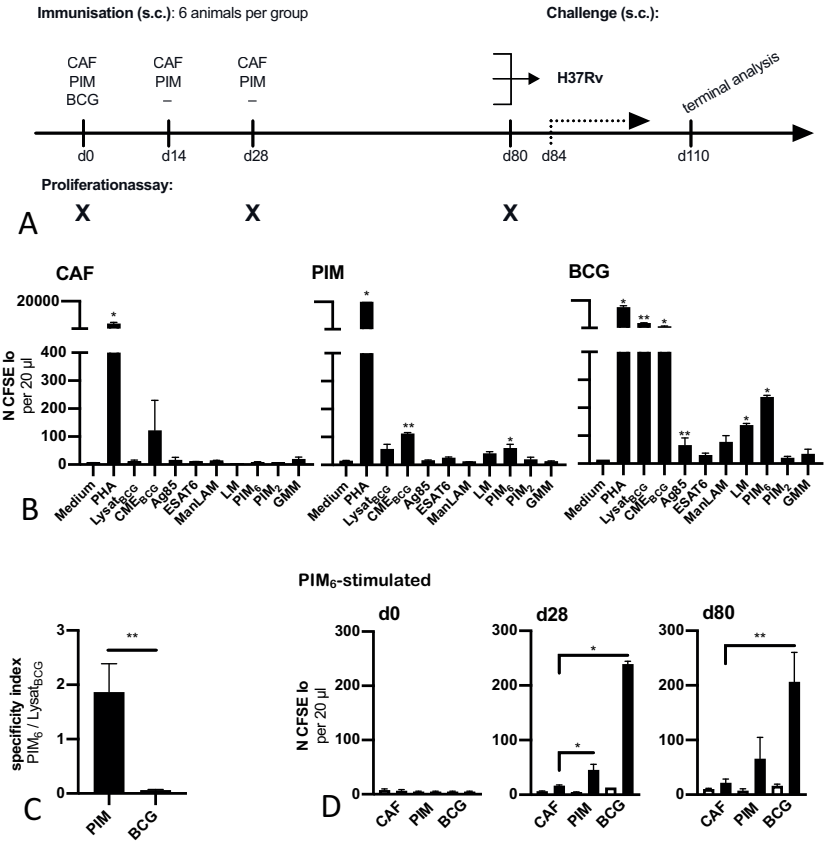
Immunisation (s.c.): 6 animals per group
Challenge (s.c.):
CAF
PIM
BCG
CAF
PIM
–
CAF
PIM
–
H37Rv
terminal analysis
d0
d14
d28
d80
d84
d110
Proliferationassay:
A
X
X
X
CAF
PIM
BCG
N CFSE lo
per 20 µl
B
Medium
PHA
Lysat BCG
CMF BCG
Ag85
ESAT6
ManLAM
LM
PIM6
PIM2
GMM
PIM6-stimulated
d0
d28
d80
specificity index
PIM6 / Lysat BCG
C
D
PIM
BCG
CAF

Fig 3

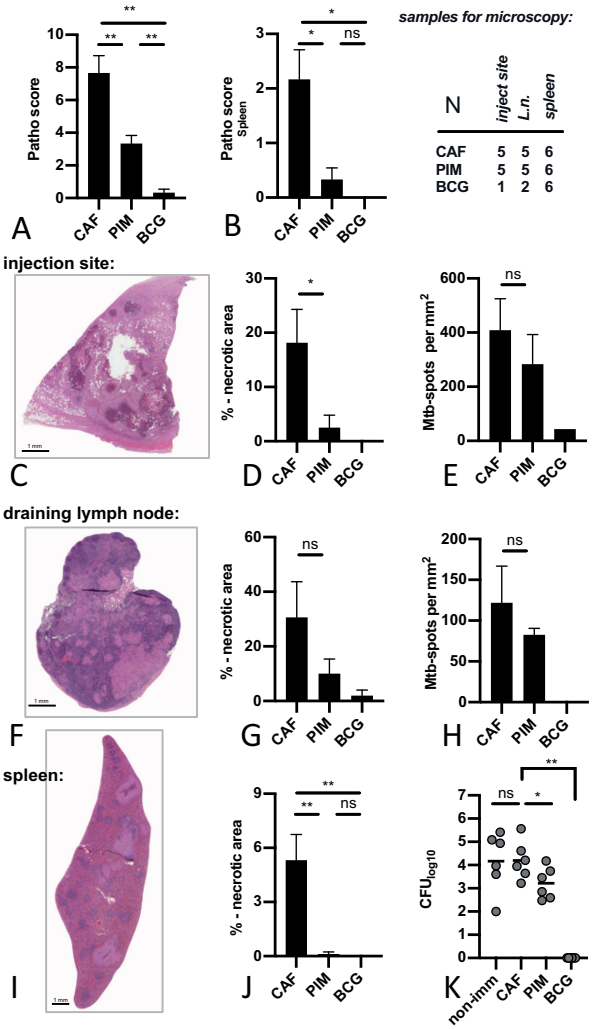
Patho score
CAF
PIM
BCG
A
Patho score Spleen
B
samples for microscopy:
N inject site L.n. spleen
CAF 5 5 6
PIM 5 5 6
BCG 1 2 6
injection site:
C
% - necrotic area
D
Mtb-spots per mm2
E
draining lymph node:
F
G
H
spleen:
I
J
CFUlog10
non-imm
K
ns

Fig 4


draining lymph node
before Mtb-challenge
draining lymph node
4 weeks after Mtb-challenge
injection site granuloma
4 weeks after Mtb-challenge
IFNγ 0.2 0.1 0.2 | 190.2 21.3 * 9.2 ** | 139.9 693.2 a 26.3 *
IL2 2.1 1.3 2.1 | 9.0 1.5 11.8 | 15.5 34.1 4.1
IL4 0.0 0.1 0.1 | 0.0 0.0 0.0 | 0.0 0.0 0.0
IL17 0.2 0.2 0.2 | 10.5 17.2 15.0 | 3.7 5.2 0.8 a
TNFα 0.6 0.6 0.6 | 7.7 2.5 * 2.3 * | 2.8 3.9 0.5 ****
TGFβ 16.0 13.1 19.4 | 32.7 71.0 82.7 ** | 1.2 1.3 3.6 **
GM-CSF 1.7 1.8 2.9 | 38.0 23.2 16.3 | 77.8 195.0 38.3
IL1 23.9 31.6 40.3 | 84.8 20.7 * 63.3 | 78.9 168.6 69.0
IL18 96.0 73.0 153.1 | 283.7 213.3 509.2 * | 112.2 446.7 a 671.8 *
IL6 0.5 0.8 * 1.3 | 18.8 4.5 * 7.3 | 11.7 42.6 28.6
IL12 0.6 0.5 0.7 | 1.8 2.0 2.8 | 0.4 2.0 27.6 *
IL23 0.1 0.1 0.1 | 15.7 2.7 7.7 | 2.9 5.6 1.3
CCL3 8.7 32.0 13.9 | 3755.5 271.3 ** 227.0 ** | 1829.2 6661.9 224.0
CCL5 152.6 104.9 189.7 | 13275.2 2592.0 4067.0 | 2988.6 8359.1 1285.0
CXCL8 1.0 3.3 1.2 | 156.5 5.5 * 9.2 * | 299.0 1315.6 56.2 *
CXCL10 20.3 27.9 43.4 | 1024.2 249.5 * 247.2 | 547.3 2767.6 a 280.0
CXCL11 4.8 8.5 7.8 | 1627.0 160.2 * 75.5 ** | 897.4 4366.0 a 227.7 a
Cathelicidin 4.7 2.7 6.5 | 54.5 134.3 19.3 | 4.6 26.3 a 21.8
Granzyme K 88.6 76.3 108.7 | 591.2 289.2 394.2 | 322.4 1516.6 a 478.3
CD1b1 34.5 22.7 29.4 | 1.5 4.5 16.3 ** | 7.2 6.5 24.5
CD1b2 10.0 11.2 12.8 | 2.4 1.2 2.5 | 4.6 3.1 5.6
CD1b3 108.2 132.5 123.9 | 18.2 46.1 * 45.1 ** | 49.3 46.0 113.1
CD1b4 133.0 152.8 115.9 | 5.8 12.7 51.4 ** | 5.9 20.0 a 9.1
MHC-I 1652.4 1884.4 1570.2 | 1500.8 1403.6 1396.1 | 3246.3 5995.9 4486.6
MHC-II 157.3 105.7 136.2 | 82.9 153.8 * 154.6 * | 106.1 372.2 757.7
β2m 1207.9 1406.6 1876.8 | 604.1 782.2 1255.6 * | 692.5 2083.2 7140.5
CAF PIM BCG CAF PIM BCG CAF PIM BCG
15 000
10 000
5 000
0
transcript levels
(relative to β-Actin)
A
a: p<0.1

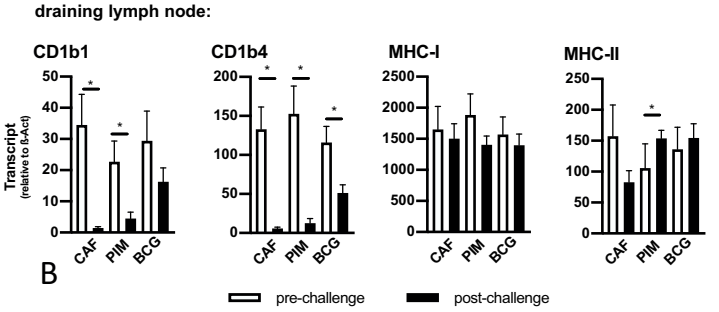
draining lymph node:
CD1b1
CD1b4
MHC-I
MHC-II
Transcript
(relative to β-Act)
CAF PIM BCG
B
pre-challenge
post-challenge

Fig 5

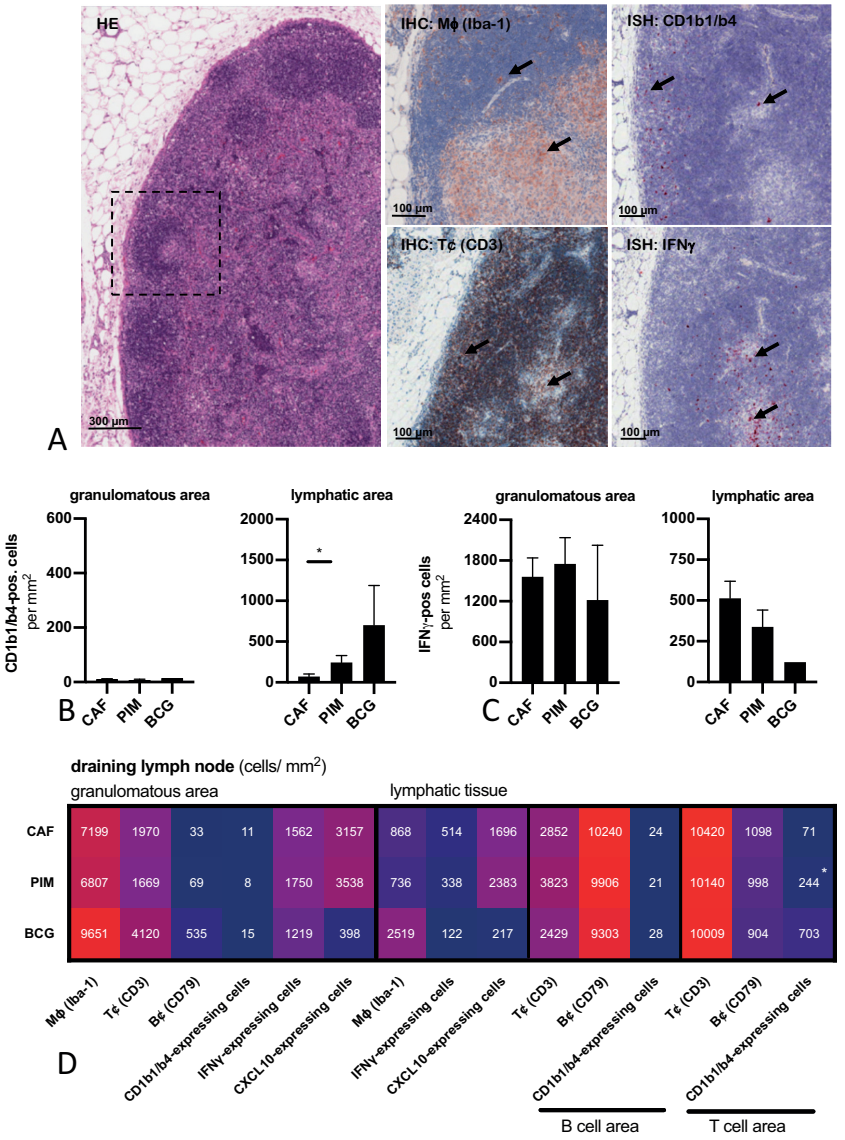
A
HE
IHC: Mϕ (Iba-1)
ISH: CD1b1/b4
IHC: Tc (CD3)
ISH: IFNγ
300 µm
100 µm
B
granulomatous area
lymphatic area
CD1b1/b4-pos. cells per mm2
CAF
PIM
BCG
C
granulomatous area
lymphatic area
IFNγ-pos cells per mm2
D
draining lymph node (cells/ mm2)
granulomatous area
lymphatic tissue
CAF 7199 1970 33 11 1562 3157 868 514 1696 2852 10240 24 10420 1098 71
PIM 6807 1669 69 8 1750 3538 736 338 2383 3823 9906 21 10140 998 244*
BCG 9651 4120 535 15 1219 398 2519 122 217 2429 9303 28 10009 904 703
Mϕ (Iba-1)
Tc (CD3)
Bc (CD79)
CD1b1/b4-expressing cells
IFNγ-expressing cells
CXCL10-expressing cells
B cell area
T cell area

Supplemental Table 1 – Pathology Score adapted from (27, 28)

Parameters	Score used
Inoculation site granuloma (right axillary subcutis)	
Granuloma(s) ≥3.5 cm in diameter with caseous necrosis	4
Granuloma(s) ≥2.5 cm in diameter with caseous necrosis	3
Granuloma(s) ≥1.5 cm in diameter ± caseous necrosis	2
Granuloma(s) ≥0.5 cm in diameter	1
No lesion	0
Right axillary lymph node	
Granuloma(s) ≥2.0 cm in diameter with caseous necrosis	4
Granuloma(s) ≥1.5 cm in diameter with caseous necrosis	3
Granuloma(s) ≥1.0 cm in diameter ± caseous necrosis	2
Granuloma(s) ≥0.5 cm in diameter	1
No lesion respectively of normal size (≤0.5 cm)	0
Spleen*	
Numerous granulomas (miliary type)	4
Many granulomas	3
Few granulomas	2
Single granulomas	1
No lesion	0
Liver*	
Numerous granulomas (miliary type)	4
Many granulomas	3
Few granulomas	2
Single granulomas	1
No lesion	0

*granulomas in spleen and liver were randomly distributed and 0.3 - 0.4 cm in diameter large

Supplemental Table 2 – qRT-PCR primer

gene	FORWARD-Primer	REVERSE-Primer	Annealing T°	amplicon size
ifng	ATTTCGGTCAATGACGAGCAT	GTTTCCTCTGGTTCGGTGACA	60 °C	90 bp
il2	GCAGTGCACCTACTTCAAGC	ACGCCTTCCAAGAGTGTCTG	60 °C	88 bp
il4	TCACGGACGTCTTTGCTGAT	CTCCCTCTCTGTTTGGGCAG	60 °C	120 bp
il17	CCTGGGACGCCTTCTTCAAT	TGGACACCCTGGATTTCGTG	60 °C	99 bp
tnfa	ACGCTCACACTCAGATCAGC	GCTGGTTTGCCACAACATGA	60 °C	70 bp
tgfb	GCTGCGAATGCAGAGACTCA	AGGTAGCGCCAGGAATTGTT	61 °C	84 bp
gm-csf	GAGGGCTCCTTGACCTTGATG	ATACAGGAAGTTTCCGGGGTCG	60 °C	70 bp
il1	GTTTCAGGCAGACCGTCTCA	GGAAGCAAGGGTCTCAGGTC	60 °C	106 bp
il18	GACTCCGACTGTGCAGACAA	CCCGTTACACGTCACAGAGA	60 °C	108 bp
il6	TTCCTCTCCACAAGCACCTTC	TATCAGCTGTGAAGTCGTGCT	60 °C	106 bp
il12p35	AAAACCAGCACCGTGAAAGC	GGCAACTCCCATTGGTTGTG	60 °C	100 bp
il23	GACGTTGATCAGCGACTCCC	CAGCCATCCCCACATAGGAT	60 °C	76 bp
ccl3	CCACGTGCATACGTAGCTGA	CTCCCGGCCTCTCTTGGTTA	60 °C	87 bp
ccl5	CCGCACCCACATCAAGGAAT	ACACACCTGGCGGTTCTTTC	61 °C	91 bp
cxcl8	GGCAGCCTTCCTGCTCTCT	CAGCTCCGAGACCAACTTTGT	61 °C	65 bp
cxcl10	CTCTGAGTGGGACTCAAGGAAT	AGGACTTTGGATTAACAGGTTGAGT	59 °C	90 bp
cxcl11	ACAGTTGTTCAAGGCTTCCC	GGCTTTTGCAATATCTGCCACTT	58 °C	96 bp
cathelicidin	AACGAAAACCTCTTCCGCCT	GCTTCGGACTATACGGGTCG	60 °C	73 bp
grzK	CCAGTCCGACAGCAATCACA	GCTGGCCTTCGACAAACAAAA	60 °C	98 bp
cd1b1	GCTTGGTAGCTTTGACAGCG	ACCTCTTCATTGCTGAAGTTTGC	60 °C	81 bp
cd1b2	TGCCTTTCCGGAGCCAATTT	GCTTGATTTTGTGCCCAGGT	61 °C	78 bp
cd1b3	ACTCAGGATGCCTTCCAAGAA	CTCCCAACCAGCCTGAGAGTT	59 °C	103 bp
cd1b4	GTGGATGCGGGGTGATAAGG	ATGTCTCATCAGCATTGGGCA	61 °C	71 bp
mhc-i	GAGAACGGGAAGGAGACGC	GGGTGACCTGTTCCTTGGAG	60 °C	85 bp
mhc-ii	TACCTGCCTTTCGTGCCATC	GGATGGGGCTTCGATCTTCA	60 °C	112 bp
b2m	TGCCTTATGCATCCAGTAAGAAAA	TGGAAGGGCAAACATGCAGA	59 °C	100 bp
β-act	ATGACGATATCGCTGCGCTC	CCATGCCTACCATGACTCCC	60 °C	138 bp

Primer for the indicated guinea pig genes were designed using the NCBI Primer-BLAST tool to span an amplicon size between 60 and 140 bp.

Supplemental Table 3 – antibodies

Antibody	Type	Antigen	Host	Dilution	Duration	AR	Temperature	Supplier	Article number
CD79α	HM57	CD79 α	mouse	1:50	Overnight	HTAR[a]	4°C	LSBio Sciences	LS-B4504
CD3	Polyclonal	CD3	rabbit	1:100	Overnight	HTAR[a]	4°C	Agilent	A045229-2
Iba-1	Polyclonal	Iba1 Fusion Protein Ag1363	rabbit	1:500	Overnight	HTAR[b]	4°C	Proteintech	10904-1-AP
M. tuberculosis	Polyclonal	PPD from *M. tuberculosis*	rabbit	1:500	Overnight	HTAR[b]	4°C	BioRad	OBT0974

a: HTAR: High-temperature antigen retrieval solution (20 minutes at 115°C in TRIS/EDTA-buffer, pH 9)

b: HTAR: High-temperature antigen retrieval solution (20 minutes at 115°C in citrate buffer, pH 6)

Abbreviations: AR: Antigen retrieval; Iba-1: allograft inflammatory factor 1; PPD: Purified protein derivative

Figure S1

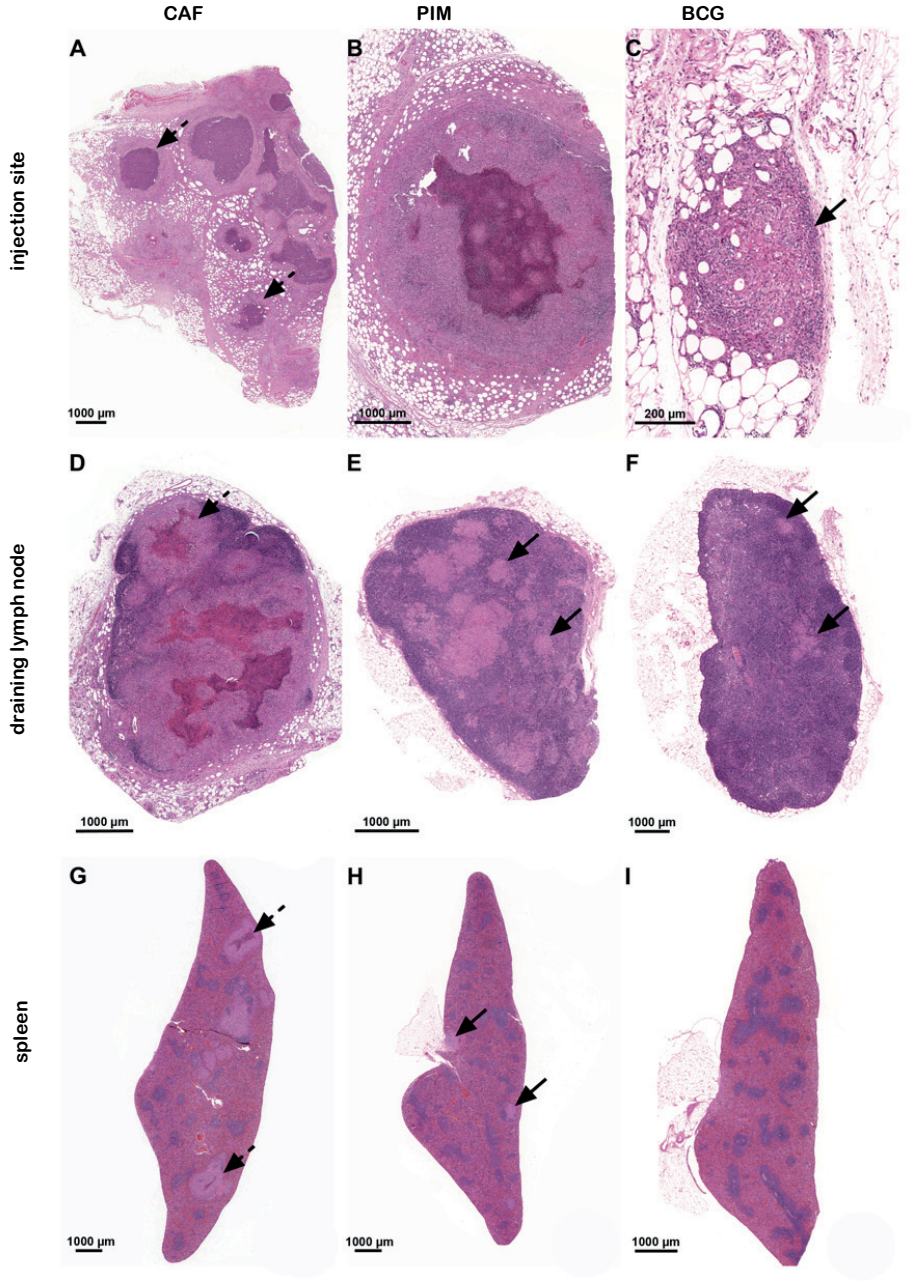
CAF
PIM
BCG
injection site
draining lymph node
spleen
A
B
C
D
E
F
G
H
I
1000 µm
1000 µm
200 µm
1000 µm
1000 µm
1000 µm
1000 µm
1000 µm
1000 µm

Figure S1 – Representative images of granulomas at the injection site, in the draining axillary lymph node and the spleen

Four weeks after s.c. challenge with virulent *Mtb*, PIM_6-, CAF01-, and BCG-vaccinated guinea pigs developed granulomas at the injection site, in the draining right axillary lymph node and spleen. Tissue sections were stained with hematoxylin and eosin and scanned as digital image. Granulomas of varying size and features developed in each subcutis, lymph node or spleen.
(A) Multiple granulomas with extensive necrosis (dashed arrows) are present at the injection site of this CAF01-vaccinated animal. (B) In this PIM_6-vaccinated animal similar granulomas are seen, but the necrosis is smaller. (C) In this BCG-vaccinated animal granulomas are reduced in size and are non-necrotic (arrow).
(D) Up to 90% of the lymph node in this CAF01-vaccinated animal is replaced by multiple granulomas with extensive necrosis (dashed arrow). (E) In this PIM_6-vaccinated animal multiple smaller non-necrotic granulomas (arrows) and fewer larger necrotic granulomas are seen. (F) Only few non-necrotic granulomas are detected in the paracortex of this lymph node from a BCG-vaccinated guinea pig.
(G) The spleen of this CAF01-vaccinated guinea pig shows multiple granulomas, mostly in association with the periarteriolar lymphoid sheaths (PALS) of the white pulp, some of them are of the necrotic type (dashed arrow). (H) Few non-necrotic granulomas (arrows) are seen near the PALS in this PIM6-vaccinated animal. (I) No granulomas are present in this the spleen of this BCG-vaccinated animal.

Figure S2

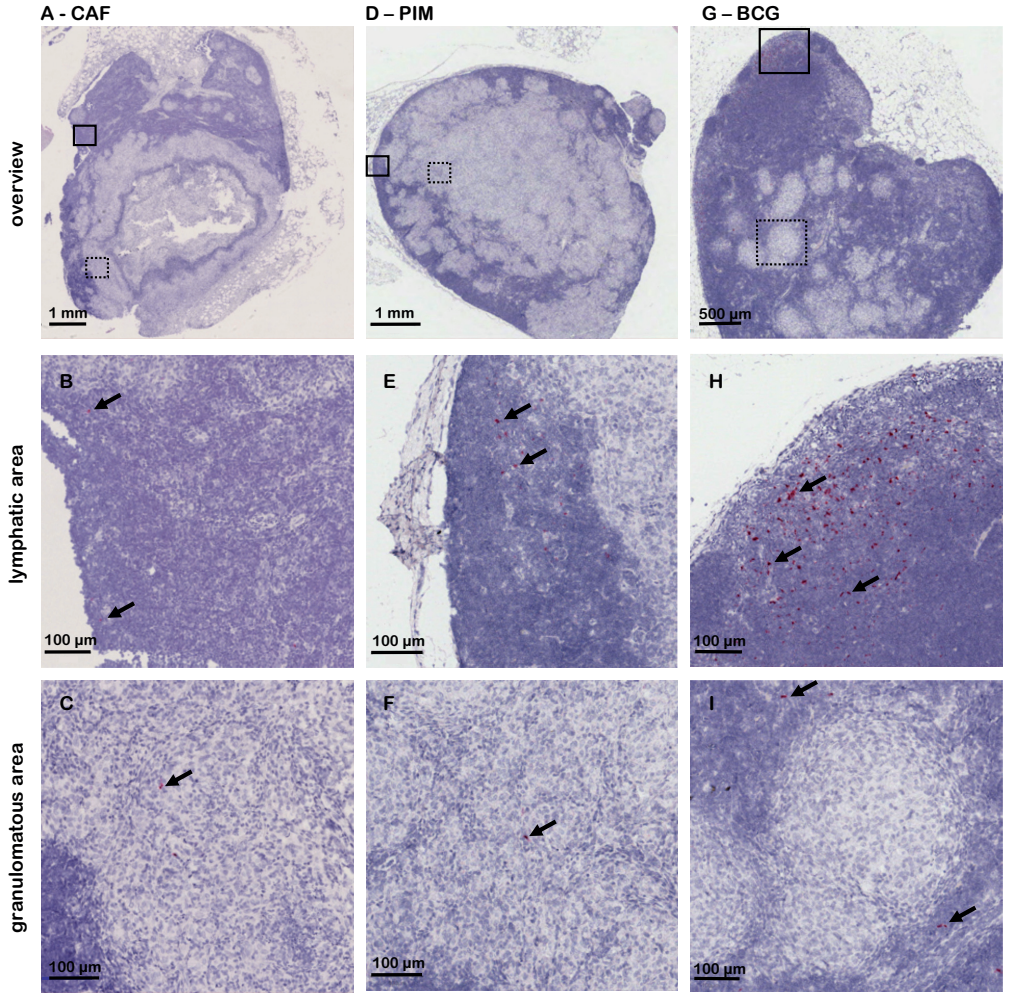
A - CAF
D – PIM
G – BCG
overview
lymphatic area
granulomatous area
1 mm
1 mm
500 µm
B
E
H
100 µm
100 µm
100 µm
C
F
I
100 µm
100 µm
100 µm

Figure S2 –CD1b1/b4-expressing cells are mainly found in the subcapsular region of the draining lymph nodes of PIM_6- or BCG-vaccinated animals

Four weeks after s.c. challenge with *Mtb*, PIM_6-vaccinated [PIM] and control guinea pigs [CAF, BCG] were euthanized and necropsied. FFPE-sections of the draining lymph nodes were investigated by in situ hybridization (ISH) for the expression of CD1b1/b4 (red). Hematoxylin (blue) was used for counterstaining. A-C: In this lymph node of a CAF01-vaccinated guinea pig an extensive necrotic granuloma formation is seen (A). Only few CD1b1/b4-expressing cells are detected in the lymphatic area (B, solid rectangle) and in the macrophage-rich rim of the granuloma (C, dotted rectangle). D-F: Multiple, non-necrotic granulomas deface the axillary lymph node of this PIM_6-vaccinated animal (D). Several CD1b1-expressing cells populate the subcapsular lymphatic area of the lymph node (E, solid rectangle). Only few, individual CD1b1/b4-expressing cells are detected in the macrophage-rich zone of the granuloma (F, dotted rectangle). G-I: In a BCG-vaccinated guinea pig the draining lymph node shows few, non-coalescing, non-necrotic granulomas (G). Numerous CD1b1/b4-expressing cells are present in the subcapsular lymphatic area (H, solid rectangle), no CD1b1/4-expressing cells are detected in the macrophage-rich area of a granuloma (I, dotted rectangle). Arrows indicate CD1b1/b4- expressing cells.

Figure S3

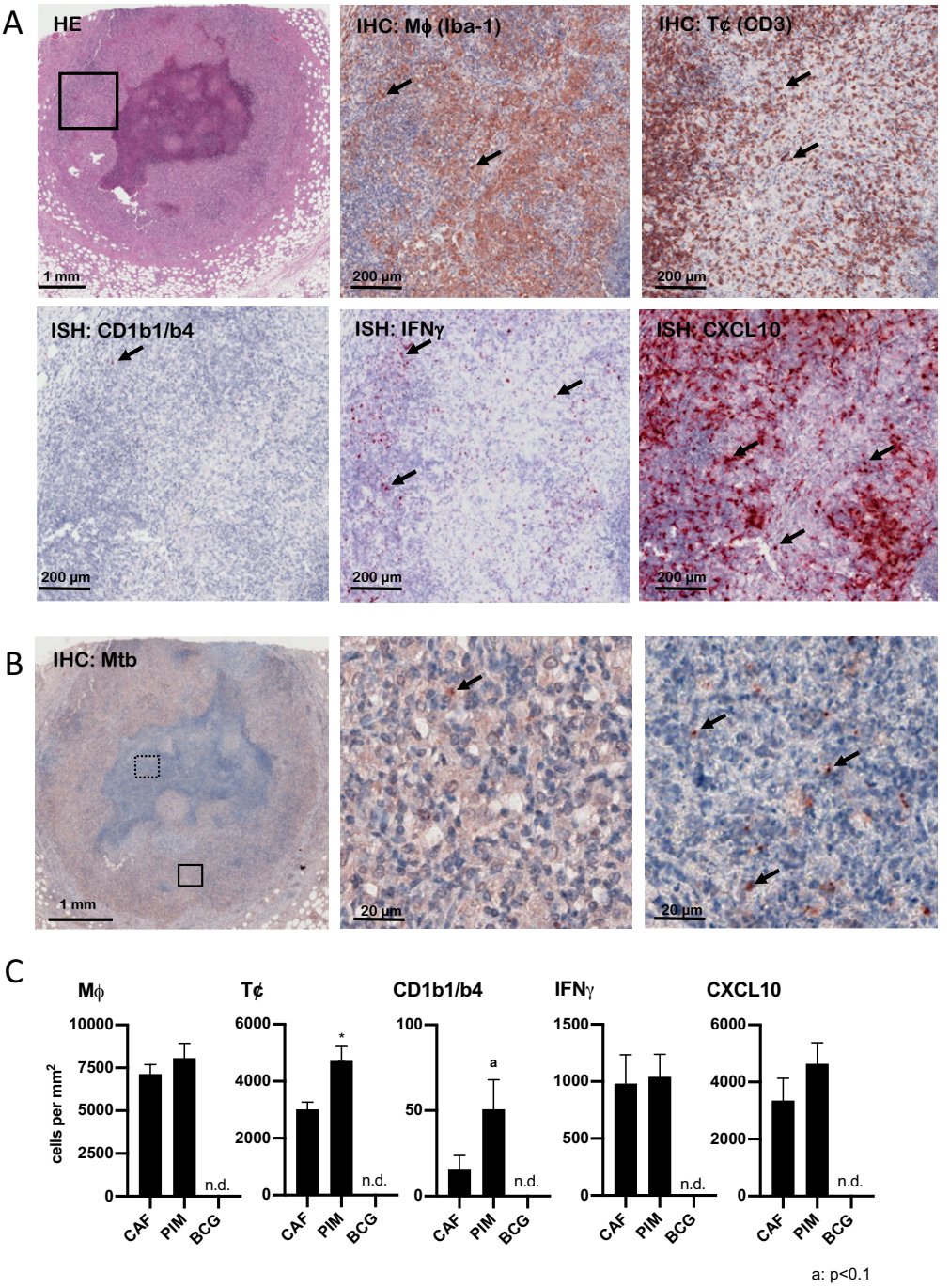
A
HE
1 mm
IHC: Mϕ (Iba-1)
200 µm
IHC: Tϕ (CD3)
200 µm
ISH: CD1b1/b4
200 µm
ISH: IFNγ
200 µm
ISH: CXCL10
200 µm
B
IHC: Mtb
1 mm
20 µm
20 µm
C
Mϕ
Tϕ
CD1b1/b4
IFNγ
CXCL10
cells per mm²
10000
7500
5000
2500
0
6000
4000
2000
100
50
1500
1000
500
n.d.
*
a
CAF
PIM
BCG
a: p<0.1

Figure S3 – Comprehensive pathohistological analysis of an injection site granuloma

Four weeks after challenge, sections of the injection site granuloma were investigated by in situ hybridization (ISH) and immunohistochemistry (IHC). (A) Representative stainings of a granuloma from a PIM_6-vaccinated animal are shown: The HE staining provides an overview, the black quadrant is shown in higher magnification for the specific stainings: In the upper panel from left to right: IHC: Iba-1-antibody, IHC: CD3-antibody; in the lower panel from left to right: ISH: CD1b1/4-probe, ISH: IFNγ-probe, ISH: CXCL-10-probe. (B) Consecutive FFPE-sections of the same granuloma were immuno-stained with an antibody specific for *M. tuberculosis.* The micrograph on the left gives an overview, the solid rectangle delineates a macrophage-rich area, which is shown in higher magnification in the middle graph. Few Mtb-specific spots are identified (black arrows). The dotted rectangle delineates part of the necrotic area, which is shown in higher magnification on the right. Several antibody-positive Mtb-spots are indicated by black arrows. (C) The number of Iba-1-positive macrophages, CD3-positive T cells and CD1b1/4-, IFNγ– and CXCL-10-expressing cells in the injection site granuloma was quantified by WSI analysis for PIM_6- and mock-vaccinated animals. Black bars represent the group mean, error bars the standard error of the mean. Asterisks indicate the level of significance as calculated by Mann-Whitney test in comparison to the CAF01-vaccinated group.

Figure S4

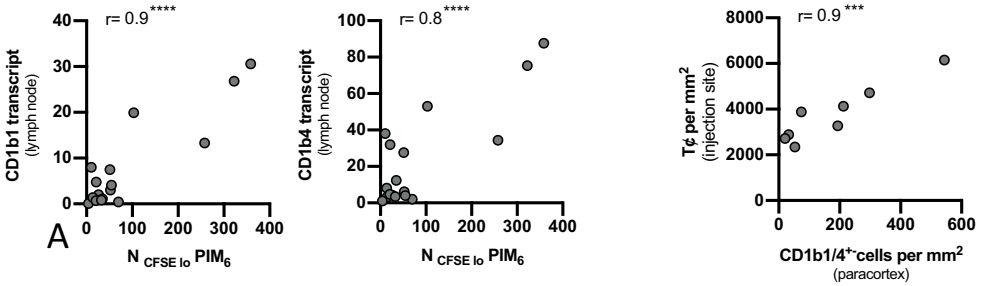

Figure S4– Correlation analysis

Four weeks after s.c. challenge with virulent H37Rv, PIM_6-vaccinated [PIM] and control guinea pigs [CAF, BCG] were euthanized and dissected. (A) The transcript levels of CD1b1 and CD1b4 in the draining lymph node four weeks after virulent H37Rv challenge were quantified by qRT-PCR in relation to β-Actin. The number of T cells proliferating in response to PIM_6 28 days after the first vaccination ($N_{CFSE\ lo}\ PIM_6$) was quantified by flow cytometry. Data was available for all animals from all groups (n=18). The Pearson correlation coefficient between the number of PIM_6-specific T cells and the CD1b expression level four weeks after the challenge was calculated and is indicated (r). (B) Four weeks after the challenge, FFPE-sections of the draining lymph nodes were investigated by in situ hybridization (ISH) for the expression of CD1b1/4 and quantified by WSI analysis. From the same animals FFPE-sections of the injection site granuloma were stained with a CD3-specific antibody. The number of granuloma infiltrating T cells was quantified by WSI analysis. Data from five PIM_6-vaccinated and five CAF-vaccinated control animals were available. The Pearson correlation coefficient was calculated between the number of T cells in the injection site granuloma and the number of CD1b1/4-expressing cells in the paracortex of the draining lymph node and is indicated (r). Grey circles represent individual animals. Asterisks indicate the level of significance.

Figure S5

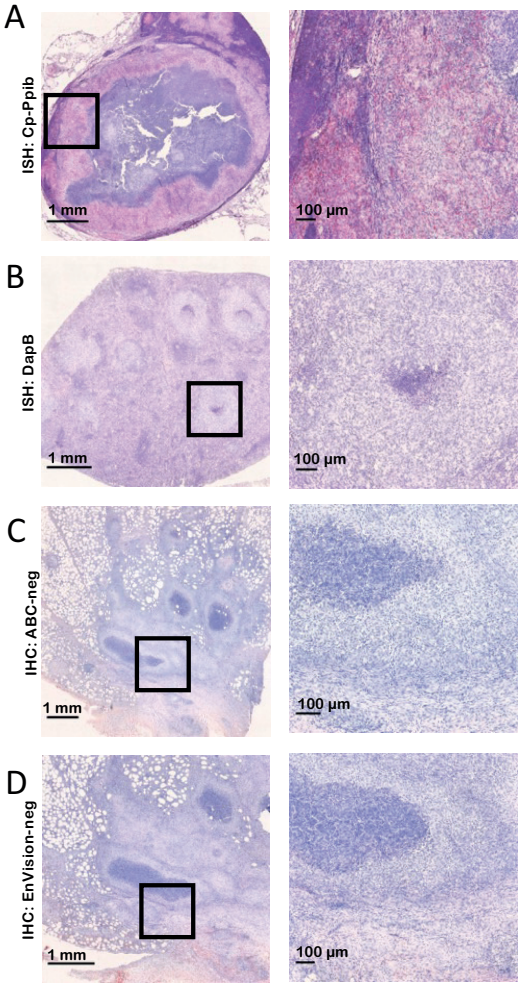

Figure S5 – Representative micrographs of control slides

Four weeks after challenge, sections were investigated by *in situ* hybridization (ISH) and immunohistochemistry (IHC). Negative and positive control slides were made to validate each staining. For every staining the left micrograph gives an overview. The black frames delineate a visual field that is shown in higher magnification on the right. (A) Probe Cp-Ppib was used as positive control for ISH. (B) Probe DapB was used as a negative control for ISH. (C) The ABC-system was used without primary antibody as a negative control for CD79-staining. (D) EnVision-system was used without a primary antibody as a negative control for CD3-, Iba-1- and *Mtb*-staining.

(III) Pharmacokinetics and Efficacy of the Benzothiazinone BTZ-043 against Tuberculous Mycobacteria inside Granulomas in the Guinea Pig Model

Emmelie Eckhardt, Yan Li, Svenja Mamerow, Jan Schinköthe, Julia Sehl-Ewert, Julia Dreisbach, Björn Corleis, Anca Dorhoi, Jens Teifke, Christian Menge, Florian Kloss, Max Bastian

Antimicrobial Agents and Chemotherapy, Accepted 16.02.2022

DOI: 10.1128/aac.01438-22

AMERICAN SOCIETY FOR MICROBIOLOGY | Antimicrobial Agents and Chemotherapy®

EXPERIMENTAL THERAPEUTICS

Pharmacokinetics and Efficacy of the Benzothiazinone BTZ-043 against Tuberculous Mycobacteria inside Granulomas in the Guinea Pig Model

Emmelie Eckhardt,[a] Yan Li,[b] Svenja Mamerow,[c] Jan Schinköthe,[d] Julia Sehl-Ewert,[a] Julia Dreisbach,[e,f] Björn Corleis,[a] Anca Dorhoi,[a] Jens Teifke,[a] Christian Menge,[c] Florian Kloss,[b] Max Bastian[a]

[a]Friedrich-Loeffler-Institut, Federal Research Institute for Animal Health, Greifswald, Germany
[b]Transfer Group Anti-infectives, Leibniz Institute for Natural Product Research and Infection Biology, Leibniz-HKI, Jena, Germany
[c]Friedrich-Loeffler-Institut, Federal Research Institute for Animal Health, Jena, Germany
[d]Institute of Veterinary Pathology, Faculty of Veterinary Medicine, Leipzig University, Leipzig, Germany
[e]Division of Infectious Diseases and Tropical Medicine, University Hospital of the University of Munich (LMU), Munich, Germany
[f]German Center for Infection Research (DZIF), Partner Site Munich, Munich, Germany

ABSTRACT Tuberculosis (TB), caused by *Mycobacterium tuberculosis*, is the world's leading cause of mortality from a single bacterial pathogen. With increasing frequency, emergence of drug-resistant mycobacteria leads to failures of standard TB treatment regimens. Therefore, new anti-TB drugs are urgently required. BTZ-043 belongs to a novel class of nitrobenzothiazinones, which inhibit mycobacterial cell wall formation by covalent binding of an essential cysteine in the catalytic pocket of decaprenylphosphoryl-β-D-ribose oxidase (DprE1). Thus, the compound blocks the formation of decaprenylphosphoryl-β-D-arabinose, a precursor for the synthesis of arabinans. An excellent *in vitro* efficacy against *M. tuberculosis* has been demonstrated. Guinea pigs are an important small-animal model to study anti-TB drugs, as they are naturally susceptible to *M. tuberculosis* and develop human-like granulomas after infection. In the current study, dose-finding experiments were conducted to establish the appropriate oral dose of BTZ-043 for the guinea pig. Subsequently, it could be shown that the active compound was present at high concentrations in *Mycobacterium bovis* BCG-induced granulomas. To evaluate its therapeutic effect, guinea pigs were subcutaneously infected with virulent *M. tuberculosis* and treated with BTZ-043 for 4 weeks. BTZ-043-treated guinea pigs had reduced and less necrotic granulomas than vehicle-treated controls. In comparison to the vehicle controls a highly significant reduction of the bacterial burden was observed after BTZ-043 treatment at the site of infection and in the draining lymph node and spleen. Together, these findings indicate that BTZ-043 holds great promise as a new antimycobacterial drug.

KEYWORDS BTZ-043, guinea pig, *Mycobacterium tuberculosis*, *Mycobacterium bovis* BCG, MDR-TB, treatment, new antibiotics

Tuberculosis (TB) in humans is caused by *Mycobacterium tuberculosis* and by other bacteria of the *M. tuberculosis* complex (MTC). TB is the world's leading cause of mortality from a single bacterial pathogen. In 2020, about 10 million people fell ill with TB and about 1.5 million deaths were estimated (1). Although treatment of TB is complicated, consisting of 6 months of treatment with a regimen of four different drugs, 85% of newly diagnosed patients are successfully treated (1). Commercially available antimycobacterial substances can be differentiated into first-line (e.g., rifampicin, isoniazid [INH], and ethambutol) and second-line drugs, which are used in combination to treat TB (2, 3). An increasing problem is the emergence of resistant mycobacteria,

Copyright © 2023 American Society for Microbiology. All Rights Reserved.

Address correspondence to Max Bastian, max.bastian@fli.de.

The authors declare no conflict of interest.

Received 24 October 2022
Returned for modification 7 December 2022
Accepted 16 February 2023

Downloaded from https://journals.asm.org/journal/aac on 29 March 2023 by 193.22.115.2.

which are either rifampicin resistant (RR-TB), resistant to rifampicin and isoniazid (MDR-TB), or extensively drug-resistant (XDR-TB). XDR-TB strains are MDR-TB strains which developed an additional resistance to fluoroquinolones and any of the second-line drugs (4). According to the WHO, in 2019, about half a million people developed RR-TB, of whom around 75% were MDR (5). The highest frequency of drug-resistant TB is found in countries of the former Soviet Union, with over 50% of relapse TB cases being MDR-TB. Globally, 3.3% of new and 17.7% of relapse TB cases developed RR- or MDR-TB in 2019 (5). With the increase of drug-resistant TB, appropriate treatment is getting more complicated and expensive. Drug-resistant TB leads to higher mortality rates. Therefore, new treatment approaches and drug regimens have to be developed and tested (6–10).

The structure of their cell wall is unique to mycobacteria, and enzymes involved in cell wall synthesis are therefore prominent targets for current and newly developed anti-TB drugs (11). One of the most promising substances is the benzothiazinone BTZ-043, which was first proposed as an anti-TB drug by Makarov et al. in 2009 (12). BTZ-043 inhibits *M. tuberculosis* cell wall synthesis by blocking decaprenylphosphoryl-β-D-ribose oxidase (DprE1) (13, 14). Consequently, cell wall arabinans cannot be formed, resulting in cell lysis and bacterial death. A very low MIC and good *in vitro* efficacy of BTZ-043 against different mycobacteria and nocardia have been demonstrated (15–17). In combination with other anti-TB drugs, such as rifampicin or isoniazid, benzothiazinones show a promising additive effect; a synergistic effect with bedaquiline is observed *in vitro* (18) and *in vivo* (17). Toxicologically, BTZ-043 showed no negative effects at therapeutic drug levels and no genotoxicity or mutagenicity in rats (19). In studies with BALB/c mice, no adverse effects after single-dose (5 g/kg of body weight) or repeated (25 and 250 mg/kg) treatment with BTZ-043 were observed (12).

Theoretically, a mutation at the Cys387 position of DprE1 could confer resistance against BTZ-043 (11), but all clinical isolates tested in a European study were found to be uniformly susceptible (20). BTZ-043 is currently undergoing phase II clinical trials within a partnership of German academic institutions and involvement of four leading consortia, the German Center for Infection Research (DZIF), the PanACEA consortium, Unite4TB, and InfectControl (21).

Although the compound has already been advanced to clinical phase trials, so far, there are no published studies that elucidate whether BTZ-043 is able to penetrate poorly vascularized granulomatous tissues and exert its antibacterial effect there. Guinea pigs have been long used as animal models to understand and describe TB infection, as they show many features of human TB disease. In particular, upon TB infection they develop necrotizing, caseating granulomas that resemble TB granulomas in human patients (22). To test the effect of BTZ-043 in a TB granuloma model, we made use of our long-standing experience with guinea pigs. In a dose-finding study, the appropriate dose of BTZ-043 for guinea pigs was determined. Subsequently, the level of BTZ-043 in *Mycobacterium bovis* BCG-induced granulomas was assessed. Finally, we investigated the therapeutic effect of BTZ-043 in guinea pigs previously infected with virulent mycobacteria.

RESULTS

Plasma levels of BTZ-043 and its metabolite after oral BTZ-043 administration to guinea pigs. Plasma levels of BTZ-043 and its metabolites were analyzed in healthy animals after oral administration. To this end, 50 mg/kg of BTZ-043 was given orally to four guinea pigs. As shown in Fig. 1A, BTZ-043 (M0) reached a maximum plasma level of 1,442 ng/mL in one animal (peak; mean, 1,205 ng/mL after 1 h). The levels of the main amino-metabolite (M1) were very low over the entire testing period, with a maximum plasma level of 380 ng/mL in one guinea pig after 2 h (mean, 150 ng/mL). Since relevant levels were only reached for 2 h, additional doses, i.e., 200 mg/kg of either micronized or wet-milled BTZ-043 and 400 mg/kg of BTZ-043, were evaluated. The experiments were conducted in the same animals with a washout period of at least 7 weeks between treatments. After treatment with a dosage of 200 mg/kg (micronized), plasma levels of M0 peaked after 1 h (853 ng/mL) and of M1 after 2 h (1,851 ng/mL)

Downloaded from https://journals.asm.org/journal/aac on 29 March 2023 by 193.22.115.2.

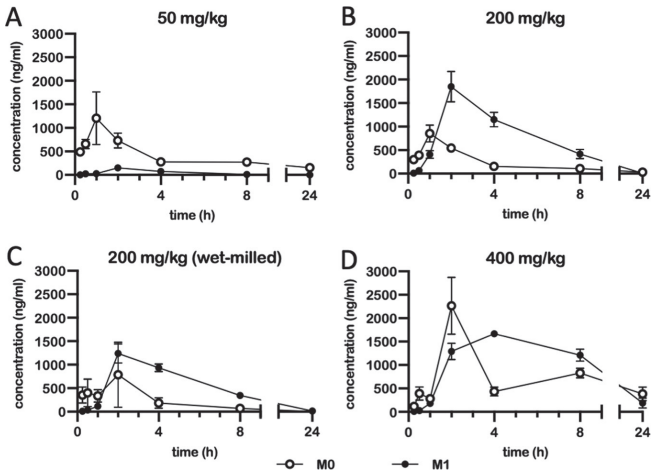

FIG 1 Plasma levels of BTZ-043 and its metabolite after oral BTZ-043 administration to guinea pigs. Four guinea pigs were given an oral dose of BTZ-043 (either 50 mg/kg, 200 mg/kg, or 400 mg/kg (all micronized) or 200 mg/kg (wet milled)). After 15 and 30 min and at 1, 2, 4, 8, and 24 h, blood was obtained from the vena saphena lateralis. The blood was centrifuged and plasma was separated into two samples, which were stabilized with ascorbic acid. After extraction, the samples were measured by mass spectrometry. The plasma levels of BTZ-043 (M0) and its metabolite M1 are shown for each time point as the group mean. Error bars represent the standard errors of the means.

but rapidly declined thereafter and reached baseline level after 24 h (Fig. 1B). For 200 mg/kg of wet-milled BTZ-043 the results were similar, but maximum plasma levels were lower, reaching 787 ng/mL for M0 and 1,237 ng/mL for M1 after 2 h (Fig. 1C). At a dosage of 400 mg/kg of BTZ-043, plasma levels finally remained elevated over 24 h (Fig. 1D). They peaked again after 2 h, with maximum levels of 2,265 ng/mL for M0 and 1,288 ng/mL for M1. Hence, 400 mg/kg was chosen as the appropriate dose for a longer treatment scheme (see also Table S2 in the supplemental material).

After multidose application of BTZ-043, plasma levels remained elevated after 24 h. To study the pharmacokinetics (PK) of BTZ-043 in guinea pigs after multidose application, six guinea pigs were treated orally with 400 mg/kg of BTZ-043 on 8 consecutive days (Fig. 2A). Plasma levels reached a concentration of 1,331 ng/mL for M0 and 2,147 ng/mL for M1 after 1 h and remained detectable over the first 24 h (Fig. 2B). On the last sampling day (Fig. 2C), samples taken prior to oral administration represent time zero. Metabolite levels were recorded in these samples as follows: M0, 1,391 ng/mL, and M1, 1,823 ng/mL. Metabolite concentrations peaked 1 h after treatment (M0, 2,176 ng/mL) or after 2 h (M1, 5,185 ng/mL) and remained over 1,000 ng/mL for the rest of the observation period, i.e., 1,171 ng/mL and 1,861 ng/mL for M0 and M1, respectively, after 24 h. During treatment weight gain was interrupted, but the animals regained weight at a normal rate immediately after treatment stopped (Fig. S1A).

High levels of BTZ-043 were reached in BCG-induced granulomas. To evaluate the tissue concentration of BTZ-043, six guinea pigs were inoculated subcutaneously with 1×10^3 CFU of BCG in the left and right axillary region each. After 28 days, small, palpable nodules had formed at the site of inoculation. Twenty-eight days after inoculation, guinea pigs were treated for 7 days with a daily oral dose of 400 mg/kg of BTZ-043 (Fig. 3A). During treatment, weight gain was slightly reduced (Fig. S1B). Afterwards, at day 35 postinoculation, guinea pigs were euthanized to harvest BCG-induced injection site granulomas. In guinea pigs at early time points, BCG induces lesions very similar to those induced by virulent mycobacteria, but BCG can be processed under biosafety level 2 (BSL2) conditions. It was therefore possible to analyze granuloma specimens by mass spectrometry

Downloaded from https://journals.asm.org/journal/aac on 29 March 2023 by 193.22.115.2.

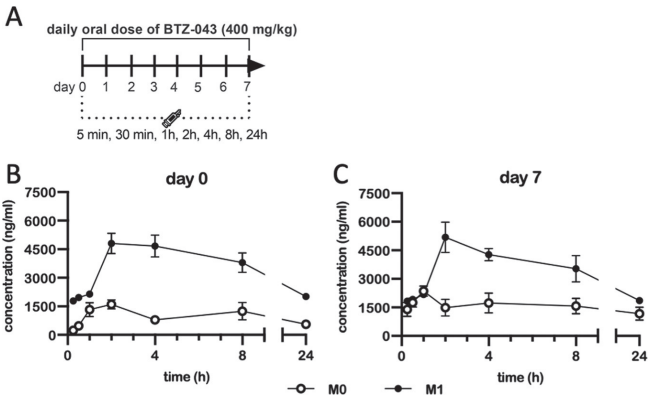

FIG 2 After multidose application of BTZ-043, plasma levels remained elevated after 24 h. (A) Six guinea pigs were given repeated single daily oral doses of 400 mg/kg of BTZ-043 over 7 consecutive days. On the first and last day, blood was obtained from the vena saphena lateralis at 15 and 30 min and at 1, 2, 4, 8, and 24 h after administration. The blood was centrifuged and plasma was separated into two samples, which were stabilized with ascorbic acid. After extraction, the samples were measured by mass spectrometry. The group mean of the plasma levels from BTZ-043 (M0) and its metabolite (M1) for each time point is shown for day 1 (B) and day 7 (C). Error bars represent the standard errors of the means.

under native conditions. BTZ-043 and its metabolite M1 were measured in relatively high concentrations compared to plasma levels (M0, 6,743 ng/g; M1, 8,768 ng/g) within granulomas. (Fig. 3B). In BTZ-043-treated animals, CFU counts in BCG granulomas were reduced by two log scales compared to those in untreated guinea pigs (Fig. 3C).

BTZ-043 treatment significantly reduced *M. tuberculosis*-induced pathology. Eighteen guinea pigs were infected subcutaneously in the left axillary region with 1×10^3 CFU of the virulent *M. tuberculosis* strain H37Rv. Fourteen days after infection, oral treatment was initiated and continued for the next 28 days (Fig. 4A). During repeated dosing

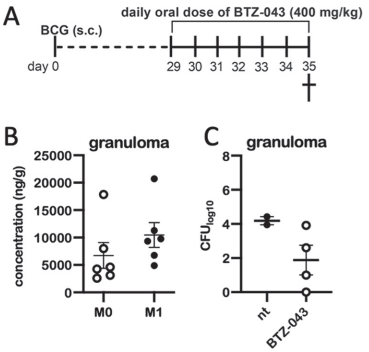

FIG 3 High levels of BTZ-043 are reached in BCG-induced granulomas. (A) Six guinea pigs were inoculated subcutaneously with 1×10^6 CFU of BCG Pasteur 1173. After 28 days, treatment with a daily oral dose of 400 mg/kg of BTZ-043 was started and continued for 7 consecutive days. At day 35, guinea pigs were euthanized and BCG-induced granulomas at the injection site were taken for analysis. (B) Parts of granulomas were cryopreserved and levels of BTZ-043 (M0) and its metabolite (M1) were measured via mass spectrometry. Individual levels and the means of M0 and M1 are shown for each of the six animals. Error bars represent the standard errors of the means. (C) For four treated animals, parts of granulomas were homogenized, serially diluted, and plated on 7H11 agar plates. After 3 weeks, CFU were counted. Results from two additional guinea pigs that were inoculated with BCG but not treated (nt) are depicted for comparison.

Downloaded from https://journals.asm.org/journal/aac on 29 March 2023 by 193.22.115.2.

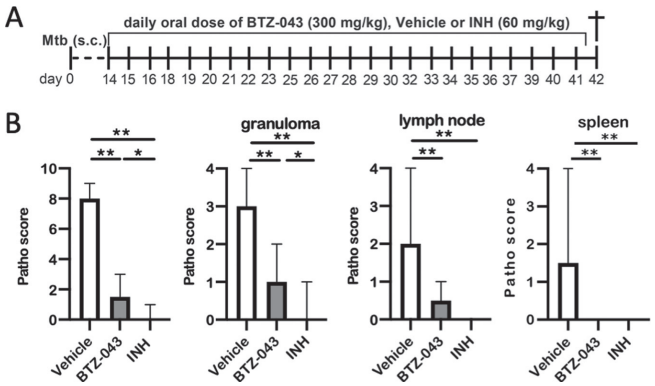

FIG 4 BTZ-043 treatment significantly reduced *M. tuberculosis*-induced pathology. (A) Guinea pigs (n = 6, each) were infected subcutaneously with 1×10^3 CFU of virulent *M. tuberculosis* strain H37Rv. After 14 days, treatment with a daily oral dose of 300 mg/kg of BTZ-043 was started and continued for 28 days. As a control, guinea pigs were treated with either vehicle solution or 60 mg/kg of isoniazid (INH). (B) After 4 weeks, guinea pigs were euthanized and necropsied. Granulomas at the infection site, the draining axillary lymph node, and spleen were macroscopically scored. Bars represent the group medians with ranges, and asterisks represent the level of significance as calculated by nonparametric Mann-Whitney U test (*, $P \leq 0.05$; **, $P \leq 0.01$).

of 400 mg/kg (in noninfected animals; see above), transient neurological signs such as tumbling or stupor were observed in some animals. Therefore, for the challenge trial, a dosage of 300 mg/kg of BTZ-043 was used. Vehicle-treated (1% carboxymethyl cellulose [CMC], 0.5% Tween 80) animals served as negative controls and isoniazid-treated (60 mg/kg) animals as positive controls. INH dosage was adapted from a previous publication (23). BTZ-043-treated animals showed the lowest weight gain in comparison to both control groups (Fig. S1C). At day 42, guinea pigs were euthanized and necropsied. The gross pathology scores of infection site granulomas, left axillary lymph nodes, and spleens were calculated. In comparison to those of vehicle-treated controls, the number and size of granulomas at the infection site and in the draining axillary lymph nodes was significantly reduced in BTZ-043- and INH-treated animals. Systemic spread, as determined by granulomatous splenitis, was completely absent in these two groups (Fig. 4B). Microscopic analysis of hematoxylin-eosin (HE)-stained tissue sections of the infection sites revealed that the size of granulomas (as determined by the absolute area in representative sections) and the percentage of necrosis within were significantly reduced in BTZ-043-treated guinea pigs in comparison to the vehicle group (Fig. 5A). Similar findings were evident in the draining axillary lymph nodes (Fig. 5B). For the spleen, granulomas were only detectable in animals of the vehicle control group (Fig. 5C). In infection site granulomas of BTZ-043-treated animals, slightly lower macrophage and higher T-cell counts were present than for vehicle- or INH-treated animals (Fig. S3A); this tendency did not reach significance. A similar nonsignificant trend was observed in draining axillary lymph nodes. Interestingly, in the lymph node, BTZ-043-treated animals showed 10-fold-higher numbers of B cells in the granulomatous region (Fig. S3B).

BTZ-043 treatment led to a significantly lower burden of virulent *M. tuberculosis* H37Rv. After 4 weeks of treatment, CFU of virulent *M. tuberculosis* H37Rv were determined at the site of infection, in the draining lymph node, and in the spleen. Compared to vehicle controls, significantly lower mycobacterial loads were observed at the site of infection in BTZ-043- and INH-treated animals (Fig. 6A). This reduction was even more striking in the lymph nodes (Fig. 6B). In contrast to vehicle controls in BTZ-043- or INH-treated guinea pigs, no mycobacteria were detectable in the spleen (Fig. 6C). Accordingly, when we analyzed additional organ samples outside the primary complex consisting of infection site granuloma and draining axillary lymph node, only

Downloaded from https://journals.asm.org/journal/aac on 29 March 2023 by 193.22.115.2.

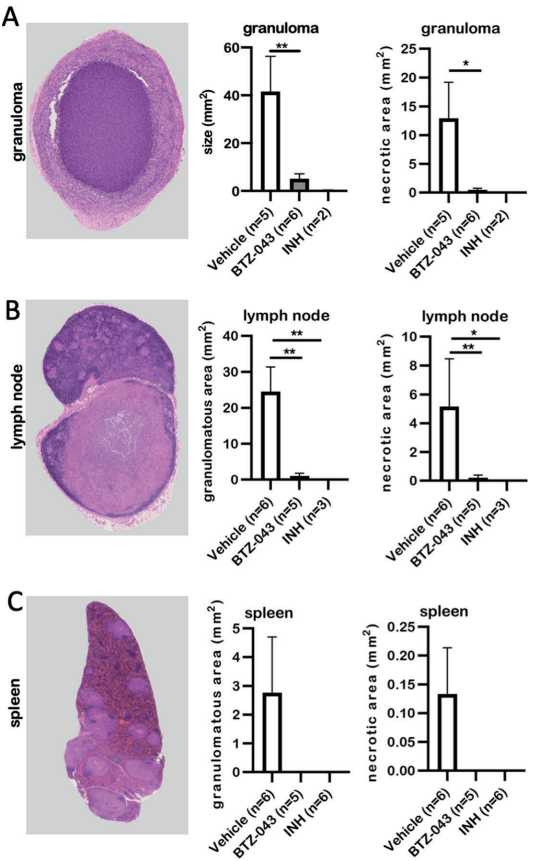

FIG 5 BTZ-043 treatment significantly reduced *M. tuberculosis*-induced necrotic lesions. Six weeks after infection and after 4 weeks of treatment, BTZ-043-treated or control animals (vehicle or INH) were euthanized and dissected and organ samples were collected. Formalin-fixed, paraffin-embedded sections of the infection site granuloma (A), the axillary lymph node (B), and the spleen (C) were HE stained, whole-slide images were obtained, and absolute granuloma areas as well as area of caseous necrosis were measured. Representative microphotographs for the respective organ are shown on the left. In the middle, the quantitative analysis of the granulomatous area is shown for the three groups. Graphs on the right depict the quantitative analysis of necrotic lesions. Bars show group means, error bars indicate the standard errors of the means, and asterisks indicate the level of significance as calculated by nonparametric Mann-Whitney U test (*, $P \leq 0.05$; **, $P \leq 0.01$).

in vehicle controls could lesions be detected: two out of six (33%) animals in the vehicle group had moderate, multifocal granulomas in the lymphonodus tracheobronchialis and mild, oligofocal, periportal centered granulomas in the liver of one animal. In the granulomas of the lung lymph node, single to a few acid-fast mycobacteria were visible (Fig. S2C to F).

DISCUSSION

In the middle of the 20th century, the discovery of antibiotics active against mycobacteria was an important turning point in the battle against TB (4). Uncountable numbers of deaths and severe TB cases could be averted through these new medications.

Downloaded from https://journals.asm.org/journal/aac on 29 March 2023 by 193.22.115.2.

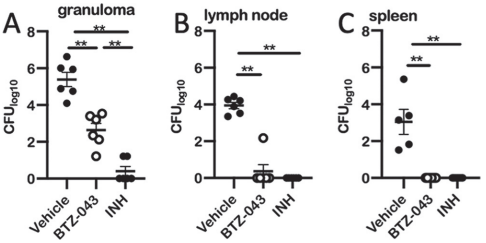

FIG 6 BTZ-043 treatment significantly reduced burden of virulent *M. tuberculosis* H37Rv. Six weeks after infection with virulent *M. tuberculosis* H37Rv, BTZ-043-treated or control animals (vehicle or INH) were euthanized and dissected and organ samples were obtained. Tissue samples of injection site granulomas (A), draining axillary lymph nodes (B), and the spleen (C) were homogenized and the number of CFU determined. Dots represent individual values for each animal. Black bars represent the group means and error bars the standard errors of the means. Asterisks show level of significance as calculated by nonparametric Mann-Whitney U test (**, $P \leq 0.01$).

However, since the 1990s, multidrug-resistant TB-causing strains have gained increasing relevance. In 2021, approximately 7% of all culture-confirmed cases worldwide were RR- or MDR-TB (1). Patients with MDR-TB need prolonged courses of treatment with a complicated treatment regimen involving several second-line drugs. This leads to more severe adverse effects and up to 100-fold-higher expenditures compared to those for drug-sensitive TB cases (24). The urgent need for new drugs that are as efficient and cost-effective as current first-line antibiotics has bolstered research and development efforts across academia, pharmaceutical companies, and public-private partnerships. A recent encouraging review gives a comprehensive overview over the pipeline of investigational drugs that are already approved or in clinical phase trials (25). One of these promising compounds is BTZ-043. Makarov et al. observed that BTZ-043 had very good activity against the different *M. tuberculosis* strains tested, including MDR and XDR strains (12). Furthermore, the *in vitro* MIC was found to be lower than those of other antimycobacterial drugs (26). In several animal models, oral administration of BTZ-043 yielded detectable plasma levels, with doses varying from 5 mg/kg to 300 mg/kg BTZ-043 in mice (12, 16) and 60 to 470 mg/kg in rats (15; unpublished data) and at up to 2,000 mg/kg BTZ-043 in minipigs (unpublished data). Although after single doses the levels rapidly decline over 24 h, good antimicrobial activity was observed in the mouse infection model (12). However, one general concern with the BALB/c mouse model is that mice normally do not develop caseating granulomas upon infection with *M. tuberculosis*. The aim of the current study was therefore to establish a preclinical model that would allow studying granuloma penetration and the effect of BTZ-043 on granuloma resident mycobacteria. As goats and cattle develop caseating granulomas and, like humans, have interlobular lung septa that help to encapsulate mycobacterial lesions, they have been proposed as experimental models to study the pathobiology of granuloma formation (27). However, by oral and even intravenous administration of BTZ-043 no detectable plasma levels of BTZ-043 could be reached in goats (unpublished data). We therefore made use of another preclinical TB model: guinea pigs, which have been used since the early days of TB research (28). They are highly susceptible to mycobacterial infections and develop granulomas very similar to those seen in human TB patients (22). In the current study, we were able to confirm that oral administration of BTZ-043 to guinea pigs resulted in plasma levels that were very similar to those reported for mice (12). With the maximum dose of 400 mg/kg, some of the adolescent animals in the multidose study developed transient, mild neurological symptoms. Adolescent animals are likely to be particularly susceptible to such side effects due to low adipose tissue levels resulting in differential drug distribution. In older animals receiving the high-dose bolus, no adverse effects were observed. Similarly, when the reduced dose of 300 mg/kg was applied in the treatment and challenge trial, no neurological symptoms occurred. In the

Downloaded from https://journals.asm.org/journal/aac on 29 March 2023 by 193.22.115.2.

ongoing clinical trial, particular attention will be paid to potential adverse reactions. However, in relation to the metabolic weight, the highest dosage in the clinical trial is 5-fold lower than the dosage used in guinea pigs (21). Therefore, the occurrence of neurological symptoms is unlikely.

In the current study, we could for the first time directly determine the concentration of the active compound in *mycobacterium*-induced granulomas. Our observations in BCG-inoculated animals indicate that the compound is enriched in the granuloma, as the concentration in the tissue homogenates was about 7-fold higher than the corresponding plasma levels. This indicates that BTZ-043 is able to penetrate mature granulomas, reaching tissue levels that are clearly higher than the MIC. The M1 metabolite is the nitroreduction product of BTZ-043. Its MIC (500 ng/mL) is orders of magnitude higher than that of BTZ-043 (1 ng/mL) (12). However, the tissue levels of M1 in the granuloma suggest that it also contributed to antimicrobial activity. A fine differentiation of tissue concentrations, as has been described for moxifloxacin in lung granulomas of TB-infected rabbits (29), was beyond the scope of our study. However, as revealed by Ziehl-Neelsen staining in TB-infected vehicle controls, most acid-fast mycobacteria were observed extracellularly in the necrotic, caseous area of the granulomas (see Fig. S2 in the supplemental material). Hence, the significant reduction of the bacterial burden in BTZ-043-treated animals compared to vehicle controls—both in BCG-vaccinated animals and after virulent *M. tuberculosis* challenge—provides additional, indirect evidence that the active compound reached poorly vascularized areas, where the mycobacteria reside. This reduction of bacterial burden at the site of infection and in the draining axillary lymph node and the complete prevention of bacterial dissemination by BTZ-043 treatment were the most important outcomes of this study. While all animals of the vehicle control group had multiple granulomas in the spleen, and some showed lesions in the lung lymph nodes and liver, no lesions whatsoever were observed outside the primary complex in treated animals. This went along with significantly reduced macroscopic granuloma scores at the site of infection and in the draining lymph nodes. Also, at the microscopic level, this was reflected by significantly smaller granulomas and an almost complete absence of necrotic lesions in BTZ-043-treated animals. The immunophenotyping showed a nonsignificant increase in absolute T-cell counts in the infection site granuloma and in granulomatous areas of the lymph node in BTZ-043-treated animals in comparison to vehicle controls (Fig. S3). This nonsignificant trend is clearly no proof of an immunostimulatory effect of BTZ-043. However, the mere possibility of a complementary, immune-enhancing effect should be investigated in more detail, because other antimycobacterial drugs, such as rifampicin and INH, have been described to have a dampening effect on antimycobacterial immune responses (30, 31).

In our hands with the 28-day treatment regimen, INH had a better effect than BTZ-043. This observation is in line with previous studies from Lechartier et al. and Makarov et al., in which INH also showed a slightly better *in vitro* (18) and *in vivo* (17) efficacy than BTZ-043. At the same time, in a large European study including 240 clinical isolates, all tested INH-resistant *M. tuberculosis* isolates proved uniformly susceptible to BTZ-043 (20). Hence, in cases of MDR-TB, BTZ-043 is expected to be as effective as with drug-sensitive strains. In addition, work is ongoing to enhance the efficacy of BTZ-043: in a recent, so-far-unpublished study in BALB/c mice, 4-fold-higher plasma levels of BTZ-043 were achieved compared to those in previous mouse studies. Together with a prolonged treatment, this resulted in substantially higher killing rates after BTZ-043 than after INH treatment (unpublished data). Along that line, Makarov et al. already pointed out in their first, seminal publication that the efficacy of BTZ-043 is dependent on the duration of therapy rather than on the actual dose (12). So, with 28 days of treatment a highly significant and convincing therapeutic effect was observed, but it can be expected that prolonged therapy will further enhance the antimycobacterial effect of BTZ-043.

In summary, we have shown that the guinea pig is well suited to study the pharmacodynamics and pharmacokinetics of BTZ-043. The model is available to test the

Downloaded from https://journals.asm.org/journal/aac on 29 March 2023 by 193.22.115.2.

compound in combination therapies with first-line drugs, such as INH or rifampicin (18), or to evaluate new derivatives of BTZ-043 (32–34). Most importantly, our current study unequivocally shows that BTZ-043 is able to penetrate the TB granuloma and that the treatment of *M. tuberculosis*-infected guinea pigs is safe and highly effective.

MATERIALS AND METHODS

Treatment. The benzothiazinone BTZ-043 (for detailed information, see Table S1 in the supplemental material) was administered as microcrystalline suspensions (micronized material or obtained through wet milling) in 1% carboxymethyl cellulose (CMC; medium viscosity) and 0.5% Tween 80 (Sigma-Aldrich, Germany). The amount of BTZ-043 in the formulation depended on the dosage (constant dosing volumes of 2 g/kg). In the dose-finding study, different doses and formulations were tested to establish the most effective dose. Hence, guinea pigs were treated with 50 mg/kg, 200 mg/kg, and 400 mg/kg (micronized). A comparison with a wet-milled formulation was done for the 200-mg/kg dose. For the multidose application and the BCG treatment study, a dose of 400 mg/kg (micronized) of BTZ-043 was used, and for the treatment after *M. tuberculosis* infection, a dose of 300 mg/kg (micronized) of BTZ-043 was used. The medication was stirred half an hour prior to each application for optimal homogeneity.

Isoniazid (INH), formulated with 30 mg/g in sterile water, at a dose of 60 mg/kg served as a positive control (23). As a negative control, a vehicle solution with 1% CMC and 0.5% Tween 80 was used.

Bacteria. For infection of guinea pigs, *Mycobacterium bovis* BCG strain Pasteur 1173 (kindly provided by Walter Mattheis, Paul-Ehrlich-Institut [PEI], Langen, Germany) or the *M. tuberculosis* H37Rv strain (kindly provided by Stefan H. E. Kaufmann, Max-Planck-Institute for Infection Biology, Berlin, Germany) was used. Bacteria were grown in oleic acid-albumin-dextrose-catalase (OADC)-enriched 7H9 medium (Becton, Dickinson, Germany) supplemented with 0.05% Tween 80 (Sigma-Aldrich, Germany). When grown to an optical density (OD) of 1.0, they were centrifuged and diluted in phosphate-buffered saline (PBS; in-house) for subcutaneous injection into guinea pigs.

Animal experiments. A total number of 34 3-month-old female Dunkin-Hartley guinea pigs were obtained from Charles River Germany and housed in groups of 2 or 3 animals. The guinea pigs were housed in open cages in the institute's biosafety level 2 or 3 animal facilities. Dry pellets, hay, and water were offered *ad libitum*; the light regime followed a natural day and night cycle and temperature was regulated automatically to 21°C. The cages were enriched with a plastic shelter and paper tunnels. Before the trial, animals were able to adjust to housing and handling during an acclimatization phase of 2 weeks. Animals were weighed weekly during the acclimatization period and daily during multidose studies.

The animal trial protocol was approved by the regulatory authority, the State Office of Agriculture, Food Safety and Fishery in Mecklenburg-Western Pomerania (LALLF MV, 7221.3-1-008/20). All animal experiments were carried out following German animal welfare regulations.

Experimental design. (i) Dose-finding study. In a dose-finding-study, four guinea pigs were first given 50 mg/kg of BTZ-043 orally. After an appropriate resting and washout phase of at least 7 weeks in between, escalating doses of 200 mg/kg and 400 mg/kg were administered to the same animals. Following oral application of BTZ-043, blood was obtained from the vena saphena lateralis after 15 and 30 min and at 1, 2, 4, 8, and 24 h. Measurement of plasma concentrations was conducted as described below.

(ii) Multidose application. Six guinea pigs were given 400 mg/kg of BTZ-043 orally for 8 consecutive days. On the first and last day, blood was obtained as described above and bioanalysis was done as described below.

(iii) BTZ-043 in granulomas. Six animals were injected subcutaneously with a dose of 1×10^3 CFU of BCG strain Pasteur 1173 resuspended in 0.25 mL of PBS. Equal amounts of this injection suspension were administered in the left and the right axillary region to induce granuloma formation on each side. After 28 days, 400 mg/kg of BTZ-043 was given orally once daily for 7 consecutive days. On day 35, guinea pigs were euthanized by CO_2 inhalation under deep anesthesia using ketamine (Livisto, Germany) and xylazine (CP-Pharma, Germany). Injection site granulomas were collected and split into equal parts for bacteriology and BTZ-043 concentration determination. CFU were determined as described for *M. tuberculosis*-challenged animals (see below).

(iv) BTZ-043 after *M. tuberculosis* infection. Eighteen guinea pigs were infected subcutaneously with 1×10^3 CFU of virulent *M. tuberculosis* strain H37Rv in the left axillary region. After 14 days, treatment was started and given once daily for 28 consecutive days. One group of six animals received a daily oral dose of 300 mg/kg of BTZ-043. As a positive control, six guinea pigs were given 60 mg/kg of INH, and as a negative control, six animals received vehicle solution. After 28 days of treatment, i.e., 42 days after inoculation, guinea pigs were euthanized and necropsied. Tissue samples were collected for further bacteriological and histological analyses (see below).

Sample workflow for BTZ-043 bioanalysis. (i) Sample preparation. Immediately after blood withdrawal from the vena saphena, the blood was stored on ice and quickly centrifuged at 1,600 relative centrifugal force (rcf) for 10 min at 4°C. The plasma was then separated in duplicates and stabilized with ascorbic acid (2.5 mg/mL). Injection site granulomas from the guinea pigs were immediately cryopreserved and kept frozen at −80°C until analysis.

(ii) Pretreatment for plasma samples. Aliquots of 10 μL were mixed with 10 μL of ascorbic acid solution (250 mg/mL in deionized water), 10 μL of internal standard (IS) (800 ng/mL in methanol (MeOH)), and 70 μL of degassed MeOH. After mixing for 2 min using an Eppendorf ThermoMixer C at 4°C and centrifugation at 16,100 rcf for 2 min at 4°C, supernatants were taken immediately for quantification.

Downloaded from https://journals.asm.org/journal/aac on 29 March 2023 by 193.22.115.2.

(iii) Pretreatment for granuloma samples. Prior to homogenization of granuloma tissue samples from BCG-injected and BTZ-043-treated guinea pigs, a stability test was performed to ascertain that BTZ-043 and its main metabolites did not degrade due to the heat created from homogenization beads. Blank granuloma tissue and the experimental granuloma tissue samples were homogenized in Precellys lysing kits CK14 (2 mL, prefilled with ceramic beads; Bertin Technologies SAS, France) using a Precellys 24 tissue homogenizer (Bertin Technologies SAS). Tissue was accurately weighted, and 9-fold (wt/wt) PBS (Lonza, USA) was added. Instead of homogenizing tissue samples continuously for 60 s, the procedure was repeated 3 times by homogenizing the samples for 20 s at 5,500 rpm and intermediary cooling in an ice bath for 5 min to avoid overheating. Tissue homogenates were stored at −80°C until use. Additionally, a recovery test was performed on the granuloma homogenates by spiking BTZ-043 and its different metabolites into the tissue homogenization preparations. Recoveries were around 80 to 86%, validating the process of homogenization of granuloma samples.

Bioanalysis. (i) Stock and working solutions. Under physiological conditions, BTZ-043 (M0) is metabolized into (besides minor metabolites) its main metabolites M1 (amino-metabolite) and M2 (hydride Meisenheimer complex). M2 is unstable under atmospheric conditions and is prone to oxidize to the parent compound (BTZ-043) *ex vivo*, which can be suppressed through addition of ascorbic acid. As only M0 and, to a lesser extent, M1 are known to have antibacterial activity, we focused on these metabolites in Results.

(ii) Calibration and QC samples. Calibration and quality control (QC) samples were obtained by adding constant volumes of different analyte working dilutions (10 μL) into blank plasma (115 μL). The spiking was limited to a final solvent content maximum of 8% (vol/vol). The calibration standards and QC samples of the cocktail solution (M0 and M1) were prepared in blank plasma (stabilized with ascorbic acid at 2.5 mg/mL). See calibration standards and QC samples in Table S3.

(iii) Quantification of BTZ-043 and its main metabolites. Samples were analyzed using a Vanquish Horizon ultrahigh-performance liquid chromatography (UHPLC) system (Thermo Fisher Scientific, Germany) coupled to a Thermo Scientific QExactive HF-X Orbitrap mass spectrometer using a UPLC column (Acquity HSS T3; Waters; 1.8-μm particle size; 2.1 by 50 mm) and a precolumn (Acquity HSS T3 VanGuard precolumn; Waters; 1.8-μm particle size; 2.1 by 5 mm). The column temperature was maintained at 25°C, and the samples were kept at 4°C. The UHPLC system was operated at a flow rate of 0.6 mL/min and an injection volume of 5 μL. Mobile phases consisted of 0.1% (vol/vol) formic acid in water (eluent A) and 0.1% (vol/vol) formic acid in acetonitrile (ACN) (eluent B). Chromatographic separation was achieved as follows: 0 to 4 min, linear gradient from 5% to 98% eluent B; 4 to 6.5 min, isocratic at 98% eluent B; 6.5 to 7 min, linear gradient from 98% to 5% eluent B; and 7 to 9 min, isocratic at 5% eluent B. The high-resolution mass spectra were acquired with electrospray ionization in the positive mode. A scan range of *m/z* 120 to 1,800 was chosen, and the maximum injection time was set to 200 ms. Ion source parameters were as follows: spray voltage, 3.5 kV; capillary temperature, 320°C; S-lens radiofrequency (RF) level, 40; sheath gas pressure, 50 (N_2 > 95%); auxiliary gas pressure, 10 (N_2 > 95%); and auxiliary gas heater temperature, 300°C. The value for the automatic gain control (AGC) target was set to 10^6, resolution was 60,000, and chromatographic peak width (full width at half maximum [FWHM]) was 15 s. Samples were measured when good calibration curves of analytes and valid QC results were obtained. During analysis, ACN solution was injected after every four samples. QC samples were injected after a batch of 24 to 30 samples, as well as after all the samples. All the samples were measured within 6 h after the sample pretreatment and were stored at −80°C after the analysis.

Data analysis of BTZ-043 measurements. (i) Evaluation of analytical data. Chromatographic data were integrated and evaluated using the software TraceFinder (Thermo Fisher) with the following parameters: calculation method, peak area ratio; regression type, linear; weighting factor, $1/x^2$; and rounding of results, three significant figures.

Measured concentrations were listed and summarized for each sampling time point and animal by calculation of means and standard deviation per time point.

(ii) PK evaluation. The pharmacokinetic (PK) assessment was performed based on mean concentrations. The following PK parameters were determined by noncompartmental methods using Phoenix WinNonlin 7.0: maximum concentration (C_{max}), time to maximum concentration (T_{max}), area under the curve from 0 to t area under the curve over the observation period (AUC_{0-t}), calculated total area under the curve (AUC_{0-inf}), the proportion of the total AUC after the observation period (%AUC_{extra}), if applicable. Measured concentrations and PK parameters were summarized by group mean values and standard deviation. For T_{max}, the median was reported. All calculated parameters were rounded to three figures.

Necropsy and sampling of *M. tuberculosis*-infected guinea pigs. Forty-two days after *M. tuberculosis* infection and after 28 days of treatment, guinea pigs were euthanized under anesthesia (see above) with pentobarbital (Release; WDT, Germany) followed by a full necropsy. Samples from infection site, draining left axillary lymph node, and spleen were taken and used for bacterial cultivation and histopathological analysis. Heart, trachea, cranial and caudal lung lobe, lymphonodus tracheobronchialis, stomach, duodenum, jejunum, ileum, colon, liver, pancreas, kidney, and brain were additionally sampled for histopathological analysis. Samples for histopathology were immediately fixated in formaldehyde and after 3 weeks in paraffin wax-embedded (FFPE) tissue blocks. Samples for bacterial enumeration of CFU were homogenized and plated on the same day. Samples of tissues were split in equal parts for bacteriological and histopathological analyses. In cases where the samples were too small to perform both analyses, CFU determination was prioritized.

Macroscopic scoring of gross lesions was performed for the infection site, left axillary lymph node, and spleen by assessing formation of granulomas, number and size of granulomas, and presence of necrosis. The scores were derived from an ordinal scale of 0 to 4 based on the modified Mitchison scoring system detailed in Table S1 (35, 36).

Downloaded from https://journals.asm.org/journal/aac on 29 March 2023 by 193.22.115.2.

Measurement of bacterial growth. Tissue samples from the injection site granuloma, draining left axillary lymph node, and spleen were diluted in 1 mL of PBS containing 0.05% Tween 80 (Sigma-Aldrich, Germany). Samples were homogenized and the homogenate was 1:10 serially diluted from 1:100 to 1:1,000,000. Fifty microliters of each solution was plated on 7H11 agar (Sigma-Aldrich, Germany) supplemented with 5 g/L of glycerin, 100 mL/L of OADC (Becton, Dickinson, Germany), and 500 μL/L of ampicillin (Carl Roth, Germany). Agar plates were incubated at 37°C for 3 weeks before counting the number of CFU.

Microscopic analysis. (i) FFPE tissue preparation and histochemistry. FFPE tissues were cut at 3 μm and hematoxylin-eosin (HE) as well as Ziehl-Neelsen or Fite-Faraco staining was performed to visualize acid-fast mycobacteria in granulomas according to standard laboratory protocols (37).

(ii) Immunohistochemistry. To visualize B cells, T cells, and macrophages, primary antibodies were used as described in Table S4. As secondary antibody, a biotinylated goat anti-mouse IgG (1:200; Vector Laboratories, Burlingame, CA; for CD79a) antibody was used with subsequent avidin-biotin-peroxidase (ABC) complex (Vector Laboratories) for 30 min at room temperature. For visualization of T cells and macrophages, the EnVision+ system (Dako, USA) was used.

(iii) Whole-slide image (WSI) analysis. The stained slides were scanned with a NanoZoomer S60 digital slide scanner (Hamamatsu, Germany) in 40× mode. For all digital analysis of the scanned slides, QuPath version 0.2.3. (38) was used.

As we prioritized assessment of CFU, in some animals there was not enough tissue left for microscopic analysis of infection site granulomas. The exact numbers of analyzed tissue samples are given in the respective figures for each treated group. The areas of organs as well as granulomatous and necrotic areas within granulomas were determined on HE-stained slides by WSI. Positive cells obtained in immunophenotyped consecutive sections were automatically enumerated with QuPath using the program cell detection algorithm (38). For each consecutive section, several visual fields representative for the area of tissue and granuloma were analyzed at a magnification of ×400. For each immunophenotyped WSI, the detection parameters were adjusted and all analyses were manually supervised.

Statistics. GraphPad Prism version 8.1.0 was used to analyze and visualize the data. Differences at a P value of <0.05 were considered significant. Quantitative data are expressed as group means plus/minus standard errors of the means (SEM). Semiquantitative data (gross pathology scoring) are depicted as medians with ranges. The results between groups were compared using Mann-Whitney U test.

SUPPLEMENTAL MATERIAL

Supplemental material is available online only.

SUPPLEMENTAL FILE 1, PDF file, 12.6 MB.

ACKNOWLEDGMENTS

We thank Walter Mattheis and Stefan H. E. Kaufmann for the provision of bacterial strains. We are particularly grateful to Wiebke Lange, Silvia Schuparis, Gabriele Czerwinski, and Ulrike Zedler for their excellent technical support. We emphasize the contribution of Frank Klipp, Bärbel Bergmann, and all the animal care takers, and we sincerely acknowledge the help of Angele Breithaupt, Bärbel Hammerschmidt, and Charlotte Schröder.

We have no financial conflict of interest.

This study was funded by the Federal Ministry for Education and Research as part of the InfectControl Consortium (grant no. 03ZZ0803B for M.B., 03ZZ0803A and 03ZZ0835A for F.K., and 03ZZ0826 for Y.L.).

REFERENCES

1. World Health Organization. 2021. Global tuberculosis report 2021. World Health Organization, Geneva, Switzerland.
2. Lenaerts AJ, Degroote MA, Orme IM. 2008. Preclinical testing of new drugs for tuberculosis: current challenges. Trends Microbiol 16:48–54. https://doi.org/10.1016/j.tim.2007.12.002.
3. Tandon R, Nath M. 2017. Tackling drug-resistant tuberculosis: current trends and approaches. Mini Rev Med Chem 17:549–570. https://doi.org/10.2174/1389557516666160606204639.
4. Matteelli A, Roggi A, Carvalho AC. 2014. Extensively drug-resistant tuberculosis: epidemiology and management. Clin Epidemiol 6:111–118. https://doi.org/10.2147/CLEP.S35839.
5. World Health Organization. 2020. Global tuberculosis report 2020. World Health Organization, Geneva, Switzerland.
6. Evangelopoulos D, McHugh TD. 2015. Improving the tuberculosis drug development pipeline. Chem Biol Drug Des 86:951–960. https://doi.org/10.1111/cbdd.12549.
7. Philips JA, Ernst JD. 2012. Tuberculosis pathogenesis and immunity. Annu Rev Pathol 7:353–384. https://doi.org/10.1146/annurev-pathol-011811-132458.
8. Lange C, Aarnoutse R, Chesov D, van Crevel R, Gillespie SH, Grobbel H-P, Kalsdorf B, Kontsevaya I, van Laarhoven A, Nishiguchi T, Mandalakas A, Merker M, Niemann S, Köhler N, Heyckendorf J, Reimann M, Ruhwald M, Sanchez-Carballo P, Schwudke D, Waldow F, DiNardo AR. 2020. Perspective for precision medicine for tuberculosis. Front Immunol 11:566608. https://doi.org/10.3389/fimmu.2020.566608.
9. Köser CU, Javid B, Liddell K, Ellington MJ, Feuerriegel S, Niemann S, Brown NM, Burman WJ, Abubakar I, Ismail NA, Moore D, Peacock SJ, Török ME. 2015. Drug-resistance mechanisms and tuberculosis drugs. Lancet 385:305–307. https://doi.org/10.1016/S0140-6736(14)62450-8.
10. Shetye GS, Franzblau SG, Cho S. 2020. New tuberculosis drug targets, their inhibitors, and potential therapeutic impact. Transl Res 220:68–97. https://doi.org/10.1016/j.trsl.2020.03.007.
11. Vilchèze C. 2020. Mycobacterial cell wall: a source of successful targets for old and new drugs. Appl Sci 10:2278. https://doi.org/10.3390/app10072278.
12. Makarov V, Manina G, Mikusova K, Möllmann U, Ryabova O, Saint-Joanis B, Dhar N, Pasca MR, Buroni S, Lucarelli AP, Milano A, de Rossi E, Belanova M, Bobovska A, Dianiskova P, Kordulakova J, Sala C, Fullam E, Schneider P, McKinney JD, Brodin P, Christophe T, Waddell S, Butcher P, Albrethsen J,

Downloaded from https://journals.asm.org/journal/aac on 29 March 2023 by 193.22.115.2.

Rosenkrands I, Brosch R, Nandi V, Bharath S, Gaonkar S, Shandil RK, Balasubramanian V, Balganesh T, Tyagi S, Grosset J, Riccardi G, Cole ST. 2009. Benzothiazinones kill Mycobacterium tuberculosis by blocking arabinan synthesis. Science 324:801–804. https://doi.org/10.1126/science.1171583.

13. Trefzer C, Škovierová H, Buroni S, Bobovská A, Nenci S, Molteni E, Pojer F, Pasca MR, Makarov V, Cole ST, Riccardi G, Mikušová K, Johnsson K. 2012. Benzothiazinones are suicide inhibitors of mycobacterial decaprenylphosphoryl-β-D-ribofuranose 2′-oxidase DprE1. J Am Chem Soc 134:912–915. https://doi.org/10.1021/ja211042r.
14. Neres J, Pojer F, Molteni E, Chiarelli LR, Dhar N, Boy-Röttger S, Buroni S, Fullam E, Degiacomi G, Lucarelli AP, Read RJ, Zanoni G, Edmondson DE, de Rossi E, Pasca MR, McKinney JD, Dyson PJ, Riccardi G, Mattevi A, Cole ST, Binda C. 2012. Structural basis for benzothiazinone-mediated killing of Mycobacterium tuberculosis. Sci Transl Med 4:150ra121. https://doi.org/10.1126/scitranslmed.3004395.
15. Gao C, Peng C, Shi Y, You X, Ran K, Xiong L, Ye T, Zhang L, Wang N, Zhu Y, Liu K, Zuo W, Yu L, Wei Y. 2016. Benzothiazinethione is a potent preclinical candidate for the treatment of drug-resistant tuberculosis. Sci Rep 6:29717. https://doi.org/10.1038/srep29717.
16. González-Martínez NA, Lozano-Garza HG, Castro-Garza J, de Osio-Cortez A, Vargas-Villarreal J, Cavazos-Rocha N, Ocampo-Candiani J, Makarov V, Cole ST, Vera-Cabrera L. 2015. In vivo activity of the benzothiazinones PBTZ169 and BTZ043 against Nocardia brasiliensis. PLoS Negl Trop Dis 9:e0004022. https://doi.org/10.1371/journal.pntd.0004022.
17. Makarov V, Lechartier B, Zhang M, Neres J, van der Sar AM, Raadsen SA, Hartkoorn RC, Ryabova OB, Vocat A, Decosterd LA, Widmer N, Buclin T, Bitter W, Andries K, Pojer F, Dyson PJ, Cole ST. 2014. Towards a new combination therapy for tuberculosis with next generation benzothiazinones. EMBO Mol Med 6:372–383. https://doi.org/10.1002/emmm.201303575.
18. Lechartier B, Hartkoorn RC, Cole ST. 2012. In vitro combination studies of benzothiazinone lead compound BTZ043 against Mycobacterium tuberculosis. Antimicrob Agents Chemother 56:5790–5793. https://doi.org/10.1128/AAC.01476-12.
19. Working Group for New TB Drugs. 2020. BTZ-043. https://www.newtbdrugs.org/pipeline/compound/btz-043. Accessed 22 February 2022.
20. Pasca MR, Degiacomi G, Ribeiro ALdJL, Zara F, de Mori P, Heym B, Mirrione M, Brerra R, Pagani L, Pucillo L, Troupioti P, Makarov V, Cole ST, Riccardi G. 2010. Clinical isolates of Mycobacterium tuberculosis in four European hospitals are uniformly susceptible to benzothiazinones. Antimicrob Agents Chemother 54:1616–1618. https://doi.org/10.1128/AAC.01676-09.
21. Hoelscher M. 2022. A prospective phase Ib/IIa, active-controlled, randomized, open-label study to evaluate the safety, tolerability, extended early bactericidal activity and pharmacokinetics of multiple oral doses of BTZ-043 tablets in subjects with newly diagnosed, uncomplicated, smear-positive, drug-susceptible pulmonary tuberculosis. https://www.clinicaltrials.gov/ct2/show/NCT04044001. Accessed 20 September 2022.
22. Clark S, Hall Y, Williams A. 2014. Animal models of tuberculosis: guinea pigs. Cold Spring Harb Perspect Med 5:a018572. https://doi.org/10.1101/cshperspect.a018572.
23. Ahmad Z, Klinkenberg LG, Pinn ML, Fraig MM, Peloquin CA, Bishai WR, Nuermberger EL, Grosset JH, Karakousis PC. 2009. Biphasic kill curve of isoniazid reveals the presence of drug-tolerant, not drug-resistant, Mycobacterium tuberculosis in the guinea pig. J Infect Dis 200:1136–1143. https://doi.org/10.1086/605605.
24. Institute of Medicine Forum on Drug Discovery, Development, and Translation, Science, Russian Academy of Medical Science. 2011. The new profile of drug-resistant tuberculosis in Russia: a global and local perspective: summary of a joint workshop. National Academies Press, Washington, DC.
25. Black TA, Buchwald UK. 2021. The pipeline of new molecules and regimens against drug-resistant tuberculosis. J Clin Tuberc Other Mycobact Dis 25:100285. https://doi.org/10.1016/j.jctube.2021.100285.
26. da Silva PB, Campos DL, Ribeiro CM, da Silva IC, Pavan FR. 2017. New antimycobacterial agents in the pre-clinical phase or beyond: recent advances in patent literature (2001–2016). Expert Opin Ther Pat 27:269–282. https://doi.org/10.1080/13543776.2017.1253681.
27. Liebler-Tenorio EM, Heyl J, Wedlich N, Figl J, Köhler H, Krishnamoorthy G, Nieuwenhuizen NE, Grode L, Kaufmann SHE, Menge C. 2022. Vaccine-induced subcutaneous granulomas in goats reflect differences in host–mycobacterium interactions between BCG- and recombinant BCG-derivative vaccines. Int J Mol Sci 23:10992. https://doi.org/10.3390/ijms231910992.
28. Koch R. 1882. Die Ätiologie der Tuberkulose. Berl Klin Wochenschr 19:1–5. https://doi.org/10.1007/978-3-662-56454-7_5.
29. Prideaux B, Dartois V, Staab D, Weiner DM, Goh A, Via LE, Barry CE, Stoeckli M. 2011. High-sensitivity MALDI-MRM-MS imaging of moxifloxacin distribution in tuberculosis-infected rabbit lungs and granulomatous lesions. Anal Chem 83:2112–2118. https://doi.org/10.1021/ac1029049.
30. Kasik JE, Monick M, Thompson JS. 1976. Immunosuppressant activity of the ansamycins. Antimicrob Agents Chemother 9:470–473. https://doi.org/10.1128/AAC.9.3.470.
31. Tousif S, Singh DK, Ahmad S, Moodley P, Bhattacharyya M, van Kaer L, Das G. 2014. Isoniazid induces apoptosis of activated CD4+ T cells: implications for post-therapy tuberculosis reactivation and reinfection. J Biol Chem 289:30190–30195. https://doi.org/10.1074/jbc.C114.598946.
32. Richter A, Seidel RW, Goddard R, Eckhardt T, Lehmann C, Dörner J, Siersleben F, Sondermann T, Mann L, Patzer M, Jäger C, Reiling N, Imming P. 2022. BTZ-derived benzisothiazolinones with in vitro activity against Mycobacterium tuberculosis. ACS Med Chem Lett 13:1302–1310. https://doi.org/10.1021/acsmedchemlett.2c00215.
33. Madikizela B, Eckhardt T, Goddard R, Richter A, Lins A, Lehmann C, Imming P, Seidel RW. 2021. Synthesis, structural characterization and antimycobacterial evaluation of several halogenated non-nitro benzothiazinones. Med Chem Res 30:1523–1533. https://doi.org/10.1007/s00044-021-02735-4.
34. Liu L, Kong C, Fumagalli M, Savková K, Xu Y, Huszár S, Sammartino JC, Fan D, Chiarelli LR, Mikušová K, Sun Z, Qiao C. 2020. Design, synthesis and evaluation of covalent inhibitors of DprE1 as antitubercular agents. Eur J Med Chem 208:112773. https://doi.org/10.1016/j.ejmech.2020.112773.
35. Mitchison DA, Wallace JG, Bhatia AL, Selkon JB, Subbaiah TV, Lancaster MC. 1960. A comparison of the virulence in guinea-pigs of South Indian and British tubercle bacilli. Tubercle 41:1–22. https://doi.org/10.1016/s0041-3879(60)80019-0.
36. Jain R, Dey B, Dhar N, Rao V, Singh R, Gupta UD, Katoch VM, Ramanathan VD, Tyagi AK. 2008. Enhanced and enduring protection against tuberculosis by recombinant BCG-Ag85C and its association with modulation of cytokine profile in lung. PLoS One 3:e3869. https://doi.org/10.1371/journal.pone.0003869.
37. Mulisch M, Welsch U. 2015. Romeis-Mikroskopische Technik. Springer, Berlin, Germany.
38. Bankhead P, Loughrey MB, Fernández JA, Dombrowski Y, McArt DG, Dunne PD, McQuaid S, Gray RT, Murray LJ, Coleman HG, James JA, Salto-Tellez M, Hamilton PW. 2017. QuPath: open source software for digital pathology image analysis. Sci Rep 7:16878. https://doi.org/10.1038/s41598-017-17204-5.

Downloaded from https://journals.asm.org/journal/aac on 29 March 2023 by 193.22.115.2.

Supplemental Table 1 – Pathology Score adapted from (24, 25)

Parameters	Score used
Inoculation site granuloma (right axillary subcutis)	
Granuloma(s) ≥3.5 cm in diameter with caseous necrosis	4
Granuloma(s) ≥2.5 cm in diameter with caseous necrosis	3
Granuloma(s) ≥1.5 cm in diameter ± caseous necrosis	2
Granuloma(s) ≥0.5 cm in diameter	1
No lesion	0
Right axillary lymph node	
Granuloma(s) ≥2.0 cm in diameter with caseous necrosis	4
Granuloma(s) ≥1.5 cm in diameter with caseous necrosis	3
Granuloma(s) ≥1.0 cm in diameter ± caseous necrosis	2
Granuloma(s) ≥0.5 cm in diameter	1
No lesion respectively of normal size (≤0.5 cm)	0
Spleen*	
Numerous granulomas (miliary type)	4
Many granulomas	3
Few granulomas	2
Single granulomas	1
No lesion	0
Liver*	
Numerous granulomas (miliary type)	4
Many granulomas	3
Few granulomas	2
Single granulomas	1
No lesion	0

*granulomas in spleen and liver were randomly distributed and 0.3 - 0.4 cm in diameter large

Supplemental Table 2 – PK parameters for M0 and M1 calculated by WinNonLin

Administration	Variable	C_{max} [ng/mL]	T_{max} [h]	AUC_{0-t} [h*ng/mL]	AUC_{0-inf} [h*ng/mL]	AUC_{extra} [%]
50 mg/kg micronized	M0	1239	1	5042	7626	34
	M1	119	2	352	-	-
200 mg/kg (micronized)	M0	984	1	3566	4053	12
	M1	1786	2	10003	10036	0
200 mg/kg (wet-milled)	M0	885	2	3305	3312	0
	M1	1377	2	8489	8560	1
400 mg/kg (micronized)	M0	2213	2	15220	39819	62
	M1	1678	4	19034	-	-

Note: "-" means that data were not available by the calculation of WinNonLin.

Fig S1

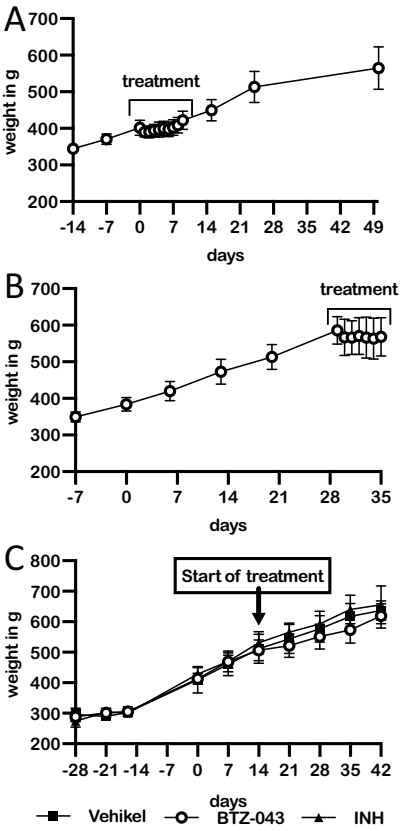

Supplement Figure 1 During BTZ-043 treatment guinea pigs show decelerated weight gain: For calculation of the right medication dosage and medical assessment guinea pigs were weighed regularly during the trials. (A) The weight curve of the multidose application study is shown, were guinea pigs were given daily 400 mg/kg BTZ-043 orally. Guinea pigs were weighed daily during and weekly before and after treatment. Error bars indicate the standard error of the mean (SEM). (B) Guinea pigs were s.c. infected with BCG on day zero and treated with 400 mg/kg BTZ-043 orally for seven days from day 29 on. The weight was measured weekly before and daily during the trial. Error bars indicate the SEM. (C) All guinea pigs were infected s.c. with virulent mycobacteria on day 0. From day 14 on they were either treated orally with 300 mg/kg BTZ-043 or 60 mg/kg isoniazid (INH) daily. As negative control guinea pigs were given vehicle solution. Guinea pigs were weighed weakly. Error bars indicate the SEM.

Fig S2

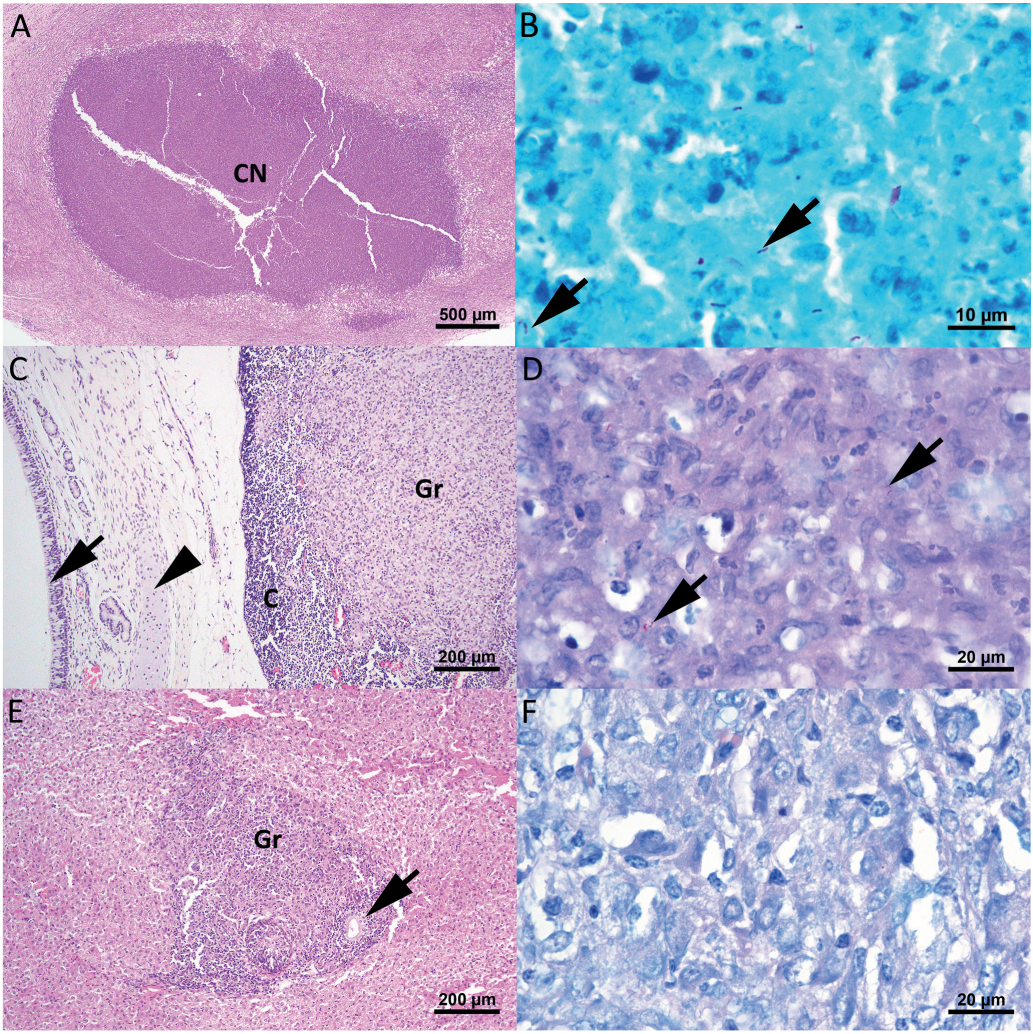

Supplemental Figure 2 Lesion characteristics and detection of acid-fast mycobacteria (AFB) in the vehicle control group 42 days after subcutaneous infection

(A) Granuloma in the axillary subcutaneous infection site of animal no. 4 with a central core of caseous necrosis (CN) and a peripheral rim of activated macrophages and fibrosis. (B) Within the caseous necrosis shown in Figure A few extracellular acid fast mycobacteria (arrows) are detectable. (C) Next to the trachea with intact respiratory epithelium (arrow) and cartilage (arrowhead), an extensive non-caseating granuloma (Gr) is evident in the *Ln. tracheobronchialis* of animal no. 4. (D) Few AFB reside in the cytoplasm of activated macrophages (arrows). (E) In the liver of animal no. 5 a non-caseating granuloma is shown in the periportal zone as outlined by a bile duct (arrow). (F) The hepatic granuloma is devoid of AFB. A, C, E; Hematoxylin eosin stain; Ziehl-Neelsen stain; F, H; Fite-Faraco-stain.

Fig S3

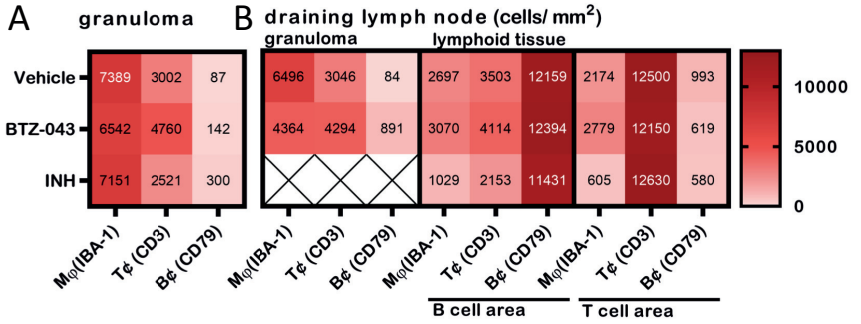

Supplement Figure 3 Guinea pigs treated with BTZ-043 have higher T cell numbers in granuloma and lymph node: Formaldehyde fixed, paraffin embedded tissue sections of the infection site granulomas and draining lymph nodes from all groups were investigated with selected immune cell markers by immunohistochemistry (IHC). (A) Consecutive sections of granulomas were stained for macrophage marker Iba-1, T cell marker CD3 and B cell marker CD79. Positive cells were counted using QuPath. The heatmap shows a comprehensive overview of the numbers of positive cells per mm^2 counted within the granulomas. Rows correspond to the three treated groups, columns to the tested surface marker or transcript. Figures represent mean values. (B) As above consecutive slides of axillary lymph nodes were stained for macrophages, T cells and B cells and positive cells were counted. It was differentiated between normal lymph node parenchyma (lymphoid tissue) with the corresponding T and B cell areas and granulomas (granulomatous area).

4 Contributions to publications

(I) Animal models for human group 1 CD1 protein function

Emmelie Eckhardt, Max Bastian

Molecular Immunology (130), S.159-163

DOI: 10.1016/j.molimm.2020.12.018.

Emmelie Eckhardt: Literature research, Writing – Original Draft, Review & Editing, Visualization

Max Bastian: Conceptualization, Literature research, Writing – Original Draft, Review & Editing

(II) Donor unrestricted T cells matter: Phosphatidylinositolmannoside vaccination induces lipid-specific Th1-responses and partially protects guinea pigs from Mycobacterium tuberculosis challenge

Emmelie Eckhardt, Jan Schinköthe, Marcel Gischke, Julia Sehl-Ewert, Björn Corleis, Anca Dorhoi, Jens Teifke, Dirk Albrecht, Annemieke Geluk, Martine Gilleron, Max Bastian

Submitted to Scientific Reports

(09.01.2023, Manuscript: SREP-23-00073)

Emmelie Eckhardt: Experimentation, Data Analysis, Writing

Jan Schinköthe: Experimentation, Data Analysis, Writing

Marcel Gischke: Experimentation, Data Analysis

Julia Sehl-Ewert: Experimentation

Björn Corleis: Critical Infrastructure, Writing/ Reviewing

Anca Dorhoi: Critical Infrastructure, Conceptualization, Writing/ Correction

Jens Teifke: Critical Infrastructure and Reagents, Conceptualization, Supervision, Writing/ Correction

Dirk Albrecht: Experimentation, Data Analysis

Annemieke Geluk: Critical Reagents, Conceptualization

Martine Gilleron: Critical Reagents, Conceptualization, Writing

Max Bastian: Experimentation, Data Analysis, Conceptualization, Funding, Writing

(III) Pharmacokinetics and Efficacy of the Benzothiazinone BTZ-043 against Tuberculous Mycobacteria inside Granulomas in the Guinea Pig Model

Emmelie Eckhardt, Yan Li, Svenja Mamerow, Jan Schinköthe, Julia Sehl-Ewert, Julia Dreisbach, Björn Corleis, Anca Dorhoi, Jens Teifke, Christian Menge, Florian Kloss, Max Bastian

Antimicrobial Agents and Chemotherapy, Accepted 16.02.2022

DOI: 10.1128/aac.01438-22

Emmelie Eckhardt: Data curation, Formal analysis, Investigation, Methodology, Visualization, Writing - original draft, Writing - review & editing

Yan Li: Formal analysis, Investigation, Methodology

Svenja Mamerow: Conceptualization, Funding acquisition, Investigation, Methodology, Project administration, Writing - review & editing

Jan Schinköthe: Data curation, Formal analysis, Investigation, Methodology, Validation, Visualization, Writing - original draft, Writing - review & editing

Julia Sehl-Ewert: Investigation, Methodology, Writing - review & editing

Julia Dreisbach: Conceptualization, Formal analysis, Funding acquisition, Resources, Validation, Writing - review & editing

Anca Dorhoi: Investigation, Methodology, Resources, Writing - review & editing

Jens P. Teifke: Conceptualization, Investigation, Supervision, Visualization, Writing - review & editing

Christian Menge: Conceptualization, Funding acquisition, Methodology, Project administration, Writing - review & editing

Florian Kloss: Conceptualization, Data curation, Formal analysis, Funding acquisition, Investigation, Writing - review & editing

Max Bastian: Conceptualization, Data curation, Formal analysis, Funding acquisition, Investigation, Methodology, Project administration, Resources, Supervision Visualization, Writing - original draft, Writing - review & editing

In agreement (Paper I to III):

Place, Date	Prof. Dr. Jens P. Teifke
	Dr. Max Bastian
	Emmelie Eckhardt

5 Discussion

Globally, tuberculosis is the deadliest disease caused by a single bacterial pathogen. It poses an enormous health risk to children and adults, especially in low- and middle-income countries, where 98 % of tuberculosis cases occur. Due to the lack of adequate diagnosis, treatment and prevention strategies, the situation in these countries is particularly difficult (World Health Organization, 2022a).

The WHO has established a plan to end the global tuberculosis epidemic (World Health Organization, 2015), but none of the milestones in WHO's End tuberculosis strategy by 2020 have been achieved (World Health Organization, 2021). While the tuberculosis incidence rate should have been reduced by 20 % between 2015 to 2020, there was only an 11 % reduction in the number of cases. For the number of deaths, it was a 9.2 % reduction instead of the WHO's target of 35 % (World Health Organization, 2021). Internationally, strategies need to be developed to make the burden tolerable for communities affected by tuberculosis (Erlinger et al., 2019; Stracker et al., 2019), and an important approach is to develop new tools to prevent and cure tuberculosis.

There are a number of challenges that need to be overcome: First, the only vaccine approved today, BCG, shows only variable protection. In particular, it does not protect against the epidemiologically most important pulmonary manifestation and therefore fails to control tuberculosis transmission (Colditz et al., 1994; Moliva et al., 2015). Efforts to develop new vaccine candidates are ongoing, and some of these candidates are currently undergoing various phases of clinical trials (Sable et al., 2019; Fatima et al., 2020; Schrager et al., 2020; Scriba et al., 2020). These vaccine candidates include subunit vaccines (protein adjuvants or viral vectors), live attenuated vaccines, and inactivated whole cell vaccines (Scriba et al., 2020). To date, however, none of these candidates has been able to outperform BCG and has been approved (Fatima et al., 2020). Another pressing concern is the increasing prevalence of multi- or extensively drug-resistant tuberculosis-strains (World Health Organization, 2021). Thus, the second important topic in tuberculosis research is the development of new antimicrobial agents and therapeutic regimens that are effective against drug-resistant *Mtb*.

The aim of this thesis was to contribute to these areas of tuberculosis research by refining the guinea pig tuberculosis model. To this end, sophisticated techniques were developed to investigate systemic and local tissue responses following virulent *Mtb*-infection. These techniques were then used in two different experimental approaches. In the first, an unconventional, lipid-based vaccine candidate to explore the antimycobacterial capabilities of T cells responding to a defined mycobacterial glycolipid, was tested. In the second project, the therapeutic effect of the new anti-mycobacterial compound BTZ-043 was investigated.

There are several widely used suitable animal models for different aspects of tuberculosis research, such as NHP, some rodents (mice, guinea pigs, rats), ruminants (cattle, goats) or non-mammals (zebrafish, fruit flies) (Gong et al., 2020; Yang et al., 2021).
Since the choice of animal model for an experiment is crucial for its feasibility and explanatory power, some aspects had to be fulfilled for the studies performed. It was important to use animals, that are naturally susceptible to tuberculosis, that are comparable to human tuberculosis infections in terms of pathology and immunology, and that can be handled well and kept safely under biosafety level 3 conditions. Therefore, guinea pigs were used for both projects, because they can be naturally infected with tuberculosis (Dharmadhikari et al., 2011), develop aspects of human tuberculosis (Turner et al., 2003; McMurray, 2014), and are easy to handle. In addition, there are longstanding experiences using them as small animal model (Bastian et al., 2011; Spohr et al., 2015; Kaufmann, 2016). Therefore, guinea pigs were an excellent model for these studies. Other animal models for tuberculosis such as mice, rats or zebrafish were unsuitable, because they do not naturally resemble human tuberculosis, or others such as cattle, goats or NHPs are more expensive, more complicated to keep and handle or even fraught with ethical concerns (Gong et al., 2020; Ramos et al., 2020).

Another crucial aspect of guinea pigs for the vaccinology study was that they express a functional CD1 type 1 system (Dascher et al., 1999; Hiromatsu et al., 2002). In a review paper (**publication I**), we highlighted and discussed the specificities of guinea pigs and other animal models for human CD1 type 1 protein function. CD1 type 1 molecules, expressed

mainly on professional APCs (Dougan et al., 2007), are essential and unique for the presentation of lipid antigens to T cells carrying a variable αβ-TCR (Beckman et al., 1994). While their structure and interaction with ligands are fairly well understood (Jackman et al., 1999; Moody et al., 2005), there is only a partial understanding and knowledge of the specific functions of CD1-restricted T cells. To study the *in vivo* functions of CD1 and induced T cell responses, initially only guinea pigs (Dascher et al., 2003), and later also cattle (Nguyen et al., 2009; Nguyen et al., 2015) and NHPs (Li et al., 2011) were used because they all naturally express CD1 type 1 molecules. In contrast, mice naturally do not express CD1 type 1 molecules. Therefore, the first description of a human CD1a/b/c-transgenic mouse strain in 2009 was a major breakthrough (Felio et al., 2009). The model has been used several times and has shed light on mechanistic aspects of CD1b T cell interactions since then (Li et al., 2011; Bagchi et al., 2017). However, in this mouse strain, the transgene is under the control of its native xenogenic, human promoter (Felio et al., 2009). Therefore, it is questionable whether the expression pattern and thus the function of the CD1 type 1-system in the transgenic model reflects the situation under natural conditions. In **publication I**, we discuss in detail the advantages and disadvantages of the different animal models and describe the various approaches used by researchers to address a broad range of problems including autoimmunity (Bagchi et al., 2017), studies of the gut microbiome (Gerb et al., 2021), and, of course, the function of CD1 type 1 molecules in infectious diseases such as *Staphylococcus aureus* or mycobacterial infections (Van Rhijn et al., 2009; Visvabharathy et al., 2020).

Lipid-reactive, CD1-restricted T cells are potentially interesting contributors to the antimycobacterial immunity, because mycobacteria express a wide variety of different lipids that are not covalently linked to the outer layer of the cell wall. Many of these lipids are known to represent CD1 ligands (Minnikin et al., 2002) and may be additional target antigens that could be incorporated into future tuberculosis vaccine formulations. In our vaccination experiment (**publication II**), PIM_6 was used as a mycobacterial lipid antigen to investigate the role and function of the corresponding CD1-restricted T cells in granuloma formation and maintenance and to evaluate the efficacy of PIM_6 vaccination in the guinea pig model.

PIM_6 is abundant on the outer leaflet of the inner membrane of mycobacteria (Bansal-Mutalik & Nikaido, 2014) making it an ideal target for recognition by immune cells. Since PIM species are not commercially available, they must either be purified from mycobacterial biomass or chemically synthesized (Gilleron et al., 2001; Boonyarattanakalin et al., 2008; Rahlwes et al., 2019; Nobre et al., 2022). Native preparations in particular are known to frequently contain contaminating lipopeptides, making the purity of these preparations a critical issue (Nobre et al., 2022).

PIM_6 was chosen as the vaccine antigen because strong T cell proliferation was observed when cells from animals vaccinated with BCG were stimulated with the lipid (publication II, Fig. 1A). Along these lines, the immune response of PBMCs from human tuberculosis patients to LAM, PIM and purified-protein derivate (PPD) was recently investigated by mass cytometry and high-multiplex immunoassay, revealing interesting patterns of chemokine induction after stimulation with PIM, that were markedly different from stimulation with PPD (Silva et al., 2021). Interestingly, T cell subsets also differed between stimulation with PPD or PIM, and a partial dependency on interaction with TLR2 was observed after PIM stimulation (Silva et al., 2021).

Previous studies in guinea pig have shown that vaccination with mycobacterial lipids, e.g. whole lipid extracts or PIM_2, provides protection against virulent *Mtb*-challenge. However, these studies did not further investigate the induced T cell responses (Dascher et al., 2003; Larrouy-Maumus et al., 2017). Therefore, in our study (**publication II**), characteristics of the immune response after BCG and PIM_6 vaccination were analyzed and compared using different methods before and after virulent *Mtb*-challenge. Using transcriptomic analysis, the expression of different cyto- and chemokines was detected, with a less proinflammatory cytokine pattern in the draining lymph node of PIM_6- or BCG-vaccinated animals. In the injection site granuloma, the expression levels of proinflammatory cytokines were higher in the PIM_6-group than in the CAF01-group. Histologic staining revealed not only the distribution of immune cells such as macrophages, T cells, and B cells and the expression of the tuberculosis-conducive cytokine IFN-γ, as has been shown previously (Fenhalls et al., 2002b; Fenhalls et al., 2002a; Turner et al., 2003), but also the expression of CXCL10 and

CD1 molecules in the tissue. Consistent with the findings of Fenhalls and coworkers, IFN-γ-expression was found predominantly inside the granulomas (Fenhalls et al., 2002a). Similarly, the proinflammatory chemokine CXCL10 was mainly associated with macrophages. In contrast, CD1b molecules were not shown to be expressed in large numbers inside the granuloma or on macrophages, but were expressed in the lymph node paracortex. As the PIM_6-vaccinated guinea pigs in our study were partially protected from infection with *Mtb*, this suggests that colocalization of CD1b molecules with T cells is more critical than widespread presence of CD1b for effective activation of the immune response and detection of mycobacterial lipid antigens. Pathological scores and the number of CFUs were significantly lower in the PIM_6 group than in the negative control group. Nevertheless, it also became clear, that immunization with PIM_6 and the resulting T cell responses alone are not sufficient to be used in a future vaccine approach against tuberculosis, as BCG-vaccinated guinea pigs were better protected in our experiments. However, as part of a subunit approach with other components, it could contribute to protection.

Only a vaccine that elicits stronger immune reactions and better protection than BCG can be considered as a future vaccine candidate (Sable et al., 2019). In the past, all vaccine approaches tested, proved to be no more efficient than BCG. Therefore, it is important that in recent years many vaccine approaches are based on knowledge about immunological aspects of tuberculosis infection (Fatima et al., 2020; Kaufmann, 2020b). Therefore, a thorough understanding of the mechanisms by which lipid antigens are presented and the role CD1-restricted T cells play in the antimycobacterial immune response would be an important prerequisite to fully exploit the potential of these antigens in tuberculosis vaccine research. To date, the rich repertoire of mycobacterial lipid antigens has not been conclusively tested (Sarmiento et al., 2019), and most subunit tuberculosis vaccine candidates are based on adjuvanted mycobacterial protein antigens (Gillard et al., 2016; Sable et al., 2019; Kaufmann, 2020a; Jenum et al., 2021; Woodworth et al., 2021). Other innovative strategies should also be considered to have a broad spectrum of potential vaccines that can be successful in the fight against tuberculosis. In our study, live attenuated BCG conferred more convincing protection than the lipid-based subunit candidate. This

may suggest that the concept of a live attenuated vaccine is more promising than the subunit approach. In fact, there are currently two very advanced live vaccine candidates in the pipeline. One is the genetically attenuated *Mtb*-strain MTBVAC (Martín et al., 2021). It showed good protection and attenuation in animals (Martín et al., 2006; Aguiló et al., 2016), a good safety profile in initial human studies (Tameris et al., 2019), and is being tested in a Phase III efficacy trial in South Africa since 2022 (Martín et al., 2021). The other one is VPM1002, a genetically modified BCG strain, which is already in phase III efficacy trials since 2018 (Kaufmann, 2021). This candidate has already demonstrated a good safety and immunogenicity profile in adults (Grode et al., 2013) and newborns (Loxton et al., 2017). The immune response following mycobacterial infection was considered in the development of the vaccine. Stefan Kaufmann and colleagues exchanged the gene encoding BCG urease C for the gene encoding *Listeria monocytogenes* listeriolysin O (Nieuwenhuizen et al., 2017). Therefore, VPM1002 vaccination induces not only a CD4 T_H1 response like conventional BCG, but also CD8 cytolytic T cells, resulting in improved efficacy (Nieuwenhuizen et al., 2017; Kaufmann, 2020b).

Another critical aspect of vaccinology is the impact of adjuvants on the induced immune response (Awate et al., 2013; Del Giudice et al., 2018; Pulendran et al., 2021). Tuberculosis vaccines require the induction of a robust T cell response in combination with a good safety profile. CAF01 is undoubtedly a strong and potent immunomodulator inducing T_H1 and T_H17 responses and is successfully used in different vaccine approaches (see 2.5 CAF01). Therefore, combining the PIM_6 preparation with CAF01 was an appropriate choice for our study (**publication II**). However, there are other effective T cell adjuvants (Hadden, 1994) such as AS02 (Garçon et al., 2007), 1,2-dioleoyl-3-trimethylammonium propane/D35/aluminum salt adjuvant (Haseda et al., 2021) or other CAF-preparations (e.g. CAF05, CAF06) (Pedersen et al., 2018), that could be considered as delivery systems for PIM_6 or other mycobacterial lipid antigens and could affect the outcome of immune response and protection.

The route of vaccination also has a major impact on the efficacy of a vaccine. For **publication II,** guinea pigs were vaccinated subcutaneously with PIM_6 or BCG and infected with *Mtb*,

as this provided the opportunity to study and compare the granuloma formation in the subcutis, dissemination of the bacteria in tissue, and the appearance of immune cells. Remarkably, BCG was administered per os when it was first introduced (Calmette, 1931), whereas the WHO now recommends intradermal application (Kuan et al., 2020).

Darrah et al. recently demonstrated the extent to which the route of vaccination alters the outcome of tuberculosis in NHPs (Darrah et al., 2020). They vaccinated animals either intradermally, intravenously or via an aerosol. Intravenous vaccination at a dose of $5x10^7$ CFUs resulted in a significantly better T cell response and protection of NHPs following a *Mtb*-challenge, demonstrating the possible potential of BCG when administered by a different route.

Intravenous administration might be appropriate for individual patients in a hygienic setting, but it is questionable whether this route is feasible for mass vaccination campaigns. Nevertheless, several viable injection routes should be considered when testing a new vaccine candidate or antigen. In the guinea pig model, intramuscular or subcutaneous injection can be practically investigated as well as mucosal application via the oral or nasal route and is also easily feasible in humans.

So, in this study (**publication II**) a strong T cell proliferation to PIM_6 after BCG vaccination was observed. When vaccinated with PIM_6, guinea pigs responded with a robust, vaccine-specific T cell response and a less proinflammatory cyto- and chemokine profile after *Mtb*-challenge. Furthermore, pathological scores and bacterial counts were reduced in PIM_6-vaccinated animals. CD1-expression was increased and CD1-expressing cells were mainly located in the paracortex of the lymph nodes. In summary, it can be concluded that PIM_6-specific T cells clearly contribute to protection from *Mtb*. Further efforts should address the mechanism and localization of this presentation and how the CD1-mediated protection can be strengthened.

For **publication III** in this dissertation, we used our expertise in the guinea pig model to test the pharmacokinetics and efficacy of the novel anti-tuberculosis drug BTZ-043.

Initially, the guinea pig was established as a good model for pharmacokinetics of BTZ-043 at a dose of 400 mg/kg. Since the goal was to find an animal model to test the ability of BTZ-

043 to reach bacteria inside granulomas, previously used animal models such as rats (Gao et al., 2016) or mice (Makarov et al., 2009; González-Martínez et al., 2015) were not suitable. Neither develop human-like granulomas after tuberculosis infection (Gong et al., 2020). BTZ-043 was also tested in the goat model, but the animals metabolized the compound so rapidly that no plasma levels were detected (unpublished data).

However, in the guinea pig, robust plasma levels of BTZ-043 were detectable over a 24-h period after both a single-dose and multiple doses. Furthermore, when BCG-vaccinated animals were treated with BTZ-043, the compound was detected in BCG-induced granulomas at high concentrations. Finally, the efficacy of BTZ-043 was tested in the treatment of *Mtb*-infected guinea pigs, and a significant reduction of pathology and bacterial counts was observed.

Despite four weeks of BTZ-043 treatment and a significant reduction of bacteria and pathological score, some residual bacteria and small persistent lesions were still detectable at the injection site and draining lymph node. This may be due to the comparatively short duration of treatment and the use of a single drug, as the standard treatment regimen for tuberculosis is a combination of two to four drugs over a of six-month period (Kumar & Kon, 2017).

It is also clear that mycobacteria have evolved the strategy of shutting down their metabolism to evade host immune system defense mechanisms (Gengenbacher & Kaufmann, 2012; Peddireddy et al., 2017). This may also have influenced the outcome of BTZ-043 treatment and explain the difference between the very low *in vitro* MIC of BTZ-043 (Makarov et al., 2014; Gao et al., 2016) and the induced plasma levels and resulting efficacy in granulomas *in vivo*.

In the so-called dormant state, mycobacteria are less susceptible to substances that interfere with metabolic processes. Accordingly, BTZ-043 was shown to be less effective in an *in vitro* dormancy-state model using *Mtb* strain 18b (Sala et al., 2010). One approach to address this problem is to prolong the duration of therapy. Since this comes with the risk of reduced patient compliance and premature discontinuation of therapy, alternative strategies are currently being investigated: Genes involved in the reactivation process of dormant mycobacteria, such as Rpf or DosR regulon genes, could be potential drug targets to

reactivate bacteria and make them susceptible to the corresponding drugs (Peddireddy et al., 2017). Although this appealing theoretical concept is still far from practical application, it might be usable in the future. Until then, combinations of anti-tuberculosis drugs have to be applied.

In **publication III**, differences in the plasma levels were observed in adult (publication III, Fig 1D) and juvenile guinea pigs (publication III, Fig 2B) after one dose of 400 mg/kg BTZ-043. BTZ-043 and its metabolite were detectable at significantly higher concentrations in the younger animals. In addition, some of the younger guinea pigs showed mild neurological signs 30 min to 4 h after BTZ-043 treatment. These details suggest that the absorption, distribution and/or metabolism of BTZ-043 is age-dependent, a phenomenon known for different drugs in human medicine. Age dependent changes in gastrointestinal physiology as well as transporters and enzymes, body composition, and other aspects, as reviewed by van den Anker et al., influence drug uptake and efficacy in human neonates and children (van den Anker et al., 2018). Moreover, the efficacy and side effects of antibiotics and other medications may be different in the elderly than in younger adults, on whom the drugs are mainly tested (Klotz, 2009; Pea, 2018). Here, in addition to some factors related to those in children, interactions with other drugs typically taken by older people for various reasons may be important (Klotz, 2009; Pea, 2018). These issues should not hinder the use of BTZ-043, as no adverse effects, neurological or otherwise, have been noted in adult guinea pigs. However, they should be considered when determining the treatment dose of BTZ-043 in humans.

The emergence of drug-resistance is not only a problem in tuberculosis, but also in many other bacteria that develop antibiotic-resistance and persistence, leading to treatment failure and recurrence of infections (Aslam et al., 2018; Huemer et al., 2020) and causing a global health crisis (World Health Organization, 2012).

The fact, that the development of new compounds is slow and tedious (Evangelopoulos & McHugh, 2015; da Silva et al., 2017; Berdigaliyev & Aljofan, 2020) highlights the importance of new promising drugs like BTZ-043.

Although it may not be as effective in the guinea pig model as standard drugs such as INH, it can make all the difference for someone suffering from MDR-/XDR-tuberculosis. When new drugs are approved for tuberculosis, care should be taken to use them judiciously. Either they can be used only to treat patients with resistant tuberculosis as a last resort, or they will be included in standard treatment. Drugs, that perform better than standard treatment in clinical trials are likely to be used for all tuberculosis patients. Nevertheless, it would be prudent to use some drugs only in resistant cases, because the history of tuberculosis treatment has taught us that mycobacteria are likely to develop resistance to new medications fairly soon (Keshavjee & Farmer, 2012). Therefore, it is even more important to keep mycobacteria susceptible to new agents for as long as possible by strengthening healthcare infrastructure, and monitoring patients receiving tuberculosis treatment (World Health Organization, 2022b, 2022c). In tuberculosis, treatment discontinuation and poor patient compliance are the main drivers for the development of antimicrobial resistance (Nguyen, 2016; Dheda et al., 2017; Goossens et al., 2020; Singh et al., 2020). Therefore, socio-economic interventions in tuberculosis-affected communities and the development and research of new compounds such as BTZ-043 must be pursued together to end the tuberculosis-epidemic.

Overall, **publication III** demonstrated the convincing effect of the novel anti-tuberculosis drug BTZ-043 in the guinea pig model and highlighted some aspects that should be investigated in further studies.

In summary, this work demonstrates the importance of the guinea pig model for tuberculosis research. Questions about immune response and protection following a novel vaccine approach that addresses the CD1 T cell axis were answered, including activation of specific T cells, cyto- and chemokine profiles, and impact on pathology and bacterial load following challenge infection. In addition, the ability of the innovative antituberculotic drug BTZ-043 to penetrate the granuloma and its high efficacy in *Mtb*-infected guinea pigs was demonstrated. Taken together, these studies contribute to the research and development of innovative approaches to end the global tuberculosis epidemic.

6 Summary

Human tuberculosis is caused by bacteria of the *Mycobacterium tuberculosis* complex, mainly by *Mycobacterium tuberculosis* (*Mtb*) itself. *Mtb* causes numerous infections, illnesses and deaths each year and is the leading cause of death among bacterial pathogens worldwide.

In this thesis, I addressed two major problems in tuberculosis control and eradication: the lack of an efficient vaccine against tuberculosis and the increasing emergence of drug-resistant *Mtb*-strains. The main focus has been on the hallmark of tuberculosis-infection, the granuloma, which represents the niche of persistence for mycobacteria but is also important for the development of host immune responses.

Guinea pigs were the animal of choice for the studies performed because they are naturally susceptible to *Mtb* and develop granulomas after infection that are comparable to those of human tuberculosis patients. It was also significant for the first project that guinea pigs have a functional CD1 type 1 system, homologue to those in humans. The avenues of exploration and knowledge about human CD1 type 1 protein function and the resulting T cell responses, have been summarized in a review paper (publication I).

In the first project (publication II), it was shown that vaccination with PIM_6 induced a PIM-specific, CD1-restricted T-cell response. After infection with virulent *Mtb*, vaccinated animals showed milder pathology as evidenced by smaller and fewer necrotic granulomas and less bacterial load compared with nonvaccinated guinea pigs. Histological and transcriptomic analyses demonstrated lower proinflammatory cyto- and chemokine levels in protected animals, whereas CD1b expression was upregulated in draining lymph nodes. Overall, this strongly suggests a contribution of PIM-specific T cells to the protection of guinea pigs after vaccination.

For the second project (publication III), the efficacy and pharmacokinetics of the new anti-tuberculosis drug BTZ-043 were investigated in the guinea pig. First, a dose-finding study was conducted to determine the appropriate dosage (400 mg/kg) of BTZ-043 in the guinea pig, in which plasma levels of the drug and its metabolite were detectable in plasma for

24 h. Subsequent multidose studies demonstrated that BTZ-043 was detectable in plasma at effective concentrations after multiple applications and also reached BCG-induced granulomas at high concentrations. Finally, treatment with BTZ-043 was shown to reduce pathology and bacterial load in granuloma, draining lymph nodes, and spleen in guinea pigs.

In conclusion, the work and results of this dissertation contribute to the research and development of new and innovative methods to control and eradicate tuberculosis.

6 Zusammenfassung

Bakterien des *Mycobacterium-tuberculosis*-Komplexes, allen voran *Mycobacterium tuberculosis* (*Mtb*) selbst, sind Erreger der humanen Tuberkulose und damit Ursache für zahlreiche Infektionen, Erkrankungen und Todesfälle jedes Jahr. So ist Tuberkulose weltweit die Haupttodesursache durch einen einzelnen bakteriellen Erreger und von ungeheurer Relevanz.

In der vorliegenden Doktorarbeit habe ich mich mit zwei Hauptproblemen der Tuberkulose-Bekämpfung beschäftigt: der Ermangelung eines effektiven Impfstoffes gegen Tuberkulose und der zunehmenden Entstehung von behandlungsresistenten Tuberkulose-Stämmen. Der Fokus lag dabei auf dem Tuberkulose-induzierten Granulom, ein typisches Merkmal der Erkrankung, welches sowohl als Nische für den Erreger als auch als Ort der Immunreaktion des Wirtes fungiert.

Für beide Problemstellungen diente das Meerschweinchen als Modelltier, da es auf natürlichem Wege mit Mykobakterien infizierbar ist und sich im Laufe der Infektion Granulome ähnlich denen des Menschen bilden. Für die erste Fragestellung war des Weiteren relevant, dass Meerschweinchen ein funktionales CD1-Typ-1-System besitzen, welches homolog zu dem im Menschen ist. Die Möglichkeiten, die sich daraus zur Erforschung und dem Verständnis der Funktion der humanen CD1-Typ 1 Proteine und die daraus resultierende T-Zell Antwort ergibt, wurden für das Meerschweinchen und weitere Tierarten in einem Review (Publikation I) ausführlich beschrieben.

Für die 2. Publikation wurde untersucht, wie sich die Immunisierung von Meerschweinchen mit dem mykobakteriellen Lipid-Antigen PIM_6 auf die T-Zell Antwort, die Granulombildung und den Schutz vor Tuberkulose auswirkt. Es konnte gezeigt werden, dass durch die Vakzinierung mit PIM_6 PIM-spezifische, CD1-restringierte T-Zellen induziert werden. Nach Infektion mit virulenten *Mtb* zeigten die geimpften Meerschweinchen eine deutlich mildere Pathologie, unter anderem mit kleineren und weniger nekrotischen Granulomen, sowie eine reduzierte Bakterienlast. Bei den geschützten Tieren konnten mittels histologischer und transkriptomischer

Untersuchungen niedrigere proinflammatorische Zyto- und Chemokinlevel nachgewiesen werden, während in den Lymphknoten die CD1b-Level erhöht waren. Zusammengenommen deutet dies auf einen Beitrag der PIM-spezifischen T-Zellen zum partiellen Schutz der Tiere durch die Impfung hin.

Für die 3. Publikation wurde die Effizienz und Pharmakokinetik von dem neuen anti-Tuberkulose-Wirkstoff BTZ-043 im Meerschweinchenmodell untersucht. In einer Dosis-Findungs-Studie wurde durch Einmalgaben von BTZ-043 eine geeignete Dosis zur Mehrfachbehandlung von Meerschweinchen festgelegt (400 mg/kg), bei welcher das Medikament und sein Metabolit über 24 h stabil im Plasma nachweisbar sind. In den darauffolgenden Studien konnte gezeigt werden, dass BTZ-043 nach Mehrfachbehandlung sowohl in geeigneter Konzentration im Plasma nachweisbar ist, als auch in BCG-induzierten Granulomen. Abschließend konnte in einer Infektionsstudie mit virulenten *Mtb* gezeigt werden, dass die Behandlung von Meerschweinchen mit BTZ-043 zu einer Reduktion der Pathologie und der Bakterienlast in Granulomen, drainierendem Lymphknoten und der Milz führt.

Zusammenfassend tragen die Ergebnisse dieser Doktorarbeit also zur Erforschung neuer und innovativer Methoden zur Bekämpfung der Tuberkulose bei: zum einen in der Untersuchung und Testung eines Lipid-Antigens zur Immunisierung als Grundlagenforschung und zum anderen die Evaluierung des bereits in Phase II befindlichen Medikaments BTZ-043 gegen Tuberkulose im Meerschweinchen.

7 References

Abdallah, A. M., Hill-Cawthorne, G. A., Otto, T. D., Coll, F., Guerra-Assunção, J. A., Gao, G., Naeem, R., Ansari, H., Malas, T. B., Adroub, S. A., Verboom, T., Ummels, R., Zhang, H., Panigrahi, A. K., McNerney, R., Brosch, R., Clark, T. G., Behr, M. A., Bitter, W., & Pain, A. (2015). Genomic expression catalogue of a global collection of BCG vaccine strains show evidence for highly diverged metabolic and cell-wall adaptations. *Scientific Reports*, *5*(1), 15443. https://doi.org/10.1038/srep15443

Abengozar-Muela, M., Esparza, M. V., Garcia-Ros, D., Vásquez, C. E., Echeveste, J. I., Idoate, M. A., Lozano, M. D., Melero, I., & Andrea, C. E. de (2020). Diverse immune environments in human lung tuberculosis granulomas assessed by quantitative multiplexed immunofluorescence. *Modern Pathology : An Official Journal of the United States and Canadian Academy of Pathology, Inc*, *33*(12), 2507–2519. https://doi.org/10.1038/s41379-020-0600-6

Aguiló, N., Uranga, S., Marinova, D., Monzón, M., Badiola, J., & Martín, C. (2016). MTBVAC vaccine is safe, immunogenic and confers protective efficacy against *Mycobacterium tuberculosis* in newborn mice. *Tuberculosis (Edinburgh, Scotland)*, *96*, 71–74. https://doi.org/10.1016/j.tube.2015.10.010

Ahmed, A., Rakshit, S., Adiga, V., Dias, M., Dwarkanath, P., D'Souza, G., & Vyakarnam, A. (2021). A century of BCG: Impact on tuberculosis control and beyond. *Immunological Reviews*, *301*(1), 98–121. https://doi.org/10.1111/imr.12968

Algood, H. M., Chan, J., & Flynn, J. L. (2003). Chemokines and tuberculosis. *Cytokine & Growth Factor Reviews*, *14*(6), 467–477. https://doi.org/10.1016/S1359-6101(03)00054-6

Angula, K. T., Legoabe, L. J., & Beteck, R. M. (2021). Chemical Classes Presenting Novel Antituberculosis Agents Currently in Different Phases of Drug Development: A 2010-2020 Review. *Pharmaceuticals (Basel, Switzerland)*, *14*(5), 461. https://doi.org/10.3390/ph14050461

Apt, A. S., Kramnik, I., & McMurray, D. N. (2020). Editorial: Mycobacteria-Host Interactions: Genetics, Immunity, Pathology. *Frontiers in Cellular and Infection Microbiology*, *10*, 611216. https://doi.org/10.3389/fcimb.2020.611216

Aranaz, A., De Juan, L., Montero, N., Sánchez, C., Galka, M., Delso, C., Alvarez, J., Romero, B., Bezos, J., Vela, A. I., Briones, V., Mateos, A., & Domínguez, L. (2004). Bovine tuberculosis (*Mycobacterium bovis)* in wildlife in Spain. *Journal of Clinical Microbiology*, *42*(6), 2602–2608. https://doi.org/10.1128/JCM.42.6.2602-2608.2004

Aslam, B., Wang, W., Arshad, M. I., Khurshid, M., Muzammil, S., Rasool, M. H., Nisar, M. A., Alvi, R. F., Aslam, M. A., Qamar, M. U., Salamat, M. K. F., & Baloch, Z. (2018). Antibiotic resistance: a rundown of a global crisis. *Infection and Drug Resistance*, *11*, 1645–1658. https://doi.org/10.2147/IDR.S173867

Awate, S., Babiuk, L. A., & Mutwiri, G. (2013). Mechanisms of action of adjuvants. *Frontiers in Immunology*, *4*, 114. https://doi.org/10.3389/fimmu.2013.00114

Awuh, J. A., & Flo, T. H. (2017). Molecular basis of mycobacterial survival in macrophages. *Cellular and Molecular Life Sciences*, *74*(9), 1625–1648. https://doi.org/10.1007/s00018-016-2422-8

Bagchi, S., He, Y., Zhang, H., Cao, L., Van Rhijn, I., Moody, D. B., Gudjonsson, J. E., & Wang, C.-R. (2017). CD1b-autoreactive T cells contribute to hyperlipidemia-induced skin inflammation in mice. *The Journal of Clinical Investigation*, *127*(6), 2339–2352. https://doi.org/10.1172/JCI92217

Balabanova, Y., Fedorin, I., Kuznetsov, S., Graham, C., Ruddy, M., Atun, R., Coker, R., & Drobniewski, F. (2004). Antimicrobial prescribing patterns for respiratory diseases including tuberculosis in Russia: a possible role in drug resistance? *Journal of Antimicrobial Chemotherapy*, *54*(3), 673–679. https://doi.org/10.1093/jac/dkh383

Ballou, C. E., Vilkas, E., & Lederer, E. (1963). Structural Studies on the Myo-inositol Phospholipids of *Mycobacterium tuberculosis* (var. bovis, strain BCG). *Journal of Biological Chemistry*, *238*(1), 69–76. https://doi.org/10.1016/S0021-9258(19)83963-7

Banasik, B. N., Perry, C. L., Keith, C. A., Bourne, N., Schäfer, H., & Milligan, G. N. (2019). Development of an anti-guinea pig CD4 monoclonal antibody for depletion of CD4+ T cells in vivo. *Journal of Immunological Methods*, *474*, 112654. https://doi.org/10.1016/j.jim.2019.112654

Bansal-Mutalik, R., & Nikaido, H. (2014). Mycobacterial outer membrane is a lipid bilayer and the inner membrane is unusually rich in diacyl phosphatidylinositol dimannosides. *Proceedings of the National Academy of Sciences of the United States of America*, *111*(13), 4958–4963. https://doi.org/10.1073/pnas.1403078111

Barberis, I., Bragazzi, N. L., Galluzzo, L., & Martini, M. (2017). The history of tuberculosis: from the first historical records to the isolation of Koch's bacillus. *Journal of Preventive Medicine and Hygiene*, *58*(1), E9-E12.

Barr, D. A., Lewis, J. M., Feasey, N., Schutz, C., Kerkhoff, A. D., Jacob, S. T., Andrews, B., Kelly, P., Lakhi, S., Muchemwa, L., Bacha, H. A., Hadad, D. J., Bedell, R., van Lettow, M., Zachariah, R., Crump, J. A., Alland, D., Corbett, E. L., Gopinath, K., . . . Meintjes, G. (2020). *Mycobacterium tuberculosis* bloodstream infection prevalence, diagnosis, and mortality risk in seriously ill adults with HIV: a systematic review and meta-analysis of individual patient data. *The Lancet Infectious Diseases*, *20*(6), 742–752. https://doi.org/10.1016/S1473-3099(19)30695-4

Basaraba, R. J. (2008). Experimental tuberculosis: the role of comparative pathology in the discovery of improved tuberculosis treatment strategies. *Tuberculosis*, *88*, S35-S47. https://doi.org/10.1016/S1472-9792(08)70035-0

Bastian, M., Braun, T., Bruns, H., Röllinghoff, M., & Stenger, S. (2008). Mycobacterial lipopeptides elicit $CD4^+$ CTLs in *Mycobacterium tuberculosis*-infected humans. *Journal of Immunology*, *180*(5), 3436–3446. https://doi.org/10.4049/jimmunol.180.5.3436

Bastian, M., Holsteg, M., Hanke-Robinson, H., Duchow, K., & Cussler, K. (2011). Bovine Neonatal Pancytopenia: is this alloimmune syndrome caused by vaccine-induced alloreactive antibodies? *Vaccine*, *29*(32), 5267–5275. https://doi.org/10.1016/j.vaccine.2011.05.012

Batt, S. M., Minnikin, D. E., & Besra, G. S. (2020). The thick waxy coat of mycobacteria, a protective layer against antibiotics and the host's immune system. *The Biochemical Journal*, *477*(10), 1983–2006. https://doi.org/10.1042/BCJ20200194

Beckman, E. M., Porcelli, S. A., Morita, C. T., Behar, S. M., Furlong, S. T., & Brenner, M. B. (1994). Recognition of a lipid antigen by CD1-restricted alpha beta+ T cells. *Nature*, *372*(6507), 691–694. https://doi.org/10.1038/372691a0

Behar, S. M., & Cardell, S. (2000). Diverse CD1d-restricted T cells: diverse phenotypes, and diverse functions. *Seminars in Immunology*, *12*(6), 551–560. https://doi.org/10.1006/smim.2000.0273

Behar, S. M., Divangahi, M., & Remold, H. G. (2010). Evasion of innate immunity by *Mycobacterium tuberculosis*: is death an exit strategy? *Nature Reviews Microbiology*, *8*(9), 668–674. https://doi.org/10.1038/nrmicro2387

Behr, M. A., & Small, P. M. (1999). A historical and molecular phylogeny of BCG strains. *Vaccine*, *17*(7-8), 915–922. https://doi.org/10.1016/s0264-410x(98)00277-1

Berdigaliyev, N., & Aljofan, M. (2020). An overview of drug discovery and development. *Future Medicinal Chemistry*, *12*(10), 939–947. https://doi.org/10.4155/fmc-2019-0307

Berg, M. K., Yu, Q., Salvador, C. E., Melani, I., & Kitayama, S. (2020). Mandated Bacillus Calmette-Guérin (BCG) vaccination predicts flattened curves for the spread of COVID-19. *Science Advances*, *6*(32). https://doi.org/10.1126/sciadv.abc1463

Bernasconi, N. L., Traggiai, E., & Lanzavecchia, A. (2002). Maintenance of serological memory by polyclonal activation of human memory B cells. *Science*, *298*(5601), 2199–2202. https://doi.org/10.1126/science.1076071

Berrington, W. R., & Hawn, T. R. (2007). *Mycobacterium tuberculosis*, macrophages, and the innate immune response: does common variation matter? *Immunological Reviews*, *219*, 167–186. https://doi.org/10.1111/j.1600-065X.2007.00545.x

Bhatt, K., Verma, S., Ellner, J. J., & Salgame, P. (2015). Quest for correlates of protection against tuberculosis. *Clinical and Vaccine Immunology : CVI*, *22*(3), 258–266. https://doi.org/10.1128/CVI.00721-14

Birkness, K. A., Guarner, J., Sable, S. B., Tripp, R. A., Kellar, K. L., Bartlett, J., & Quinn, F. D. (2007). An in vitro model of the leukocyte interactions associated with granuloma formation in Mycobacterium tuberculosis infection. *Immunology and Cell Biology*, *85*(2), 160–168. https://doi.org/10.1038/sj.icb.7100019

Bitencourt, J., Peralta-Álvarez, M. P., Wilkie, M., Jacobs, A. J., Wright, D., Salman Almujri, S., Li, S., Harris, S. A., Smith, S. G., Elias, S. C., White, A. D., Satti, I., Sharpe, S. S., O'Shea, M. K., McShane, H., & Tanner, R. (2021). Induction of Functional Specific Antibodies, IgG-Secreting Plasmablasts and Memory B Cells Following BCG Vaccination. *Frontiers in Immunology*, *12*, 798207. https://doi.org/10.3389/fimmu.2021.798207

Bloom, B. R., Atun, R., Cohen, T., Dye, C., Fraser, H., Gomez, G. B., Knight, G., Murray, M. B., Nardell, E. A., Rubin, E. J., Salomon, J., Vassall, A., Volchenkov, G., White, R., Wilson, D., & Yadav, P. (2017). Major Infectious Diseases: Tuberculosis. https://doi.org/10.1596/978-1-4648-0524-0_ch11

Bobak, C. A., Abhimanyu, N., Natarajan, H., Gandhi, T., Grimm, S. L., Nishiguchi, T., Koster, K., Longlax, S. C., Dlamini, Q., Kahari, J., Mtetwa, G., Cirillo, J. D., O'Malley, J., Hill, J. E., Coarfa, C., & DiNardo, A. R. (2022). Increased DNA methylation, cellular senescence and premature epigenetic aging in guinea pigs and humans with tuberculosis. *Aging*, *14*(5), 2174–2193. https://doi.org/10.18632/aging.203936

Boonyarattanakalin, S., Liu, X., Michieletti, M., Lepenies, B., & Seeberger, P. H. (2008). Chemical synthesis of all phosphatidylinositol mannoside (PIM) glycans from *Mycobacterium tuberculosis*. *Journal of the American Chemical Society*, *130*(49), 16791–16799. https://doi.org/10.1021/ja806283e

Borkute, R. R., Woelke, S., Pei, G., & Dorhoi, A. (2021). Neutrophils in Tuberculosis: Cell Biology, Cellular Networking and Multitasking in Host Defense. *International Journal of Molecular Sciences*, *22*(9). https://doi.org/10.3390/ijms22094801

Bozzano, F., Marras, F., & Maria, A. de (2014). Immunology of tuberculosis. *Mediterranean Journal of Hematology and Infectious Diseases*, *6*(1), e2014027. https://doi.org/10.4084/MJHID.2014.027

Brennan, P. J., & Nikaido, H. (1995). The envelope of mycobacteria. *Annual Review of Biochemistry*, *64*, 29–63. https://doi.org/10.1146/annurev.bi.64.070195.000333

Brigl, M., & Brenner, M. B. (2004). CD1: antigen presentation and T cell function. *Annual Review of Immunology*, *22*, 817–890. https://doi.org/10.1146/annurev.immunol.22.012703.104608

Briken, V., Porcelli, S. A., Besra, G. S., & Kremer, L. (2004). Mycobacterial lipoarabinomannan and related lipoglycans: from biogenesis to modulation of the immune response. *Molecular Microbiology*, *53*(2), 391–403. https://doi.org/10.1111/j.1365-2958.2004.04183.x

Brill, K. J., Li, Q., Larkin, R., Canaday, D. H., Kaplan, D. R., Boom, W. H., & Silver, R. F. (2001). Human natural killer cells mediate killing of intracellular *Mycobacterium tuberculosis* H37Rv via granule-independent mechanisms. *Infection and Immunity*, *69*(3), 1755–1765. https://doi.org/10.1128/IAI.69.3.1755-1765.2001

Bruchfeld, J., Correia-Neves, M., & Källenius, G. (2015). Tuberculosis and HIV Coinfection. *Cold Spring Harbor Perspectives in Medicine*, *5*(7), a017871. https://doi.org/10.1101/cshperspect.a017871

Cáceres, N., Tapia, G., Ojanguren, I., Altare, F., Gil, O., Pinto, S., Vilaplana, C., & Cardona, P. J. (2009). Evolution of foamy macrophages in the pulmonary granulomas of experimental tuberculosis models. *Tuberculosis (Edinburgh, Scotland)*, *89*(2), 175–182. https://doi.org/10.1016/j.tube.2008.11.001

Calabi, F., & Milstein, C. (2000). The molecular biology of CD1. *Seminars in Immunology*, *12*(6), 503–509. https://doi.org/10.1006/smim.2000.0271

Cala-De Paepe, D., Layre, E., Giacometti, G., Garcia-Alles, L.-F., Mori, L., Hanau, D., Libero, G. de, La Salle, H. d., Puzo, G., & Gilleron, M. (2012). Deciphering the role of CD1e protein in mycobacterial phosphatidyl-myo-inositol mannosides (PIM) processing for presentation by CD1b to T lymphocytes. *The Journal of Biological Chemistry*, *287*(37), 31494–31502. https://doi.org/10.1074/jbc.M112.386300

Calmette, A. (1931). Preventive Vaccination Against Tuberculosis with BCG. *Proceedings of the Royal Society of Medicine*, *24*(11), 1481–1490. https://doi.org/10.1177/003591573102401109

Cambier, C. J., Takaki, K. K., Larson, R. P., Hernandez, R. E., Tobin, D. M., Urdahl, K. B., Cosma, C. L., & Ramakrishnan, L. (2014). Mycobacteria manipulate macrophage recruitment through coordinated use of membrane lipids. *Nature*, *505*(7482), 218–222. https://doi.org/10.1038/nature12799

Cegielski, J. P., & McMurray, D. N. (2004). The relationship between malnutrition and tuberculosis: evidence from studies in humans and experimental animals. *The International Journal of Tuberculosis and Lung Disease: The Official Journal of the International Union Against Tuberculosis and Lung Disease*, *8*(3), 286–298.

Chatterjee, D., Hunter, S. W., McNeil, M. R., & Brennan, P. J. (1992). Lipoarabinomannan. Multiglycosylated form of the mycobacterial mannosylphosphatidylinositols. *Journal of Biological Chemistry*, *267*(9), 6228–6233. https://doi.org/10.1016/S0021-9258(18)42685-3

Cheville, N. F. (Ed.). (2009). *Ultrastructural Pathology: The Comparative Cellular Basis of Disease* (Second Edition). Wiley-Blackwell.

Chiaradia, L., Lefebvre, C., Parra, J., Marcoux, J., Burlet-Schiltz, O., Etienne, G., Tropis, M., & Daffé, M. (2017). Dissecting the mycobacterial cell envelope and defining the composition of the native mycomembrane. *Scientific Reports*, *7*(1), 12807. https://doi.org/10.1038/s41598-017-12718-4

Christensen, D. (2017). Development and Evaluation of CAF01. In V. E. Schijns & D. T. O'Hagan (Eds.), *Immunopotentiators in Modern Vaccines (Second Edition)* (333–345). Academic Press. https://doi.org/10.1016/B978-0-12-804019-5.00017-7

Christensen, D., Agger, E. M., Andreasen, L. V., Kirby, D., Andersen, P., & Perrie, Y. (2009). Liposome-based cationic adjuvant formulations (CAF): past, present, and future. *Journal of Liposome Research*, *19*(1), 2–11. https://doi.org/10.1080/08982100902726820

Christensen, D., Christensen, J. P., Korsholm, K. S., Isling, L. K., Erneholm, K., Thomsen, A. R., & Andersen, P. (2017). Seasonal Influenza Split Vaccines Confer Partial Cross-Protection against Heterologous Influenza Virus in Ferrets When Combined with the CAF01 Adjuvant. *Frontiers in Immunology*, *8*, 1928. https://doi.org/10.3389/fimmu.2017.01928

Churchyard, G. J., Kim, P., Shah, N. S., Rustomjee, R., Gandhi, N. R., Mathema, B., Dowdy, D., Kasmar, A. G., & Cardenas, V. (2017). What We Know About Tuberculosis Transmission: An Overview. *The Journal of Infectious Diseases*, *216*(suppl_6), 629-635. https://doi.org/10.1093/infdis/jix362

Ciabattini, A., Pettini, E., Fiorino, F., Pastore, G., Andersen, P., Pozzi, G., & Medaglini, D. (2016). Modulation of Primary Immune Response by Different Vaccine Adjuvants. *Frontiers in Immunology*, *7*, 427. https://doi.org/10.3389/fimmu.2016.00427

Cirovic, B., Bree, L. C. J. de, Groh, L., Blok, B. A., Chan, J., van der Velden, W. J. F. M., Bremmers, M. E. J., van Crevel, R., Händler, K., Picelli, S., Schulte-Schrepping, J., Klee, K., Oosting, M., Koeken, V. A. C. M., van Ingen, J., Li, Y., Benn, C. S., Schultze, J. L., Joosten, L. A. B., . . . Schlitzer, A. (2020). BCG Vaccination in Humans Elicits Trained Immunity via the Hematopoietic Progenitor Compartment. *Cell Host & Microbe*, *28*(2), 322-334.e5. https://doi.org/10.1016/j.chom.2020.05.014

Clark, S. O., Hall, Y., & Williams, A. (2014). Animal models of tuberculosis: Guinea pigs. *Cold Spring Harbor Perspectives in Medicine*, *5*(5), a018572. https://doi.org/10.1101/cshperspect.a018572

Clemmensen, H. S., Dube, J.-Y., McIntosh, F., Rosenkrands, I., Jungersen, G., Aagaard, C., Andersen, P., Behr, M. A., & Mortensen, R. (2021). In vivo antigen expression regulates CD4 T cell differentiation and vaccine efficacy against *Mycobacterium tuberculosis* infection. *MBio*, *12*(2), e00226-21. https://doi.org/10.1128/mBio.00226-21

Colditz, G. A., Brewer, T. F., Berkey, C. S., Wilson, M. E., Burdick, E., Fineberg, H. V., & Mosteller, F. (1994). Efficacy of BCG vaccine in the prevention of tuberculosis. Meta-analysis of the published literature. *The Journal of the American Medical Association*, *271*(9), 698–702.

Comas, I., Chakravartti, J., Small, P. M., Galagan, J., Niemann, S., Kremer, K., Ernst, J. D., & Gagneux, S. (2010). Human T cell epitopes of *Mycobacterium tuberculosis* are evolutionarily hyperconserved. *Nature Genetics*, *42*(6), 498–503. https://doi.org/10.1038/ng.590

Corbel, M. J., Fruth, U., Griffiths, E., & Knezevic, I. (2004). Report on a WHO consultation on the characterisation of BCG strains, Imperial College, London 15-16 December 2003. *Vaccine*, *22*(21-22), 2675–2680. https://doi.org/10.1016/j.vaccine.2004.01.050

Cox, H. S., Orozco, J. D., Male, R., Ruesch-Gerdes, S., Falzon, D., Small, I., Doshetov, D., Kebede, Y., & Aziz, M. (2004). Multidrug-resistant tuberculosis in central Asia. *Emerging Infectious Diseases*, *10*(5), 865–872. https://doi.org/10.3201/eid1005.030718

Creissen, E., Izzo, L., Dawson, C., & Izzo, A. A. (2021). Guinea Pig Model of *Mycobacterium tuberculosis* Infection. *Current Protocols*, *1*(12), e312. https://doi.org/10.1002/cpz1.312

da Silva, D. A. A., da Silva, M. V., Barros, C. C. O., Alexandre, P. B. D., Timóteo, R. P., Catarino, J. S., Sales-Campos, H., Machado, J. R., Rodrigues, D. B. R., Oliveira, C. J., & Rodrigues, V. (2018). TNF-α blockade impairs in vitro tuberculous granuloma formation and down modulate Th1, Th17 and Treg cytokines. *PLoS ONE*, *13*(3), e0194430. https://doi.org/10.1371/journal.pone.0194430

da Silva, P. B., Campos, D. L., Ribeiro, C. M., da Silva, I. C., & Pavan, F. R. (2017). New antimycobacterial agents in the pre-clinical phase or beyond: recent advances in patent literature (2001-2016). *Expert Opinion on Therapeutic Patents*, *27*(3), 269–282. https://doi.org/10.1080/13543776.2017.1253681

Daffé, M., & Marrakchi, H. (2019). Unraveling the Structure of the Mycobacterial Envelope. *Microbiology Spectrum*, 1087–1095. https://doi.org/10.1128/9781683670131.ch65

Daffé, M., Quémard, A., & Marrakchi, H. (2017). Mycolic Acids: From Chemistry to Biology. In O. Geiger (Ed.), *Biogenesis of Fatty Acids, Lipids and Membranes* (1–36). Springer International Publishing. https://doi.org/10.1007/978-3-319-43676-0_18-1

Daniel, T. M. (2006). The history of tuberculosis. *Respiratory Medicine*, *100*(11), 1862–1870. https://doi.org/10.1016/j.rmed.2006.08.006

Daniel, T. M. (2011). Hermann Brehmer and the origins of tuberculosis sanatoria. *The International Journal of Tuberculosis and Lung Disease: The Official Journal of the International Union Against Tuberculosis and Lung Disease*, *15*(2), 161-2. https://doi.org/10.5588/ijtld.08.0472

Darrah, P. A., Zeppa, J. J., Maiello, P., Hackney, J. A., Wadsworth, M. H., Hughes, T. K., Pokkali, S., Swanson, P. A., Grant, N. L., Rodgers, M. A., Kamath, M., Causgrove, C. M., Laddy, D. J., Bonavia, A., Casimiro, D., Lin, P. L., Klein, E., White, A. G., Scanga, C. A., . . . Seder, R. A. (2020). Prevention of tuberculosis in macaques after intravenous BCG immunization. *Nature*, *577*(7788), 95–102. https://doi.org/10.1038/s41586-019-1817-8

Dascher, C. C. (2007). Evolutionary biology of CD1. *Current Topics in Microbiology and Immunology*, *314*, 3–26. https://doi.org/10.1007/978-3-540-69511-0_1

Dascher, C. C., Hiromatsu, K., Naylor, J. W., Brauer, P. P., Brown, K. A., Storey, J. R., Behar, S. M., Kawasaki, E. S., Porcelli, S. A., Brenner, M. B., & LeClair, K. P. (1999). Conservation of a CD1 multigene family in the guinea pig. *Journal of Immunology*, *163*(10), 5478–5488.

Dascher, C. C., Hiromatsu, K., Xiong, X., Morehouse, C., Watts, G., Liu, G., McMurray, D. N., LeClair, K. P., Porcelli, S. A., & Brenner, M. B. (2003). Immunization with a mycobacterial lipid vaccine improves pulmonary pathology in the guinea pig model of tuberculosis. *International Immunology*, *15*(8), 915–925. https://doi.org/10.1093/intimm/dxg091

Davidson, J. A., Loutet, M. G., O'Connor, C., Kearns, C., Smith, R. M., Lalor, M. K., Thomas, H. L., Abubakar, I., & Zenner, D. (2017). Epidemiology of *Mycobacterium bovis* disease in humans in England, Wales, and Northern Ireland, 2002–2014. *Emerging Infectious Diseases*, *23*(3), 377–386. https://doi.org/10.3201/eid2303.161408

Davis, J. M., & Ramakrishnan, L. (2009). The role of the granuloma in expansion and dissemination of early tuberculous infection. *Cell*, *136*(1), 37–49. https://doi.org/10.1016/j.cell.2008.11.014

De Libero, G., Collmann, A., & Mori, L. (2009). The cellular and biochemical rules of lipid antigen presentation. *European Journal of Immunology*, *39*(10), 2648–2656. https://doi.org/10.1002/eji.200939425

De Libero, G., & Mori, L. (2014). The T-Cell Response to Lipid Antigens of *Mycobacterium tuberculosis*. *Frontiers in Immunology*, *5*, 219. https://doi.org/10.3389/fimmu.2014.00219

Del Giudice, G., Rappuoli, R., & Didierlaurent, A. M. (2018). Correlates of adjuvanticity: A review on adjuvants in licensed vaccines. *Seminars in Immunology*, *39*, 14–21. https://doi.org/10.1016/j.smim.2018.05.001

Dharmadhikari, A. S., Basaraba, R. J., van der Walt, M. L., Weyer, K., Mphahlele, M., Venter, K., Jensen, P. A., First, M. W., Parsons, S., McMurray, D. N., Orme, I. M., & Nardell, E. A. (2011). Natural infection of guinea pigs exposed to patients with highly drug-resistant tuberculosis. *Tuberculosis (Edinburgh, Scotland)*, *91*(4), 329–338. https://doi.org/10.1016/j.tube.2011.03.002

Dheda, K., Gumbo, T., Gandhi, N. R., Murray, M. B., Theron, G., Udwadia, Z. F., Migliori, G. B., & Warren, R. M. (2014). Global control of tuberculosis: from extensively drug-resistant to untreatable tuberculosis. *The Lancet Respiratory Medicine*, *2*(4), 321–338. https://doi.org/10.1016/S2213-2600(14)70031-1

Dheda, K., Gumbo, T., Maartens, G., Dooley, K. E., McNerney, R., Murray, M. B., Furin, J., Nardell, E. A., London, L., Lessem, E., Theron, G., van Helden, P. D., Niemann, S., Merker, M., Dowdy, D., van Rie, A., Siu, G. K. H., Pasipanodya, J. G., Rodrigues, C., . . . Warren, R. M. (2017). The epidemiology, pathogenesis, transmission, diagnosis, and management of multidrug-resistant, extensively drug-resistant, and incurable tuberculosis. *The Lancet Respiratory Medicine*, *5*(4), 291–360. https://doi.org/10.1016/S2213-2600(17)30079-6

Dommergues, M. A., La Rocque, F. de, Guy, C., Lécuyer, A., Jacquet, A., Guérin, N., Fagot, J. P., Boucherat, M., d'Athis, P., & Cohen, R. (2009). Local and regional adverse reactions to BCG-SSI vaccination: a 12-month cohort follow-up study. *Vaccine*, *27*(50), 6967–6973. https://doi.org/10.1016/j.vaccine.2009.09.073

Dougan, S. K., Kaser, A., & Blumberg, R. S. (2007). CD1 Expression on Antigen-Presenting Cells. In *T Cell Activation by CD1 and Lipid Antigens* (113–141). Springer, Berlin, Heidelberg. https://doi.org/10.1007/978-3-540-69511-0_5

Driessen, N. N., Ummels, R., Maaskant, J. J., Gurcha, S. S., Besra, G. S., Ainge, G. D., Larsen, D. S., Painter, G. F., Vandenbroucke-Grauls, C. M. J. E., Geurtsen, J., & Appelmelk, B. J. (2009). Role of Phosphatidylinositol Mannosides in the Interaction between Mycobacteria and DC-SIGN ▿ †. *Infection and Immunity*, *77*(10), 4538–4547. https://doi.org/10.1128/IAI.01256-08

Dulberger, C. L., Rubin, E. J., & Boutte, C. C. (2020). The mycobacterial cell envelope - a moving target. *Nature Reviews Microbiology*, *18*(1), 47–59. https://doi.org/10.1038/s41579-019-0273-7

DZIF. (2022, April 25). *New drug substance BTZ-043 for tuberculosis | German Center for Infection Research*. https://www.dzif.de/en/new-drug-substance-btz-043-tuberculosis

Egen, J. G., Rothfuchs, A. G., Feng, C. G., Winter, N., Sher, A., & Germain, R. N. (2008). Macrophage and T Cell Dynamics during the Development and Disintegration of Mycobacterial Granulomas. *Immunity*, *28*(2), 271–284. https://doi.org/10.1016/j.immuni.2007.12.010

Ehlers, S., & Schaible, U. E. (2012). The granuloma in tuberculosis: dynamics of a host-pathogen collusion. *Frontiers in Immunology*, *3*, 411. https://doi.org/10.3389/fimmu.2012.00411

Erlinger, S., Stracker, N., Hanrahan, C., Nonyane, S., Mmolawa, L., Tampi, R. P., Tucker, A., West, N., Lebina, L., Martinson, N., & Dowdy, D. (2019). Tuberculosis patients with higher levels of poverty face equal or greater costs of illness. *The International Journal of Tuberculosis and Lung Disease: The Official Journal of the International Union Against Tuberculosis and Lung Disease*, *23*(11), 1205–1212. https://doi.org/10.5588/ijtld.18.0814

Eruslanov, E. B., Lyadova, I. V., Kondratieva, T. K., Majorov, K. B., Scheglov, I. V., Orlova, M. O., & Apt, A. S. (2005). Neutrophil responses to *Mycobacterium tuberculosis* infection in genetically susceptible and resistant mice. *Infection and Immunity*, *73*(3), 1744–1753. https://doi.org/10.1128/IAI.73.3.1744-1753.2005

Eum, S.-Y., Kong, J.-H., Hong, M.-S., Lee, Y.-J., Kim, J.-H., Hwang, S.-H., Cho, S.-N., Via, L. E., & Barry, C. E. (2010). Neutrophils are the predominant infected phagocytic cells in the airways of patients with active pulmonary TB. *Chest*, *137*(1), 122–128. https://doi.org/10.1378/chest.09-0903

European Directorate for the Quality of Medicine and Health Care (2020). Europäisches Arzneibuch 10.0.

Evangelopoulos, D., & McHugh, T. D. (2015). Improving the tuberculosis drug development pipeline. *Chemical Biology & Drug Design*, *86*(5), 951–960. https://doi.org/10.1111/cbdd.12549

Fatima, S., Kumari, A., Das, G., & Dwivedi, V. P. (2020). Tuberculosis vaccine: A journey from BCG to present. *Life Sciences*, *252*, 117594. https://doi.org/10.1016/j.lfs.2020.117594

Felio, K., Nguyen, H., Dascher, C. C., Choi, H.-J., Li, S., Zimmer, M. I., Colmone, A., Moody, D. B., Brenner, M. B., & Wang, C.-R. (2009). CD1-restricted adaptive immune responses to Mycobacteria in human group 1 CD1 transgenic mice. *The Journal of Experimental Medicine*, *206*(11), 2497–2509. https://doi.org/10.1084/jem.20090898

Fenhalls, G., Stevens, L., Bezuidenhout, J., Amphlett, G. E., Duncan, K., Bardin, P., & Lukey, P. T. (2002a). Distribution of IFN-gamma, IL-4 and TNF-alpha protein and CD8 T cells producing IL-12p40 mRNA in human lung tuberculous granulomas. *Immunology*, *105*(3), 325–335. https://doi.org/10.1046/j.1365-2567.2002.01378.x

Fenhalls, G., Stevens, L., Moses, L., Bezuidenhout, J., Betts, J. C., van Helden, P. D., Lukey, P. T., & Duncan, K. (2002b). In situ detection of *Mycobacterium tuberculosis* transcripts in human lung granulomas reveals differential gene expression in necrotic lesions. *Infection and Immunity*, *70*(11), 6330–6338. https://doi.org/10.1128/iai.70.11.6330-6338.2002

Fischer, K., Scotet, E., Niemeyer, M., Koebernick, H., Zerrahn, J., Maillet, S., Hurwitz, R., Kursar, M., Bonneville, M., Kaufmann, S. H. E., & Schaible, U. E. (2004). Mycobacterial phosphatidylinositol mannoside is a natural antigen for CD1d-restricted T cells. *Proceedings of the National Academy of Sciences of the United States of America*, *101*(29), 10685–10690. https://doi.org/10.1073/pnas.0403787101

Fox, W. (1868). A lecture on the artificial production of tubercle in the lower animals. *British Medical Journal*, *1*(386), 499–502. https://doi.org/10.1136/bmj.1.386.499

Gadola, S. D., Zaccai, N. R., Harlos, K., Shepherd, D., Castro-Palomino, J. C., Ritter, G., Schmidt, R. R., Jones, E. Y., & Cerundolo, V. (2002). Structure of human CD1b with bound ligands at 2.3 A, a maze for alkyl chains. *Nature Immunology*, *3*(8), 721–726. https://doi.org/10.1038/ni821

Gao, C., Peng, C., Shi, Y., You, X., Ran, K., Xiong, L., Ye, T., Zhang, L., Wang, N., Zhu, Y., Liu, K., Zuo, W., Yu, L., & Wei, Y. (2016). Benzothiazinethione is a potent preclinical candidate for the treatment of drug-resistant tuberculosis. *Scientific Reports*, *6*(1), 29717. https://doi.org/10.1038/srep29717

Garcia-Alles, L.-F., Collmann, A., Versluis, C., Lindner, B., Guiard, J., Maveyraud, L., Huc, E., Im, J. S., Sansano, S., Brando, T., Julien, S., Prandi, J., Gilleron, M., Porcelli, S. A., La Salle, H. d., Heck, A. J. R., Mori, L., Puzo, G., Mourey, L., & Libero, G. de (2011). Structural reorganization of the antigen-binding groove of human CD1b for presentation of mycobacterial

sulfoglycolipids. *Proceedings of the National Academy of Sciences of the United States of America*, *108*(43), 17755–17760. https://doi.org/10.1073/pnas.1110118108

Garçon, N., Chomez, P., & van Mechelen, M. (2007). GlaxoSmithKline Adjuvant Systems in vaccines: concepts, achievements and perspectives. *Expert Review of Vaccines*, *6*(5), 723–739. https://doi.org/10.1586/14760584.6.5.723

Geldmacher, C., Ngwenyama, N., Schuetz, A., Petrovas, C., Reither, K., Heeregrave, E. J., Casazza, J. P., Ambrozak, D. R., Louder, M., Ampofo, W., Pollakis, G., Hill, B., Sanga, E., Saathoff, E., Maboko, L., Roederer, M., Paxton, W. A., Hoelscher, M., & Koup, R. A. (2010). Preferential infection and depletion of *Mycobacterium tuberculosis*-specific CD4 T cells after HIV-1 infection. *The Journal of Experimental Medicine*, *207*(13), 2869–2881. https://doi.org/10.1084/jem.20100090

Gengenbacher, M., & Kaufmann, S. H. E. (2012). *Mycobacterium tuberculosis*: success through dormancy. *Fems Microbiology Reviews*, *36*(3), 514–532. https://doi.org/10.1111/j.1574-6976.2012.00331.x

Gerb, S. A., Dashek, R. J., Ericsson, A. C., Griffin, R., & Franklin, C. L. (2021). The Effects of Ketamine on the Gut Microbiome on CD1 Mice. *Comparative Medicine*, *71*(4), 295–301. https://doi.org/10.30802/AALAS-CM-20-000117

Gillard, P., Yang, P.-C., Danilovits, M., Su, W.-J., Cheng, S.-L., Pehme, L., Bollaerts, A., Jongert, E., Moris, P., Ofori-Anyinam, O., Demoitié, M.-A., & Castro, M. (2016). Safety and immunogenicity of the M72/AS01E candidate tuberculosis vaccine in adults with tuberculosis: A phase II randomised study. *Tuberculosis (Edinburgh, Scotland)*, *100*, 118–127. https://doi.org/10.1016/j.tube.2016.07.005

Gilleron, M., Lepore, M., Layre, E., Cala-De Paepe, D., Mebarek, N., Shayman, J. A., Canaan, S., Mori, L., Carrière, F., Puzo, G., & Libero, G. de (2016). Lysosomal Lipases PLRP2 and LPLA2 Process Mycobacterial Multi-acylated Lipids and Generate T Cell Stimulatory Antigens. *Cell Chemical Biology*, *23*(9), 1147–1156. https://doi.org/10.1016/j.chembiol.2016.07.021

Gilleron, M., Quesniaux, V. F. J., & Puzo, G. (2003). Acylation state of the phosphatidylinositol hexamannosides from *Mycobacterium bovis* bacillus Calmette Guerin and mycobacterium tuberculosis H37Rv and its implication in Toll-like receptor response. *Journal of Biological Chemistry*, *278*(32), 29880–29889. https://doi.org/10.1074/jbc.M303446200

Gilleron, M., Ronet, C., Mempel, M., Monsarrat, B., Gachelin, G., & Puzo, G. (2001). Acylation state of the phosphatidylinositol mannosides from *Mycobacterium bovis* bacillus Calmette Guérin and ability to induce granuloma and recruit natural killer T cells. *Journal of Biological Chemistry*, *276*(37), 34896–34904. https://doi.org/10.1074/jbc.M103908200

Gong, W., Liang, Y., & Wu, X. (2020). Animal Models of Tuberculosis Vaccine Research: An Important Component in the Fight against Tuberculosis. *BioMed Research International*, *2020*, 4263079. https://doi.org/10.1155/2020/4263079

González-Martínez, N. A., Lozano-Garza, H. G., Castro-Garza, J., Osio-Cortez, A. de, Vargas-Villarreal, J., Cavazos-Rocha, N., Ocampo-Candiani, J., Makarov, V., Cole, S. T., & Vera-Cabrera, L. (2015). In Vivo Activity of the Benzothiazinones PBTZ169 and BTZ043 against Nocardia brasiliensis. *PLoS Neglected Tropical Diseases*, *9*(10), e0004022. https://doi.org/10.1371/journal.pntd.0004022

Goossens, S. N., Sampson, S. L., & van Rie, A. (2020). Mechanisms of Drug-Induced Tolerance in *Mycobacterium tuberculosis*. *Clinical Microbiology Reviews*, *34*(1). https://doi.org/10.1128/CMR.00141-20

Grange, J. M., & Stanford, J. L. (1990). BCG vaccination and cancer. *Tubercle*, *71*(1), 61–64. https://doi.org/10.1016/0041-3879(90)90063-E

Griffith, A. S. (1937). Bovine tuberculosis in man. *Tubercle*, *18*(12), 529–543. https://doi.org/10.1016/S0041-3879(37)80200-7

Grode, L., Ganoza, C. A., Brohm, C., Weiner, J., Eisele, B., & Kaufmann, S. H. E. (2013). Safety and immunogenicity of the recombinant BCG vaccine VPM1002 in a phase 1 open-label randomized clinical trial. *Vaccine*, *31*(9), 1340–1348. https://doi.org/10.1016/j.vaccine.2012.12.053

Guallar-Garrido, S., Almiñana-Rapún, F., Campo-Pérez, V., Torrents, E., Luquin, M., & Julián, E. (2021). BCG Substrains Change Their Outermost Surface as a Function of Growth Media. *Vaccines*, *10*(1). https://doi.org/10.3390/vaccines10010040

Guerin, M. E., Korduláková, J., Alzari, P. M., Brennan, P. J., & Jackson, M. (2010). Molecular basis of phosphatidyl-myo-inositol mannoside biosynthesis and regulation in mycobacteria. *The Journal of Biological Chemistry*, *285*(44), 33577–33583. https://doi.org/10.1074/jbc.R110.168328

Guermonprez, P., Valladeau, J., Zitvogel, L., Théry, C., & Amigorena, S. (2002). Antigen presentation and T cell stimulation by dendritic cells. *Annual Review of Immunology*, *20*, 621–667. https://doi.org/10.1146/annurev.immunol.20.100301.064828

Guirado, E., & Schlesinger, L. S. (2013). Modeling the *Mycobacterium tuberculosis* Granuloma - the Critical Battlefield in Host Immunity and Disease. *Frontiers in Immunology*, *4*, Article 98. https://doi.org/10.3389/fimmu.2013.00098

Gupta, R. K., Lucas, S. B., Fielding, K. L., & Lawn, S. D. (2015). Prevalence of tuberculosis in post-mortem studies of HIV-infected adults and children in resource-limited settings: a systematic review and meta-analysis. *AIDS (London, England)*, *29*(15), 1987–2002. https://doi.org/10.1097/QAD.0000000000000802

Hadden, J. W. (1994). T-cell adjuvants. *International Journal of Immunopharmacology*, *16*(9), 703–710. https://doi.org/10.1016/0192-0561(94)90090-6

Haseda, Y., Munakata, L., Kimura, C., Kinugasa-Katayama, Y., Mori, Y., Suzuki, R., & Aoshi, T. (2021). Development of combination adjuvant for efficient T cell and antibody response induction against protein antigen. *PLoS ONE*, *16*(8), e0254628. https://doi.org/10.1371/journal.pone.0254628

Hilgers, L., & Snippe, H. (1992). DDA as an immunological adjuvant. *Research in Immunology*, *143*(5), 494–503. https://doi.org/10.1016/0923-2494(92)80060-x

Hinshaw, H., Pyle, M. M., & Feldman, W. H. (1947). Streptomycin in tuberculosis. *The American Journal of Medicine*, *2*(5), 429–435. https://doi.org/10.1016/0002-9343(47)90087-9

Hiromatsu, K., Dascher, C. C., Sugita, M., Gingrich-Baker, C., Behar, S. M., LeClair, K. P., Brenner, M. B., & Porcelli, S. A. (2002). Characterization of guinea-pig group 1 CD1 proteins. *Immunology*, *106*(2), 159–172. https://doi.org/10.1046/j.1365-2567.2002.01422.x

Ho, R. S., Fok, J. S., Harding, G. E., & Smith, D. W. (1978). Host-Parasite Relationships in Experimental Airborne Tuberculosis. VII. Fate of *Mycobacterium tuberculosis* in Primary Lung Lesions and in Primary Lesion-Free Lung Tissue Infected as a Result of Bacillemia. *The Journal of Infectious Diseases*, *138*(2), 237–241.

Huber, A., Killy, B., Grummel, N., Bodendorfer, B., Paul, S., Wiesmann, V., Naschberger, E., Zimmer, J., Wirtz, S., Schleicher, U., Vera, J., Ekici, A. B., Dalpke, A., & Lang, R. (2020). Mycobacterial

Cord Factor Reprograms the Macrophage Response to IFN-γ towards Enhanced Inflammation yet Impaired Antigen Presentation and Expression of GBP1. *The Journal of Immunology*, *205*(6), 1580–1592. https://doi.org/10.4049/jimmunol.2000337

Huemer, M., Mairpady Shambat, S., Brugger, S. D., & Zinkernagel, A. S. (2020). Antibiotic resistance and persistence-Implications for human health and treatment perspectives. *EMBO Reports*, *21*(12), e51034. https://doi.org/10.15252/embr.202051034

Hunter, R. L. (2011). Pathology of post primary tuberculosis of the lung: an illustrated critical review. *Tuberculosis (Edinburgh, Scotland)*, *91*(6), 497–509. https://doi.org/10.1016/j.tube.2011.03.007

Huppmann, M., Baumgarten, A., Ziegler, A.-G., & Bonifacio, E. (2005). Neonatal Bacille Calmette-Guerin vaccination and type 1 diabetes. *Diabetes Care*, *28*(5), 1204–1206. https://doi.org/10.2337/diacare.28.5.1204

Hurt, R. (2004). Tuberculosis sanatorium regimen in the 1940s: a patient's personal diary. *Journal of the Royal Society of Medicine*, *97*(7), 350–353. https://doi.org/10.1258/jrsm.97.7.350

Jackman, R. M., Moody, D. B., & Porcelli, S. A. (1999). Mechanisms of lipid antigen presentation by CD1. *Critical Reviews in Immunology*, *19*(1), 49–63.

Jackson, M. (2014). The mycobacterial cell envelope-lipids. *Cold Spring Harbor Perspectives in Medicine*, *4*(10), a021105. https://doi.org/10.1101/cshperspect.a021105

Jacobs, A. J., Mongkolsapaya, J., Screaton, G. R., McShane, H., & Wilkinson, R. J. (2016). Antibodies and tuberculosis. *Tuberculosis (Edinburgh, Scotland)*, *101*, 102–113. https://doi.org/10.1016/j.tube.2016.08.001

Jamaati, H., Mortaz, E., Pajouhi, Z., Folkerts, G., Movassaghi, M., Moloudizargari, M., Adcock, I. M., & Garssen, J. (2017). Nitric Oxide in the Pathogenesis and Treatment of Tuberculosis. *Frontiers in Microbiology*, *8*, Article 2008. https://doi.org/10.3389/fmicb.2017.02008

Jarlier, V., & Nikaido, H. (1994). Mycobacterial cell wall: structure and role in natural resistance to antibiotics. *FEMS Microbiology Letters*, *123*, 11–18. https://doi.org/10.1111/j.1574-6968.1994.tb07194.x

Jasenosky, L. D., Scriba, T. J., Hanekom, W. A., & Goldfeld, A. E. (2015). T cells and adaptive immunity to *Mycobacterium tuberculosis* in humans. *Immunological Reviews*, *264*, 74–87. https://doi.org/10.1111/imr.12274

Jenum, S., Tonby, K., Rueegg, C. S., Ruhwald, M., Kristiansen, M. P., Bang, P., Olsen, I. C., Sellæg, K., Røstad, K., Mustafa, T., Taskén, K., Kvale, D., Mortensen, R., & Dyrhol-Riise, A. M. (2021). A Phase I/II randomized trial of H56:IC31 vaccination and adjunctive cyclooxygenase-2-inhibitor treatment in tuberculosis patients. *Nature Communications*, *12*(1), 6774. https://doi.org/10.1038/s41467-021-27029-6

Jo, E.-K. (2008). Mycobacterial interaction with innate receptors: TLRs, C-type lectins, and NLRs. *Current Opinion in Infectious Diseases*, *21*(3), 279–286. https://doi.org/10.1097/QCO.0b013e3282f88b5d

Kanabalan, R. D., Le Lee, J., Lee, T. Y., Chong, P. P., Hassan, L., Ismail, R., & Chin, V. K. (2021). Human tuberculosis and *Mycobacterium tuberculosis* complex: A review on genetic diversity, pathogenesis and omics approaches in host biomarkers discovery. *Microbiological Research*, *246*, 126674.

Kang, P. B., Azad, A. K., Torrelles, J. B., Kaufman, T. M., Beharka, A., Tibesar, E., DesJardin, L. E., & Schlesinger, L. S. (2005). The human macrophage mannose receptor directs *Mycobacterium tuberculosis* lipoarabinomannan-mediated phagosome biogenesis. *The Journal of Experimental Medicine*, *202*(7), 987–999. https://doi.org/10.1084/jem.20051239

Kaufmann, E. (2016). *Detection and characterization of lipopeptide-specific T cells in guinea pigs sensitized with bacteria of the Mycobacterium tuberculosis complex* [Dissertation]. Justus-Liebig-Universität Gießen.

Kaufmann, E., Spohr, C., Battenfeld, S., Paepe, D. C.-D., Holzhauser, T., Balks, E., Homolka, S., Reiling, N., Gilleron, M., & Bastian, M. (2016). BCG Vaccination Induces Robust CD4+ T Cell Responses to *Mycobacterium tuberculosis* Complex-Specific Lipopeptides in Guinea Pigs. *Journal of Immunology*, *196*(6), 2723–2732. https://doi.org/10.4049/jimmunol.1502307

Kaufmann, S. H. E. (2020a). Neue Impfstoffe gegen Tuberkulose [New vaccines against tuberculosis]. *Bundesgesundheitsblatt - Gesundheitsforschung - Gesundheitsschutz*, *63*(1), 56–64. https://doi.org/10.1007/s00103-019-03065-y

Kaufmann, S. H. E. (2020b). Vaccination Against Tuberculosis: Revamping BCG by Molecular Genetics Guided by Immunology. *Frontiers in Immunology*, *11*, 316. https://doi.org/10.3389/fimmu.2020.00316

Kaufmann, S. H. E. (2021). Vaccine Development Against Tuberculosis Over the Last 140 Years: Failure as Part of Success. *Frontiers in Microbiology*, *12*, Article 750124. https://doi.org/10.3389/fmicb.2021.750124

Keshavjee, S., & Farmer, P. E. (2012). Tuberculosis, drug resistance, and the history of modern medicine. *The New England Journal of Medicine*, *367*(10), 931–936. https://doi.org/10.1056/NEJMra1205429

Khader, S. A., Bell, G. K., Pearl, J. E., Fountain, J. J., Rangel-Moreno, J., Cilley, G. E., Shen, F., Eaton, S. M., Gaffen, S. L., Swain, S. L., Locksley, R. M., Haynes, L., Randall, T. D., & Cooper, A. M. (2007). IL-23 and IL-17 in the establishment of protective pulmonary CD4+ T cell responses after vaccination and during *Mycobacterium tuberculosis* challenge. *Nature Immunology*, *8*(4), 369–377. https://doi.org/10.1038/ni1449

Kim, M.-J., Wainwright, H. C., Locketz, M., Bekker, L.-G., Walther, G. B., Dittrich, C., Visser, A., Wang, W., Hsu, F.-F., Wiehart, U., Tsenova, L., Kaplan, G., & Russell, D. G. (2010). Caseation of human tuberculosis granulomas correlates with elevated host lipid metabolism. *EMBO Molecular Medicine*, *2*(7), 258–274. https://doi.org/10.1002/emmm.201000079

Kleinsteuber, K. (2012). *T-Zell Polarisierung bei der humanen Tuberkulose: Charakterisierung der Rolle von Suppressor of Cytokine Signaling (SOCS)-3 bei der Aktivierung und Differenzierung von CD4+ T-Zellen [*Dissertation]. Universität Hamburg.

Klotz, U. (2009). Pharmacokinetics and drug metabolism in the elderly. *Drug Metabolism Reviews*, *41*(2), 67–76. https://doi.org/10.1080/03602530902722679

Knudsen, N. P. H., Olsen, A., Buonsanti, C., Follmann, F., Zhang, Y., Coler, R. N., Fox, C. B., Meinke, A., D'Oro, U., Casini, D., Bonci, A., Billeskov, R., Gregorio, E. de, Rappuoli, R., Harandi, A. M., Andersen, P., & Agger, E. M. (2016). Different human vaccine adjuvants promote distinct antigen-independent immunological signatures tailored to different pathogens. *Scientific Reports*, *6*, Article 19570. https://doi.org/10.1038/srep19570

Koch, R. (1882). Die Ätiologie der Tuberkulose. *Berliner klinische Wochenschrift*, *Nr. 15* https://doi.org/10.1007/978-3-662-56454-7_5

Koch, R. (1891). Über bakteriologische Forschung. In: Verhandlungen des X. Internationalen Medizinischen Kongresses, Berlin.

Kolls, J. K., & Khader, S. A. (2010). The role of Th17 cytokines in primary mucosal immunity. *Cytokine & Growth Factor Reviews*, *21*(6), 443–448. https://doi.org/10.1016/j.cytogfr.2010.11.002

Kuan, R., Muskat, K., Peters, B., & Lindestam Arlehamn, C. S. (2020). Is mapping the BCG vaccine-induced immune responses the key to improving the efficacy against tuberculosis? *Journal of Internal Medicine*, *288*(6), 651–660. https://doi.org/10.1111/joim.13191

Kumar, K., & Kon, O. M. (2017). Diagnosis and treatment of tuberculosis: latest developments and future priorities. *Annals of Research Hospitals*, *1*(5), 1. https://doi.org/10.21037/arh.2017.08.08

La Salle, H. d., Mariotti, S., Angenieux, C., Gilleron, M., Garcia-Alles, L.-F., Malm, D., Berg, T., Paoletti, S., Maître, B., Mourey, L., Salamero, J., Cazenave, J. P., Hanau, D., Mori, L., Puzo, G., & Libero, G. de (2005). Assistance of microbial glycolipid antigen processing by CD1e. *Science*, *310*(5752), 1321–1324. https://doi.org/10.1126/science.1115301

Ladefoged, A., Bunch-Christensen, K., & Guld, J. (1976). Tuberculin sensitivity in guinea-pigs after vaccination with varying doses of BCG of 12 different strains. *Bulletin of the World Health Organization*, *53*(4), 435–443.

Larrouy-Maumus, G., Layre, E., Clark, S. O., Prandi, J., Rayner, E., Lepore, M., Libero, G. de, Williams, A., Puzo, G., & Gilleron, M. (2017). Protective efficacy of a lipid antigen vaccine in a guinea pig model of tuberculosis. *Vaccine*, *35*(10), 1395–1402. https://doi.org/10.1016/j.vaccine.2017.01.079

Lechartier, B., Hartkoorn, R. C., & Cole, S. T. (2012). In vitro combination studies of benzothiazinone lead compound BTZ043 against *Mycobacterium tuberculosis*. *Antimicrobial Agents and Chemotherapy*, *56*(11), 5790–5793. https://doi.org/10.1128/AAC.01476-12

Lee, Y. C., & Ballou, C. E. (1965). Complete structures of the glycophospholipids of mycobacteria. *Biochemistry*, *4*(7), 1395–1404. https://doi.org/10.1021/bi00883a026

Leentjens, J., Kox, M., Stokman, R., Gerretsen, J., Diavatopoulos, D. A., van Crevel, R., Rimmelzwaan, G. F., Pickkers, P., & Netea, M. G. (2015). BCG Vaccination Enhances the Immunogenicity of Subsequent Influenza Vaccination in Healthy Volunteers: A Randomized, Placebo-Controlled Pilot Study. *The Journal of Infectious Diseases*, *212*(12), 1930–1938. https://doi.org/10.1093/infdis/jiv332

Lehmann, J. (1946). Para-Aminosalicylic acid in the Treatment of Tuberculosis. *The Lancet*, *247*(6384), 15–16. https://doi.org/10.1016/S0140-6736(46)91185-3

Lenaerts, A. J., Hoff, D. R., Aly, S., Ehlers, S., Andries, K., Cantarero, L., Orme, I. M., & Basaraba, R. J. (2007). Location of persisting mycobacteria in a Guinea pig model of tuberculosis revealed by r207910. *Antimicrobial Agents and Chemotherapy*, *51*(9), 3338–3345. https://doi.org/10.1128/AAC.00276-07

Li, H., & Javid, B. (2018). Antibodies and tuberculosis: finally coming of age? *Nature Reviews Immunology*, *18*(9), 591–596. https://doi.org/10.1038/s41577-018-0028-0

Li, H., Wang, X.-X., Wang, B., Fu, L., Liu, G., Lu, Y., Cao, M., Huang, H., & Javid, B. (2017). Latently and uninfected healthcare workers exposed to TB make protective antibodies against *Mycobacterium tuberculosis*. *Proceedings of the National Academy of Sciences of the United States of America*, *114*(19), 5023–5028. https://doi.org/10.1073/pnas.1611776114

Li, S., Choi, H.-J., Felio, K., & Wang, C.-R. (2011). Autoreactive CD1b-restricted T cells: a new innate-like T-cell population that contributes to immunity against infection. *Blood*, *118*(14), 3870–3878. https://doi.org/10.1182/blood-2011-03-341941

Lima, V. M., Bonato, V. L., Lima, K. M., Dos Santos, S. A., Dos Santos, R. R., Gonçalves, E. D., Faccioli, L. H., Brandão, I. T., Rodrigues-Junior, J. M., & Silva, C. L. (2001). Role of trehalose dimycolate in recruitment of cells and modulation of production of cytokines and NO in tuberculosis. *Infection and Immunity*, *69*(9), 5305–5312. https://doi.org/10.1128/iai.69.9.5305-5312.2001

Lin, P. L., & Flynn, J. L. (2015). CD8 T cells and *Mycobacterium tuberculosis* infection. *Seminars in Immunopathology*, *37*(3), 239–249. https://doi.org/10.1007/s00281-015-0490-8

Lin, P. L., Rutledge, T., Green, A. M., Bigbee, M., Fuhrman, C., Klein, E., & Flynn, J. L. (2012). CD4 T cell depletion exacerbates acute *Mycobacterium tuberculosis* while reactivation of latent infection is dependent on severity of tissue depletion in cynomolgus macaques. *AIDS Research and Human Retroviruses*, *28*(12), 1693–1702. https://doi.org/10.1089/aid.2012.0028

Lindenstrøm, T., Agger, E. M., Korsholm, K. S., Darrah, P. A., Aagaard, C., Seder, R. A., Rosenkrands, I., & Andersen, P. (2009). Tuberculosis subunit vaccination provides long-term protective immunity characterized by multifunctional CD4 memory T cells. *The Journal of Immunology*, *182*(12), 8047–8055. https://doi.org/10.4049/jimmunol.0801592

Lindenstrøm, T., Woodworth, J. S., Dietrich, J., Aagaard, C., Andersen, P., & Agger, E. M. (2012). Vaccine-induced th17 cells are maintained long-term postvaccination as a distinct and phenotypically stable memory subset. *Infection and Immunity*, *80*(10), 3533–3544. https://doi.org/10.1128/IAI.00550-12

Lönnroth, K., Jaramillo, E., Williams, B. G., Dye, C., & Raviglione, M. (2009). Drivers of tuberculosis epidemics: the role of risk factors and social determinants. *Social Science & Medicine (1982)*, *68*(12), 2240–2246. https://doi.org/10.1016/j.socscimed.2009.03.041

López-Serrano, S., Cordoba, L., Pérez-Maillo, M., Pleguezuelos, P., Remarque, E. J., Ebensen, T., Guzmán, C. A., Christensen, D., Segalés, J., & Darji, A. (2021). Immune Responses to Pandemic H1N1 Influenza Virus Infection in Pigs Vaccinated with a Conserved Hemagglutinin HA1 Peptide Adjuvanted with CAF®01 or CDA/αGalCerMPEG. *Vaccines*, *9*(7). https://doi.org/10.3390/vaccines9070751

Lowe, D. M., Bandara, A. K., Packe, G. E., Barker, R. D., Wilkinson, R. J., Griffiths, C. J., & Martineau, A. R. (2013). Neutrophilia independently predicts death in tuberculosis. *The European Respiratory Journal*, *42*(6), 1752–1757. https://doi.org/10.1183/09031936.00140913

Loxton, A. G., Knaul, J. K., Grode, L., Gutschmidt, A., Meller, C., Eisele, B., Johnstone, H., van der Spuy, G., Maertzdorf, J., Kaufmann, S. H. E., Hesseling, A. C., Walzl, G., & Cotton, M. F. (2017). Safety and Immunogenicity of the Recombinant *Mycobacterium bovis* BCG Vaccine VPM1002 in HIV-Unexposed Newborn Infants in South Africa. *Clinical and Vaccine Immunology : CVI*, *24*(2). https://doi.org/10.1128/CVI.00439-16

Lu, L. L., Chung, A. W., Rosebrock, T. R., Ghebremichael, M., Yu, W. H., Grace, P. S., Schoen, M. K., Tafesse, F., Martin, C., Leung, V., Mahan, A. E., Sips, M., Kumar, M. P., Tedesco, J., Robinson, H., Tkachenko, E., Draghi, M., Freedberg, K. J., Streeck, H., . . . Alter, G. (2016). A Functional Role for Antibodies in Tuberculosis. *Cell*, *167*(2), 433-443.e14. https://doi.org/10.1016/j.cell.2016.08.072

Luca, S., & Mihaescu, T. (2013). History of BCG Vaccine. *Maedica*, *8*(1), 53–58.

Ly, L. H., Russell, M. I., & McMurray, D. N. (2007). Microdissection of the cytokine milieu of pulmonary granulomas from tuberculous guinea pigs. *Cellular Microbiology*, *9*(5), 1127–1136. https://doi.org/10.1111/j.1462-5822.2006.00854.x

Makarov, V., Lechartier, B., Zhang, M., Neres, J., van der Sar, A. M., Raadsen, S. A., Hartkoorn, R. C., Ryabova, O. B., Vocat, A., Decosterd, L. A., Widmer, N., Buclin, T., Bitter, W., Andries, K., Pojer, F., Dyson, P. J., & Cole, S. T. (2014). Towards a new combination therapy for tuberculosis with next generation benzothiazinones. *EMBO Molecular Medicine*, *6*(3), 372–383. https://doi.org/10.1002/emmm.201303575

Makarov, V., Manina, G., Mikušová, K., Möllmann, U., Ryabova, O. B., Saint-Joanis, B., Dhar, N., Pasca, M. R., Buroni, S., Lucarelli, A. P., Milano, A., Rossi, E. de, Belanova, M., Bobovská, A., Dianiskova, P., Korduláková, J., Sala, C., Fullam, E., Schneider, P., . . . Cole, S. T. (2009). Benzothiazinones kill *Mycobacterium tuberculosis* by blocking arabinan synthesis. *Science*, *324*(5928), 801–804. https://doi.org/10.1126/science.1171583

Marino, S., Cilfone, N. A., Mattila, J. T., Linderman, J. J., Flynn, J. L., & Kirschner, D. E. (2015). Macrophage polarization drives granuloma outcome during Mycobacterium tuberculosis infection. *Infection and Immunity*, *83*(1), 324–338. https://doi.org/10.1128/IAI.02494-14

Martín, C., Marinova, D., Aguiló, N., & Gonzalo-Asensio, J. (2021). MTBVAC, a live TB vaccine poised to initiate efficacy trials 100 years after BCG. *Vaccine*, *39*(50), 7277–7285. https://doi.org/10.1016/j.vaccine.2021.06.049

Martín, C., Williams, A., Hernandez-Pando, R., Cardona, P. J., Gormley, E., Bordat, Y., Soto, C. Y., Clark, S. O., Hatch, G. J., Aguilar, D., Ausina, V., & Gicquel, B. (2006). The live *Mycobacterium tuberculosis* phoP mutant strain is more attenuated than BCG and confers protective immunity against tuberculosis in mice and guinea pigs. *Vaccine*, *24*(17), 3408–3419. https://doi.org/10.1016/j.vaccine.2006.03.017

Matteelli, A., Roggi, A., & Carvalho, A. C. (2014). Extensively drug-resistant tuberculosis: epidemiology and management. *Clinical Epidemiology*, *6*, 111–118. https://doi.org/10.2147/CLEP.S35839

Mayer-Barber, K. D., & Barber, D. L. (2015). Innate and Adaptive Cellular Immune Responses to *Mycobacterium tuberculosis* Infection. *Cold Spring Harbor Perspectives in Medicine*, *5*(12). https://doi.org/10.1101/cshperspect.a018424

McMurray, D. N. (2014). Guinea Pig Model of Tuberculosis. In *Tuberculosis* (135–147). John Wiley & Sons, Ltd. https://doi.org/10.1128/9781555818357.ch9

Merker, M., Barbier, M., Cox, H. S., Rasigade, J.-P., Feuerriegel, S., Kohl, T. A., Diel, R., Borrell, S., Gagneux, S., Nikolayevskyy, V., Andres, S., Nübel, U., Supply, P., Wirth, T., & Niemann, S. (2018). Compensatory evolution drives multidrug-resistant tuberculosis in Central Asia. *ELife*, *7*. https://doi.org/10.7554/eLife.38200

Migliori, G. B., Sotgiu, G., D'Ambrosio, L., Centis, R., Lange, C., Bothamley, G., Cirillo, D. M., Lorenzo, S. de, Guenther, G., Kliiman, K., Muetterlein, R., Spinu, V., Villar, M., Zellweger, J. P., Sandgren, A., Huitric, E., & Manissero, D. (2012). TB and MDR/XDR-TB in European Union and European Economic Area countries: managed or mismanaged? *The European Respiratory Journal*, *39*(3), 619–625. https://doi.org/10.1183/09031936.00170411

Minnikin, D. E., Kremer, L., Dover, L. G., & Besra, G. S. (2002). The methyl-branched fortifications of *Mycobacterium tuberculosis*. *Chemistry and Biology*, *9*(5), 545–553. https://doi.org/10.1016/S1074-5521(02)00142-4

Moliva, J. I., Turner, J., & Torrelles, J. B. (2015). Prospects in *Mycobacterium bovis* Bacille Calmette et Guérin (BCG) vaccine diversity and delivery: why does BCG fail to protect against tuberculosis? *Vaccine*, *33*(39), 5035–5041. https://doi.org/10.1016/j.vaccine.2015.08.033

Moody, D. B. (2007). T Cell Activation by CD1 and Lipid Antigens. https://doi.org/10.1007/978-3-540-69511-0

Moody, D. B., Zajonc, D. M., & Wilson, I. A. (2005). Anatomy of CD1-lipid antigen complexes. *Nature Reviews Immunology*, *5*(5), 387–399. https://doi.org/10.1038/nri1605

Morra, M. E., Kien, N. D., Elmaraezy, A., Abdelaziz, O. A. M., Elsayed, A. L., Halhouli, O., Montasr, A. M., Vu, T. L.-H., Ho, C., Foly, A. S., Phi, A. P., Abdullah, W. M., Mikhail, M., Milne, E., Hirayama, K., & Huy, N. T. (2017). Early vaccination protects against childhood leukemia: A systematic review and meta-analysis. *Scientific Reports*, *7*(1), 15986. https://doi.org/10.1038/s41598-017-16067-0

Murphy, K. (2012). *Janeway's Immunobiology: 8th Edition* (8th ed.). Garland Science, Taylor & Francis Group, LLC.

Mutis, T., Cornelisse, Y. E., & Ottenhoff, T. H. (1993). Mycobacteria induce CD4+ T cells that are cytotoxic and display Th1-like cytokine secretion profile: heterogeneity in cytotoxic activity and cytokine secretion levels. *European Journal of Immunology*, *23*(9), 2189–2195. https://doi.org/10.1002/eji.1830230921

NCATS Inxight Drugs. (2022, June 8). *BTZ-043*. https://drugs.ncats.io/drug/G55ZH52P57

Neres, J., Pojer, F., Molteni, E., Chiarelli, L. R., Dhar, N., Boy-Röttger, S., Buroni, S., Fullam, E., Degiacomi, G., Lucarelli, A. P., Read, R. J., Zanoni, G., Edmondson, D. E., Rossi, E. de, Pasca, M. R., McKinney, J. D., Dyson, P. J., Riccardi, G., Mattevi, A., . . . Binda, C. (2012). Structural basis for benzothiazinone-mediated killing of *Mycobacterium tuberculosis*. *Science Translational Medicine*, *4*(150), 150ra121. https://doi.org/10.1126/scitranslmed.3004395

Nerlich, A. G., Haas, C. J., Zink, A., Szeimies, U., & Hagedorn, H. G. (1997). Molecular evidence for tuberculosis in an ancient Egyptian mummy. *Lancet*, *350*(9088), 1404. https://doi.org/10.1016/S0140-6736(05)65185-9

Netea, M. G., Domínguez-Andrés, J., Barreiro, L. B., Chavakis, T., Divangahi, M., Fuchs, E., Joosten, L. A. B., van der Meer, J. W. M., Mhlanga, M. M., Mulder, W. J. M., Riksen, N. P., Schlitzer, A., Schultze, J. L., Stabell Benn, C., Sun, J. C., Xavier, R. J., & Latz, E. (2020). Defining trained immunity and its role in health and disease. *Nature Reviews Immunology*, *20*(6), 375–388. https://doi.org/10.1038/s41577-020-0285-6

Netea, M. G., van der Meer, J. W. M., & van Crevel, R. (2021). BCG vaccination in health care providers and the protection against COVID-19. *The Journal of Clinical Investigation*, *131*(2). https://doi.org/10.1172/JCI145545

Nguyen, L. (2016). Antibiotic resistance mechanisms in *M. tuberculosis*: an update. *Archives of Toxicology*, *90*(7), 1585–1604. https://doi.org/10.1007/s00204-016-1727-6

Nguyen, T. K. A., Koets, A. P., Santema, W. J., Van Eden, W., Rutten, V. P. M. G., & Van Rhijn, I. (2009). The mycobacterial glycolipid glucose monomycolate induces a memory T cell response comparable to a model protein antigen and no B cell response upon experimental vaccination of cattle. *Vaccine*, *27*(35), 4818–4825. https://doi.org/10.1016/j.vaccine.2009.05.078

Nguyen, T. K. A., Reinink, P., El Messlaki, C., Im, J. S., Ercan, A., Porcelli, S. A., & Van Rhijn, I. (2015). Expression patterns of bovine CD1 in vivo and assessment of the specificities of the

anti-bovine CD1 antibodies. *PLoS ONE*, *10*(3), e0121923. https://doi.org/10.1371/journal.pone.0121923

Nieberle, K. (1929). Studien zur pathologischen Anatomie und Pathogenese der Tuberkulose der Haustiere: Der Primärkomplex beim Kalb. *Archiv Für Wissenschafftliche Und Praktische Tierheilkunde / Organ Der Gesellschaft Deutscher Naturforscher Und Ärzte*(1), 3–20.

Nieberle, K. (1938). *Tuberkulose und Fleischhygiene: Untersuchungen über die pathologische Anatomie und Pathogenese der Tuberkulose mit besonderer Berücksichtigung ihrer Bedeutung für die Beurteilung des Fleisches der tuberkulösen Schlachttiere*. Gustav Fischer.

Nieuwenhuizen, N. E., Kulkarni, P. S., Shaligram, U., Cotton, M. F., Rentsch, C. A., Eisele, B., Grode, L., & Kaufmann, S. H. E. (2017). The Recombinant Bacille Calmette-Guérin Vaccine VPM1002: Ready for Clinical Efficacy Testing. *Frontiers in Immunology*, *8*, 1147. https://doi.org/10.3389/fimmu.2017.01147

Nobre, R. N., Esteves, A. M., Borges, N., Rebelo, S., Liu, Y., Mancia, F., & Santos, H. (2022). Production and Purification of Phosphatidylinositol Mannosides from *Mycobacterium smegmatis* Biomass. *Current Protocols*, *2*(6), e458. https://doi.org/10.1002/cpz1.458

Nugent, G., Whitford, J., Yockney, I. J., & Cross, M. L. (2012). Reduced spillover transmission of *Mycobacterium bovis* to feral pigs (Sus scofa) following population control of brushtail possums (Trichosurus vulpecula). *Epidemiology and Infection*, *140*(6), 1036–1047. https://doi.org/10.1017/S0950268811001579

Oettinger, T., Jørgensen, M., Ladefoged, A., Hasløv, K., & Andersen, P. (1999). Development of the *Mycobacterium bovis* BCG vaccine: review of the historical and biochemical evidence for a genealogical tree. *Tubercle and Lung Disease*, *79*(4), 243–250. https://doi.org/10.1054/tuld.1999.0206

Oleszycka, E., & Lavelle, E. C. (2014). Immunomodulatory properties of the vaccine adjuvant alum. *Current Opinion in Immunology*, *28*, 1–5. https://doi.org/10.1016/j.coi.2013.12.007

Ordway, D. J., Palanisamy, G. S., Henao-Tamayo, M., Smith, E. E., Shanley, C. A., Orme, I. M., & Basaraba, R. J. (2007). The cellular immune response to *Mycobacterium tuberculosis* infection in the guinea pig. *Journal of Immunology*, *179*(4), 2532–2541. https://doi.org/10.4049/jimmunol.179.4.2532

Orme, I. M., & Basaraba, R. J. (2014). The formation of the granuloma in tuberculosis infection. *Seminars in Immunology*, *26*(6), 601–609. https://doi.org/10.1016/j.smim.2014.09.009

Ortalo-Magné, A., Dupont, M. A., Lemassu, A., Andersen, A. B., Gounon, P., & Daffé, M. (1995). Molecular composition of the outermost capsular material of the tubercle bacillus. *Microbiology (Reading, England)*, *141*(7), 1609–1620. https://doi.org/10.1099/13500872-141-7-1609

Pagán, A. J., & Ramakrishnan, L. (2018). The Formation and Function of Granulomas. *Annual Review of Immunology*, *36*, 639–665. https://doi.org/10.1146/annurev-immunol-032712-100022

Pai, M., Behr, M. A., Dowdy, D., Dheda, K., Divangahi, M., Boehme, C. C., Ginsberg, A. M., Swaminathan, S., Spigelman, M., Getahun, H., Menzies, D., & Raviglione, M. (2016). Tuberculosis. *Nature Reviews. Disease Primers*, *2*, 16076. https://doi.org/10.1038/nrdp.2016.76

Palanisamy, G. S., Smith, E. E., Shanley, C. A., Ordway, D. J., Orme, I. M., & Basaraba, R. J. (2008). Disseminated disease severity as a measure of virulence of *Mycobacterium tuberculosis* in the guinea pig model. *Tuberculosis*, *88*(4), 295–306. https://doi.org/10.1016/j.tube.2007.12.003

Pasca, M. R., Degiacomi, G., Ribeiro, Ana Luisa de Jesus Lopes, Zara, F., Mori, P. de, Heym, B., Mirrione, M., Brerra, R., Pagani, L., Pucillo, L., Troupioti, P., Makarov, V., Cole, S. T., & Riccardi, G. (2010). Clinical isolates of *Mycobacterium tuberculosis* in four European hospitals are uniformly susceptible to benzothiazinones. *Antimicrobial Agents and Chemotherapy*, *54*(4), 1616–1618. https://doi.org/10.1128/AAC.01676-09

Pea, F. (2018). Pharmacokinetics and drug metabolism of antibiotics in the elderly. *Expert Opinion on Drug Metabolism & Toxicology*, *14*(10), 1087–1100. https://doi.org/10.1080/17425255.2018.1528226

Peddireddy, V., Doddam, S. N., & Ahmed, N. (2017). Mycobacterial Dormancy Systems and Host Responses in Tuberculosis. *Frontiers in Immunology*, *8*, 84. https://doi.org/10.3389/fimmu.2017.00084

Pedersen, G. K., Andersen, P., & Christensen, D. (2018). Immunocorrelates of CAF family adjuvants. *Seminars in Immunology*, *39*, 4–13. https://doi.org/10.1016/j.smim.2018.10.003

Petroff, S. A., & Branch, A. (1928). Bacillus Calmette-Guérin (B.C.G.): Animal Experimentation and Prophylactic Immunization of Children. *American Journal of Public Health and the Nation's Health*, *18*(7), 843–864. https://doi.org/10.2105/ajph.18.7.843-b

Pettenati, C., & Ingersoll, M. A. (2018). Mechanisms of BCG immunotherapy and its outlook for bladder cancer. *Nature Reviews Urology*, *15*(10), 615–625. https://doi.org/10.1038/s41585-018-0055-4

Pfyffer, G. E. (2015). Mycobacterium: General Characteristics, Laboratory Detection, and Staining Procedures. In *Manual of Clinical Microbiology* (536–569). John Wiley & Sons, Ltd. https://doi.org/10.1128/9781555817381.ch30

Podell, B. K., Ackart, D. F., Obregon-Henao, A., Eck, S. P., Henao-Tamayo, M., Richardson, M., Orme, I. M., Ordway, D. J., & Basaraba, R. J. (2014). Increased severity of tuberculosis in Guinea pigs with type 2 diabetes: a model of diabetes-tuberculosis comorbidity. *The American Journal of Pathology*, *184*(4), 1104–1118. https://doi.org/10.1016/j.ajpath.2013.12.015

Porcelli, S. A., Brenner, M. B., Greenstein, J. L., Balk, S. P., Terhorst, C., & Bleicher, P. A. (1989). Recognition of cluster of differentiation 1 antigens by human CD4-CD8-cytolytic T lymphocytes. *Nature*, *341*(6241), 447–450. https://doi.org/10.1038/341447a0

Porcelli, S. A., Morita, C. T., & Brenner, M. B. (1992). CD1b restricts the response of human CD4-8- T lymphocytes to a microbial antigen. *Nature*, *360*(6404), 593–597. https://doi.org/10.1038/360593a0

Pulendran, B., Arunachalam, P. S., & O'Hagan, D. T. (2021). Emerging concepts in the science of vaccine adjuvants. *Nature Reviews Drug Discovery*, *20*(6), 454–475. https://doi.org/10.1038/s41573-021-00163-y

Queval, C. J., Brosch, R., & Siméone, R. (2017). The Macrophage: A Disputed Fortress in the Battle against *Mycobacterium tuberculosis*. *Frontiers in Microbiology*, *8*, 2284. https://doi.org/10.3389/fmicb.2017.02284

Rahlwes, K. C., Puffal, J., & Morita, Y. S. (2019). Purification and Analysis of Mycobacterial Phosphatidylinositol Mannosides, Lipomannan, and Lipoarabinomannan. *Methods in Molecular Biology (Clifton, N.J.)*, *1954*, 59–75. https://doi.org/10.1007/978-1-4939-9154-9_6

Ramos, L., Lunney, J. K., & Gonzalez-Juarrero, M. (2020). Neonatal and infant immunity for tuberculosis vaccine development: importance of age-matched animal models. *Disease Models & Mechanisms*, *13*(9). https://doi.org/10.1242/dmm.045740

Reece, S. T., & Kaufmann, S. H. E. (2012). Floating between the poles of pathology and protection: Can we pin down the granuloma in tuberculosis? *Current Opinion in Microbiology*, *15*(1), 63–70. https://doi.org/10.1016/j.mib.2011.10.006

Reinink, P., & Van Rhijn, I. (2016). Mammalian CD1 and MR1 genes. *Immunogenetics*, *68*(8), 515–523. https://doi.org/10.1007/s00251-016-0926-x

Ristori, G., Faustman, D., Matarese, G., Romano, S., & Salvetti, M. (2018). Bridging the gap between vaccination with Bacille Calmette-Guérin (BCG) and immunological tolerance: the cases of type 1 diabetes and multiple sclerosis. *Current Opinion in Immunology*, *55*, 89–96. https://doi.org/10.1016/j.coi.2018.09.016

Rodrigues, L. C., Diwan, V. K., & Wheeler, J. G. (1993). Protective effect of BCG against tuberculous meningitis and miliary tuberculosis: A meta-analysis. *International Journal of Epidemiology*, *22*(6), 1154–1158. https://doi.org/10.1093/ije/22.6.1154

Rodrigues, T. S., Conti, B. J., Fraga-Silva, T. F. d. C., Almeida, F., & Bonato, V. L. (2020). Interplay between alveolar epithelial and dendritic cells and *Mycobacterium tuberculosis*. *Journal of Leukocyte Biology*, *108*(4), 1139–1156. https://doi.org/10.1002/JLB.4MR0520-112R

Rodriguez-Takeuchi, S. Y., Renjifo, M. E., & Medina, F. J. (2019). Extrapulmonary Tuberculosis: Pathophysiology and Imaging Findings. *Radiographics : A Review Publication of the Radiological Society of North America, Inc*, *39*(7), 2023–2037. https://doi.org/10.1148/rg.2019190109

Rossouw, M., Nel, H. J., Cooke, G. S., van Helden, P. D., & Hoal, E. G. (2003). Association between tuberculosis and a polymorphic NFκB binding site in the interferon γ gene. *The Lancet*, *361*(9372), 1871–1872. https://doi.org/10.1016/S0140-6736(03)13491-5

Rubin, E. J. (2009). The granuloma in tuberculosis--friend or foe? *The New England Journal of Medicine*, *360*(23), 2471–2473. https://doi.org/10.1056/NEJMcibr0902539

Russell, D. G., Cardona, P. J., Kim, M.-J., Allain, S., & Altare, F. (2009). Foamy macrophages and the progression of the human tuberculosis granuloma. *Nature Immunology*, *10*(9), 943–948. https://doi.org/10.1038/ni.1781

Sable, S. B., Posey, J. E., & Scriba, T. J. (2019). Tuberculosis Vaccine Development: Progress in Clinical Evaluation. *Clinical Microbiology Reviews*, *33*(1). https://doi.org/10.1128/CMR.00100-19

Sakamoto, K. (2012). The pathology of *Mycobacterium tuberculosis* infection. *Veterinary Pathology*, *49*(3), 423–439. https://doi.org/10.1177/0300985811429313

Sala, C., Dhar, N., Hartkoorn, R. C., Zhang, M., Ha, Y. H., Schneider, P., & Cole, S. T. (2010). Simple model for testing drugs against nonreplicating *Mycobacterium tuberculosis*. *Antimicrobial Agents and Chemotherapy*, *54*(10), 4150–4158. https://doi.org/10.1128/AAC.00821-10

Sancho-Vaello, E., Albesa-Jové, D., Rodrigo-Unzueta, A., & Guerin, M. E. (2017). Structural basis of phosphatidyl-myo-inositol mannosides biosynthesis in mycobacteria. *Biochimica Et Biophysica Acta (BBA) - Molecular and Cell Biology of Lipids*, *1862*(11), 1355–1367. https://doi.org/10.1016/j.bbalip.2016.11.002

Sani, M., Houben, E. N. G., Geurtsen, J., Pierson, J., Punder, K. de, van Zon, M., Wever, B., Piersma, S. R., Jiménez, C. R., Daffé, M., Appelmelk, B. J., Bitter, W., van der Wel, N., & Peters, P. J. (2010). Direct visualization by cryo-EM of the mycobacterial capsular layer: a labile structure containing ESX-1-secreted proteins. *PLoS Pathogens*, *6*(3), e1000794. https://doi.org/10.1371/journal.ppat.1000794

Sarmiento, M. E., Alvarez, N., Chin, K. L., Bigi, F., Tirado, Y., García, M. A., Anis, F. Z., Norazmi, M. N., & Acosta, A. (2019). Tuberculosis vaccine candidates based on mycobacterial cell envelope components. *Tuberculosis (Edinburgh, Scotland)*, *115*, 26–41. https://doi.org/10.1016/j.tube.2019.01.003

Saunders, B. M., & Britton, W. J. (2007). Life and death in the granuloma: immunopathology of tuberculosis. *Immunology and Cell Biology*, *85*(2), 103–111. https://doi.org/10.1038/sj.icb.7100027

Saunders, M. J., & Evans, C. A. (2020). COVID-19, tuberculosis and poverty: preventing a perfect storm. *The European Respiratory Journal*, *56*(1). https://doi.org/10.1183/13993003.01348-2020

Schäfer, H., & Burger, R. (2012). Tools for cellular immunology and vaccine research the in the guinea pig: monoclonal antibodies to cell surface antigens and cell lines. *Vaccine*, *30*(40), 5804–5811. https://doi.org/10.1016/j.vaccine.2012.07.012

Schaible, U. E., & Kaufmann, S. H. E. (2000). CD1 molecules and CD1-dependent T cells in bacterial infections: a link from innate to acquired immunity? *Seminars in Immunology*, *12*(6), 527–535. https://doi.org/10.1006/smim.2000.0272

Schatz, A., & Waksman, S. A. (1944). Effect of Streptomycin and Other Antibiotic Substances upon *Mycobacterium tuberculosis* and Related Organisms. *Experimental Biology and Medicine*, *57*(2), 244–248. https://doi.org/10.3181/00379727-57-14769

Schlesinger, L. S. (1993). Macrophage phagocytosis of virulent but not attenuated strains of *Mycobacterium tuberculosis* is mediated by mannose receptors in addition to complement receptors. *Journal of Immunology*, *150*(7), 2920–2930.

Schlesinger, L. S. (1996). Entry of *Mycobacterium tuberculosis* into Mononuclear Phagocytes. In T. M. Shinnick (Ed.), *Current Topics in Microbiology and Immunology. Tuberculosis* (71–96). Springer Berlin Heidelberg. https://doi.org/10.1007/978-3-642-80166-2_4

Schrager, L. K., Vekemens, J., Drager, N., Lewinsohn, D. M., & Olesen, O. F. (2020). The status of tuberculosis vaccine development. *The Lancet Infectious Diseases*, *20*(3), e28-e37. https://doi.org/10.1016/s1473-3099(19)30625-5

Scriba, T. J., Coussens, A. K., & Fletcher, H. A. (2017). Human Immunology of Tuberculosis. *Microbiology Spectrum*, *5*(1), Article 5.1.15. https://doi.org/10.1128/microbiolspec.TBTB2-0016-2016

Scriba, T. J., Netea, M. G., & Ginsberg, A. M. (2020). Key recent advances in TB vaccine development and understanding of protective immune responses against *Mycobacterium tuberculosis*. *Seminars in Immunology*, 101431. https://doi.org/10.1016/j.smim.2020.101431

Segura-Cerda, C. A., López-Romero, W., & Flores-Valdez, M. A. (2019). Changes in Host Response to *Mycobacterium tuberculosis* Infection Associated With Type 2 Diabetes: Beyond Hyperglycemia. *Frontiers in Cellular and Infection Microbiology*, *9*, 342. https://doi.org/10.3389/fcimb.2019.00342

Selwyn, P. A., Hartel, D., Lewis, V. A., Schoenbaum, E. E., Vermund, S. H., Klein, R. S., Walker, A. T., & Friedland, G. H. (1989). A prospective study of the risk of tuberculosis among intravenous drug users with human immunodeficiency virus infection. *The New England Journal of Medicine*, *320*(9), 545–550. https://doi.org/10.1056/NEJM198903023200901

Shaler, C. R., Horvath, C. N., Jeyanathan, M., & Xing, Z. (2013). Within the Enemy's Camp: contribution of the granuloma to the dissemination, persistence and transmission of

Mycobacterium tuberculosis. *Frontiers in Immunology*, *4*, 30. https://doi.org/10.3389/fimmu.2013.00030

Sia, J. K., Georgieva, M., & Rengarajan, J. (2015). Innate Immune Defenses in Human Tuberculosis: An Overview of the Interactions between *Mycobacterium tuberculosis* and Innate Immune Cells. *Journal of Immunology Research*, *2015*, 747543. https://doi.org/10.1155/2015/747543

Sieling, P. A., Hill, P. J., Dobos, K. M., Brookman, K., Kuhlman, A. M., Fabri, M., Krutzik, S. R., Rea, T. H., Heaslip, D. G., Belisle, J. T., & Modlin, R. L. (2008). Conserved mycobacterial lipoglycoproteins activate TLR2 but also require glycosylation for MHC class II-restricted T cell activation. *Journal of Immunology*, *180*(9), 5833–5842. https://doi.org/10.4049/jimmunol.180.9.5833

Silva, C. S., Sundling, C., Folkesson, E., Fröberg, G., Nobrega, C., Canto-Gomes, J., Chambers, B. J., Lakshmikanth, T., Brodin, P., Bruchfeld, J., Nigou, J., Correia-Neves, M., & Källenius, G. (2021). High Dimensional Immune Profiling Reveals Different Response Patterns in Active and Latent Tuberculosis Following Stimulation With Mycobacterial Glycolipids. *Frontiers in Immunology*, *12*, 727300. https://doi.org/10.3389/fimmu.2021.727300

Singh, A. K., Netea, M. G., & Bishai, W. R. (2021). BCG turns 100: its nontraditional uses against viruses, cancer, and immunologic diseases. *The Journal of Clinical Investigation*, *131*(11). https://doi.org/10.1172/JCI148291

Singh, R., Dwivedi, S. P., Gaharwar, U. S., Meena, R., Rajamani, P., & Prasad, T. (2020). Recent updates on drug resistance in *Mycobacterium tuberculosis*. *Journal of Applied Microbiology*, *128*(6), 1547–1567. https://doi.org/10.1111/jam.14478

Smith, D. W., McMurray, D. N., Wiegeshaus, E. H., Grover, A. A., & Harding, G. E. (1970). Host-parasite relationships in experimental airborne tuberculosis. IV. Early events in the course of infection in vaccinated and nonvaccinated guinea pigs. *The American Review of Respiratory Disease*, *102*(6), 937–949. https://doi.org/10.1164/arrd.1970.102.6.937

Spohr, C., Kaufmann, E., Battenfeld, S., Duchow, K., Cussler, K., Balks, E., & Bastian, M. (2015). A new lymphocyte proliferation assay for potency determination of bovine tuberculin PPDs. *Altex*, *32*(3), 201–210. https://doi.org/10.14573/altex.1502101

Stenger, S., Hanson, D. A., Teitelbaum, R., Dewan, P., Niazi, K. R., Froelich, C. J., Ganz, T., Thoma-Uszynski, S., Melián, A., Bogdan, C., Porcelli, S. A., Bloom, B. R., Krensky, A. M., & Modlin, R. L. (1998). An antimicrobial activity of cytolytic T cells mediated by granulysin. *Science*, *282*(5386), 121–125. https://doi.org/10.1126/science.282.5386.121

Stenger, S., Mazzaccaro, R. J., Uyemura, K., Cho, S., Barnes, P. F., Rosat, J. P., Sette, A., Brenner, M. B., Porcelli, S. A., Bloom, B. R., & Modlin, R. L. (1997). Differential effects of cytolytic T cell subsets on intracellular infection. *Science*, *276*(5319), 1684–1687. https://doi.org/10.1126/science.276.5319.1684

Stop TB Partnership. (2020a). *The impact of COVID-19 on the TB epidemic: A community perspective*. https://www.stoptb.org/file/9318/download

Stop TB Partnership. (2020b). *The potential impact of the COVID-19 response on tuberculosis in high-burden countries: A modelling analysis*. https://stoptb.org/assets/documents/news/Modeling%20Report_1%20May%202020_FINAL.pdf

Stracker, N., Hanrahan, C., Mmolawa, L., Nonyane, B., Tampi, R. P., Tucker, A., West, N., Lebina, L., Martinson, N., & Dowdy, D. (2019). Risk factors for catastrophic costs associated with tuberculosis in rural South Africa. *The International Journal of Tuberculosis and Lung Disease:*

The Official Journal of the International Union Against Tuberculosis and Lung Disease, *23*(6), 756–763. https://doi.org/10.5588/ijtld.18.0519

Suárez, I., Fünger, S. M., Kröger, S., Rademacher, J., Fätkenheuer, G., & Rybniker, J. (2019). The Diagnosis and Treatment of Tuberculosis. *Deutsches Ärzteblatt International*, *116*(43), 729–735. https://doi.org/10.3238/arztebl.2019.0729

Sugita, M., & Brenner, M. B. (2000). T lymphocyte recognition of human group 1 CD1 molecules: implications for innate and acquired immunity. *Seminars in Immunology*, *12*(6), 511–516. https://doi.org/10.1006/smim.2000.0277

Surmik, D., Szczygielski, T., Janiszewska, K., & Rothschild, B. M. (2018). Tuberculosis-like respiratory infection in 245-million-year-old marine reptile suggested by bone pathologies. *Royal Society Open Science*, *5*(6), 180225. https://doi.org/10.1098/rsos.180225

Takayama, K., Wang, L., & David, H. L. (1972). Effect of isoniazid on the in vivo mycolic acid synthesis, cell growth, and viability of *Mycobacterium tuberculosis*. *Antimicrobial Agents and Chemotherapy*, *2*(1), 29–35. https://doi.org/10.1128/aac.2.1.29

Tameris, M., Mearns, H., Penn-Nicholson, A., Gregg, Y., Bilek, N., Mabwe, S., Geldenhuys, H., Shenje, J., Luabeya, A. K. K., Murillo, I., Doce, J., Aguiló, N., Marinova, D., Puentes, E., Rodríguez, E., Gonzalo-Asensio, J., Fritzell, B., Thole, J., Martín, C., . . . Veldsman, A. (2019). Live-attenuated *Mycobacterium tuberculosis* vaccine MTBVAC versus BCG in adults and neonates: a randomised controlled, double-blind dose-escalation trial. *The Lancet Respiratory Medicine*, *7*(9), 757–770. https://doi.org/10.1016/S2213-2600(19)30251-6

Tangye, S. G., & Tarlinton, D. M. (2009). Memory B cells: effectors of long-lived immune responses. *European Journal of Immunology*, *39*(8), 2065–2075. https://doi.org/10.1002/eji.200939531

Torrelles, J. B., Azad, A. K., & Schlesinger, L. S. (2006). Fine discrimination in the recognition of individual species of phosphatidyl-myo-inositol mannosides from *Mycobacterium tuberculosis* by C-type lectin pattern recognition receptors. *Journal of Immunology*, *177*(3), 1805–1816. https://doi.org/10.4049/jimmunol.177.3.1805

Toyonaga, K., Miyake, Y., & Yamasaki, S. (2014). Characterization of the receptors for mycobacterial cord factor in Guinea pig. *PLoS ONE*, *9*(2), e88747. https://doi.org/10.1371/journal.pone.0088747

Treatment of pulmonary tuberculosis with streptomycin and para-aminosalicylic acid (1950). *British Medical Journal*, *2*(4688), 1073–1085. https://doi.org/10.1136/bmj.2.4688.1073

Trefzer, C., Škovierová, H., Buroni, S., Bobovská, A., Nenci, S., Molteni, E., Pojer, F., Pasca, M. R., Makarov, V., Cole, S. T., Riccardi, G., Mikušová, K., & Johnsson, K. (2012). Benzothiazinones are suicide inhibitors of mycobacterial decaprenylphosphoryl-β-D-ribofuranose 2'-oxidase DprE1. *Journal of the American Chemical Society*, *134*(2), 912–915. https://doi.org/10.1021/ja211042r

Turner, O. C., Basaraba, R. J., & Orme, I. M. (2003). Immunopathogenesis of pulmonary granulomas in the guinea pig after infection with *Mycobacterium tuberculosis*. *Infection and Immunity*, *71*(2), 864–871. https://doi.org/10.1128/iai.71.2.864-871.2003

Ulrichs, T., & Kaufmann, S. H. E. (2006). New insights into the function of granulomas in human tuberculosis. *The Journal of Pathology*, *208*(2), 261–269. https://doi.org/10.1002/path.1906

Ulrichs, T., Kosmiadi, G. A., Trusov, V., Jörg, S., Pradl, L., Titukhina, M., Mishenko, V., Gushina, N., & Kaufmann, S. H. E. (2004). Human tuberculous granulomas induce peripheral lymphoid

follicle-like structures to orchestrate local host defence in the lung. *The Journal of Pathology*, *204*(2), 217–228. https://doi.org/10.1002/path.1628

van den Anker, J., Reed, M. D., Allegaert, K., & Kearns, G. L. (2018). Developmental Changes in Pharmacokinetics and Pharmacodynamics. *The Journal of Clinical Pharmacology*, *58 Suppl 10*, S10-S25. https://doi.org/10.1002/jcph.1284

Van Rhijn, I., Nguyen, T. K. A., Michel, A., Cooper, D., Govaerts, M., Cheng, T.-Y., Van Eden, W., Moody, D. B., Coetzer, J. A. W., Rutten, V. P. M. G., & Koets, A. P. (2009). Low cross-reactivity of T-cell responses against lipids from *Mycobacterium bovis* and M. avium paratuberculosis during natural infection. *European Journal of Immunology*, *39*(11), 3031–3041. https://doi.org/10.1002/eji.200939619

Vilchèze, C. (2020). Mycobacterial Cell Wall: A Source of Successful Targets for Old and New Drugs. *Applied Sciences*, *10*(7), 2278. https://doi.org/10.3390/app10072278

Vilchèze, C., & Jacobs, W. R. (2007). The mechanism of isoniazid killing: clarity through the scope of genetics. *Annual Review of Microbiology*, *61*, 35–50. https://doi.org/10.1146/annurev.micro.61.111606.122346

Villeneuve, C., Gilleron, M., Maridonneau-Parini, I., Daffé, M., Astarie-Dequeker, C., & Etienne, G. (2005). Mycobacteria use their surface-exposed glycolipids to infect human macrophages through a receptor-dependent process. *Journal of Lipid Research*, *46*(3), 475–483. https://doi.org/10.1194/jlr.M400308-JLR200

Visvabharathy, L., Genardi, S., Cao, L., He, Y., Alonzo, F. 3., Berdyshev, E., & Wang, C.-R. (2020). Group 1 CD1-restricted T cells contribute to control of systemic *Staphylococcus aureus* infection. *PLoS Pathogens*, *16*(4), e1008443. https://doi.org/10.1371/journal.ppat.1008443

Weiss, G., & Schaible, U. E. (2015). Macrophage defense mechanisms against intracellular bacteria. *Immunological Reviews*, *264*(1), 182–203. https://doi.org/10.1111/imr.12266

Wiegeshaus, E. H., McMurray, D. N., Grover, A. A., Harding, G. E., & Smith, D. W. (1970). Host-parasite relationships in experimental airborne tuberculosis. 3. Relevance of microbial enumeration to acquired resistance in guinea pigs. *The American Review of Respiratory Disease*, *102*(3), 422–429. https://doi.org/10.1164/arrd.1970.102.3.422

Winslow, G. M., Cooper, A. M., Reiley, W., Chatterjee, M., & Woodland, D. L. (2008). Early T-cell responses in tuberculosis immunity. *Immunological Reviews*, *225*, 284–299. https://doi.org/10.1111/j.1600-065X.2008.00693.x

Woelke, S. (2020). *Identifikation und molekulare Charakterisierung hoch-immunogener mykobakterieller T-Zell-Antigene* [Dissertation]. Justus-Liebig-Universität Gießen.

Wolf, A. J., Linas, B., Trevejo-Nuñez, G. J., Kincaid, E., Tamura, T., Takatsu, K., & Ernst, J. D. (2007). *Mycobacterium tuberculosis* infects dendritic cells with high frequency and impairs their function in vivo. *Journal of Immunology*, *179*(4), 2509–2519. https://doi.org/10.4049/jimmunol.179.4.2509

Woo, M., Wood, C., Kwon, D., Park, K.-H. P., Fejer, G., & Delorme, V. (2018). *Mycobacterium tuberculosis* Infection and Innate Responses in a New Model of Lung Alveolar Macrophages. *Frontiers in Immunology*, *9*, 438. https://doi.org/10.3389/fimmu.2018.00438

Woodworth, J. S., Clemmensen, H. S., Battey, H., Dijkman, K., Lindenstrøm, T., Laureano, R. S., Taplitz, R., Morgan, J., Aagaard, C., Rosenkrands, I., Lindestam Arlehamn, C. S., Andersen, P., & Mortensen, R. (2021). A Mycobacterium tuberculosis-specific subunit vaccine that

provides synergistic immunity upon co-administration with Bacillus Calmette-Guérin. *Nature Communications*, *12*(1), 6658. https://doi.org/10.1038/s41467-021-26934-0

Working Group for New TB Drugs. (2022, February 22). *BTZ-043*. https://www.newtbdrugs.org/pipeline/compound/btz-043

World Health Organization. (2012). *The evolving threat of antimicrobial resistance: Opinions for action*. https://apps.who.int/iris/bitstream/handle/10665/44812/?sequence=1

World Health Organization. (2015). *The End TB Strategy*. https://apps.who.int/iris/bitstream/handle/10665/331326/WHO-HTM-TB-2015.19-eng.pdf?sequence=1&isAllowed=y

World Health Organization. (2022). *WHO consolidated guidelines on tuberculosis, Module 4: treatment - drug-resistant tuberculosis treatment, 2022 update*. https://www.who.int/publications/i/item/9789240063129

World Health Organization. (2018). *Global Tuberculosis Report 2018*. https://www.who.int/publications/i/item/9789241565646

World Health Organization. (2020, October 15). *Global tuberculosis report 2020*. https://www.who.int/publications/i/item/9789240013131

World Health Organization. (2021, October 14). *Global tuberculosis report 2021*. https://www.who.int/publications/i/item/9789240037021

World Health Organization. (2022a, June 30). *Tuberculosis (TB)*. https://www.who.int/news-room/fact-sheets/detail/tuberculosis

World Health Organization. (2022b, June 30). *Tuberculosis: Multidrug-resistant tuberculosis (MDR-TB)*. https://www.who.int/news-room/questions-and-answers/item/tuberculosis-multidrug-resistant-tuberculosis-(mdr-tb)

World Health Organization. (2022c, July 7). *Tackling the drug-resistant TB crisis*. https://www.who.int/activities/tackling-the-drug-resistant-tb-crisis

Wørzner, K., Sheward, D. J., Schmidt, S. T., Hanke, L., Zimmermann, J., McInerney, G., Karlsson Hedestam, G. B., Murrell, B., Christensen, D., & Pedersen, G. K. (2021). Adjuvanted SARS-CoV-2 spike protein elicits neutralizing antibodies and CD4 T cell responses after a single immunization in mice. *EBioMedicine*, *63*, 103197. https://doi.org/10.1016/j.ebiom.2020.103197

Yamazaki-Nakashimada, M. A., Unzueta, A., Berenise Gámez-González, L., González-Saldaña, N., & Sorensen, R. U. (2020). BCG: a vaccine with multiple faces. *Human Vaccines & Immunotherapeutics*, *16*(8), 1841–1850. https://doi.org/10.1080/21645515.2019.1706930

Yang, H.-J., Wang, D., Wen, X., Weiner, D. M., & Via, L. E. (2021). One Size Fits All? Not in In Vivo Modeling of Tuberculosis Chemotherapeutics. *Frontiers in Cellular and Infection Microbiology*, *11*, 613149. https://doi.org/10.3389/fcimb.2021.613149

Yang, Z., Wang, C., Wang, T., Bai, J., Zhao, Y., Liu, X., Ma, Q., Wu, X., Guo, Y., Zhao, Y., & Ren, L. (2015). Analysis of the reptile CD1 genes: evolutionary implications. *Immunogenetics*, *67*(5-6), 337–346. https://doi.org/10.1007/s00251-015-0837-2

Yonekawa, A., Saijo, S., Hoshino, Y., Miyake, Y., Ishikawa, E., Suzukawa, M., Inoue, H., Tanaka, M., Yoneyama, M., Oh-Hora, M., Akashi, K., & Yamasaki, S. (2014). Dectin-2 is a direct receptor

for mannose-capped lipoarabinomannan of mycobacteria. *Immunity*, *41*(3), 402–413. https://doi.org/10.1016/j.immuni.2014.08.005

Young, D. (2009). Animal models of tuberculosis. *European Journal of Immunology*, *39*(8), 2011–2014. https://doi.org/10.1002/eji.200939542

Zachary, J. F. (Ed.). (2021). *Pathologic Basis of Veterinary Disease* (Seventh Edition).

Zhou, J., Lv, J., Carlson, C., Liu, H., Wang, H., Xu, T., Wu, F., Song, C., Wang, X., Wang, T., & Qian, Z. (2021). Trained immunity contributes to the prevention of *Mycobacterium tuberculosis* infection, a novel role of autophagy. *Emerging Microbes & Infections*, *10*(1), 578–588. https://doi.org/10.1080/22221751.2021.1899771

Zuber, B., Chami, M., Houssin, C., Dubochet, J., Griffiths, G., & Daffé, M. (2008). Direct visualization of the outer membrane of mycobacteria and corynebacteria in their native state. *Journal of Bacteriology*, *190*(16), 5672–5680. https://doi.org/10.1128/JB.01919-07

Zuñiga, J., Torres-García, D., Santos-Mendoza, T., Rodriguez-Reyna, T. S., Granados, J., & Yunis, E. J. (2012). Cellular and humoral mechanisms involved in the control of tuberculosis. *Clinical and Developmental Immunology*, *2012*, 193923. https://doi.org/10.1155/2012/193923

8 Appendix

8.1 Eigenständigkeitserklärung

"Ich erkläre hiermit, die vorgelegte Dissertation mit dem Titel:
“Vaccination and therapeutic strategies against *M. tuberculosis* in the guinea pig model”
selbständig und ohne unerlaubte fremde Hilfe und nur mit den Hilfen angefertigt, die ich in der Dissertation angegeben habe. Alle Textstellen, die wörtlich oder sinngemäß aus veröffentlichten oder nicht veröffentlichten Schriften entnommen sind, und alle Angaben, die auf mündlichen Auskünften beruhen, sind als solche kenntlich gemacht. Bei den von mir durchgeführten und in der Dissertation erwähnten Untersuchungen habe ich die Grundsätze guter wissenschaftlicher Praxis, wie sie in der "Satzung der Justus-Liebig-Universität Gießen zur Sicherung guter wissenschaftlicher Praxis" niedergelegt sind, eingehalten."

Emmelie Margarete Eckhardt

8.2 Publications

Eckhardt, Emmelie; Bastian, Max (2020): Animal models for human group 1 CD1 protein function. In: *Molecular Immunology* (130), S. 159–163. DOI: 10.1016/j.molimm.2020.12.018.

Eckhardt, Emmelie; Bastian, Max (2021): Vaccines against Coronaviruses of Veterinary Importance. In: *Berliner und Münchener Tierärztliche Wochenschrift* 134, S. 1–12. DOI: 10.2376/1439-0299-2020-31.

Eckhardt, Emmelie; Stei, Fabian; Thal, Dana; Schinköthe, Jan (2021): Erregersteckbrief *Mycobacterium tuberculosis*. Online verfügbar unter https://www.openagrar.de/servlets/MCRFileNodeServlet/openagrar_derivate_00041876/Erregersteckbrief_Tuberkulose_Oktober-2021_0.pdf, zuletzt geprüft am 18.03.2022.

Emmelie Eckhardt, Yan Li, Svenja Mamerow, Jan Schinköthe, Julia Sehl-Ewert, Julia Dreisbach, Björn Corleis, Anca Dorhoi, Jens Teifke, Christian Menge, Florian Kloss, Max Bastian: Pharmacokinetics and Efficacy of the Benzothiazinone BTZ-043 against Tuberculous Mycobacteria inside Granulomas in the Guinea Pig Model. In: Antimicrobial Agents and Chemotherapy. DOI: 10.1128/aac.01438-22

Submitted:

Emmelie Eckhardt, Jan Schinköthe, Marcel Gischke, Julia Sehl-Ewert, Björn Corleis, Anca Dorhoi, Jens Teifke, Dirk Albrecht, Annemieke Geluk, Martine Gilleron, Max Bastian: Donor unrestricted T cells matter: Phosphatidylinositolmannoside vaccination induces lipid-specific Th1-responses and partially protects guinea pigs from Mycobacterium tuberculosis challenge. Submitted to Scientific Reports on 09.01.2023, Manuscript: SREP-23-00073

8.3 Oral and poster presentations

Emmelie Eckhardt, Jan Schinköthe, Jens Teifke, Martine Gilleron, Max Bastian (03/2020): The role and function of lipid-reactive guinea pig T cells in mycobacterial granuloma formation and maintenance. 24th Symposium „Infection and Immune Defense" of the German Society for Immunology (DGfI), Rothenfels, Germany, oral presentation.

Emmelie Eckhardt, Jan Schinköthe, Jens Teifke, Martine Gilleron, Max Bastian (06/2021): The role and function of PIM-specific, lipid-reactive T cells in mycobacterial granuloma formation and maintenance in the guinea pig. Junior Scientist Zoonosis Meeting 2021, poster presentation.

Emmelie Eckhardt, Jan Schinköthe, Jens Teifke, Martine Gilleron, Max Bastian (07/2021): The role and function of lipid-reactive guinea pig T cells in mycobacterial granuloma formation and maintenance. VIA2021 – Treffen des Veterinärimmunologischen Arbeitskreises der DGfI, oral presentation.

Emmelie Eckhardt, Jan Schinköthe, Jens Teifke, Martine Gilleron, Max Bastian (10/2021): The role and function of lipid-reactive guinea pig T cells in mycobacterial granuloma formation and maintenance. Junior Scientist Symposium 2021 (Animal welfare – Challenges and solutions for science and agriculture), poster presentation.

Emmelie Eckhardt, Jan Schinköthe, Jens Teifke, Martine Gilleron, Max Bastian (04/2022): PIM-specific, CD1b-restricted T cells contribute to granuloma integrity and immune protection against *M. tuberculosis* in the guinea pig. One Health Conference Greifswald 2022, poster presentation.

Emmelie Eckhardt, Yan Li, Svenja Mamerow, Jan Schinköthe, Julia Sehl-Ewert, Julia Dreisbach, Björn Corleis, Anca Dorhoi, Jens Teifke, Christian Menge, Florian Kloss, Max Bastian (10/2022): The new antituberculotic drug BTZ-043 in the guinea pig model. Zoonoses 2022 – International Symposium on Zoonoses Research, poster presentation.

Emmelie Eckhardt, Yan Li, Svenja Mamerow, Jan Schinköthe, Julia Sehl-Ewert, Julia Dreisbach, Björn Corleis, Anca Dorhoi, Jens Teifke, Christian Menge, Florian Kloss, Max Bastian (11/2022): BTZ-043 – a new antituberculotic drug – in the guinea pig model. Junior Scientist Symposium 2022 (Past, Present, Future – Science in Context), poster presentation.

8.4 Acknowledgments

Da sich meine tiefempfundene Dankbarkeit so oder so nicht in passenden Worten niederschreiben lässt, soll dieses eine kleine Wort ausreichen, meinen Dank an alle auszudrücken, die mich bei dem großen Projekt Doktorarbeit und meinem Weg bis dahin unterstützt haben, egal ob im Vordergrund oder Hintergrund, beruflich oder privat, in entspannten oder weniger entspannten Zeiten, in glücklichen oder betrübten Momenten, in motivierten oder unmotivierten Phasen, zweibeinig oder vierbeinig, im Labor, im Stall, am Strand oder im Grünen: **Danke!**

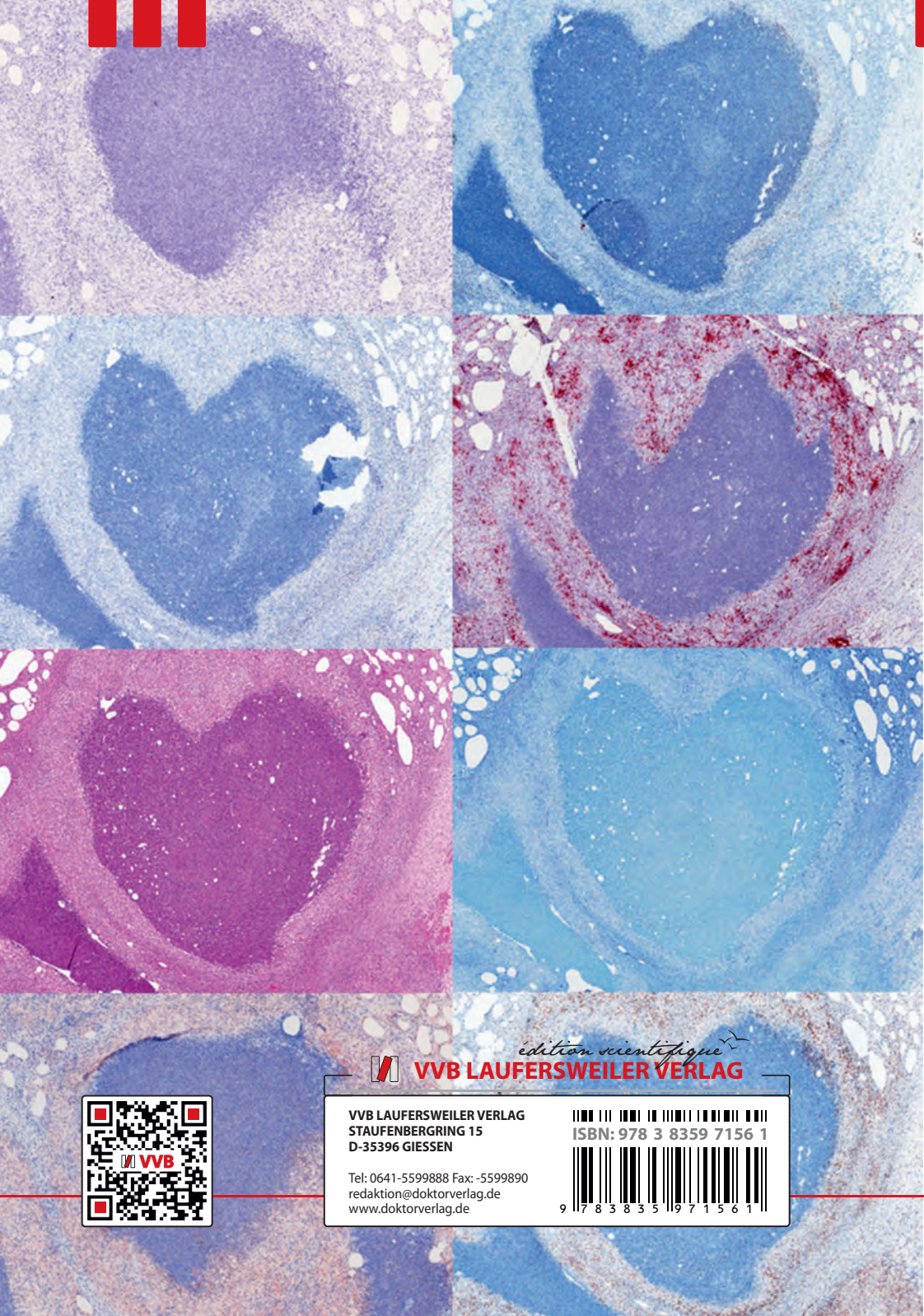

édition scientifique
VVB LAUFERSWEILER VERLAG

VVB LAUFERSWEILER VERLAG
STAUFENBERGRING 15
D-35396 GIESSEN

Tel: 0641-5599888 Fax: -5599890
redaktion@doktorverlag.de
www.doktorverlag.de

ISBN: 978 3 8359 7156 1